UNIVERSITY OF SHEFFIELD

DEPARTMENT OF CIVIL AND STRUCTURAL

ENGINEERING

ULTIMATE STRENGTH ANALYSIS OF THREE DIMENSIONAL STRUCTURES WITH FLEXIBLE RESTRAINTS

BY

Wang Yong Chang

(B.Sc)

A Thesis Submitted to the University of Sheffield for the Degree of Doctor of Philosophy

June, 1988

Certification of research

This is to certify that, except when specific reference to other investigations is made, the work described in this Thesis is the result of the investigation of the candidate.

[redacted]

Candidate

[redacted]

Supervisor

Acknowledgements

The author wishes to express his sincere gratitude to his supervisor Dr. D.A.Nethercot, Reader in the Department of Civil and Structural Engineering at the University of Sheffield, for his excellent guidance, consistent encouragement and interest in the work throughout the author's study.

The assistance provided by Professor T.H.Hanna, head of the Department and all the staff in the Department is appreciated.

Without the financial support from the Chinese Government and the British Council, it would have been impossible for the author to start, let alone finish the study.

Thanks are extended to the University's Computing Centre for various facilities provided to the author.

List of publications

Paper 1 WANG,Y.C., EL-KHENFAS,M.A. and NETHERCOT,D.A., 'Lateral-Torsional Buckling of End-Restrained Beams', Journal of Construc-tional Steel Research **7 (1987)** pp.335-362

Paper 2 WANG,Y.C., and NETHERCOT,D.A., 'Ultimate Strength Analysis of Three Dimensional Column Subassemblages with Flexible Connections', Journal of Constructional Steel Research (in press)

Paper 3 WANG,Y.C. and NETHERCOT,D.A., 'Ultimate Strength Analysis of 3-D Braced I-Beams', submitted to The Structural Engineer for publication.

Contents

List of tables

List of figures

Notations

a height of the applied load (page 21)

a offset of the beam load from column top (page 245)

A cross-section area

b $= \frac{a}{L}\sqrt{\frac{EI_y}{GK_T}}$ (page 21)

b_f flange width

c buckling load ratio (page 19)

C connection stiffness

C' ratio of collapse load to reduced Euler load

D cross-section depth

$\{\dot{d}\}$ incremental displacement vector

$\{\dot{d}_{globe}\}$ incremental displacement vector in global system

$\{\dot{d}_{local}\}$ incremental displacement vector in local system

d_Y, d_Z offsets of S_{tz} and S_{ty} in Y and Z directionsrespectively

d_{XY}, d_{XZ} offsets of S_{tx} in Y and Z directions

$\{\triangle d\}$ displacement vector

e_y, e_{yy} column load eccentricity in Y direction

e_z, e_{zz} column load eccentricity in Z direction

E Young's modulus

$\{E_n\}$ unbalanced load vector

EI_W cross-section warping rigidity

$\dot{f}_b$ bracing force increment

F applied load (page 47)

F column design load (page 175)

F ratio of collapse load to squash load (page 176)

$$F = \frac{P_{collapse}}{P_{squash}}$$

F_b bracing force

F_d $=0.01 t_f b_f \sigma_y$

F_{ob} elastic buckling stress

$\{F_n\}$ applied load vector

F_u ultimate bracing force

F^F conventional fixed end force

F_S^F modified fixed end force

$\dot{F}$ increment in applied load

$\{\dot{F}_E\}$ increments in nodal applied force vector

F_ξ, F_η, F_ζ stress resultants in ξ, η, ζ directions

G shear modulus

GK_T ,**GJ** St. Venant's torsional rigidity

h distance between flange centroids

H_{load} height of applied load

I_b beam moment of inertia

I_c column moment of inertia

I_x second moment of area about major axis

I_y second moment of area about minor axis

I_η, I_ζ second moments of area about η, ζ axes

k effective length ratio (page 8)

k_b', k_t' stiffness distribution coefficients at column bottom and top

$\mathrm{K} = \prod_{j=1}^{m} q_j^{a_j}$ dimensional factor to allow for the size of different connections; m is the total number of size parameters; a_j is the dimensionless exponent to express the effect of q_j; q_j is the numerical value of jth size parameter.

K_b beam stiffness $K_b = \frac{I_b}{L_b}$

K_c column stiffness $K_c = \frac{I_c}{L_c}$

KM_0, ϕ_0, n Ramberg-Osgood curve fitting coefficients

K_S spring stiffness matrix (page 29)

K_{tor} connection torsional stiffness

K_W warping stiffness

K_1, K_2 stiffness distribution coefficients

$$K = \frac{\textit{total column stiffness at joint}}{\textit{total stiffness of all membes at joint}}$$

$$\overline{K_{tor}} = \frac{K_{tor}}{GK_T/L}$$

$\dot{K}_b$ bracing tangential stiffness

K_b' beam effective stiffness

[**K**] stiffness matrix

[K_b] tangential stiffness matrix of braces at a node

[K_{globe}] stiffness matrix in global system

[K_{local}] stiffness matrix in local system

[$\dot{K}_b$] diagonal matrix of bracing rigidities at a node

[K_G] segment geometric stiffness matrix

[K_S] segment flexural stiffness matrix

L member length

L_b beam length

L_c column length

L_e effective length

m end moment ratio

m_x, m_y coefficients

m_η, m_ζ stress resultants about η *and* ζ axes at shear centre

M connection moment

M_{ax} allowable bending moment about minor axis

M_{centre} moment at beam centre

M_{cr} elastic buckling moment of a beam

M_c^1, M_c^2 column centre moments

$M_d = F_d \times h$

M_e moment at beam end

M_E elastic critical moment

$\overline{M_E}$ modified elastic critical moment allowing for end warping influence

M_i inelastic buckling moment of a beam

M_{max} cross-sectional plastic moment capacity (page 12)

M_{max} maximum applied moment about major axis on a member (page 176)

$M_{m.s}$ column midspan moment

M_p cross-sectional plastic moment capacity about major axis

M_{pz} cross-sectional plastic moment capacity about minor axis

M_t^1, M_t^2 column top moments

M_x, M_y bending moments about major and minor axes respectively

M_{tor} end torque

M_u ultimate bracing moment

M_y cross-sectional elastic moment limit of a beam (page 33)

M_z bending moment about minor axis

M_W bimoment

$\Delta M_1, \Delta M_2$ connection moment increments

M_ξ, M_η, M_ζ bending moments about ξ, η, ζ axes

N number of bays

p_c compressive strength

P applied load

P_b ultimate bracing force

P_c buckling load of a braced column

$P_{collapse}$ collapse load

P_{cr} buckling load of an unbraced column

P_E elastic buckling load of a braced column

P_{Euler} Euler load

$P_p = \frac{4M_p}{L}$

P_{re} applied column load

P_s, P_{squash} column squash load

P_ξ, P_η, P_ζ applied loads in ξ, η, ζ directions

$\Delta P = \Delta P_1 + \Delta P_2;$

ΔP_1: applied beam load increment;

ΔP_2: applied column load increment.

r_y radius of gyration of the beam about its minor axis

R'_x Euler load reduction coefficient modified on account of major axis bending moment and axial load

$\mathbf{S}$ conventional stiffness matrix

S_b bracing stiffness

S_{bl} limit bracing stiffness for complete bracing

$\overline{S_{bl}}$ nondimensional limit bracing stiffness for complete bracing

S_{req} bracing strength requirement

S_{rx}, S_{ry}, S_{rz} X,Y,Z-axis rotational bracing rigidities respectively

S_S modified stiffness matrix

S_{tx}, S_{ty}, S_{tz} X,Y,Z-axis translational bracing rigidities respectively

S_x cross-sectional plastic modulus

S_W warping bracing rigidity

t_f flange thickness

$\mathbf{T}$ applied beam load

$[\mathbf{T}\ ]$, $[T_1]$, $[T_2]$, $[T_3]$ transformation matrices

$[T_b\ ]$ transformation matrix due to offset of braces

$\dot{u}_b$ incremental bracing displacement

$\{u\}$ displacement vector

$\{\dot{u}_b\}$ incremental bracing displacement vector at a node

$\{u\}^*$ total displacement vector

$\delta U_{L.H.}$ strain energy due to load offsets

U_x, U_y, U_z displacements in x,y,z directions

U_X, U_Y, U_Z displacements in X,Y,Z directions

$\Delta U_Y, \Delta U_Z$ displacement differences over a member in Y and Z directions respectively

U_ξ, U_η, U_ζ displacements in ξ, η, ζ directions

$\{U_E\}$ displacement vector in member principal coordinate directions

$\{\dot{U}_E\}$ incremental nodal displacement vector

$\{U_o\}$ displacement vector in system directions

$\{U_{\bar{o}}\}$ displacement vector in member local coordinate directions

w uniform beam load

$\delta \dot{W}$ strain energy increment

$W_b = \frac{8(M_e + M_{m.s.})}{L^2}$

W_{cr} beam elastic buckling load

$\delta W_{L.H.}$ virtual work due to load offsets

$W_p = \frac{8M_p}{L^2}$

W_u ultimate applied beam load

y_c, z_c, Y_c, Z_c centroid coordinates in x-y-z and X-Y-Z systems

y_o, z_o, Y_o, Z_o shear centre coordinates in x-y-z and X-Y-Z systems

Z_x plastic cross-sectional modulus about major axis

Z_y elastic cross-sectional modulus about minor axis

α angle of cross-section principal axis to original axis

$[\alpha\ ]$ coefficient matrix

β beam buckling moment modification factor due to non-uniform bending moment distribution

β_1 end-restraint parameter for major axis

$$\frac{M_x}{\phi_x} = \left(\frac{EI_x}{L}\right)\left(\frac{2\beta_1}{1-\beta_1}\right)$$

β_2 end-restraint parameter for minor axis

$$\frac{M_y}{\phi_y} = \left(\frac{EI_y}{L}\right)\left(\frac{2\beta_2}{1-\beta_2}\right)$$

β_3 end-restraint parameter for torsion

$$\frac{M_{tor}}{\theta} = \left(\frac{GK_T}{L}\right)\left(\frac{1}{\beta_3}\right)$$

δ ratio of allowable stresses

$\Delta\delta$ column deflection increment

$\delta_{disp.}, \delta_{load}$ displacement and load convergence factors

δ_0 initial deflection magnitude

θ axial rotation of twisting

$\dot{\theta}$ first derivative of θ

$\theta_\xi, \theta_x, \theta_X$ axial rotation of twisting about ξ, x and X axes

λ slenderness (page 8)

$\lambda = \frac{S_h L^3}{48 E I_y}$ (page 19)

$\lambda = \frac{L/r_y}{\pi\sqrt{E/\sigma_y}}$ (page 177)

λ_y slenderness about minor axis $\lambda_y = \frac{L}{r_y}$

ν Poisson's ratio

σ_r residual stress

σ_y yield stress

ϕ connection rotation

Summary

This thesis reports the analytical study on the effects of various restraints on the spatial behaviour of thin-walled structures. Starting from a brief literature review, the need to conduct a systematical investigation into the problem is identified. This is carried out by first modifying an existing program for ultimate strength analysis of a beam-column member with conventional end supporting conditions (i.e. either simply supported or fixed) and then applying the modified program to solve various practical problems.

The connection is treated as a beam-column member whose stiffness matrix is obtained from its force-deformation characteristics. A multi-linear representation is chosen to simulate the nonlinear force-deformation curve for its simplicity. Unloading of the connection is considered. Only the offsets of translational braces are allowed for, although the same principle may be applied to rotational braces. Elastic-perfectly -plastic behaviour of a brace is assumed. Nevertheless, other nonlinear responses may be easily accommodated. The two major imperfections, namely initial deflection and residual stress, are included. The validity of the program has been varified by checking against various analytical and experimental results.

Four topics have been addressed by conducting appropriate parametric studies using the modified program. These are:

1. Effects of semi-rigid connections on the spatial behaviour of 3-D beams.

2. Bracing effects on 3-D I-beams.

3. Effects of semi-rigid beam-column connections on 3-D column sub-assemblages.

4. Bracing effects on 3-D column subassemblages.

The results of these studies are presented in Chapters 4,5,7 and 8 respectively. Whilst in Chapter 9, some general conclusions from this research are summarised and some future work related to this subject recommended.

Chapter 1

INTRODUCTION

1.1 General Behaviour of Semi-Rigid Connections

In ordinary analyses of structural frames, connections are always assumed to be either pins or rigid joints, although for almost every connection in reality, the truth lies between these two extremities.

For an isolated beam-column, flexible end connections have the effects of providing restraints and reducing the maximum flexural moment within the span compared with pins or reducing the moment at supports compared with rigid joints. The effect of optimizing the moment distribution along a member is clearly illustrated in figure 1.1. In most cases, some economy in the design of such restrained members is possible.

In the case of beam-column connections in a complete frame, the effects of connections are two-fold. Firstly, they are capable of offering restraints to columns, and secondly, certain moments may be transferred through con-

tions from the beams to the columns. The load-carrying capacities of such columns will depend on the relative importance of these two effects. If the former is more pronounced, the columns will fail at higher collapse loads if stiffer connections are used. However, if the latter is the main reason for the failure of columns, the previously described trend of column strength variation will be reversed.

1.2 Objectives of the Present Investigation

While studies of the in-plane behaviour of semi-rigid connections and their effects on the basic flexural behaviour of structures have been undertaken extensively both at Sheffield and elsewhere, the effects of realistic connections in three dimensions remain uncertain.

The present study attempts to provide insights into this aspect. A finite element computer program which was written by EL-KHENFAS[1] with the basic theory of element stiffness resting on the work developed by RAJASERANAN[2] to analyse three dimensional beam-columns with ideal supporting conditions was available before the commencement of the present investigation.

This program was first modified and later extended to include the effects of flexible end connections. The extension and verification of the modified version are presented in chapter 3 whereas the detailed parametric study based on the new program is provided in chapter 4. The analysis in chapter 3 is further extended to consider the bracing effects on beam-columns and this is reported in chapter 5.

For an isolated beam-column, the implicit hypthesis is that the ad-

joining members possess infinite rigidity. This is certainly not true for a practical structure. It is therefore necessary to take into consideration of the flexibility of these members. A model of a column subassemblage which consists of a column and flexible beams framed into both axes of the column through realistic connections is analysed by extending and rewriting the program described in chapter 3. Chapter 6 describes this effort and compares the analysis with other available sources. The procedure is then employed to study the interelationship between different arrangements of connections, loading conditions and column slendernesses etc. Chapter 7 gives details of this study. A simple analysis, suitable to micro- computers, which incoperates the design approach proposed in the British Standard for Steelwork[3], to obtain the ultimate load of such subassemblages is also described in this chapter. In chapter 8, an additional study is made to deal with the bracing effects on column subassemblages in a similar manner to the study conducted in chapter 5 for beam-column members. Finally, some conclusions and recommendations are suggested in chapter 9.

1.3 Limitations of the Present Investigation

Due to the basic theory adopted and the time available for this study, the present investigation contains the following limitations:

1. Small axial rotation of twisting is assumed. As a result, the application of direct torques may not give the desired answer.

2. Although the basic theory is applicable to any form of thin-walled cross-sections, only the behaviour of I-sections is studied.

3. Line elements are adopted for warping; therefore the distortion of webs and non-uniform transmission of warping at a joint are not considered.

4. Since this study is for the purpose of tracing ultimate loads only, post-buckling is ignored.

5. Cyclic loading is not considered but any sequence of statically applied loads is possible, including arrangements which lead to unloading i.e. reversal in the direction of rotation, in the connections.

6. The material is assumed to be elastic-perfectly-plastic. Furthermore, the same behaviour is assumed for both compression and tension.

7. The flexibility of the panel zone at a joint is not considered. Instead, the connection is represented by a rigid bar and a flexible spring.

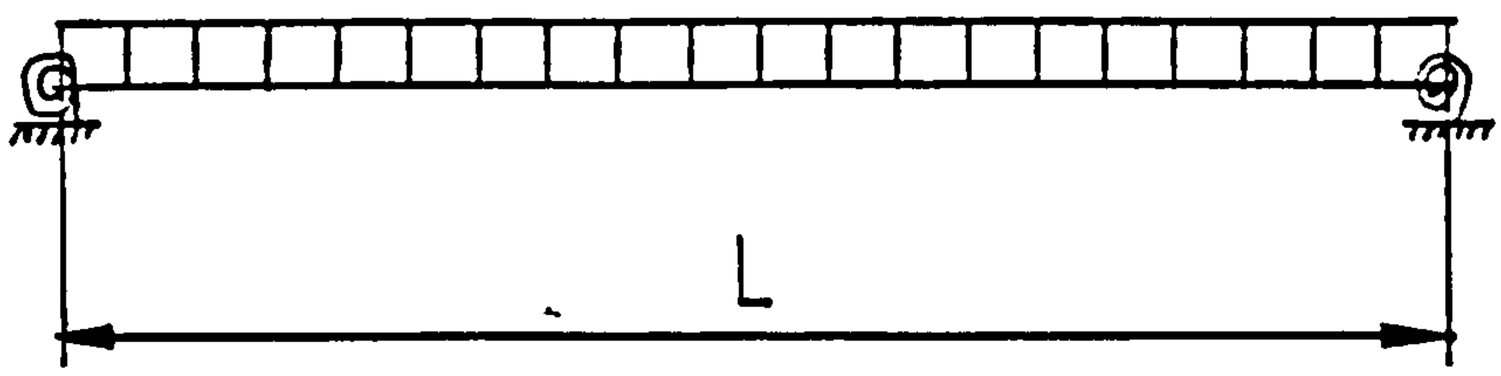

(a) A beam with semi-rigid joints

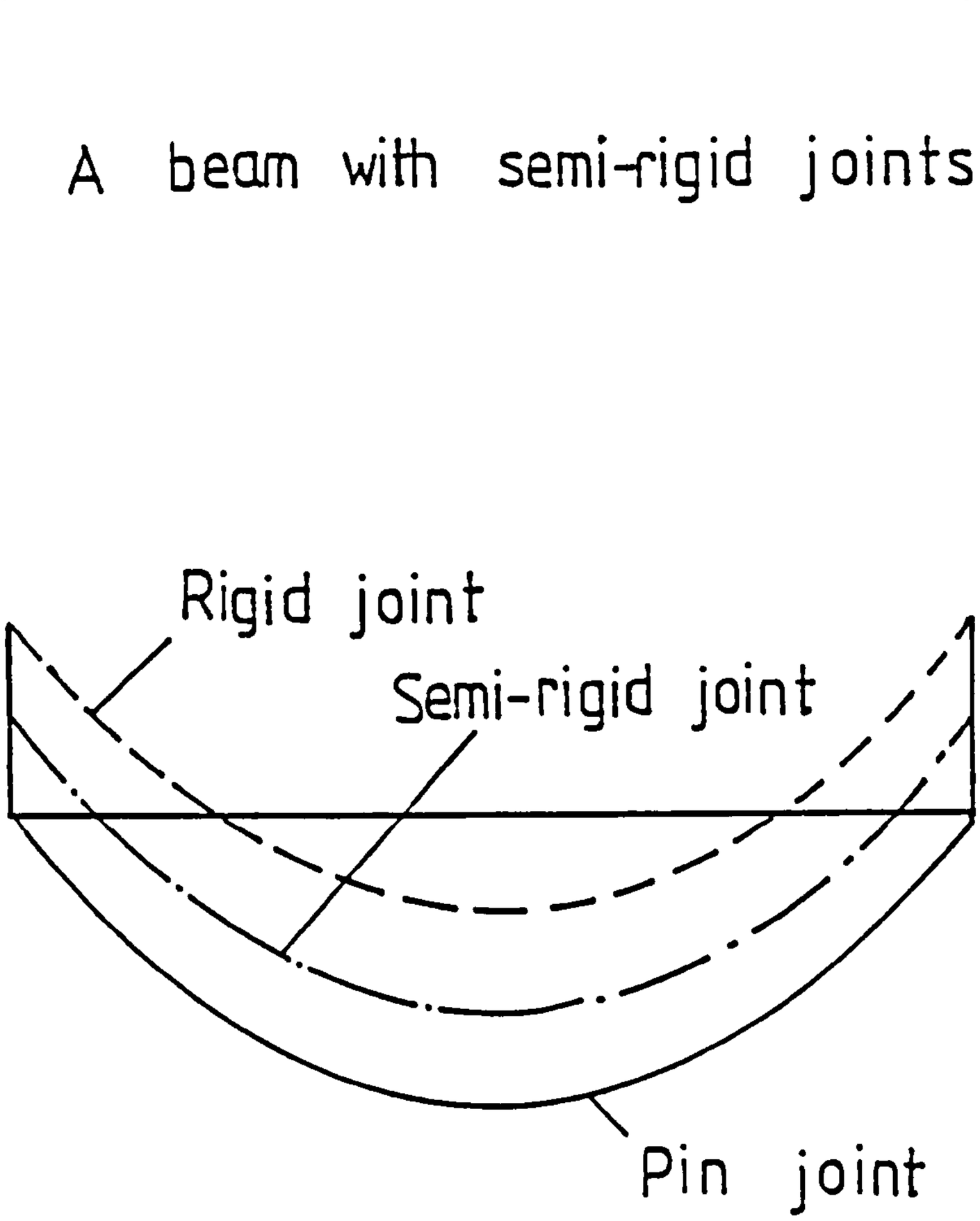

(b) Bending moment diagrams

Fig. 1·1 Effect of semi-rigid joints on bending moment in a beam

Chapter 2

REVIEW OF LITERATURE ON FLEXIBLY RESTRAINED 3-D STRUCTURES

The problems of beam-columns and frames have long been the focus of many researchers' interest with the result that various studies have been devoted to the understanding of their behaviour. This chapter attempts to give a brief review of literature in this field with special interest in the spatial behaviour of end–restrained beam-columns, braced beam-columns and beam-column subassemblages.

2.1 Two Dimensional Analyses of Flexibly Jointed Frames

The hypothesis that a beam-column connection behaves either as a pin-joint which cannot transfer any moment or a rigid joint which retains complete rotational continuity between connected members has been adopted in most analyses of planar frames, although the semi-rigid nature of a realistic connection has long been recognised. Not until quite recently, has the problem of studying flexibly connected structures received much attention. The primary obstac le to conducting such analysis is the complex behaviour of the connection itself.

The most important feature of a beam-column connection is its moment-rotation ($M - \phi$) characteristics. Over the past fifty years or so, a large number of tests have been carried out to study the connection behaviour. It is believed that the in-plane response of various types of commonly used connections is fairly well understood. Reviews by NETHERCOT[4], GOVERDHAN[5], KISHI and CHEN[6] provide connection $M-\phi$ data for virtually all available connection tests.

Typical moment-rotation curve for a representative connection is shown in figure 2.2. It can be seen that the behaviour of a semi-rigid connection is generally nonlinear throughout the entire loading stage. The characteristics of two extreme cases - rigid and pin joints - are also indicated in the figure. Once the force-deformation characteristics of a connection are known, the inclusion of its effect into structural analyses would present little difficulty.

JONES[7] was one of the first to incorporate the effects of flexible joints into structural analysis systematically. Using the finite element method, he

investigated the behaviour of planar columns with nonlinear supporting conditions. Both material and geometric imperfections were taken into consideration. The nonlinear $M - \phi$ behaviour of a connection was fitted by the B-spline curve-fitting technique. He concluded that the presence of even the most flexible connections i.e. web cleats, which are commonly hypothesized as shear connections only, could raise the buckling load of a column significantly, especially if its geometric slenderness was greater than 80.

The effective length of a restrained column which is defined as 'that length which when used in conjunction with the column curve for pinned gives the same strength as the failure load for the end-restrained columns'[7] was investigated for various connections e.g. web cleats, flange cleats etc. Based on a detailed parametric study, he concluded that the effective length ratio k did not depend on the geometrical slenderness of the column λ . This result is in accordance with the findings of SUGIMOTO and CHEN[8].

NETHERCOT and CHEN[9] identified the main considerations for determining the ultimate load capacities of end-restrained columns. Various approaches for conducting such analyses were reviewed. The column design procedure to include the effects of end-restraints was also addressed. The method which uses the concept of effective length factor was proposed.

The problem of end restrained columns was investigated by SHEN and LU[10]. This study allows for all the major nonlinear factors to be considered i.e. initial crookedness, residual stress, load eccentricities, nonlinear material properties as well as loading, unloading and reloading of yielded fibers. However, only linear end restraint characteristics were assumed. An iterative numerical integration procedure was employed to obtain the load-deflection curves. A comprehensive parametric study was conducted, based on which

the following interesting conclusions were drawn: the strength increase became smaller as the end restraint stiffness became larger; the residual stress distribution seemed to have less effect on the strength variation for end restrained columns than for pin-ended ones.

The minor axis response of restrained minor axis columns was traced by RAZZAQ[11] using the finite difference method. He concluded that 'the attainment of column maximum load is always associated with complete plastification of one or more nodes at and around the midspan', which is expected since no instability would be involved if loads were applied about the minor axis only leaving complete plastification as the sole reason for the column's failure. The restraint was assumed to behave linearly.

Using the finite element method, the behaviour of flexibly connected frames was investigated by LUI and CHEN[12]. It was assumed that the cross-section behaved elastically until the plastic moment capacity was exceeded, thus only concentrated plastification was included. The connection was taken as an element and its moment-rotation characteristic was described by an expontial function. The unloading of the connection was considered and the initial stiffness was assumed for the unloading stage. The importance of connections affecting the behaviour and ultimate strengths of steel frames was justified.

The problem of flexibly jointed frames was also looked into by GERSTLE[13]. From the analyses of a number of subassemblages representing critical portions of typical unbraced multi-storey steel frames, he found that the increase in connection stiffness would generally lead to an increase in frame strength. However, for long-span frames only a few storeys high, the provision of overstiff connections might result in a decrease in frame strength.

ANDERSON and LOK[14] presented a method of analysis to incorporate the influence of connection semi-rigidity into the conventional analysis of planar frames. In this analysis, the rotations at any connection except real pins are initially assumed to be zero. Using the conventional rigid frame analysis, the displacements and rotations are calculated, hence the member end reactions are obtained using slope-deflection equations. Incorporating connection moment-rotation characteristics, the connection rotations are assessed and these are then used to amend the applied load vector. Using this new vector of applied loads, a new vector of displacements and thus new member end reactions are obtained. This procedure is repeated until the convergence criterion is satisfied. This approach is attractive since it retains the stiffness matrix for each iteraction. Nevertheless, this analysis was limited to linear elastic behaviour and the ultimate load of the structure cannot be traced. Moreover, convergence can only be obtained for connections with high values of stiffness and approximately linear moment-rotation relationships.

DAVISON[15] tested a series of practical joints and a number of full-scale flexibly connected column subassemblages. Various aspects affecting the behaviour of connections were looked into and the in-plane $M - \phi$ behaviour of all these connections has been reported.

Parallel to DAVISON's experimental work and following JONES's recommendation, RIFAI[16] extended JONES's analysis to study the flexibly connected planar column subassemblages. Geometrical and material nonlinearities were all accounted for. The action of semi-rigid connections was included by modifying the conventional shape functions and adding the energy stored in the connection to the strain energy of the member. The B-spline technique

first used by JONES[7] was adopted to model the connection response from the tests by DAVISON[15]. The column subassemblage tests conducted by DAVISON[15] were simulated using a finite element program based on this theory. Good agreement was reached. It was concluded that the effect of semi-rigid connections was substantial regardless of the existence of beam loads. A comprehensive review of literature on the connections' effects on two-dimensional structures was provided.

Analysis of planar structures has been extensive and satisfying results in terms of both connection behaviour and their effects on planar structures have been produced. However, the behaviour of spatial structures has so far been largely overlooked due to its comparative difficulty. The remainder of this chapter is therefore devoted to this problem.

2.2 Simply Supported Beams

The expression for the elastic buckling moment of a simply supported beam with thin-walled cross-section under uniform moment is well known as[17]:

$$M_{cr} = \frac{\pi}{L}\sqrt{EI_y GK_T}\sqrt{1 + \frac{\pi^2 EI_w}{L^2 GK_T}} \tag{2.1}$$

in which L is the length of the member, EI_y is the flexural rigidity of the member about its weaker axis, GK_T and EI_w are the beam's torsional and warping rigidities.

If the beam has wide flanges or a shallow web so that the assumption of infinite flexural rigidity about the stronger axis is not realistic, equation 2.1 gives an underestimate of the critical moment, as the true buckling moment is obtained by dividing 2.1 by the following correction factor:

$$\sqrt{\left(1 - \frac{EI_y}{EI_x}\right)\left(1 - GK_T\left(1 + \frac{\pi^2 EI_w}{L^2 GK_T}\right)/EI_x\right)}$$

where EI_x is the beam's flexural rigidity about its major axis.

If the member is subject to moment gradients, the maximum moment the beam can withstand is obtained by multiplying the critical moment for uniform moment distribution by a modificaton factor β , so that

$$M_{cr(moment\ gradient)} = \beta M_{cr(uniform\ moment)} \tag{2.2}$$

Since uniform bending is the most severe case, β is no less than unity. A list of β values for different loading conditions is available in many textbooks e.g. Ref.[17] or design specifications e.g. Ref.[3].

In the case of a short beam, when a plastic hinge mechanism is able to form, the maximum moment the member is capable of sustaining is the cross-sectional plastic moment capacity, i.e.

$$M_{max} = M_p = \sigma_y S_x \tag{2.3}$$

where σ_y is the yield stress of the material and S_x is the plastic modulus of the cross-section.

For a member with intermediate slenderness, whose elastic critical moment exceeds the yield moment of the cross-section, plastification occurs before the achievement of the critical moment of the member. Elastic-plastic action will govern this region until the plastic buckling moment of the remaining elastic core of the cross-section is higher than the cross-sectional plastic moment capacity of the member. The behaviour for a simply supported perfect beam under uniform moment is featured in fig.2.1.

For a member of practical proportions, plastic action is almost always involved. Due to the action of various imperfections, e.g. initial deflection,

residual stress, load eccentricities, the determinination of the inelastic buckling load is much more complicated and a numerical approach usually has to be employed. This problem has attracted the attention of many authors and numerous papers have been publised on this subject. The book on the behaviour of spatial beam-columns by CHEN and ASTUTA[17] provides a comprehensive review in this field. More recently, extending the analytical procedure by RAJASEKARAN[2], EL-KHENFAS[1] developed a fairly rigorous method for the analysis of beam-column buckling problems.

2.3 Lateral-Torsional Buckling Analysis of 3-D Beam-Columns with End Restraints

Section 2.1 indicates that a huge body of knowledge has been formed for the understanding of connections and their effects on planar structures. However, work on the 3-D version of this problem has largely been ignored. This is due to the complexity of both the response of beam-column members and the restraint characteristics of connections. Study in this field is therefore limited; available work will be reviewed.

HECHTMAN et al[18] tested a series of full scale beams with three types of end conditions i.e. simply supported, supported by web cleats and supported by top and seat cleats. Geometrical slendernesses ranging from 110 to 441 were used. Only the ultimate loads were reported. Since some vital data e.g. connection $M-\phi$ characteristics, cross-section properties, material properties as well as initial imperfections were either not uniquely defined or not reported at all, their results are difficult to interpret. Nevertheless, the following conclusions were drawn: the existence of substantial connections

resulted in an increase in strength over the simply supported equivalent and the greater the slenderness the larger the increase. Therefore, it was proposed that this advantage be included in design; the presence of substantial connections increased the slenderness ratio at which the beam started yielding, which was obviously due to the fact that substantial connections reduced the deflection and thus the strain of beams; initial imperfections had a significant effect on the ultimate strengths of beams.

Following TIMOSENKO's energy theory[19], the effects of symmetrical elastic end restraints on the elastic lateral buckling of symmetrically loaded I-beams were analysed by TRAHAIR[20]. In this analysis, two types of buckling shapes for twist were used depending on whether the ends of the beam were free to warp or prevented from warping. Since this was an elastic bifucation problem, neither initial imperfection nor residual stress was included. The end restraint under consideration was either about the major axis or minor axis or torsional restraint. No results were reported on the combination of these restraints. Furthermore, the force-deformation characteristics of the restraint was assumed linear. Results were documented in tables and figures. Given any value which complies with the assumption, the critical load may be easily obtained by interpolation.

A study by SCHMIT[21] of the elastic lateral buckling of torsionally restrained narrow rectangular beams gave rise to the conclusion that provided the torsional restraint was greater than 40 times the beam's torsional rigidity $\frac{GK_T}{L}$, in which GK_T is the St. Venant torsional rigidity and L the beam length, an error of no more than 2 percent in the beam's load carrying capacity would be induced if infinite end torsional rigidity instead of the real value was used in the calculation of the beam's ultimate strength.

Making use of this conclusion, the Australian specification[22] proposes the corresponding limit value as

$$40\frac{GK_T}{L}\left[1+\frac{\pi^2 EI_w}{GK_T L^2}\right]$$

for an I-section beam with a warping rigidity of EI_w .

YOSHIDA and IMOTO[23] addressed the problem of inelastic lateral buckling of restrained beams using the matrix transfer method. Only linear force-deformation characteristics of restraints were incoperated. Residual stress was included, but no initial lack-of-straightness was allowed.

Using the finite difference approach, VINNOKOTA and AOSHIMA[24] studied the spatial behaviour of rotationally and directionally restrained biaxially loaded beam-column members. The rotational restraint was assumed to be elastic perfectly plastic while the directional restraint was linear. Residual stress was included but the initial deflection was neglected. After comparing the analytical results against experimental results by GENT and MILNER[25] and the analytical results by SANTATHEDAPORN and CHEN[26], the procedure was used to study the behaviour of a three dimensional beam-column subassemblage. Only the most critical column was analysed and the remaining part of the subassemblage was replaced by rotational restraints to the analysed column. The result was compared with MASSONNET's[27] interaction equations. That the result of the latter was lower was attributable to not taking into consideration the relaxation of end moments.

Unlike flexural bending or torsion, the pecularity of cross-sectional warping is uniquely associated with structures composed of thin-walled open sections. Because of the difficulty in identifying warping displacement and

warping reaction(bimoment), no attempt seems to exist to find their relationships experimetally or theoretically, nor have the effects of this type of restraint been extensively studied. OJALVO and CHAMBER[28] were among the few who considered the effect of warping restraint on the behaviour of beam-columns. By solving the differential equations with numerical integration approach, they studied the strengthening effect of warping restraints on I-beams of various lengths under uniform moment. It was found that a beam with full end fixty(prevention of lateral deflection, rotation, twisting and warping) might be capable of raising the buckling moment to several times that of a simply supported one(allowing lateral rotation and warping). Merely providing full warping restraint would enhance the buckling moment considerably. A warping restraint with a stiffness of $G(\pi^2 B^3/16)$ was capable of resulting in a buckling moment approximately the same as that for full warping restraint, in which B is the section width. Since the study was restricted to elastic behaviour, it was observed that shorter beams obtained higher strength increases for the same warping restraint. Though this may not be necessarily true for structures in reality, the significant contribution of warping restraint to the resistance to beam buckling was clearly demonstrated.

LINDER and GIETZELT[29] reported their study of the effects of end-plates on the ultimate load of laterally unsupported beams. Using beam theory, the end-plates were treated as elastic warping restraints. In order to include this warping effect in the design, the elastic critical moment M_E was replaced by $\overline{M_E}$ which reflects the end warping influence. This value was then used in the ECCS design curves. The results were compared with a limited number of test results and it seemed that the ECCS curves might

be used for beams with end-plate connections, provided the warping effect is allowed for.

The effect of end warping restraint has been addressed by VACHARAJITTIPHAN and TRAHAIR[30]. Assuming a beam is restrained at its ends by a pair of identical warping restraints with a stiffness value of K_W, it was suggested that if KL was less than one tenth of $\frac{L/a}{tanhL/2a}$, the ends of the beam would virtually have freedom to warp; if the value of KL was greater than 10 times that of $\frac{L/a}{tanhL/2a}$, the beam could be treated to be effectively prevented from warping at its ends. $K = \frac{2K_W}{EI_y}$ and $\frac{L}{a}$ indicates the relative importance of uniform torque and warping torque in contributing to the resistance to the total applied torque, $\frac{L}{a} = \sqrt{\frac{GJL^2}{EI_w}}$. The use of web stiffeners and additional webs was recognised to increase the warping restraint significantly.

2.4 Beam-Columns with Intermediate Restraints

For a practically proportioned beam-column, failure is always governed by inelastic lateral torsional buckling and the failure load is considerably lower than the full plastic capacity measured by the squash load P_{squash} for a column or the plastic moment capacity M_p of the cross-section for a beam.

Various techniques may be employed to enhance the buckling load of a member, one of which is the provision of an effective bracing system.

In practice, a main beam in a real structure is often braced e.g. by floors, purlins, secondary beams etc. It is therefore necessary to determine the strengthening effect of such braces on the main member, and in order to ensure that the braces are capable of maintaining effective restraint to the

main member, to also determine a safe value for the strength requirement of the bracing itself. Whilst numerous studies of different aspects of the bracing problem have been reported [31], the great majority of these have confined attention to the determination of the necessary bracing stiffness to achieve a certain level of improved performance from the main member. The complementary problem of assessing the associated strength requirement has been studied for comparatively few arrangements.

In this section, some of the previous work dealing with the bracing problem is reviewed.

For a simply supported perfect column braced at the mid-span by a translational brace, the approximate elastic buckling load was given in Ref.[31] as

$$P_c = \frac{\pi^2 E I_y}{L^2} + \frac{3}{16} S_b L \qquad for\ 0 < S_b < S_{bl} \tag{2.4}$$

$$P_c = \frac{4\pi^2 E I_y}{L^2} \qquad for\ S_{bl} < S_b \tag{2.5}$$

where S_{bl} is the limiting value for 'complete bracing' and

$$S_{bl} = \frac{16\pi^2 E I_y}{L^3} \tag{2.6}$$

S_b is the bracing stiffness.

The typical buckling load-bracing stiffness relationship for a discretely braced member is described in figure 2.3. Increasing the bracing rigidity will enhance the buckling load of the member until a certain value of bracing rigidity is reached at which the buckling mode of the member changes so that there is no deformation in the brace. Any bracing rigdity exceeding this critical value would cause the brace to act as an unyielding support and not induce any effect on the buckling load of the member. The inserts in

figure 2.3 illustrate the two buckling modes of a centrally braced column corresponding to different ranges of bracing stiffness.

FLINT[32] has reported some work on the effect of lateral bracing on the lateral buckling load of simply supported rectangular beams. It was proposed that the ratio of the buckling load for braced beams to that for unbraced beams be calculated in the following way:

$$c = \sqrt{1 + \lambda} \tag{2.7}$$

in which λ is the nondimensional bracing stiffness:

$$\lambda = \frac{S_b L^3}{48 E I_y} \tag{2.8}$$

By directly solving the differential equations of equilibirium or employing the energy method in cases of difficult problems, ZUK[33] derived the bracing strengths required for eight representative cases of braced beams and columns. For instance, assuming a half sine wave of initial lateral deflection form with a bow of L/1000, the elastic bracing reaction in an unyielding lateral brace is 0.53% P_c for a centrally braced column, in which P_c is the critical buckling load of the column assuming a double curvature buckling mode. For a beam possessing the same initial deflection as for the column case and under the action of an uniformly distributed moment, the bracing strength requirement would be 0.75% of the force in one flange of the beam for a central lateral brace at the beam's compression flange or 2.04% for a central lateral brace at the centroid. Though this study may give reasonable prediction for a single brace, the multiple bracing system was just briefly mentioned. It was suggested that a bracing force equal to that for a single brace would be applicable to each component of the multiple bracing system.

Assuming a fictitious hinge at the bracing point, WINTER[34] determined the mimimum rigidity required to make 'the actual elastic bracing equivalent in effect to an unyieldig support' and the strength required of such bracing when the bracing rigidity is equal to or larger than this minimum bracing rigidity. He gave the relationship between the bracing strength requirement and the bracing stiffness as

$$S_{req} = \delta_0 \frac{S_{bl}}{1 - (S_{bl}/S_b)} \qquad for\ S_b > S_{bl} \tag{2.9}$$

in which S_{req} is the bracing strength requirement, S_b and S_{bl} are respectively the bracing stiffness under consideration and the bracing stiffness for complete bracing. Equation 2.9 is qualitatively plotted in figure 2.4. Incidently, if the bracing stiffness S_b reaches the critical value S_{bl}, an infinite value of bracing force would be developed in the brace provided there is a finite initial deflection δ_0. If S_b exceeds S_{bl}, the use of a stiffer brace would require a lower strength as shown in the figure.

A limited number of test results confirmed this trend. From these tests, he pointed out that 'the greater the rigidity of the bracing the smaller the strength required of it to produce a given column capacity'. This conclusion was also reached by NETHERCOT[35] in a more limited study of columns. In the same note, he also showed that a value of $\frac{S_b}{S_{bl}}$ higher than 1.25 was necessary for a reaction of less than 2 percent of the compressive load in the main member to be developed in the brace.

WINTER slao noticed that the minimum rigidities calculated for full bracing of ideal columns were not sufficient to achieve full bracing of real i.e. imperfect columns.

Solving the differential equations of equilibrium for lateral flexure and

axial torsion, SCHMIT[21] studied the elastic buckling of an centrally loaded beam with identical elastic end torsional restraints and an elastic translational restraint at the position of the applied load. The following conclusions concerning the effects of bracing were drawn: if the end restraint should be greater than 40 times the torsional rigidity of the beam, the limiting bracing stiffness should be exceeded and the load position in the range $-0.2 < b < 0.2$, then using the lower bound, the greatest error would be no more than 2% in the estimate of P_c .

$$\frac{10.9\sqrt{EI_yGK_T}}{L^2} < P_c < \frac{11.1\sqrt{EI_yGK_T}}{L^2} \tag{2.10}$$

$$b = \frac{a}{L}\sqrt{\frac{EI_y}{GK_T}} \tag{2.11}$$

in which a is the height of the applied load and the minimum bracing rigidity S_{bl} is calculated as

$$S_{bl} = \left(\frac{2.8}{b+0.23}\right) \times \left(\frac{48EI_y}{L^3}\right) \tag{2.12}$$

Numerically integrating the simultaneous differential equations between the two ends of the beam while satisfying the equilibrum and continuity requirements at interior joints would result in a set of homogenous equations related to the boundary conditions. The determinant of the coefficients of these equations would be zero when the lateral buckling load for the beam is reached. This concept was used by HARTMANN[36] to study the elastic lateral buckling problem of continuous beams. He pointed out that for a single span beam, any bracing would have significant effect on the behaviour of the main member. However, for a multiple span beam, the axial stiffness of the interior attachment, which provided lateral restraint to the main member, was of no influence, whereas its strong axis flexural bending stiffness, which

provided torsional restraint to the main beam, showed a reasonable effect on the behaviour and ultimate load of the main member regardless of the beam type.

MASSEY[37] studied the case of a simply supported beam loaded with a uniform bending moment and prevented from buckling laterally by a rigid horizontal support positioned at the mid-span at a height above the centroid. The solution technique was tedious and the approximation introduced to describle the plastification of the cross-section was very approximate. Small scale beams were tested but the corelation with the analysis was poor.

The buckling load of a column which is discretely attached to other members providing full restraint to the flange of the main member against lateral movement and elastic restraint against twisting has been studied by DOOLEY[38] by solving energy equations of equilibrium. It was shown that if the torsional buckling mode controlled failure, the system would be equivalent to a column which was continuously attached to a foundation of uniform torsional stiffness about the attached flange. However, if the torsional stiffness of the restraint was sufficient to prevent twisting from occuring at the supporting points, the column would buckle in a mode consisting of half waves between adjacent supporting points.

This conclusion was justified by the tests reported in Ref.[39]. In this study, 50 intermediately braced columns over a range of minor axis slenderness ratios under the action of axial thrust and different eccentricities about both axes were tested. In these tests, the supporting rigs provided complete restraint to the lateral deflection but no effective torsional resistance so that the requirement of torsional buckling in Ref.[38] was satisfied. The ratio of section depth/offset of the enforced axis of twisting was set to be $1\frac{1}{3}$ to accord

with the assumption in Ref.[38]. It was observed that by merely increasing the pitches of restraints, the column only experienced a small loss in the buckling load and a slight increase in its flexibility. Therefore, the conclusion that the column could be treated as continuously attached to the supporting rig was validated.

These tests were also analysed theoritically by HARUNG and MILLAR[40]. Since columns without minor axis bending suffer less torsional deformation and the column failure is mainly due to lateral torsional buckling, the effect of the number of restraints may be less for this case. It also indicated that the effect of imperfections was small due to large eccentricities of the applied load.

A study by TAM[41] confirmed those previously described conclusions. Having extended those investigatons, he concluded that for an eccentric lateral restraint without rotational stiffness, the offset of the enforced axis of twisting had a more pronounced influence than the pitches of attachments. Furthermore, an offset of more than the depth of the section resulted in a negligible influence on the behaviour of the the braced member. However, if the attachment possessed a certain amount of rotational stiffness, i.e. providing the main member with torsional restraint, different arrangements of attachments would result in completely different behaviour of the main member since the interaction between flexural buckling and torsional buckling was induced.

Bracing strength was evaluated by MEDLAND[42] for columns of variable numbers of bays and braces. It was observed that the variation of the bracing force in the most highly loaded brace with the number of bays(N) was almost linear. Dividing this bracing force by N+1 would result in a

value approximately equal to that for a single column(N=0). The number of braces did not appear to have any significant influence on this value. It was also pointed out that bracing strength requirement varied linearly with the initial deflection magnitude, therefore, those bracing strength requirement graphs provided in Ref.[42] could be proportioned for other realistic initial deflection magnitudes.

NETHERCOT and TRAHAIR[43] studied the effect of corrugated sheeting acting as shear diaphragms on the strength of I-beams. They showed that the rigidity of the bracing would normally exceed the mimimum rigidity requirements allowing the beam to reach its M_p whereas the bracing force would often be the dominating factor. Simple methods were proposed to calculate the beam's capacity in the case of any insufficient bracing rigidity or bracing strength, and they showed that this value was often considerably higher than that of an unbraced beam.

TRAHAIR and NETHERCOT[31] summarised bracing stiffness requirements for complete bracing for various loading cases, bracing types and beam slendernesses, assuming initially perfect main members. Although limited to elastic behaviour, the results may be used as a reference point.

Experimentally, WAKAYABASHI and NAKAMURA[44] tested a series of unbraced beams and beams braced by purlins or sub-beams under the action of different moment gradients. They observed that the existence of bracing enhanced the buckling load of the beam enormously and drew the conclusion that even beams with very high slendernesses ($\frac{L}{r_y}$ up to 500) were capable of reaching the full plastic moment capacity M_p under certain types of moment gradient loading. The problem was also analysed by a finite element program. Comparison between the tests and the analysis was

reasonable but discrepencies did exist especially if the beam was braced by purlins. The imprecise modelling of the bracing characteristics was thought to be the reason.

WONG-CHUNG and KITIPORNCHAI[45] conducted a series of tests on beams with different slendernesses under quarter point loading. Partial bracing i.e. torsional bracing or lateral bracing was placed at the midspan of the beam. From the tests, it was confirmed that a lateral brace placed at the tension flange was completely ineffectve, whilst a lateral brace placed at the shear centre would be as effective as torsional bracing. They also showed that the influence of bracing could be evaluated based on the inelastic buckling capacity curve for an unbraced beam under uniform moment provided that the elastic buckling moment M_E , for determining the beam's modified slenderness, encompassed the influence of the brace. Theoretical results were also reported and a good agreement was observed.

2.5 3-D Frame Analysis

Monitoring the response of full-scale three-dimensional frames would be prohibitively costly to handle experimentally or require very powerful computational facilities. These requirements often prevent the investigation into the behaviour of such structures from being undertaken. As a result, researches on this prolem have been hampered. This section presents a review of available sources in this field.

A series of elasticaly restrained H-columns under biaxial bending was tested and analysed by GENT and MILNER[25]. The column as part of a subframe was rigidly connected to beams at its end(Fig.2.5a). The column

was first bent about both axes by applying beam loads through tightening a pair of turnbukles. When the beam loads reached certain levels, the turnbukles were then rigidly clamped and a direct column axial load was applied.

The column end moment-rotation relationship is qualitatively described in fig.2.5b. As indicated in this figure, the column initially assists in restraining the loaded beam, which produces the ascending part of the curve. Once the beam load is terminated and the column load applied, the column deformation increases its end rotation due to the effects of applied axial load and the plastic action. This increase in column end rotation relaxes the beam end moment which is equal to the column end moment, thus a descending part of column end moment-rotation curve is developed. As pointed out in Ref.[46], the ascending part depends solely on beam stiffness, whilst the descending part is controlled by column stiffness.

Load-deflection and load-moment curves were recorded for all specimens unitl the column collapsed. It was observed that because of moment shedding at the top of the column, even the most severe biaxial bending did not seriously reduce the ultimate axial load carrying capacity as compared with the value for the column when axially loaded. It was also noticed that the column buckling load was sensitive to the changes in beam stiffness.

The tested subframes were also investigated theoretically[46], However, beams were simulated as linear springs so that the problem was converted to that of restrained columns and the complexity was significantly reduced. Since only linear calculation was performed, neither residual stress nor initial crookedness was included in the analysis. The analytical procedure was rather complicated. Nevertheless, the corelation between the analytical and test results was quite satisfactory. Having compared the results from the

analysis which accounted for torsion and those neglecting torsion, it was then concluded that the torsion resulting from the second order effect of flexural bending did not affect the column's ultimate load and neither was it the reason for failure.

MILNER's tests highlighted the study in this area. Following this investigation, TAYLOR[47] tested ninteen 1/3 - 1/2 scale three-storey by two bay ridiidly jointed frames. Each frame was restrained about its minor axis by rigidly attaching a beam with a remote pin to central columns. The effects of major axis beam loading, minor axis beam loading, column slenderness ratio and minor axis restraint were investigated. From these tests, it was observed that the existence of minor axis restraint increased the collapse load of the frame in the practical range of minor axis beam stiffness to minor axis column stiffness ratio, although the rate of increase declined with an increasing ratio. Both major axis and minor axis loads were influential on the behaviour and the collapse load of the structure. Twisting was small and of little influence on the collapse load.

The Joint Committee published its first report for the design of rigid-jointed multi-storey frames in 1964[48] for mild steel structures and a renewed one in 1971[49] for high-yield-point steels without altering the basic design philosophy. It was proposed that the major axis beams (which bend or restrain the column about its major axis) be designed according to fixed ends and three plastic hinges (one at midspan and one at each end). Minor axis beams were to be designed elastically using a limited-frame consisting of the beam and adjoining members in the plane of bending of the beam. The column was designed on the basis that the total stress in the column, which included the stresses from column bending about both axes, axially applied

load and those from the axial load acting through initial deflections, should not exceed the yield stress of the material.

In order to verify the design approach proposed by the Joint Committee[48], WOOD et al[50] tested a full scale 3-storey 2×1 bay frame. It was observed that the Joint Committee's approach was accurate for beam design. However, the load-carrying capacity of the column was underestimated because of the neglect of plastic action in the column. It was therefore suggested that a more accurate criterion for collapse be sought with increased plasticity.

SMITH and ROBERTS[51] tested a full scale 3-storey 2×2 bay rigidly connected high strength steel frame with similar scope to that described above. It was found that the Joint Committee's approach was applicable to both high-yield-point steels and mild steel.

Making use of the design method proposed for two dimensional frames, LOTT et al[52] suggested an approach for designing three dimensional sub-assemblages consisting of a hollow box column and 8 wide flange beams framed into the column at both ends about both axes. The hypothesis that the column has the same cross-sectional plastic moment capacity about any axis of bending was adopted. The possibility of torsional buckling was ruled out because of the high torsional rigidity of the cross-section. Therefore, the problem was reduced to a planar one once the unbalanced column moments from beams were composed into a single plane. Both two and three dimensional specimens designed by this approach were tested and a close agreement with the predicted bahaviour was obtained. However, the limitation of this method is obvious.

Using models of scaffolds, LIGHTFOOT and LeMESSURIER[53] studied the stability of flexibly connected frames in the elastic range. The only

source which contributes to nonlinearity and instability of the structure came from axial action. The system of six degrees of freedom was adopted, i.e. 3 displacements along and 3 rotations about 3 co-ordinate axes. The conventional stiffness matrix for rigidly connected members was used.

In order to include the effect of flexibity of connections, the conventional stiffness matrix was modified employing a static condensation technique. The final form for the modified stiffness matrix and modified fixed end forces and moments take the forms:

$$S_s = K_s(S + K_s)^{-1}S \tag{2.13}$$

$$F_s^F = K_s(S + K_s)^{-1}F^F \tag{2.14}$$

in which K_s is the diagonal matrix of the various uncoupled spring stiffness matrix; S the conventional stiffness matrix of the member and F_F is the conventional matrix for the fixed-end forces and moments. The effect of offset of the bracing member was addressed, but it was concluded that the behaviour of the structure was not greatly influenced.

The analysis of three dimensional flexibly connected frames by ANG and MORRIS[54] seemed to be more concentrated on deriving the standardisation equations for various connections. In the analysis, the Ramberg-Osgood function was ultilised to simulate the moment-rotation behaviour of connections and it was written as

$$\frac{\phi}{\phi_0} = \frac{KM}{KM_0}\left(1 + \left(\frac{KM}{KM_0}\right)^{n-1}\right) \tag{2.15}$$

in which ϕ_0 ,KM_0 and n are constants to be evaluated from a Ramberg-Osgood curve fitting program; M and ϕ are the applied moment at the connection and the resulting rotation respectively; K is a dimensionless factor to account for the size of different connections.

$$K = \prod_{j=1}^{m} q_j^{a_j} \tag{2.16}$$

where q_j and a_j are the numerical value of jth size parameter and the dimensionless exponent to express its effect; m is the total number of size parameters.

It seems that the only merit of this analysis over the previously reviewed one is that it included the nonlinear effect of the connection's moment-rotation behaviour. However, the effect of axial action of the structure was neglected and the floors were assumed to act as rigid diaphragms for resisting in-plane forces so that 3 degrees of freedom i.e. two displacements and one rotation could be used to represent the in-plane action of each floor. Since the structure was assumed to behave elastically and no instability factor was included, it would be incorrect or impossible to obtain either buckling load or ultimate load of the structure. In fact, in the report, only displacements and member end forces at certain load levels were compared with other analyses to check the validity of the analytical program.

2.6 Warping and Distortion at a Joint in a Spatial Frame

For a spatial frame composed of thin-walled open cross-sections, the warping and distortion at a joint are of considerable importance in affecting the behaviour and load-carrying capacity of the structure. Due to its extreme difficulty, the problem of evaluating these effects has been largely simplified or overlooked. The assumptions of no warping restraint or continuity of warping transmission across a joint have been adopted. However, this may

be true only for some extreme cases. For most of the practical joints, the truth lies between these two extremities.

RENTON[55] studied two cases of continuity of warping restraint at a joint. These are shown in fig.2.6. SHARMAN[56] extended this conclusion in his analysis of thin-walled assemblies by assuming that a constant ratio of warping was transferred from one member to another at the joint. This constant may vary from 1 for complete equality (fig.2.6a) to -1 for complete reversal (fig.2.6b) of warping restraint. However, this constant may be difficult to ascertain.

It was pointed out in Ref.[30] that the warping of an I-section at a joint was resisted by warping and distortion of other members and stiffeners provided at the joint. Furthermore, warping and distortion were interdependent especially if the joint was unstiffened. From the analysis of an angle joint consisting of two identical I-sections with various stiffeners, which used conventional beam theory for the in-plane flexure and twisting of the flanges and stiffeners as well as the finite element method for the transverse bending and twisting of webs, it was shown that the warping restraint provided to a member was independent of the member length and there was a progressive increase in the warping restraint stiffness with the use of more stiffeners.

The work by TAM[41] proved that the hypothesis of complete continuity of warping transmission across a joint required the I-beams to be of identical dimensions and their flanges to lie in two parallel planes at an angle of 90 degree to each other. Using the finite element method, he investigated the non-uniform torsional behaviour of structural joints and frames. In his analysis, the warping and distortion were considered by relating the flange flexural moments in its plane to the resulting rotations at the ends of the

member instead of the conventional bimoment and rate of twist θ'. Assuming two dimensional deflection functions for web distortions, the resistance to distortion for an I-section member was then considered. Three orthogonal rotations of one of the flanges of the I-section shown in fig. 2.7 instead of the one dimensional treatment of a single degree of freedom θ' were adopted for the analysis of warping and distortion. Assuming identical behaviour for both flanges, three extra degrees of freedom resulted. These new degrees of freedom are vectors and tranformable. A stiffness matrix of order 18 instead of 14 was formed for each beam-column element. Results from this analysis were checked against other theoretical and experimental sources and a good corelation was observed.

2.7 Conclusion

It is not difficult to reach the following conclusion regarding the state of research in the field of flexibly supported beam-columns and semi-rigidly connected frames:

1. the two dimensional part of this problem is fairly well understood;

2. there is a lack of systematic study on the three dimensional version of this problem.

Therefore, the systematic investigation into the spatial behaviour of flexibly restrained structures forms the theme of the present study.

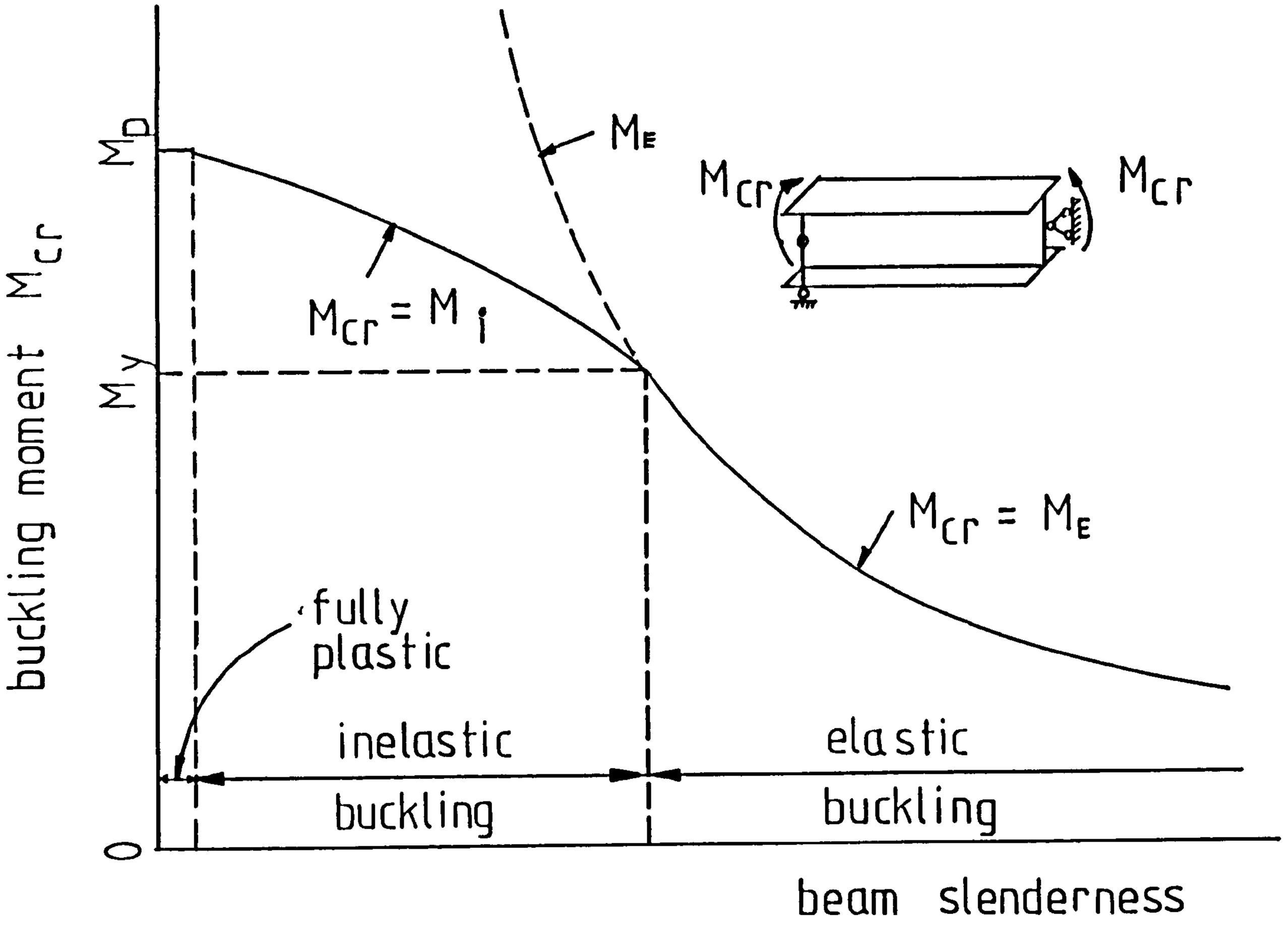

Fig. 2·1 Maximum moment capacity of a beam

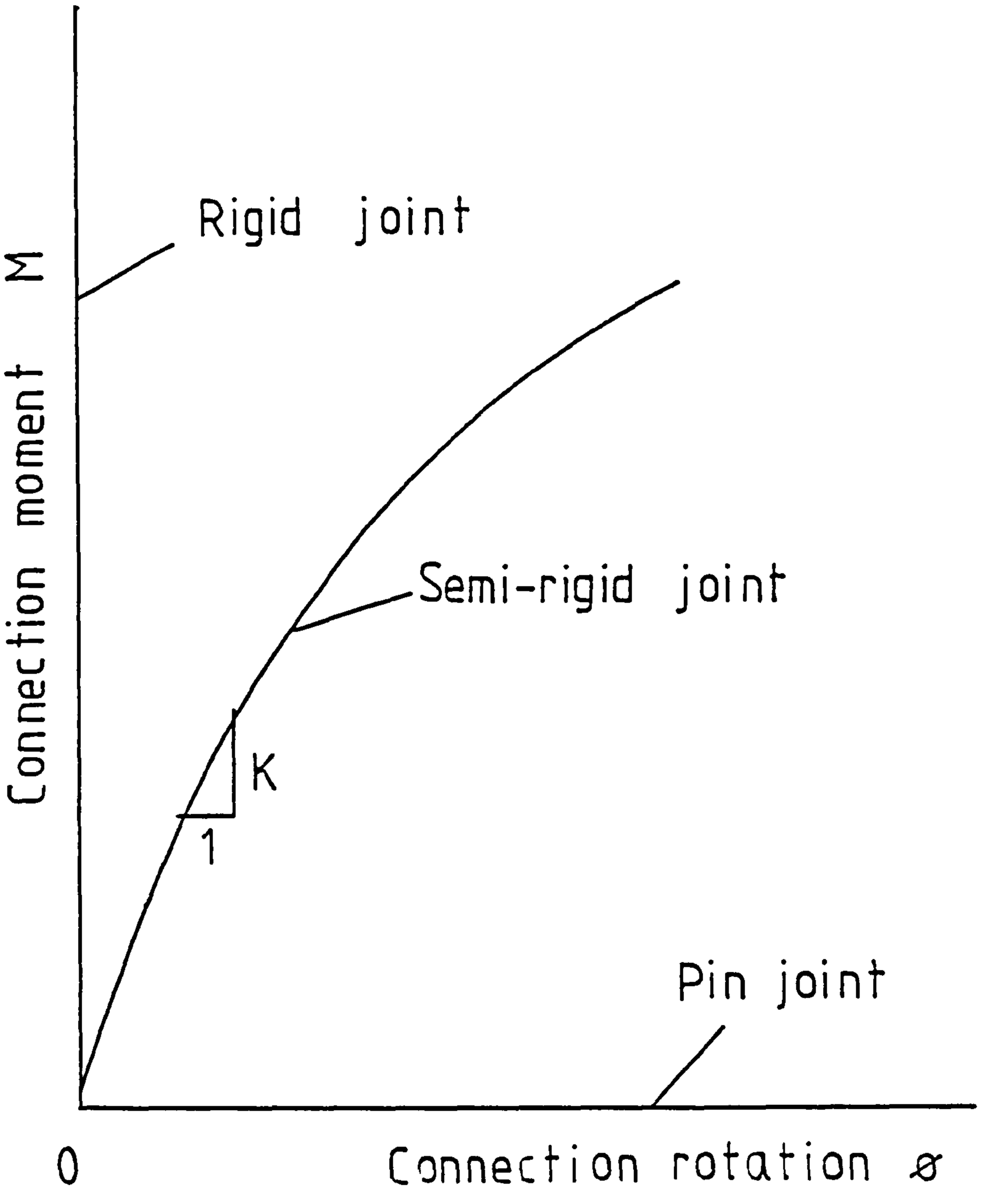

Fig. 2·2 Typical semi-rigid connection moment-rotation curve

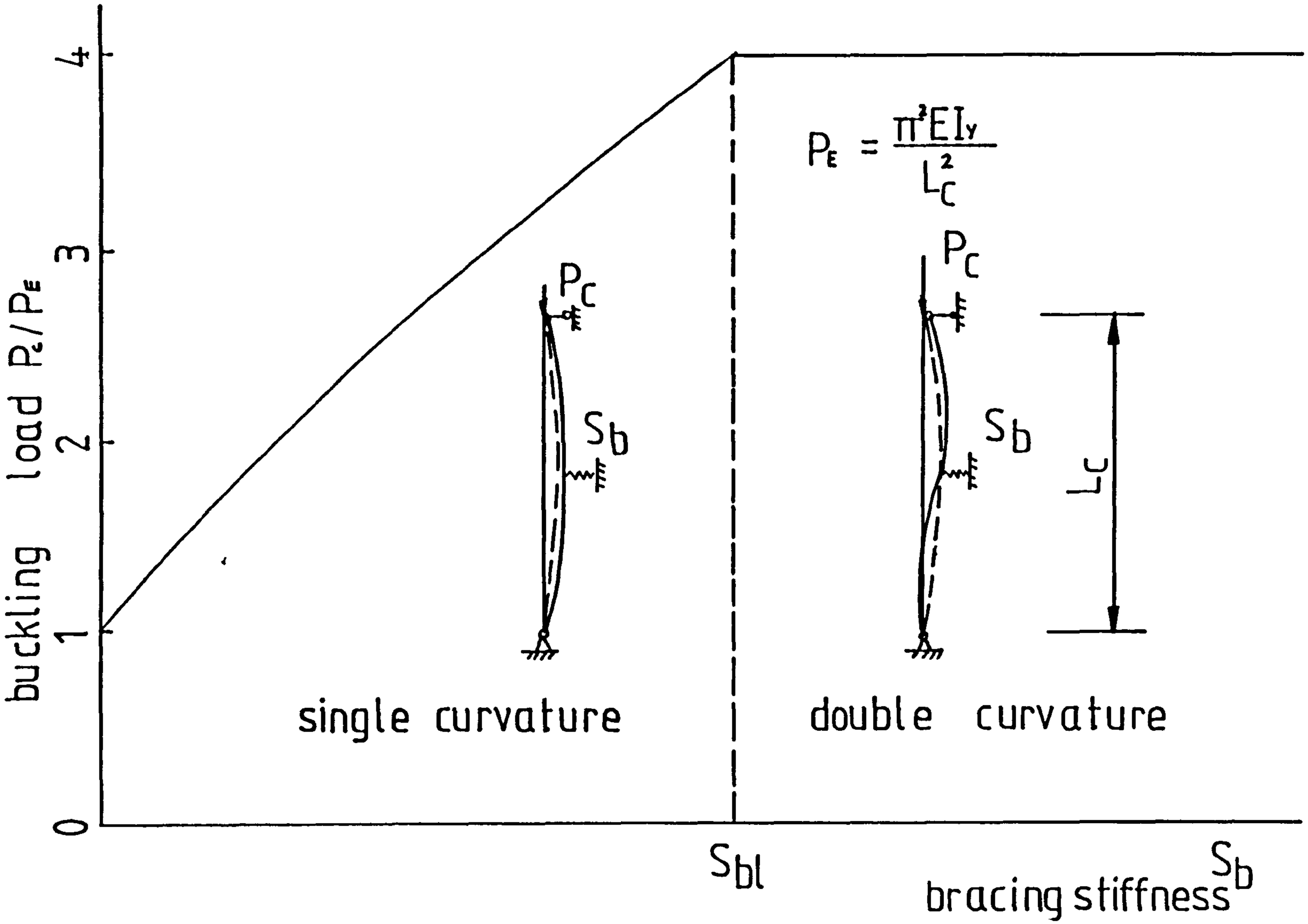

Fig. 2.3 Buckling load-bracing stiffness for centrally braced elastic column

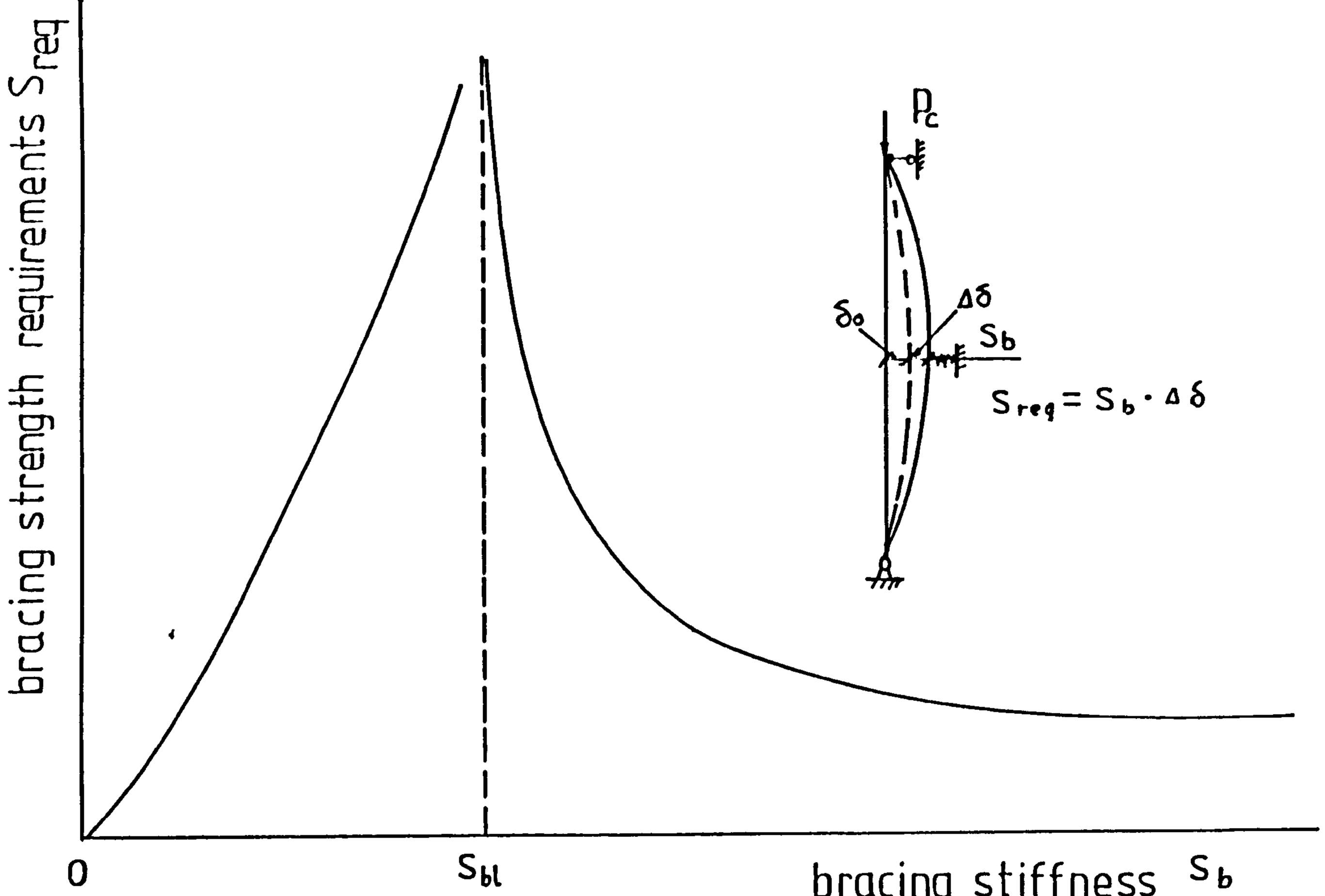

Fig. 2·4 Bracing strength requirement- bracing stiffness relationship for a centrally braced elastic column

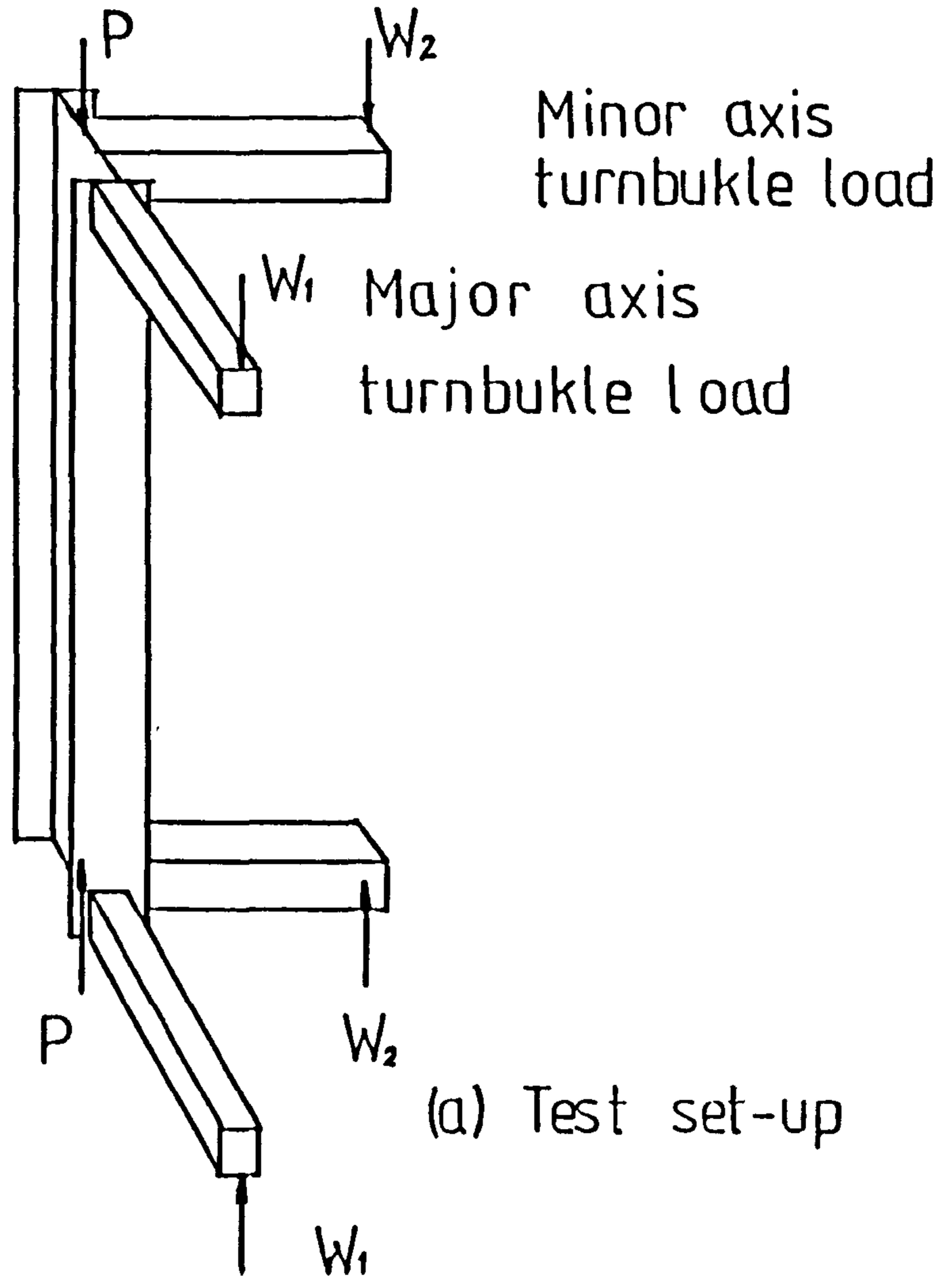

(a) Test set-up

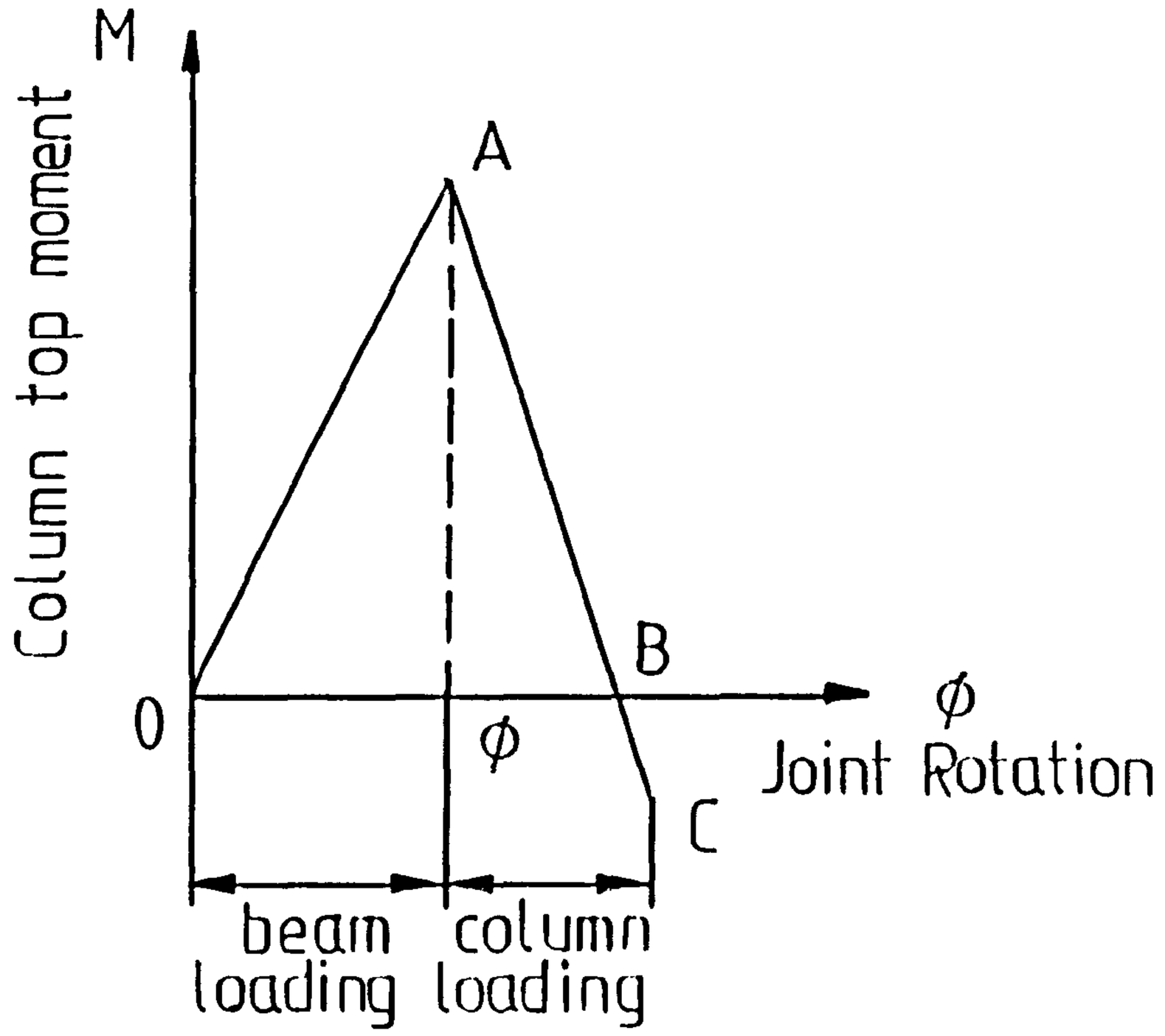

(b) Column top moment-rotation behaviour

Fig. 2·5 Study of Ref. 46

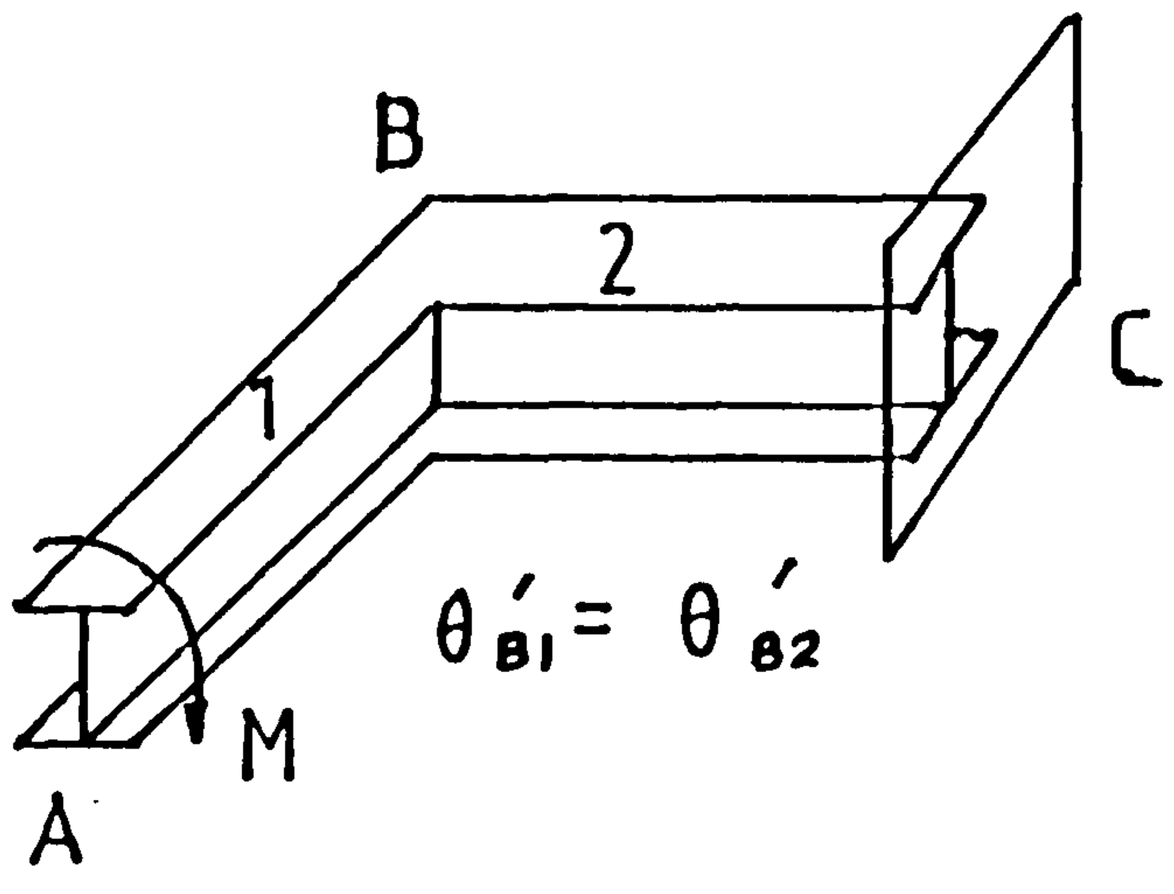

(a) complete equality

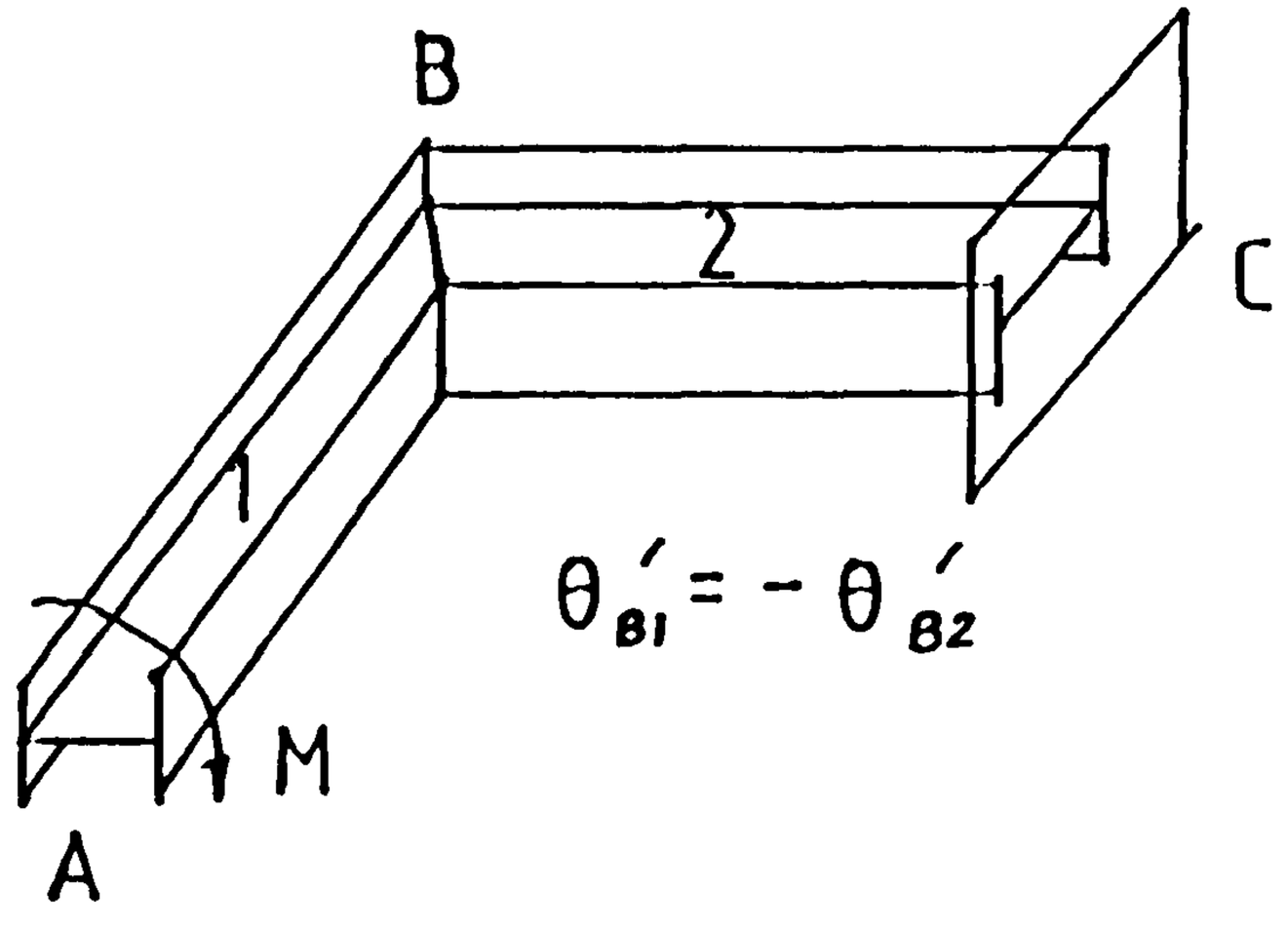

(b) complete reversal

Fig. 2·6 Two cases of complete warping transmission across a joint

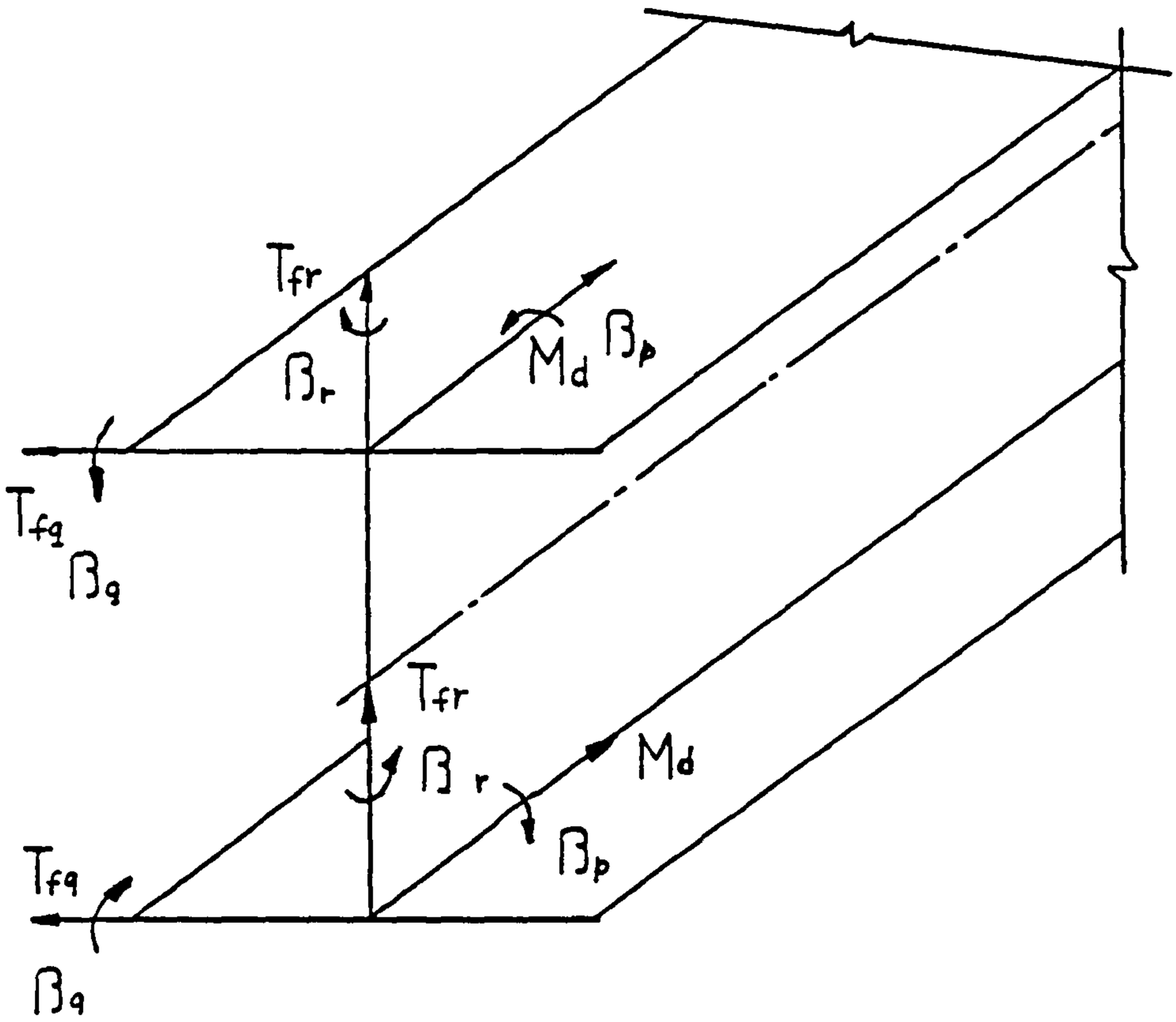

Fig. 2·7 Model adopted in Ref.41
for warping and distortion analysis

Chapter 3

FINITE ELEMENT ANALYSIS OF RESTRAINED BEAM-COLUMNS

3.1 Introduction

The study of the spatial behaviour of thin-walled beam-columns differs from that of solid ones. For the latter, twisting is small and there is no problem of cross-sectional warping, thus the two dimensional analysis may be easily extended to give a reasonably accurate predication for the three dimensional behaviour; whereas for the former, the use of open cross-sections e.g. I-sections because of their ecomony in resisting flexural bending, presents the complexity of interaction between flexural bending, torsion and warping. The conventional hypothesis of plane cross-section after deformation will likely

cause great inaccuracy in the existence of warping. However, Vlasov's[57] assumption concerning the kinematics of the thin-walled cross-sections is more general. This states that the shearing deformation in the mid-surface of the thin-walled plate is extremely small and can be neglected.

Following this assumption and using the finite element method, Rajasekaran[2] derived the stiffness of a beam-column element composed of thin-walled plates. This is used in the present analysis of restrained members. Two types of practical restraint are considered. They are flexible end support conditions which are often associated with beam-column connections and intermediate restraints to reflect the bracing effects from secondary members. The incorporation of flexible connections is performed by adding their tangent stiffnesses to the appropriate diagonal terms in the overall stiffness matrix. The bracing effect is allowed for by including the strain energy contribution from all braces and duly modifying the stiffness matrix of the member.

3.2 The Existing Program

Using the finite element method, Rajasekaran[2] presented the analysis for three-dimensional beam-column members. This is briefly summarised herein.

Referring to Fig. 3.1 for a segment of thin-walled cross-section, starting from Vlasov's assumption[57] the cross-sectional kinematic relationship is obtained. In order to reduce the complexity of the analytical procedure, it is assumed that the axial rotation of twisting θ of a segment is reasonably small so that $\sin\theta = \theta$ and $\cos\theta = 1.0$ when relating the transverse displacements at any point in the cross-section to those at principal axes. The second

order strain-displacement relationship is used to take into account the effect of geometrical changes resulting from deformation on the stability of the structure.

Applying the virtual work principle, a variational form of the incremental equations of equilibrium is obtained. Adopting a cubic displacement function for flexural bending and torsion and a linear function for axial action, the principal axis displacements along the segment are expressed by those at the ends. Applying these displacement functions (shape functions) to the incremental equations of equilibrium and carrying out integration, the externaly applied nodal loads are related to the displacements at the ends of the segment through cross-sectional properties and various stress resultants. The final equation is symbolised as follows:

$$[K_s]\{\dot{U}_E\} + [K_G]\{\dot{U}_E\} = \{\dot{F}_E\} \tag{3.1}$$

where $\{\dot{F}_E\}$ and $\{\dot{U}_E\}$ are increments in applied nodal force and resulting displacement vectors of the segment. $[K_s]$ and $[K_G]$ are flexural and geometrical stiffness matrices of the element. For convenience, these stiffness matrices are quoted in Appendix A1.

As seen in Fig. 3.1, there are 7 degrees of freedom at each node. These are 3 displacements along and 3 rotations about 3 coordinate axes respectively and the rate of axial twisting to account for warping of the thin-walled cross-section.

Two sets of coordinate axes are used for each element as shown in Fig. 3.2. The first ($\xi-\eta-\zeta$) is the instantenous principal axes which changes with the shift of centroid and shear centre due to the spread of material yielding, the second (x-y-z) is fixed on each element and moves merely because of the

element deformation. Before the assembly of stiffness matrices, the element stiffness matrices are transferred from the first set of coordinate axes to the second. The transformation matrix $[T_1]$ is also quoted in Appendix A2.

In the analysis, the geometrical imperfection is treated as an imaginary force vector. For each load increment, the unbalanced force vector after n-1 iterations is:

$$\{E_n\} = \{F_n\} - [K_s]\{u_{n-1}\} - \left[K_{G(n-1)}\right]\{u_{n-1}\} - \left[K_{G(n-1)}\right]\{u\}^* \quad (3.2)$$

in which $\{F_n\}$ is the applied load vector at the current step; $[K_s]$, $\left[K_{G(n-1)}\right]$ and $\{u_{n-1}\}$ are respectively the current flexural stiffness matrix, geometrical stiffness matrix and displacement increment vector at (n-1)th iteration and $\{u\}^*$ is the total displacement vector after n-1 iterations. The initial deflections may be included in $\{u\}^*$.

To take the cross-sectional plastification into consideration, the cross-section is divided into a number of small blocks whose elastic modulus is replaced by the tangential modulus according to the strain of each block. When calculating the stress, the residual stress may be included. Summing the contributionsfor these small areas to cross-sectional properties and stress resultants gives the corresponding values of the whole cross-section.

This approach was applied by El-Khenfas[1] and a computer program was written for it, although later the same author extended this approach to include large twisting and high-order terms in the strain-displacement relationships with the result that a much more sophisticated formulation was derived.

The program written by El-Khenfas based on the derivation by Rajasekaran is used as the starting point for the author's investigation.

3.3 Modification of Overall Stiffness Matrix

In the preceeding section, the stiffness of a beam-column element is obtained. However, the direct application of this formulation is limited. The presence of various forms of restraint will contribute to the potential energy stored in the structure and this change has to be considered consequently; the height of applied transverse loads also affects the stability. Therefore, proper modificationes of the stiffness matrix should be made to reflect these effects. This section attempts to cover this area.

3.3.1 Incorporation of Flexible Boundary Conditions

Most analyses assume extreme supporting conditions, i.e. either hinged or fixed end conditions. Consequently, stiffness values equal to either zero or infinity are introduced for these two extremities for the corresponding degrees of freedom. For members whose ends are flexibly restrained with nonlinear force-deformation characteristics, however, the stiffnesses of the restraint should be evaluated first and the tangential stiffnesses be added to the appropriate degrees of freedom.

Various techniques have been devoted to simulating the non-linear force-deformation relationships of restraints. For beam-columns restrained by moment connections, the strong axis response of the connections have been extensively studied. Jones[7] used the most accurate representation of B-spline curve-fitting technique; Lui and Chen[12] assumed the exponent function. In this investigation, a multi-linear arrangement is used to represent the force-deformation curves for the sake of simplicity. Generally, five or six segments are sufficient to provide a reasonable fit. It is assumed that

a connection loses its stiffness and behaves like a pin joint once the end restraining action exceeds a certain limiting value.

Two ways of incorporating the connection stiffness were tried. One retains the stiffness at the beginning of each load increment throughout the load step provided the increment is small; the other varies the stiffness with the change of the connection end restraint moment. It was observed that the first was more satisfactory than the second. The reason is that some connections e.g. extended end plates, may have sharp changes in their moment-rotation curves as shown in Fig. 3.3b and if their end restraint moments fall within this region, some numerical difficulties may occur. For those connections whose moment- rotation curves are reasonably smooth, both approaches are suitable. The first method has been used in the analysis presented herein.

3.3.2 Incorporation of Lateral Restraints

An I-beam with 7 types of bracing corresponding to the 7 degrees of freedom is shown in figure 3.4. The directional bracings (figure 3.4b) act remote from the shear centre and the centroid, whilst the rotational bracings (fig. 3.4c) are assumed to act through the shear centre merely for simplicity. Offset of these bracings could be accommodated without difficulty as for the case of the directional bracings. Applying the virtual work principle, the strain energy in a brace is expressed in the incremental form as:

$$\delta \dot{W} = \delta \dot{u}_b \dot{f}_b \tag{3.3}$$

where $\dot{f}_b$ and $\dot{u}_b$ are the force and displacement increments respectively in the brace.

$$\dot{f}_b = \dot{K}_b \dot{u}_b \tag{3.4}$$

in which $\dot{K}_b$ is the tangential stiffness of the brace. Therefore:

$$\delta\dot{W} = \delta\dot{u}_b \dot{K}_b \dot{u}_b \tag{3.5}$$

Summing the contributions for all braces at each node:

$$\sum \delta\dot{W} = \delta < \dot{u}_b > \left[\dot{K}_b\right] \{\dot{u}_b\} \tag{3.6}$$

where $\{\dot{u}_b\}$ is the displacement vector for the braces at the node and $\left[\dot{K}_b\right]$ is the diagonal matrix of order 7, each component of which corresponds to the value of the tangential stiffness of the individual brace given in Fig. 3.4. Thus:

$$\begin{aligned}
\dot{K}_{b11} &= S_{tx} \\
\dot{K}_{b22} &= S_{ty} \\
\dot{K}_{b33} &= S_{rz} \\
\dot{K}_{b44} &= S_{tz} \\
\dot{K}_{b55} &= S_{ry} \\
\dot{K}_{b66} &= S_{rx} \\
\dot{K}_{b77} &= S_w
\end{aligned} \tag{3.7}$$

$$\dot{K}_{bij} = 0 \quad otherwise, \ for \ i,j = 1,7$$

Also from this figure, it can be seen that

$$\{\dot{u}_b\} = [T_b]\{\dot{u}\} \tag{3.8}$$

in which $[T_b]$ is the transformation matrix due to the offset of the braces and $\{\dot{u}\}$ is the displacement vector of the node. $[T_b]$ is given in Appendix A3. Therefore:

$$\delta\dot{W} =< \delta\dot{u} > [K_b]\{\dot{u}\} \tag{3.9}$$

where $[K_b]$ is the bracing stiffness matrix given in Appendix A3.

An elastic perfectly plastic representation is assumed for the bracing, although any non-linear relationship may be employed between the bracing force and the bracing displacement. As stated previously for end connections, the bracing stiffness at the beginning of each load increment is kept unchanged throughout the load step to avoid computational inaccuracy.

3.3.3 Inclusion of Loading Height

Taking an I-beam as an example, the transverse load is often acting on the upper flange of the beam as shown in Fig. 3.5a. The offset of the applied load from the shear centre will affect the stability of the structure. As seen in Fig. 3.5b, assuming that the cross-section has undergone an axial twisting θ under the action of the applied load F and that increasing this load by a small amount of $\dot{F}$ will result in a small increment $\dot{\theta}$, there will be extra torques $(F+\dot{F})H_{load}(\theta+\dot{\theta})$ and $FH_{load}\theta$ for these adjoining configurations respectively.

The virtual work done by these torques is equivalent to the loss of the potential energy of the same amount in the member's strain energy and the increment of this energy loss is the virtual work difference between these two configurations i.e.

$$\delta\dot{U}_{L.H.} = -\delta\dot{W}_{L.H.} \tag{3.10}$$

and

$$\begin{aligned}\delta\dot{W}_{L.H.} &= -\left((F+\dot{F})H_{load}(\theta+\dot{\theta})\delta\dot{\theta} - FH_{load}\theta\delta\dot{\theta}\right) \\ &= -\left((F+\dot{F})H_{load}\dot{\theta}\delta\dot{\theta} + \dot{F}H_{load}\theta\delta\dot{\theta}\right) \qquad (3.11)\end{aligned}$$

whence:

$$\delta\dot{U}_{L.H.} = \delta\dot{\theta}(F+\dot{F})H_{load}\dot{\theta} + \dot{F}H_{load}\theta\delta\dot{\theta} \qquad (3.12)$$

Assuming small load increment i.e. lim $\dot{F}$ =0,

$$\delta\dot{U}_{L.H.} = \delta\dot{\theta}FH_{load}\dot{\theta} \qquad (3.13)$$

Equation 3.13 is equivalent to increasing the diagonal stiffness corresponding to the axial twisting by an amount of FH_{load} at the start of each loading step. From sign conventions, if a downward force is applied at the upper flange of the beam, F is negative while H_{load} is positive. Therefore, the product of FH_{load} is negative, which implies that the stability of the member is reduced. The effects of other arrangements of applied load and its position agree with theoretical observations.

3.4 Inclusion of Imperfections

The aforementioned sections present the theoretical analogy for a straight member. However, a member always possesses some residual stresses due to welding and initial deflections from fabrication and erection etc. Before embarking on the analysis of the member, the effects of imperfections should be considered.

3.4.1 Inclusion of Residual Stresses

As mentioned in section 2, the residual stress can be incorporated into the analysis when calculating the stress resultants of the cross-section. This method is adopted in the present study. Although only two types of commonly used residual stress distribution are included in this study, other types can be incorporated without involving much difficulty. These two types are:

1. Linear distribution as shown in Fig. 3.6a;

2. Parabolic distribution as shown in Fig. 3.6b.

Since residual stress is self-equilibrating, it has to be ensured that no non-zero stress resultant results from any form of distribution.

3.4.2 Inclusion of Initial Deflections

In the analysis by Rajasekaran[2], the initial deflection is converted to a set of imaginary forces as explained in section 2.

In this investigation, an additional set of coordinate axes (X-Y-Z) is used, which is fixed in space and used as the reference point for all elements. The geometrical nonlinearity is allowed for by a transformation matrix from the element coordinate system to the fixed member coordinate axes. For each element,

$$\begin{aligned} \{\dot{d}_{local}\} &= [T]\{\dot{d}_{globe}\} \\ [K]_{globe} &= [T]^T [K_{local}][T] \end{aligned} \tag{3.14}$$

and

$$[T] = \begin{bmatrix} [T_2] & [0] \\ [0] & [T_2] \end{bmatrix} \tag{3.15}$$

in which $[T_2]$ is the transformation matrix merely resulting from element displacements. It is given in Appendix A2. In constructing $[T_2]$, the initial deflections can be included. In the present study, a half sine wave is normally assumed. However, the initial deflections may be directly input for each node.

Once all stiffness matrices are transferred from element coordinate axes to the fixed member coordinate axes, they are assembled to form the member stiffness matrix.

3.4.3 Inclusion of Load Eccentricities

The eccentricities of the axial load may be converted to appropriate flexural bending moments. The offsets of transerve loads from the shear centre may be treated as equivalent torques.

3.5 Solution Technique

The resulting equation can be expressed as:

$$\{\dot{F}\} = [K]\{\dot{d}\} \tag{3.16}$$

where $\{\dot{F}\}$ and $\{\dot{d}\}$ are respectively the incremental load and resulting deformation vectors and $[K]$ is the overall stiffness matrix at the current configuration. Due to the nature of the problem considered herein, this equation is nonlinear so that an iterative approach is necessary. This is carried out using the Newton-Raphson technique. This procedure involves the evaluation of unbalanced forces.

3.5.1 Unbalanced Force

One approach for calculating the unbalanced forces is to evaluate stress resultants immediately after updating the strain and thus the stress distribution across the cross-sections at all nodes and then find out the resulting force vector at these nodes, which is the internal force vector. The difference between the applied load vector and this internal force vector is the required unbalanced force vector. Although theoretically sound, this method suffers the following disadvantages when it is implemented:

1. The non-continuity between discreted members due to deformation and material yielding may result in unbalanced forces even if the structure is in equilibrium because of computing inaccuracy. This may influence the convegence of the program or even lead to divergence;

2. Due to the different units of various force components, it would be difficult to impose a non-unit convergence factor for these unbalanced forces.

Nevertheless, the stiffness matrix is not very sensitive to small variations in stress resultants or slight alternation of the member's position after deformation. Therefore, the following approach is used in the present investigation to reduce the computational round-off error:

Fig. 3.7 describes the one-dimensional load-deflection characteristics. Assuming at one equilibrium stage, $\{\Delta d^0\}$ results under the action of $\{\Delta F^0\}$ from equation 3.16 , the internal force vector is

$$\{\Delta F_{internal}\} = \left([\alpha][K] + [1-\alpha]\left[K^{+1}\right]\right) \times \{\Delta d^0\} \tag{3.17}$$

in which $[K]$ is the stiffness matrix at the start of the iteration and $[K^{+1}]$ is that immediately after updating the deformation $\{\Delta d^0\}$ and $0 < \alpha_{i,j} < 1$. Hence, the unbalanced force vector is

$$\begin{aligned}
\{\Delta F_{unbalanced}\} &= \{\Delta F^0\} - \left([\alpha] \times [K] + [1-\alpha] \times \left[K^{+1}\right]\right) \times \{\Delta d^0\} \\
&= [\alpha] \times \left(\{\Delta F^0\} - [K] \times \{\Delta d^0\}\right) \\
&+ [1-\alpha] \times \left(\{\Delta F^0\} - \left[K^{+1}\right] \times \{\Delta d^0\}\right) \\
&= [1-\alpha] \left(\{\Delta F^0\} - \left[K^{+1}\right] \times \{\Delta d^0\}\right) \qquad (3.18)
\end{aligned}$$

Applying a small load increment, different values of $\alpha_{i,j}$ would have little effect on the reponse of the structure. Furthermore, it would be very difficult or even impossible to select an appropriate value of $\alpha_{i,j}$. Therefore, $\alpha_{i,j} = 0.5$ is randomly chosen. Therefore:

$$\{\Delta F_{unbalanced}\} = 0.5 \times \left(\{\Delta F^0\} - \left[K^{+1}\right] \times \{\Delta d^0\}\right) \qquad (3.19)$$

The next interation will be to solve the equation

$$\{\Delta F_{unbalanced}\} = \left[K^{+1}\right] \{\Delta d^1\} \qquad (3.20)$$

This process is continued until the pre-specified convergence criteria are reached. The total deformation vector Δd for the total nodal force increment ΔF is the sum of the deformation increments until convergence.

$$\{\Delta d\} = \{\Delta d^0\} + \{\Delta d^1\} + \ldots + \{\Delta d^n\} \qquad (3.21)$$

3.5.2 Convergence Criteria

Both load and displacement vectors are checked within each load increment. The convergence is thought to be reached only if both force and displacement convergence criteria are satisfied i.e.

$$\frac{\sqrt{< \Delta F_{unbalanced} > \{\Delta F_{unbalanced}\}}}{\sqrt{< \Delta F > \{\Delta F\}}} < \delta_{load} \tag{3.22}$$

and

$$\frac{\sqrt{< \Delta d^n > \{\Delta d^n\}}}{\sqrt{< \Delta d > \{\Delta d\}}} < \delta_{disp.} \tag{3.23}$$

where δ_{load} and $\delta_{disp.}$ are pre-specified small values of convergence factor for applied load and resulting displacement respectively. In the present analysis,

$$\delta_{load} = \delta_{disp.} = 0.01 \tag{3.24}$$

3.6 The Computer Program

The preceeding sections present the methods for including the effects of various restraints and various imperfections. The original program mentioned in section 2 is then modified to incorporate these effects.

Since the purpose of the program is to trace the nonlinear load-displacement response and ultimate load of a laterally restrained beam-column, the step-by-step iterative incremental approach is necessary. If the structure fails at a load level, the program restarts at the previous step with a load increment equal to one tenth of the latest one. The failure load is thought to be achieved if the load increment is smaller than the pre-specified value. The last stable load is regarded as the ultimate load of the structure. Once this value is obtained, the externally applied loads, the resulting nodal displacements and bracing reactions recorded at each step are printed out before the program is terminated.

Fig. 3.8 gives the flow chart of the program.

The modified program possesses the following main features:

1. Incorporating the effects of any types of practical restraints;

2. Tracing the load-deflection curve of a beam-column until failure;

3. Inclusion of major imperfections e.g. residual stress, initial deflections and load eccentricities.

3.7 Verification of the Computer Program

Before conducting any systematic study into the effects of various restraints on the behaviour and load-carrying capacity of beam-columns, comparison with existing analytical and experimental studies are made to check the accuracy of the program.

3.7.1 End Restrained Beam-Columns

Table 3.1 presents comparison with a selection of Trahair's[20] analytical results for elastic buckling problems with linear elastic end restraints. It was found that in no case was the difference between the two approaches more than 2 percent.

To study the effects of different connection restraints on the lateral buckling of I-beams, Hechtmann et al[18] tested a series of beams supported by web cleats and top and seat cleats. The cross-section was 10LB15 and the beam geometrical slenderness ranged from 110 to 441. A selection of the author's results are compared with Hechtmann's[18] tests in tables 3.2, 3.3 and Fig. 3.9. In both cases four results have been obtained for each test beam: a pair assuming simply supported end conditions in the vertical plane and a pair allowing for end restraint against in-plane bending. Davison[15]

used the similar connection arrangements, therefore, when conducting the comparison, his test results were used for the in-plane moment-rotation relationship. For the out-of-plane end conditions, twisting has been assumed to be prevented, no restraint to be present against lateral bending and either freedom to warp or prevention of warping was adopted.

In all 8 cases, the analysis based on simple supports and no warping restraint underestimates the test results; this was expected. Fig. 3.9 compares the test results and the pair of analytical results which include the in-plane restraint. In these figures, the ultimate load is nondimensionised by dividing it by P_p, which is the load required for a simply supported beam to reach its cross-sectional plastic moment capacity within the central segment.

$$P_p = \frac{4Mp}{L} \tag{3.25}$$

in which L is the length of the beam.

Fig. 3.9a clearly shows that for beams restrained by flange cleats, which effectively restrain the warping of their flanges, the inclusion of full warping restraint gives close agreement with the test results. On the other hand, for web cleats, which provide a much lower degree of out-of-plane and warping restraints, the test results are embraced by the analytical results as seen in Fig. 3.9b. Clearly without proper data on connection out-of-plane restraint characteristics, especially the warping restraint rigidity, it is not possible to model the tests precisely. It was also necessary to make assumptions in the analyses regarding the initial lack of straightness in the beams (a bow of L/1000 was used) and the pattern of residual stress present (a Lehigh-type distribution with a maximum compressive stress at the flange tips of 30 percent of yield was used). Thus really close agreement between the

analysis and the test results can hardly be expected. As an indication of the sensitivity of the results to 'reasonable variations' in the exact characteristics of the connection, the $M-\phi$ curve for each connection type has been displaced horizontally by 10 percent i.e. stiffness increased or decreased, and new sets of results obtained. The effect on the buckling load was no more than 2 percent in any case, thus suggesting that great precision in modelling in-plane restraint is not necessary.

3.7.2 Braced Beam-Columns

The approximate equation for the buckling load of a perfect column braced at the mid-span is given in Ref.[31] as:

$$\begin{aligned} P_c &= \frac{\pi^2 EI_y}{L^2} + \frac{3}{16} S_b L \quad for\ 0 < S_b < S_{bl} \\ P_c &= \frac{4\pi^2 EI_y}{L^2} \qquad\qquad for\ S_{bl} < S_b \end{aligned} \tag{3.26}$$

where S_b is the bracing stiffness and S_{bl} is the value for complete bracing given by

$$S_{bl} = \frac{16\pi^2 EI_y}{L^3} \tag{3.27}$$

Fig. 3.10 shows the author's results to be in general agreement with Eqs 3.26.

A series of I-beams braced either by purlins or by sub-beams has been tested by Wakabayashi and Nakamura[44]. In their analysis the purlins were modelled as torsional braces with a moment-rotation curve of the type given in Fig. 3.11a. The sub-beam was assumed to be an elastic rotational spring located at the shear centre with a moment-rotation relationship as given in Fig. 3.11b. Different moment gradients in the main beam were produced by a pair of side beams. Test values of ultimate strengths for all specimens

and load-deflection relationships for two specimens were reported and the author's analytical results have been checked against these. Table 3.4 provides the comparison for the ultimate strengths in the form of the ratio of the applied maximum moment to the plastic moment capacity of the cross-section, whilst Figs. 3.12 and 3.13 give the comparison of the load-deflection behaviour. The correlation is regarded as reasonable.

In Ref.[44] mention was made of a comparison between the test values and the authors' own analysis, although the actual ultimate load values from the analysis by Wakabayashi and Nakamura were not quoted. However, the authors did refer to some discrepancies between the theory and experiment, attributing these to the inaccuracy of the modelling of the bracing characteristics. For the present analysis, the results are generally lower than the test points; the neglect of strain hardening, particularly in cases where a large fraction of the cross-section's plastic moment capacity was reached, is thought to have had some influence here.

Eleven full-scale beams, either unbraced or with partial bracing, have been tested and analysed by Wong-Chung and Kitipornchai[45]. The comparison between their ultimate strengths and those calculated by the author is given in Table 3.5. Agreement is generally good, particularly when it is appreciated that only the mean values of yield stress and Young's modulus were provided and the initial deflection and the residual stress assumed herein are likely to be different from those reported in Ref.[45].

The above comparison are felt to provide sufficient evidence that the author's analysis is capable of accurately modelling the behaviour thus predicting the ultimate load of laterally restrained beam-columns.

3.8 Conclusion

Starting from the analytical procedure derived by Rajasekaran[2] for the spatial response of general beam-columns, the methods of including the effects of flexible end supports and intermediate bracings as well as various types of imperfections are presented. The original program is modified and the new program is then compared with other studies. From these comparisons, it is confirmed that the new program can be relied on for producing satisfactory results for the present investigation.

Table 3.1

Comparison with Ref. 20 for buckling loads

Restraint condition	Boundary conditions				Rigid		Semi-rigid		Pinned	
	β_1	β_2	β_3	K_W	Ref.20	Author's	Ref.20	Author's	Ref.20	Author's
(Major)	0.715	0	∞	0	399.8	394.0	287.5	284.5	158.4	157.0
i(b)	0.715	0	∞	∞	554.6	543.1	381.2	379.7	221.9	218.1
(Minor)	0	0.873	∞	0	789.1	784.2	565.9	549.6	358.6	356.1
iii(b)	0	0.873	∞	∞	940.3	931.5	839.7	829.6	530.6	522.0
(Torsion)	0	0	0.05	0	172.6	171.2	158.2	157.2	129.9	129.6
i(b)	0	0	0.05	∞	233.7	229.6	200.7	199.7	154.0	150.6

1. β_3 =0.2 is assumed as providing no torsional restraint; β_1, β_2 and β_3 have the same meaing as in Ref. 20; K_W is the value for end warping stiffness.

2. Values are in kN and kNm in the case of concentrated load and end moment respectively.

3. Bracketed in column 1 is the axis about which the restraint is provided; the unbracketed is the loading case referred in Ref. 20.

Table 3.2

Analytical results for laterally unsupported beams -Comparison with tests of Ref. 18 for web cleat connection

Beam No.	$\frac{L}{r_y}$	Maximum load (kN) test	Simply Supported E.W.F.	Simply Supported E.W.P.	with End Restraints E.W.F.	with End Restraints E.W.P.
47	110	181.1	121.8	193.0	136.0	211.6
49	147	104.5	62.8	99.6	72.6	113.6
51	221	49.0	28.6	46.4	35.0	55.1
53	294	28.5	17.1	26.3	22.3	32.5

E.W.F. stands for End Warping Free

E.W.P. stands for End Warping Prevented

Table 3.3

Analytical results for laterally unsupported beams -Comparison with tests of Ref. 18 for flange cleat connection

Beam No.	$\frac{L}{r_y}$	Maximum load (kN) test	Simply supported E.W.F.	Simply supported E.W.P.	with End Restraints E.W.F.	with End Restraints E.W.P.
37	110	207.5	124.0	194.0	156.0	237.2
39	147	155.5	68.8	114.0	90.0	145.4
41	221	65.4	28.6	48.2	42.4	67.8
43	294	40.5	16.5	25.5	33.8	39.5

E.W.F. stands for End Warping Free

E.W.F. stands for End Warping Prevented

Table 3.4 Comparison of author's results with tests of Ref. 44 - ultimate loads

Type of major axis moment diagram	Type of bracing	Length (m)	Slender-ness	M_u/M_p		percentage difference
				Ref. 44	Present Analysis	
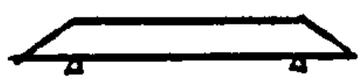	Unbraced	5.0	459	0.35	0.33	-6.0
		2.5	229	0.59	0.573	-4.4
	Unbraced	6.5	596	0.45	0.42	-7.0
		5.0	459	0.58	0.53	-8.4
		3.5	321	0.80	0.80	0.0
	Unbraced	6.5	596	0.60	0.54	-10.0
		3.5	321	0.86	0.82	-5.2
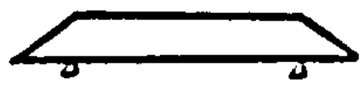	Purlins	5.0	459	0.63	0.63	0.0
		2.5	229	0.84	0.83	-1.3
	Purlins	5.0	459	0.92	0.88	-4.4
		3.5	321	1.08	0.90	-17.0
	Purlins	6.5	596	0.99	0.89	-10.0
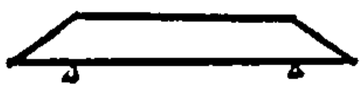	Sub-beam	5.0	459	0.52	0.49	-6.0
		2.5	229	0.90	0.83	-7.5
	Sub-beam	6.5	596	0.60	0.56	-6.3
		3.5	321	0.90	0.88	-2.3

Table 3.5 Comparison of author's results with tests of Ref. 45 - ultimate loads

Beam No.	Bracing Type	Test result Ref. 45 $\frac{M}{M_p}$	Analytical result,Ref. 45 $\frac{M}{M_p}$	Author's analysis $\frac{M}{M_p}$	Percentage difference - Author's analysis & tests
1	Unbraced	0.788	0.782	0.783	-0.7
2	Bottom flange	0.808	0.794	0.794	-1.7
3	Shear centre	0.886	0.906	0.880	-0.7
4	Torsional	0.858	0.906	0.882	+2.8
5	Unbraced	0.866	0.869	0.863	-0.3
6	Bottom flange	0.826	0.885	0.867	+5.0
7	Shear centre	0.922	0.933	0.937	+1.6
8	Torsional	0.962	0.923	0.950	-1.3
9	Unbraced	0.904	0.926	0.897	-0.8
10	Bottom flange	0.917	0.933	0.897	-2.2
11	Shear centre	1.004	1.000	0.950	-5.0

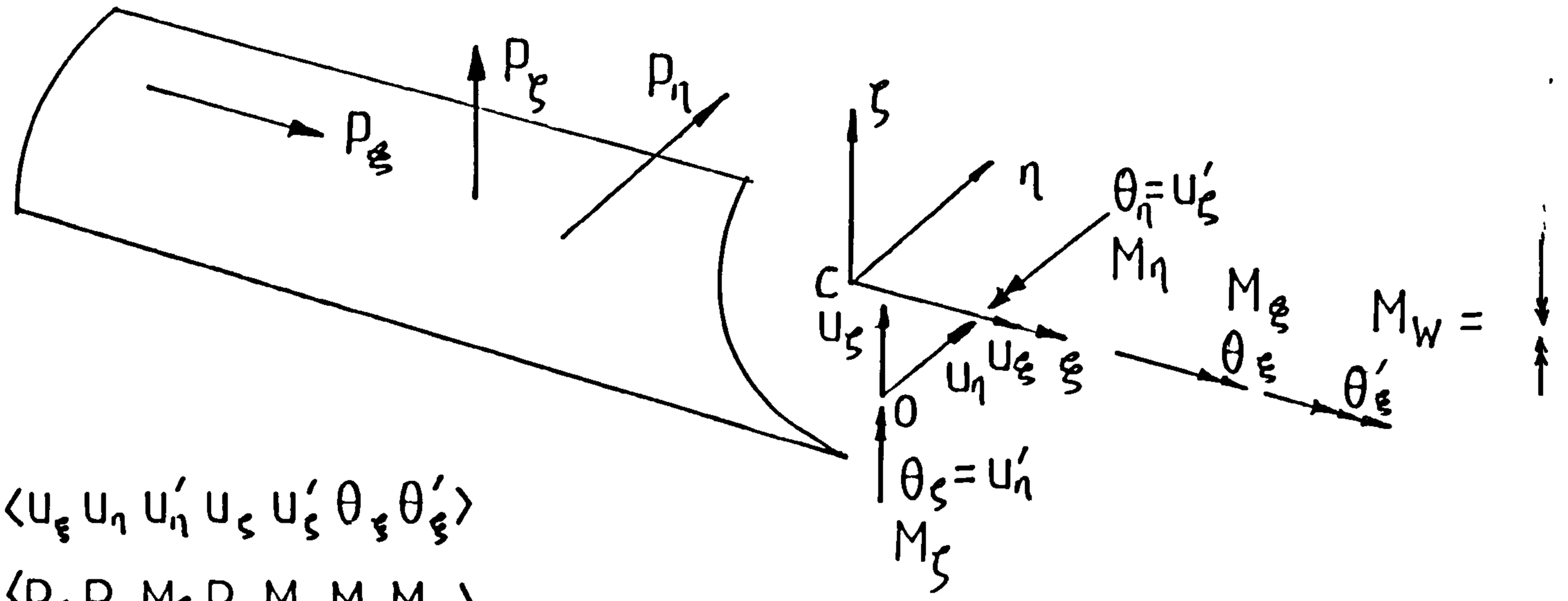

$\langle u_E \rangle = \langle u_\xi\ u_\eta\ u'_\eta\ u_\zeta\ u'_\zeta\ \theta_\xi\ \theta'_\xi \rangle$

$\langle F_E \rangle = \langle P_\xi\ P_\eta\ M_\zeta\ P_\zeta\ M_\eta\ M_\xi\ M_W \rangle$

Fig. 3·1 Positive directions for applied loads and resulting displacements at a node

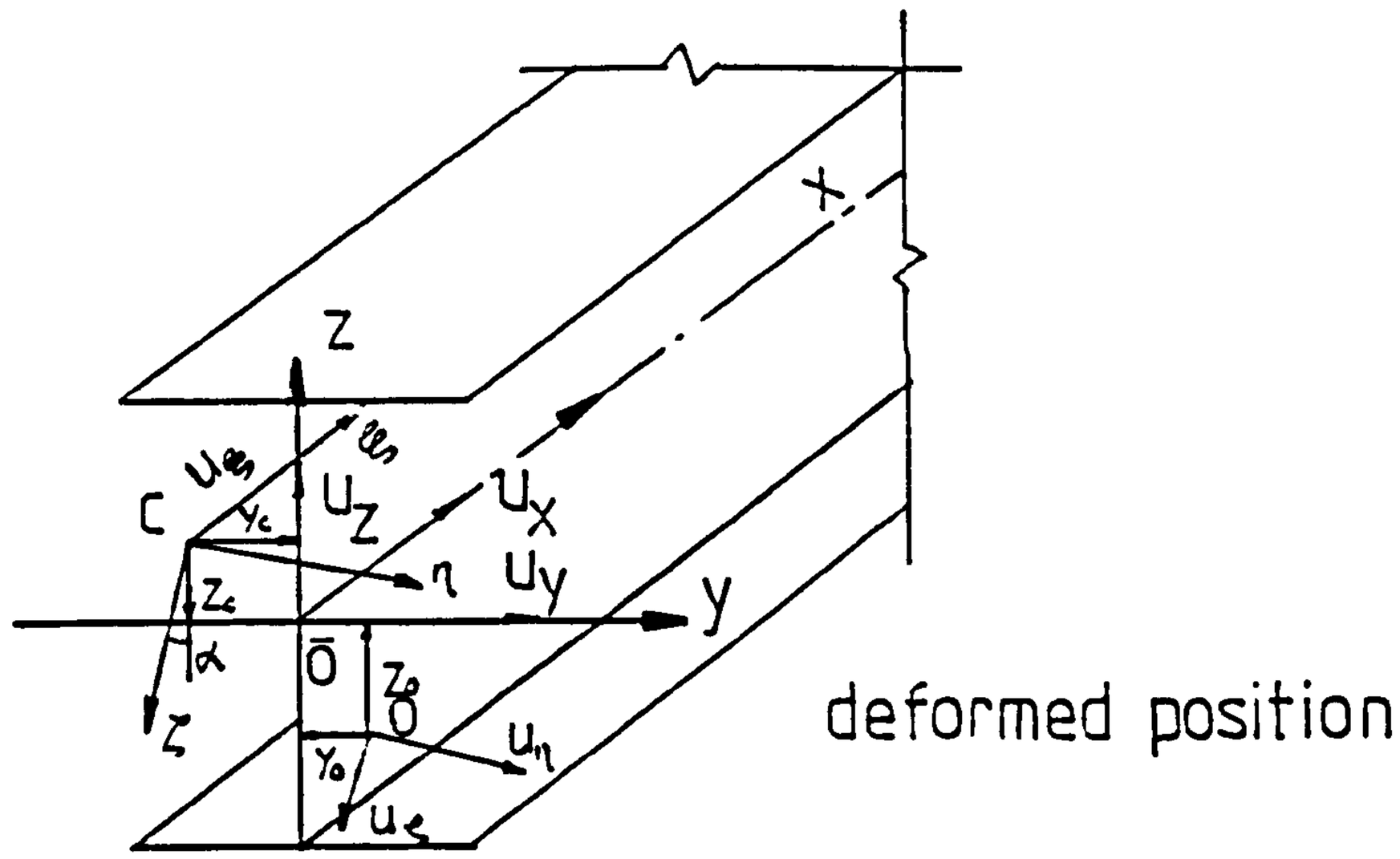

deformed position

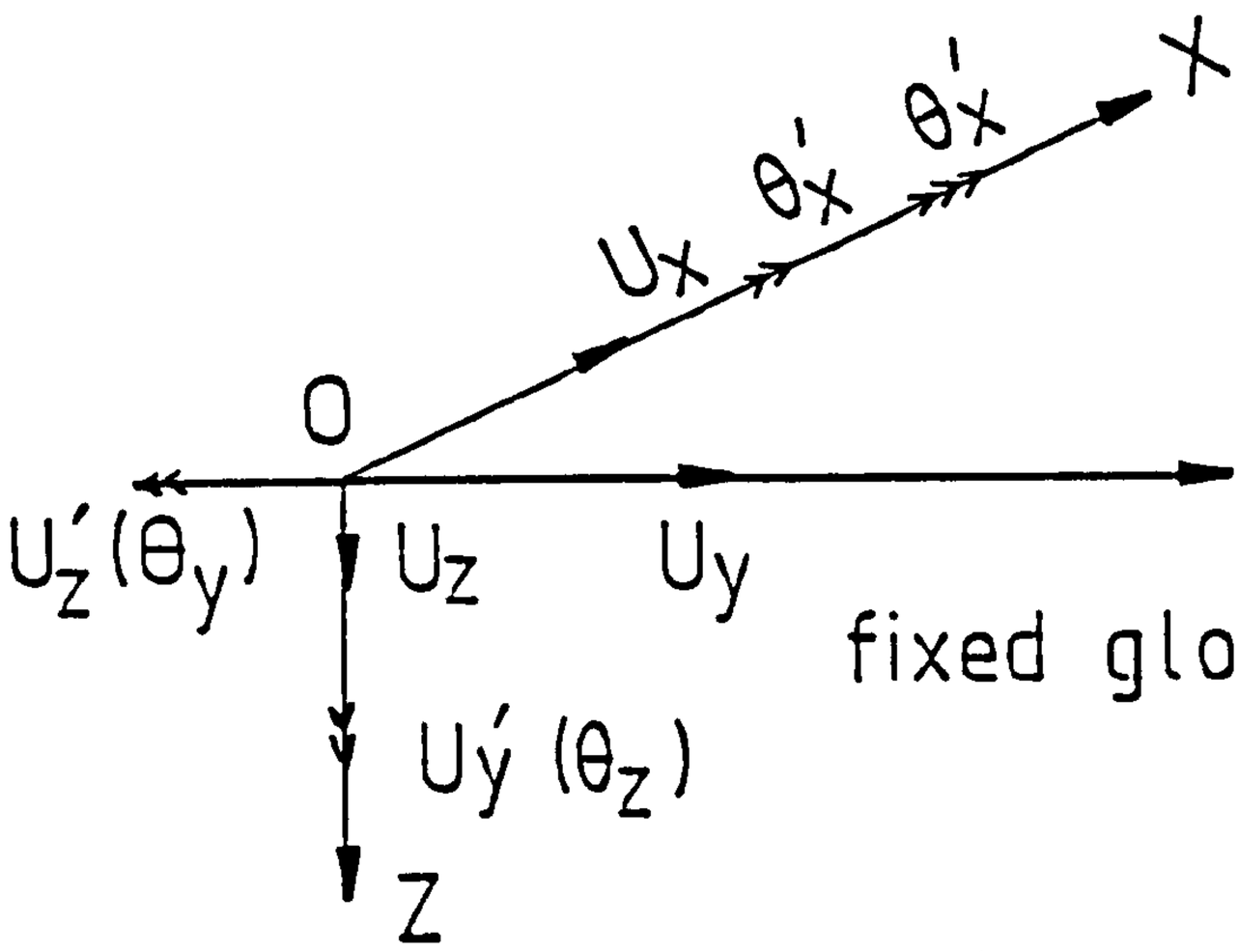

fixed global axes

$$\langle U_E \rangle = \langle U_\xi \; U_\eta \; U'_\eta \; U_\zeta \; U'_\zeta \; \theta_\xi \; \theta'_\xi \rangle$$

$$\langle U_{\bar{o}} \rangle = \langle U_X \; U_y \; U'_y \; U_Z \; U'_Z \; \theta_X \; \theta'_X \rangle$$

$$\langle U_o \rangle = \langle U_X \; U_Y \; U'_Y \; U_Z \; U'_Z \; \theta_X \; \theta'_X \rangle$$

Fig. 3·2 Definition of coordinate axes and degrees of freedom

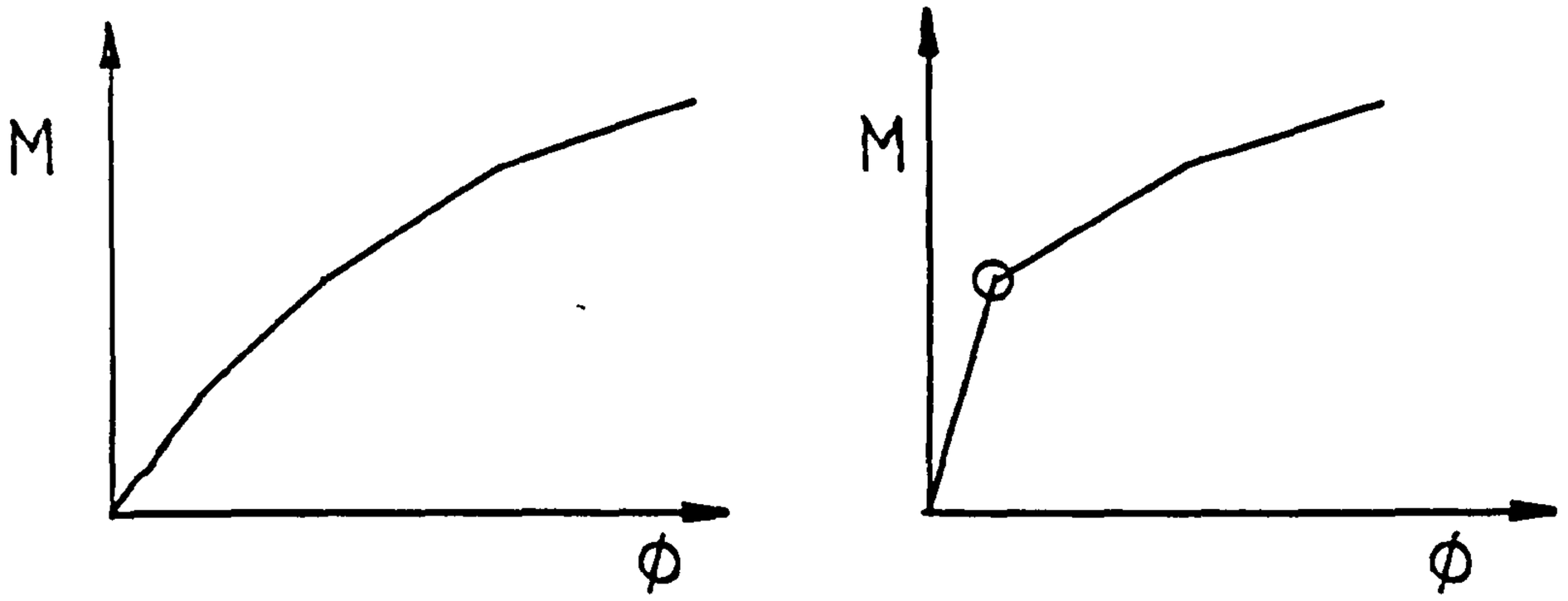

(a) Smooth curve (b) with sharp change

Fig. 3·3 Two types of M-ϕ curve

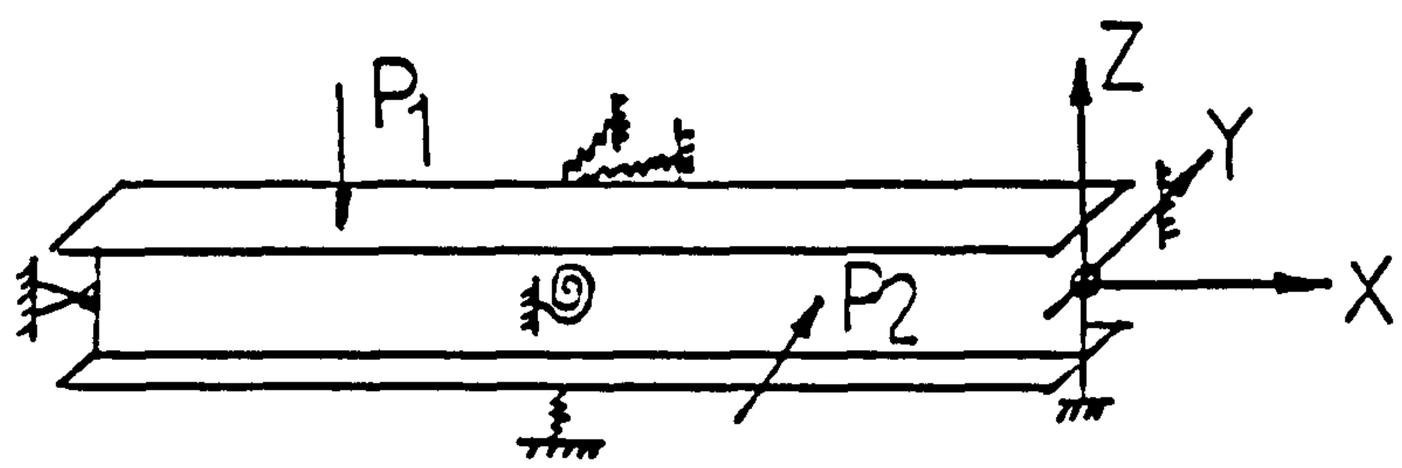

(a) General view of a braced beam

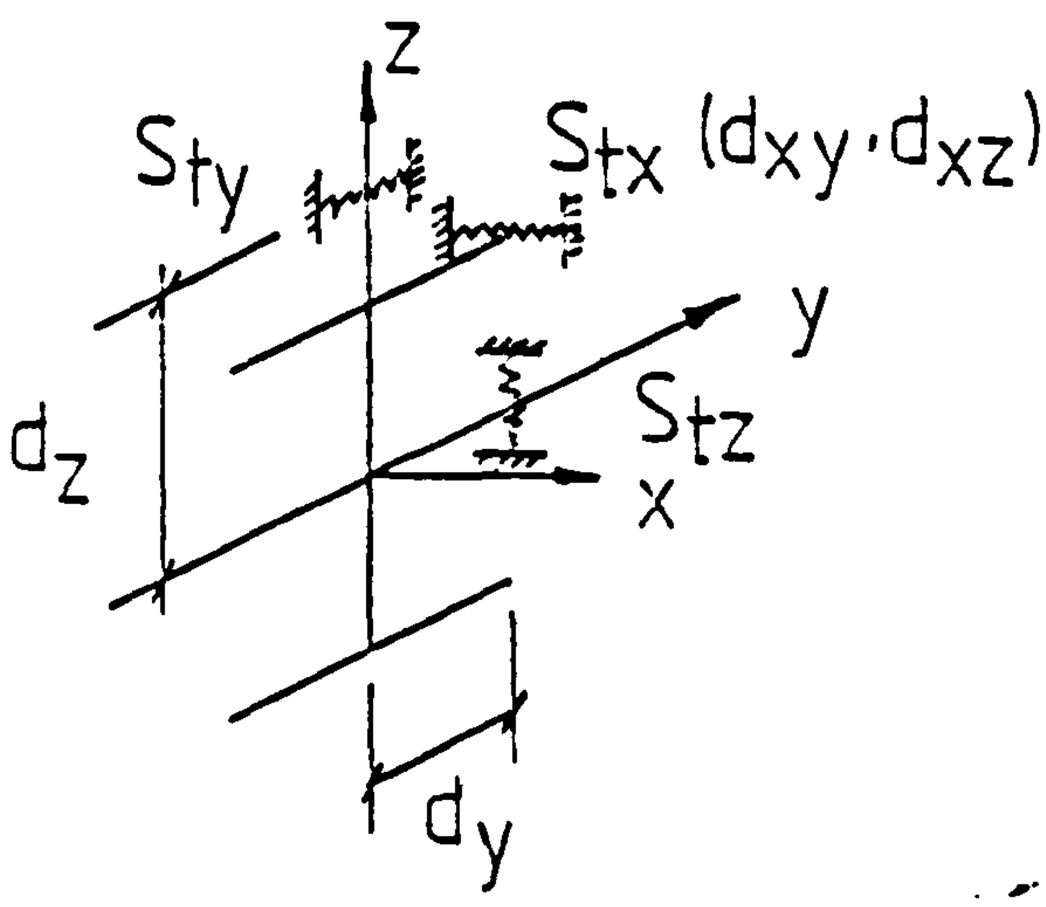

(b) Translational braces

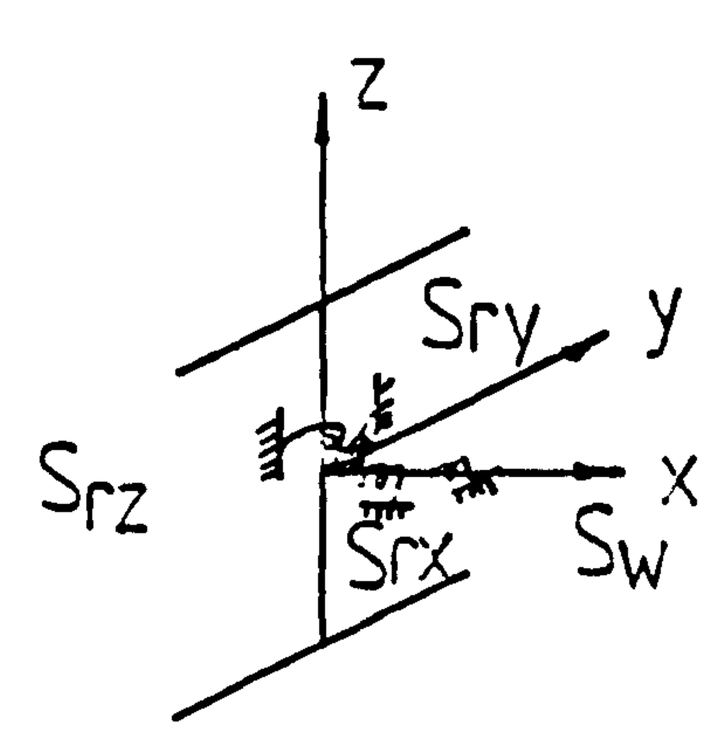

(c) Rotational braces

Fig. 3·4 Problem under consideration

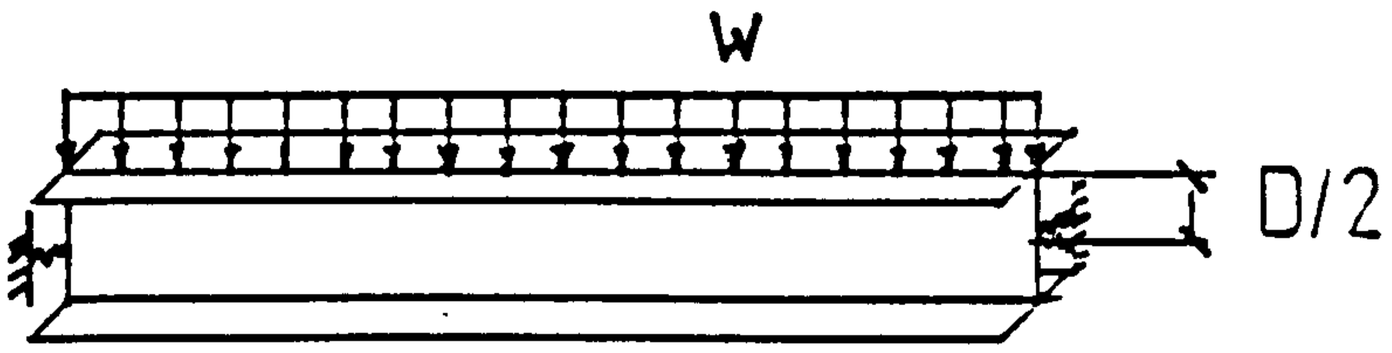

Fig. 35a An I-beam under load

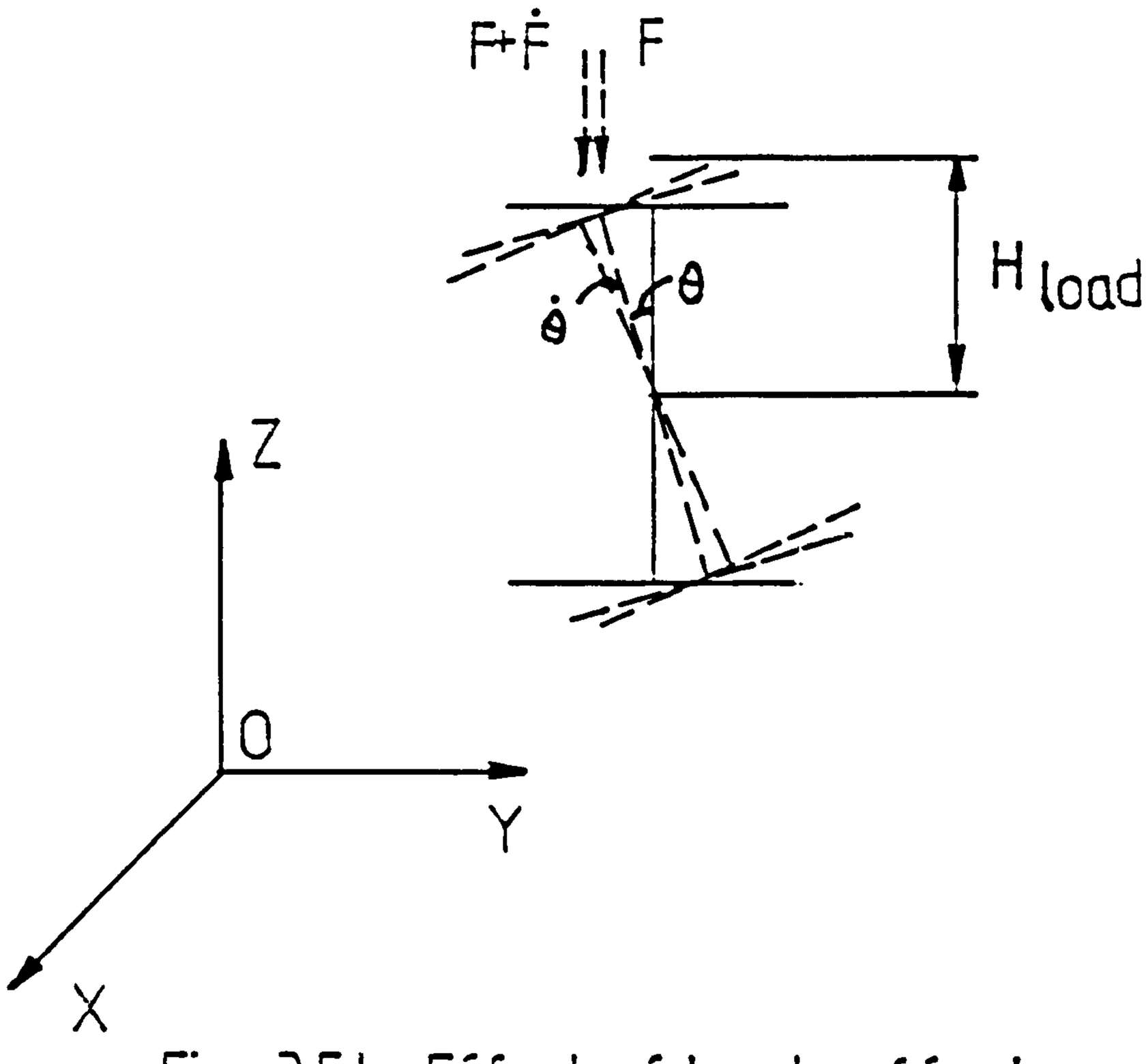

Fig. 35b Effect of load offset

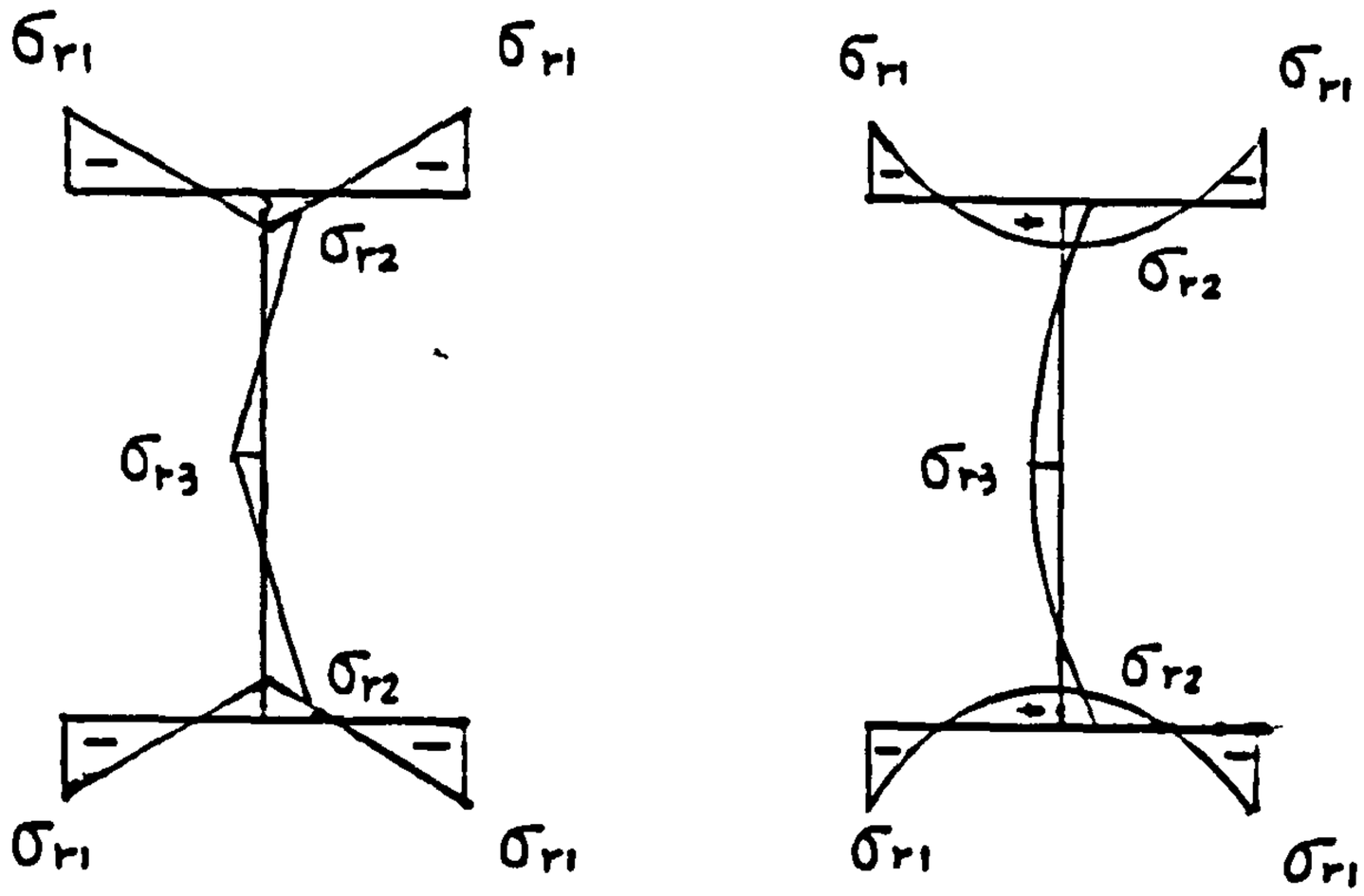

(a) Linear

(b) Parabolic

FIG. 3.6 TWO TYPES OF RESIDUAL STRESS DISTRIBUTION

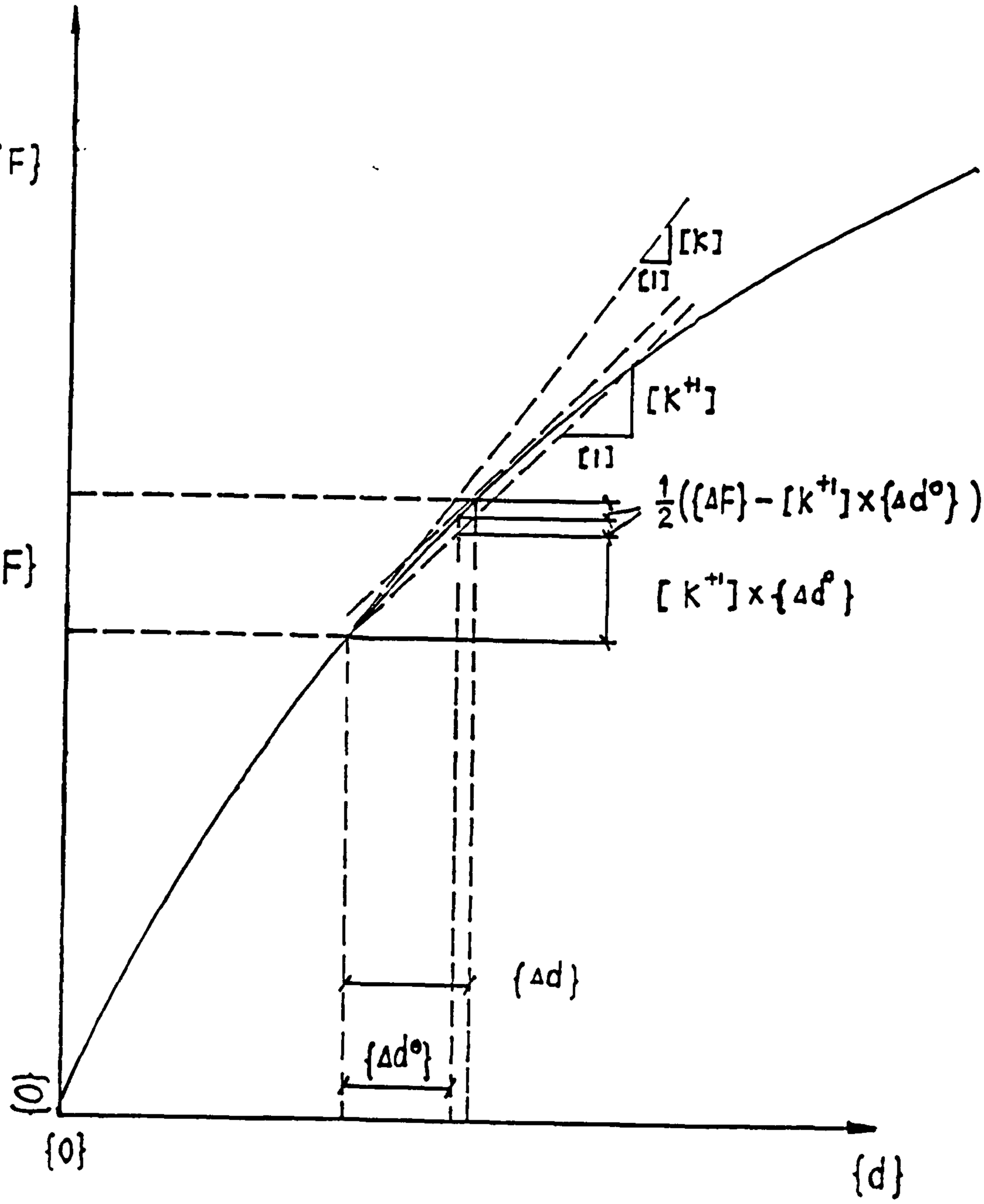

Fig. 3·7 Solution technique

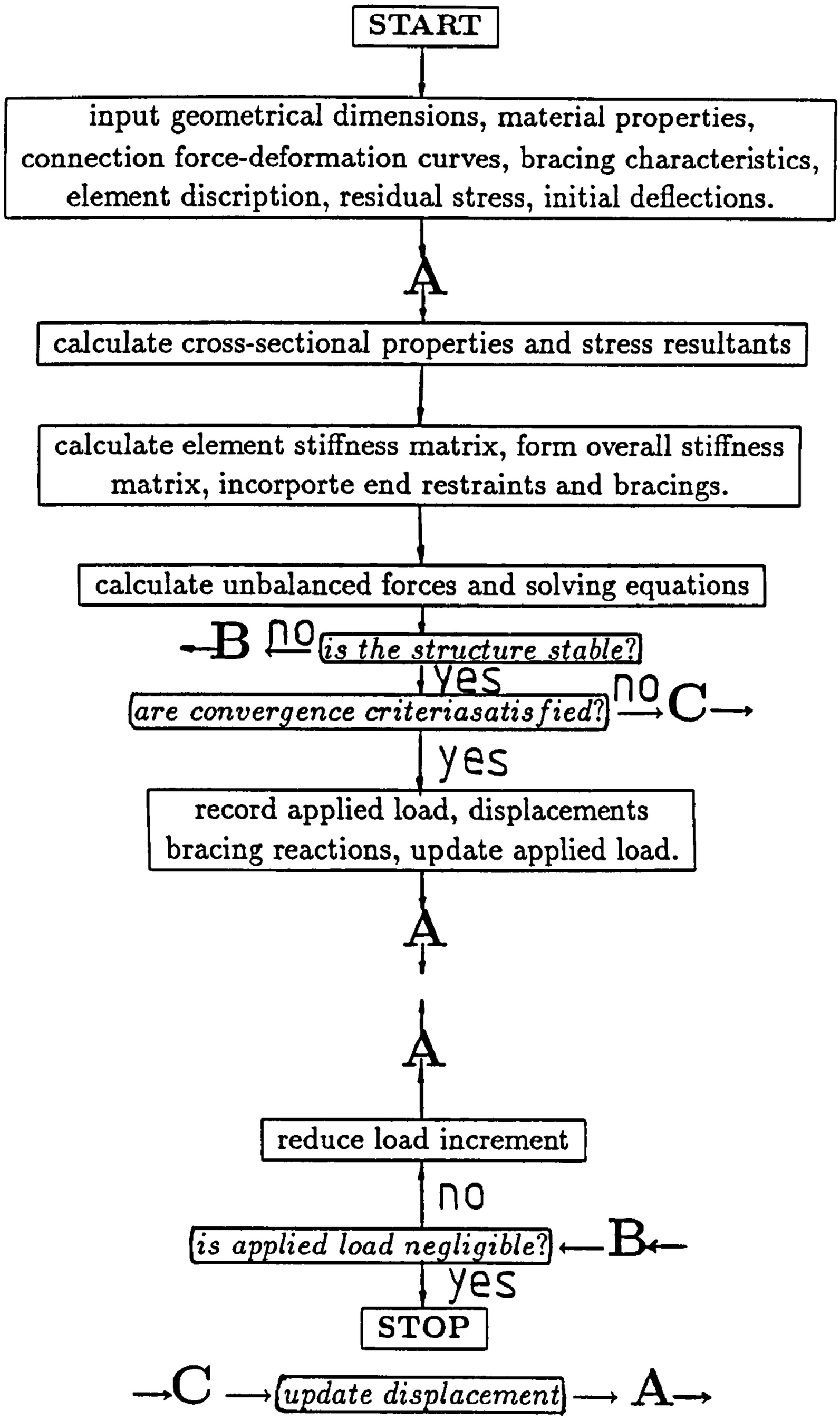

Fig. 3.8 Computer Program Flow Chart

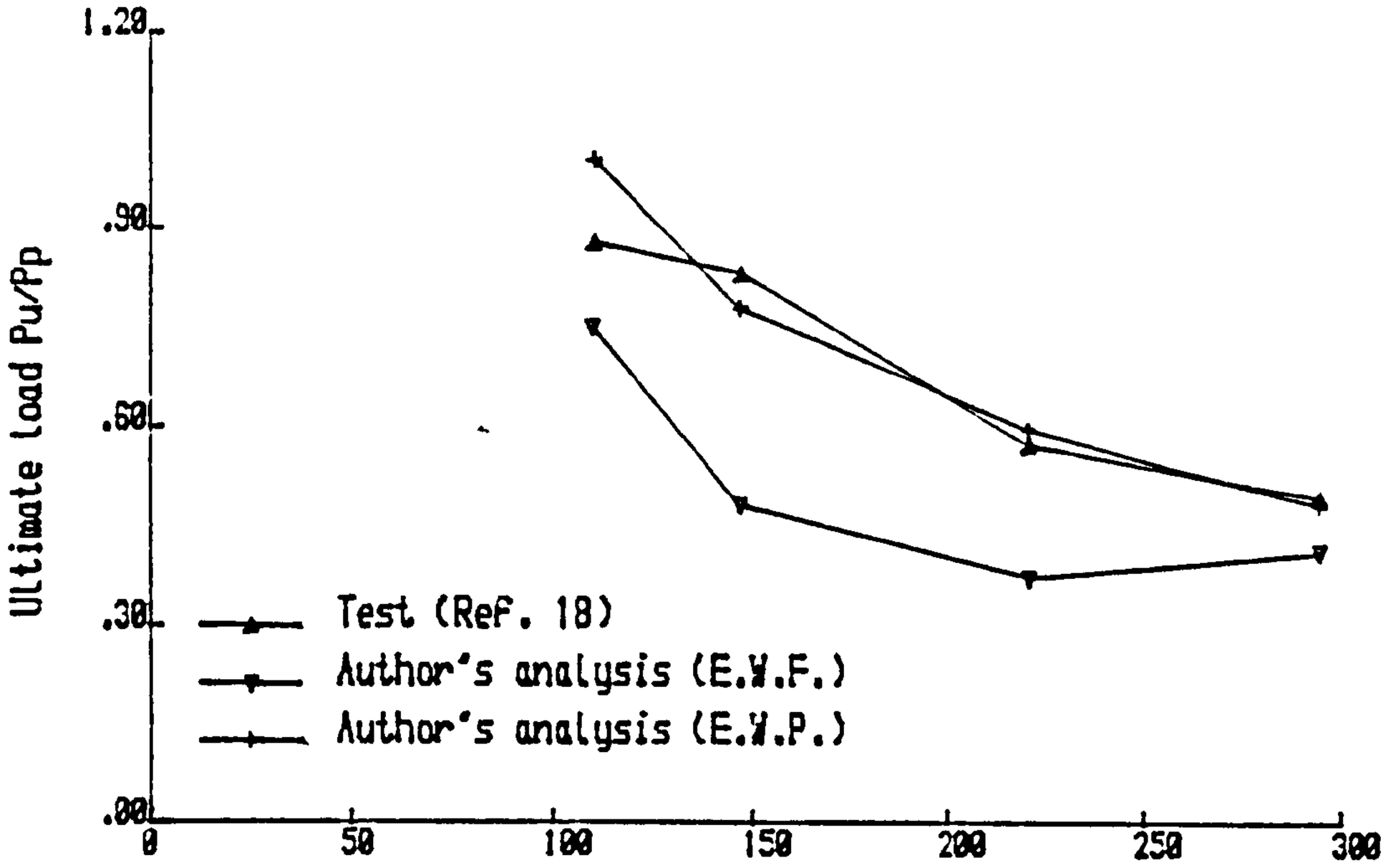

Fig. 3.9a Comparison of Author's analysis with tests of Ref. 18 For flange cleats

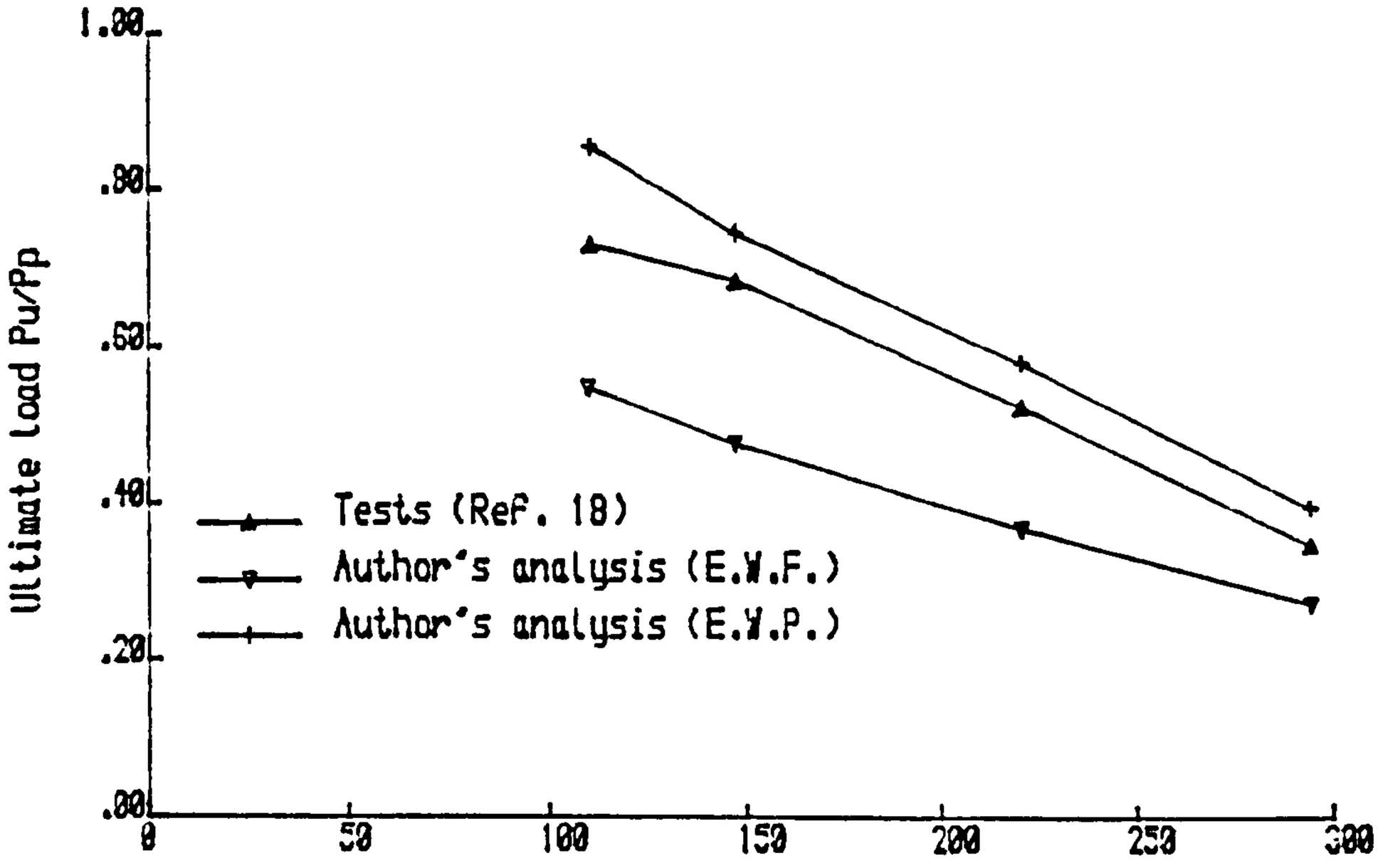

Fig. 3.9b Comparison of Author's analysis with tests of Ref. 18 For web cleat connections.

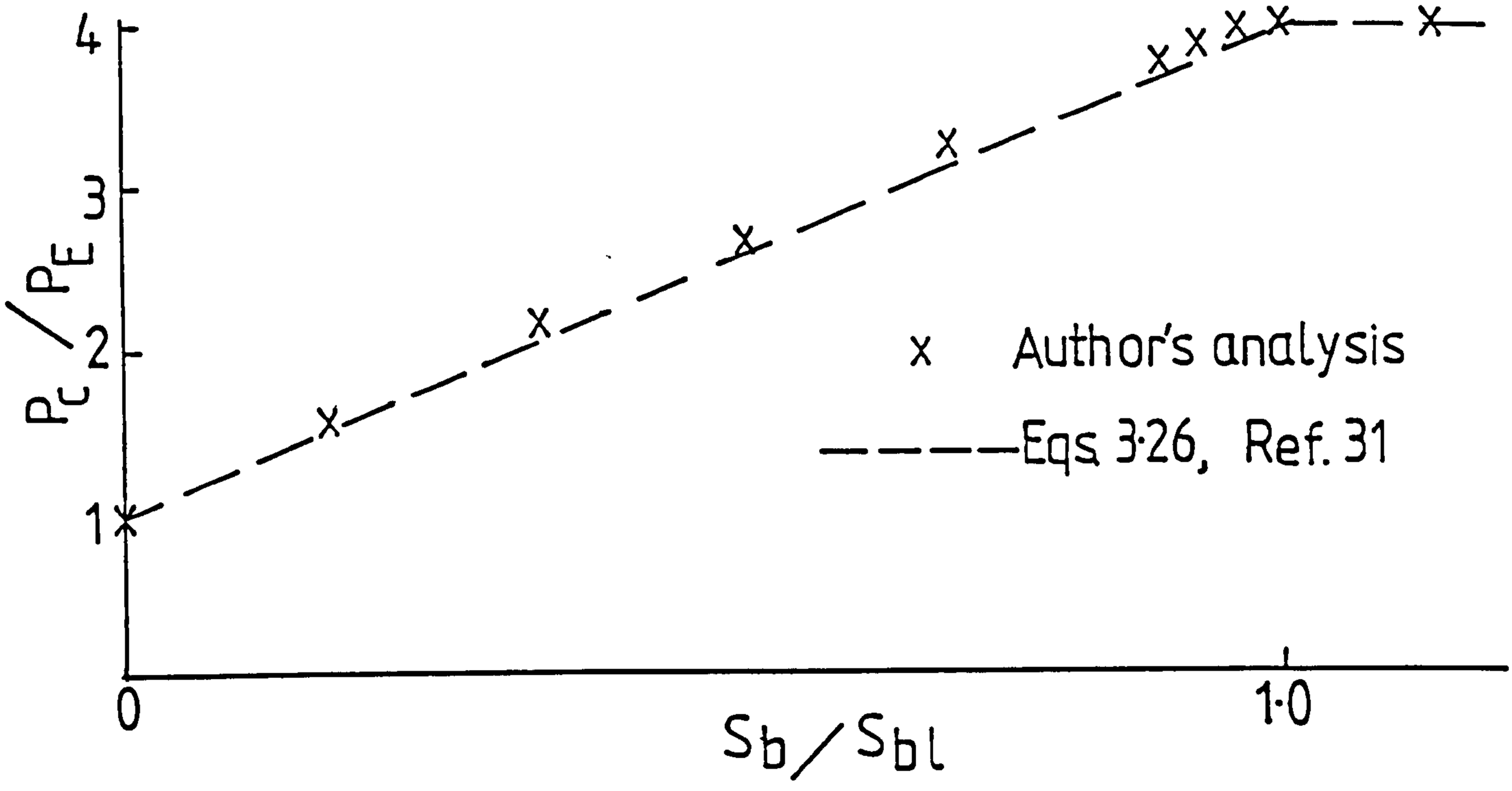

Fig.3·10 Comparison of results for centrally braced column

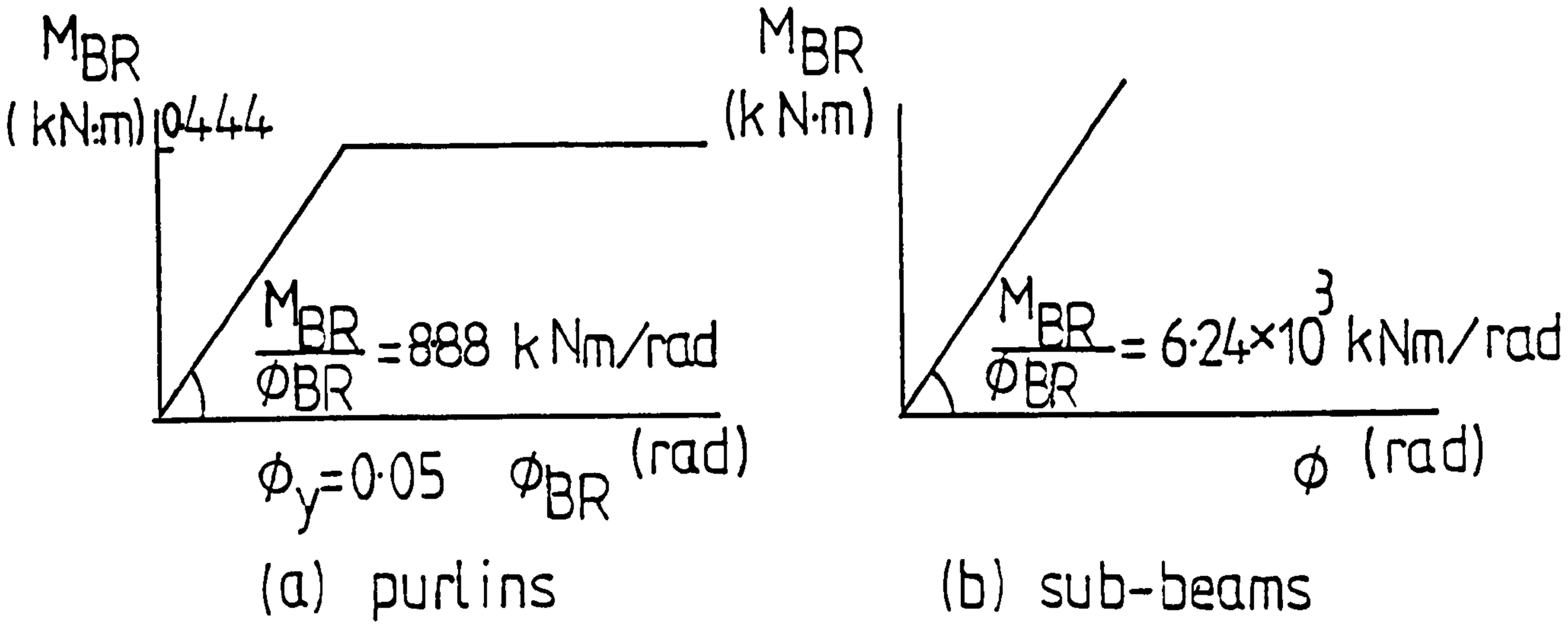

Fig.3·11 Moment-rotation characteristics for braces

$\lambda_y = 229$

Test – Ref. 44

Braced

Unbraced

Present Analysis

Braced

Unbraced

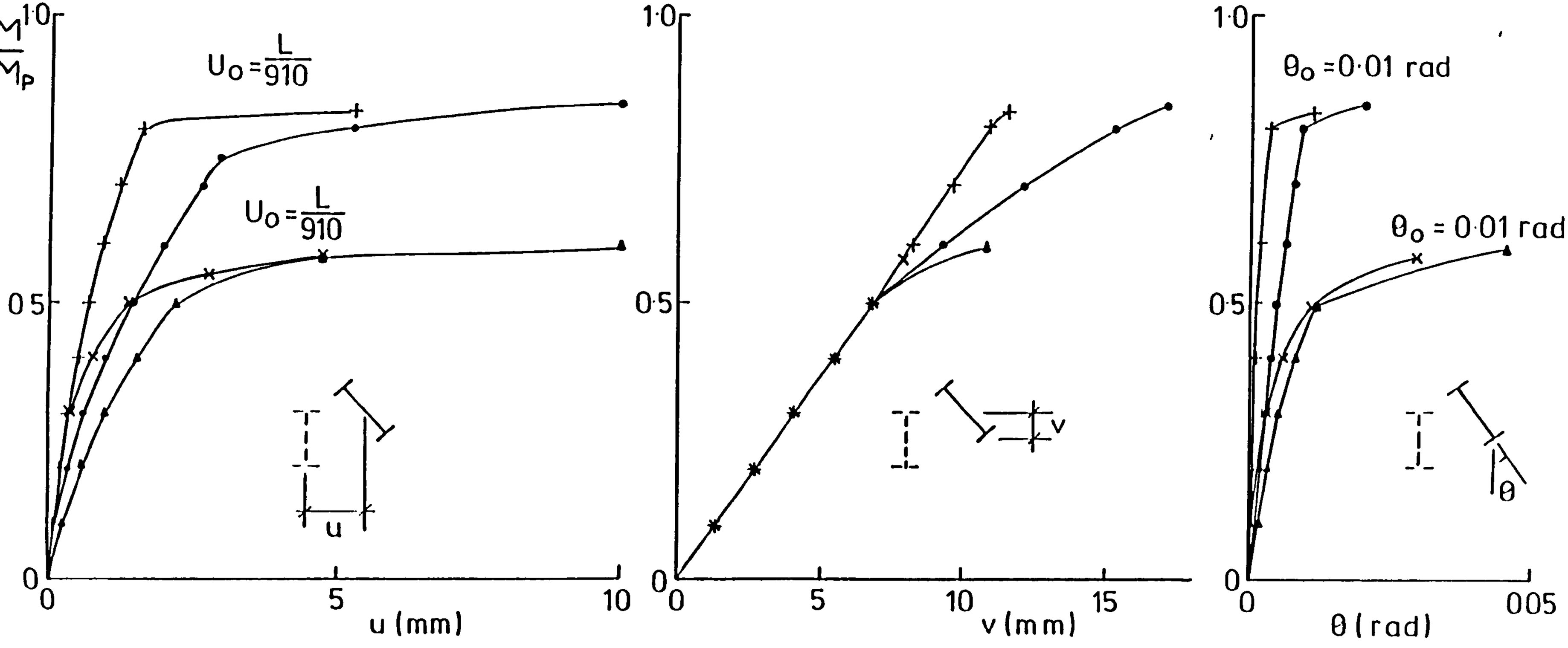

FIG. 312 COMPARISON OF AUTHOR'S RESULTS WITH TESTS OF REF. 44 UNIFORM MOMENT ON CENTRAL SEGMENT

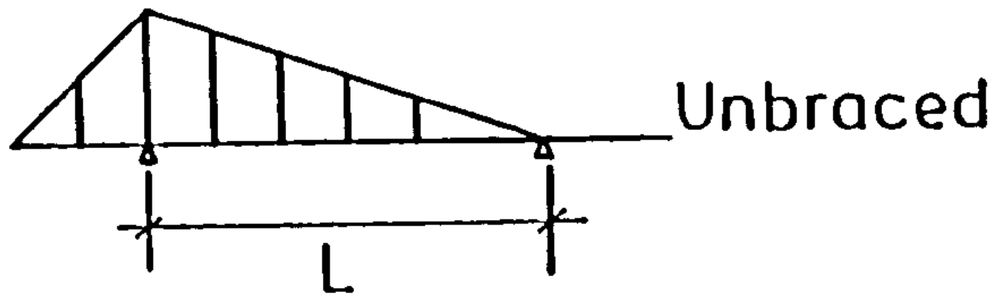

Test – Ref. 44

$\lambda_y = 321$

$\lambda_y = 596$

Present analysis

$\lambda_y = 321$

$\lambda_y = 596$

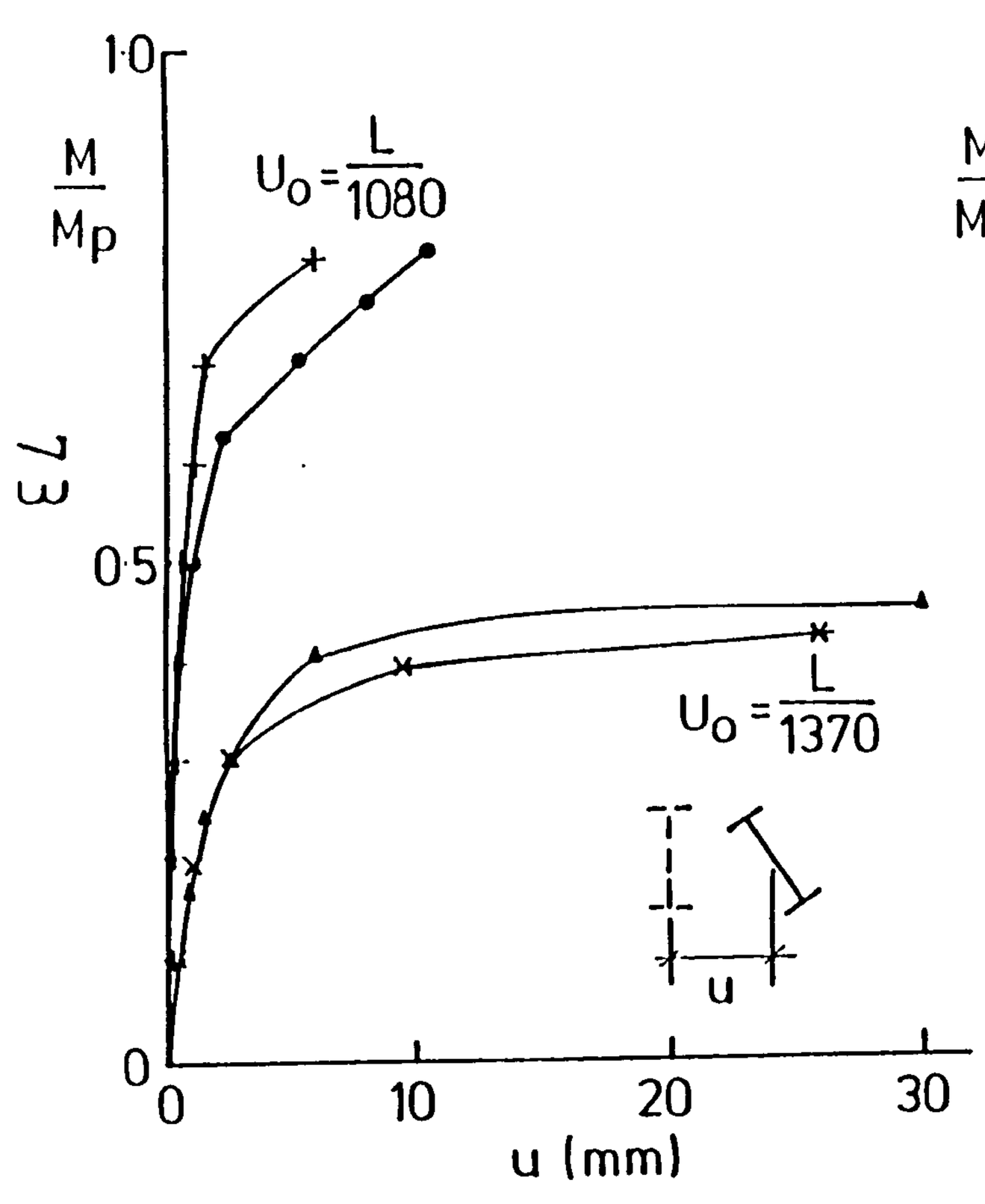

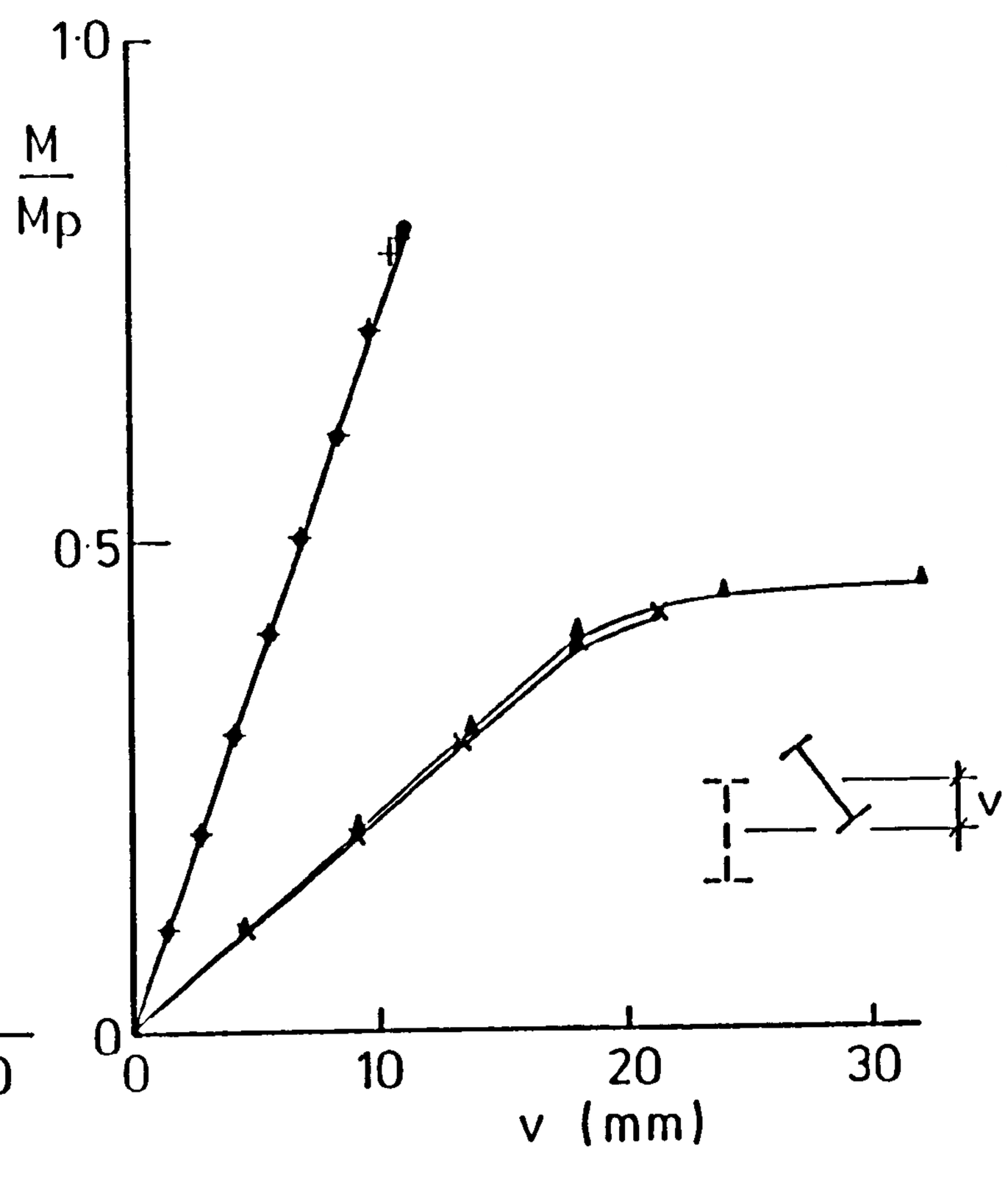

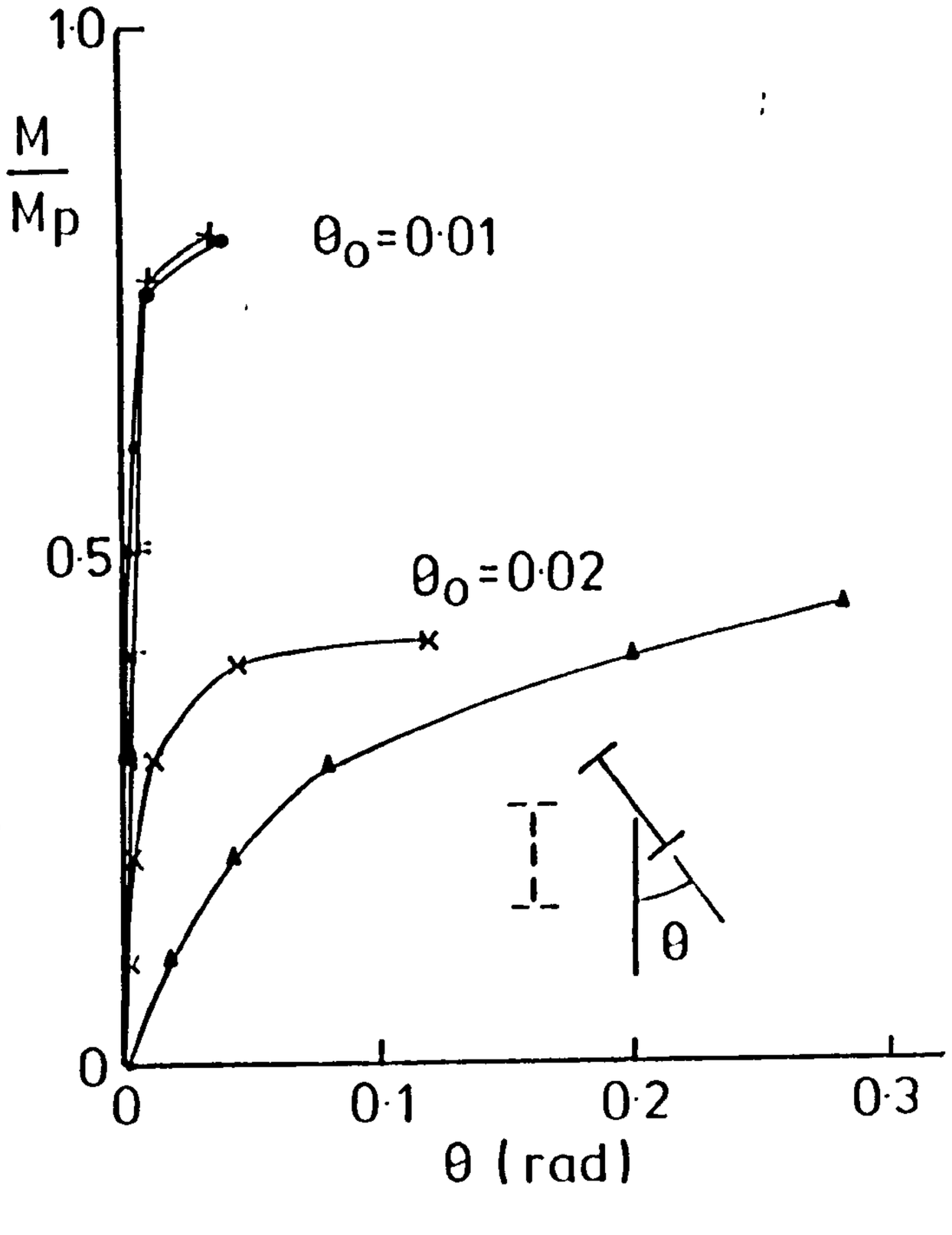

FIG. 3·13 COMPARISON OF AUTHOR'S RESULTS WITH TESTS OF REF. 44 NON-UNIFORM MOMENT ON CENTRAL SEGMENT

Chapter 4

SPATIAL BEHAVIOUR OF FLEXIBLY SUPPORTED BEAMS

4.1 Introduction

Chapter 2 indicates that a systematic study is necessary for a better understanding of the behaviour of end restrained members deforming in a three-dimensional manner. Furthermore, the application of various analyses to realistic structures with practical connections is rare. In chapter 3, an analogy has been presented to incorporate various restraining effects on the behaviour of beam-columns and close agreement with other studies was obtained, thus validating the ability of the analysis to properly deal with such topics.

In this chapter, a detailed parametric study into the spatial behaviour of end restrained beams using the computer program based on the theory of chapter 3 is reported. Results from this study are discussed and then used to

assess the recommendation given in BS5950 for the design of end restrained beams.

The most important parameter is the degree of restraint provided to the member. In this study, four types of restraint are addressed separately, namely:

1. in-plane flexural bending restraint;

2. out-of-plane flexural bending restraint;

3. torsional restraint;

4. warping restraint.

Consideration is also given to the effects of two major imperfections i.e. residual stress and initial lateral deflection.

4.2 Description of the Problem Under Investigation

The beam under study is shown in figure 4.1a. Its ends are flexibly connected to immovable supports by various restraints. A UB 254 × 22 cross-section has been used, with the range of slenderness from $\frac{L}{r_y}$ =40, at which failure is mainly due to plastic action, to $\frac{L}{r_y}$ =300, for which lateral instability dominates. Identical support conditions are assumed at both ends.

Grade 43 steel with Young's modulus E=200,000 N/mm^2, Poisson's ratio ν =0.25 and yield stress σ_y =275 N/mm^2 was assumed. The initial out-of-plane deflection is shown in Fig. 4.1c, while residual stress patterns

shown in Fig. 3.6 have been adopted with $\sigma_{r1} = 0.3\sigma_y$ in compression. Loading has been assumed to be uniformly distributed on the top flange.

4.3 Effects of In-plane Restraints

As pointed out in section 2.1, the in-plane behaviour of most commonly used connections is well understood; it is therefore possible to investigate their effects on the behaviour of beams. In this section, results for six different end conditions are presented. These are pin joints (**PJ**), web cleats(**WC**), flange cleats (**FC**), flush end plates (**FEP**), extended end plates (**EEP**) and rigid joints (**RJ**). Fig. 4.2 shows the in-plane moment-rotation data taken from the tests of Davison[15] and their multi-linear representations used herein. Also shown in the figure is the plastic moment capacity of the cross section. As for other end degrees of freedom, transverse displacements are prevented; out-of-plane rotation is allowed; axial rotation of twisting is restrained and either freedom to warp or prevention of warping is assumed.

4.3.1 Results

Figures 4.3-4.5 give three sets of load-deflection curves for $\frac{L}{r_y}$ =40,150 and 300 respectively, assuming free end warping. In these figures, the applied load is expressed non-dimensionally by dividing it by W_p, which is the load required to develop a plastic hinge at the centre of a simply supported beam,

$$W_p = \frac{8M_p}{L^2} \tag{4.1}$$

in which M_p is the plastic moment capacity of the cross section and L is the length of the beam.

Figures 4.3a,4.4a and 4.5a show the variation of out-of-plane deflection with increasing applied load, whilst Figs 4.3b,4.4b and 4.5b present the relationship between applied load and in-plane deflection at the centre of the beam.

It is clear from these figures that for stocky beams little out-of-plane deformation occurs until quite close to failure and Fig. 4.3a also shows that $\frac{W_u}{W_p}$ approaches unity even for a simply supported beam. Failure is therefore essentially by plastic hinge action. In such cases, no extra iterations are required in the program to reach convergence until quite high proportions of the failure load. On the other hand, slender beams fail at a much lower load and behave non-linearly from the beginning of the loading process, with large out-of-plane deformations being developed as shown in Figs 4.4a and 4.5a.

Both in-plane and out-of-plane deflections reduce as connection stiffness is increased. This leads to progressively higher load-carrying capacities as more substantial connections are used. This point is illustrated more clearly in Tables 4.1 and 4.2 which are respectively ultimate strengths and percentage increases produced by end restraints.

The influence of end restraint on the ultimate load is clearly greater when the beam's slenderness is higher. For instance, the increases for an extended end plate connection are 57.5%, 72.5% and 169.0% at values of $\frac{L}{r_y}$ equal to 40,150 and 300 respectively. This reflects the greater relative stiffness of the connection as the beam's flexibility increases. Figure 4.6 compares the in-plane moment diagrams at maximum load for each of the six end conditions at three representative values of $\frac{L}{r_y}$ of 40,150 and 300. These diagrams show how, for each type of restraint, the end restraining moment

is increased, leading to a progressively greater influence of end restraint with increases in slenderness. It is, of course, these more favourable patterns of moment produced by the end restraint that permit loads in excess of W_p to be carried in several instances.

Taking $\frac{L}{r_y}$ =150 as a representative case, it may be seen from Table 4.4 that the strength increases over the equivalent simply supported beam assuming free end warping are:

- Web cleat connection 11.2%
- Flange cleat connection 26.7%
- Flush end plate connection 48.6%
- Extended end plate connection 72.5%
- Rigid joint 108.6%

Figures 4.7a and 4.7b present the complete relationship between ultimate load and slenderness for the two cases of end warping free and end warping prevented for each type of end connection.

The values of Fig. 4.7a are, of course, conservative estimates of the true improvements since no out-of-plane restraint has been included. Comparison with Fig. 4.7b for fixed end warping gives some idea of the further improvements that may be possible if the necessary out-of-plane restraint characteristics of the different connection types had been properly quantified.

4.3.2 Sensitivity Study

This study has been carried out to investigate the extent to which small variations in the 'random' problem variables, i.e. initial out-of-plane deflection, residual stress and connection stiffness, affect the behaviour of the beam.

Effect of initial out-of-plane deflection

This study has been conducted assuming a Lehigh type of residual stress pattern for beams provided with either extended end plates or pin joints. Values of $\frac{\delta_0}{L}$ of 0,1/5000,1/1000,1/200 have been used.

Figure 4.8a gives the beam curves for the different levels of initial imperfection. One point that is immediately clear from this figure is that perfect beams behave rather differently from those which are initially crooked at low slenderness where plastic action is the main reason for the failure. This was also observed in Reference[58]. It follows from one of the basic assumptions of the theory of thin-walled structures. A perfect beam will have zero warping stiffness since the beam's flanges are fully yielded and the 'effective' section becomes a rectangle, whilst the different way in which yielding spreads through the cross-section makes it possible for the imperfect beam to retain some warping stiffness even at high loads. However, as the slenderness increases, less of the beam's web is yielded at failure, thus the difference in effective sections for the two cases becomes smaller. When failure is controlled by inelastic lateral instability, with only a modest degree of plasticity, the earlier yield from larger out-of-plane actions caused by the presence of the initial lateral deflections reduces the effective stiffness and the imperfect beam therefore fails at a lower load and consequently, the larger

the initial deflection the lower the ultimate load. The effect of imperfections on the behaviour of beams at high slenderness may be explained from a knowledge of yield zone penetration; discussion of this is presented in section 4.3.3. The magnitude of the initial crookedness has the anticipated sort of effect on the buckling loads of simply sypported beams i.e. it has the greatest effect in the region of medium slenderness ($\frac{L}{r_y}$ =100-200). Figure 4.8b indicates that the presence of larger initial imperfections also causes the beam to behave non-linearly at an earlier stage.

Effect of residual stress

Three cases have been compared; (a) no residual stress (**NO**), (b) Lehigh pattern of residual stress (**LEHIGH**), (c) parabolic residual stress distribution (**PARABOLIC**). $\delta_0 = \frac{L}{1000}$ was assumed in all cases for the initial out-of-plane deflection. Both extended end plate connections and pin joints were examined. Figures 4.9a and 4.9b present the beam buckling curves and load versus in-plane deflection relationships respectively. From Fig. 4.9a, the following points are of particular interest:

1. the residual stress has a small effect on the ultimate loads of beams generally;

2. the parabolic pattern of residual stress has a less severe effect than the Lehigh pattern of residual stress;

3. the effect of residual stress is dependant on the degree of yield penetration in the beam. If full plastification of one section in the beam is the reason for the beam's failure or the beam fails almost elastically, the residual stress has a negligible effect on its load-carrying capacity.

These are cases as seen in Fig. 4.9a for beams with small slendernesses as well as for simply supported beams with high slendernesses. Whereas for end restrained beams, the situation is different at higher slendernesses when a certain amount of yield occurs due to the effect of a greater degree of out-of-plane involvement. Figure 4.9b confirms that the presence of residual stress affects the beam's in-plane response only in the inelastic range.

Effect of variation in connection stiffness

The effect of varying the connection properties by displacing the connection $M - \phi$ curve by 10% horizontally has been studied for extended end plate connections and flange cleat connections. It was observed that beams with a higher ratio of connection stiffness to beam stiffness seemed to be more sensitive to small variations of the connection stiffness. Nevertheless, the buckling strength changes were less than 2% in the case of the extended end plate connection and about 1% for beams with flange cleat connections. This suggests that the 'exact' form of the connection $M - \phi$ curve is not too important a factor.

4.3.3 Spread of Yielding

Two sets of beam yield penetration and moment distribution diagrams are presented in Figs 4.10 and 4.11. The first of these has been drawn for three different end connections-rigid joints, extended end plates and pin connections-with $\frac{L}{r_y}$=150; the second is for an extended end plate connection with three different slendernesses, $\frac{L}{r_y}$ =40,150 and 300. All of these figures are for the end warping free condition and are drawn for conditions

at the maximum load level. The non-dimensional reference moment levels are based on the appropriate plastic moment capacity of the cross-section in the cases of flexural bending and the elastic limit bimoment in the case of warping. The signs of the flange tip strains caused by various positive actions referred to a beam's central cross-section are shown in Fig. 4.12a, together with the values of the first yield and fully plastic capacity of the cross-section.

It can be seen from figure 4.10 that in the case of rigid joints, part of the lower flange is yielded at the end due to the effect of the great major axis bending moment and residual stress, whereas for other connections, the end cross-sections remain elastic at failure because of small major axis bending moments. However, at the centre of the beam, elastic behaviour is preserved for beams with rigid joints while plastic action occurs for other connection arrangements. This comes from the fact that less major axis moment is generated at the beam centre for rigid connections than for other connections; and also in contributing to the yield penetration of the beam, out-of-plane effects are of great significance. It can be seen that the major axis bending moment at the beam centre for every connection arrangement is smaller than, say, that at the end for extended end plates, but the accumulation of compressive strain on the nearer half of the upper flange (viewed from the front of the beam) causes this part to yield in compression.

Fig. 4.11 shows the changing role played by end restraint with increasing beam length. These figures show that in contributing to the beam's yield penetration, the effect of in-plane bending moment decreases while that of the out-of-plane actions increases. At $\frac{L}{r_y}$ =40, the central cross-section of the beam is nearly fully yielded according to the yield penetration pattern due

to in-plane action with only a small modification from out-of-plane actions and residual stress. With the increase of the beam slenderness, this effect is reduced while the effect of out-of-plane actions become more influential. This can be observed in figure 4.11, which shows for $\frac{L}{r_y}$ =150, that a very small region with accumulated compressive strains from all actions is yielded in compression and that for $\frac{L}{r_y}$ =300, this yield zone is increased remarkably.

The above discussion may be used to explain various phenomena observed in the sensitivity study. Fig. 4.12b shows the signs of the strains from the various actions for the beam in this study at its centre. As discribed above, part of the upper flange is yielded in compression at high slendernesses, therefore, it is no longer able to sustain any additional stress; therefore, from the updated strain distribution and thus the stress distribution due to out-of-plane actions resulted from updated load increment, it can be seen that the stress resultant about major axis from the corresponding lower flange is equivalent to reducing the major axis bending moment(Fig. 4.12b). This relaxed mid-span moment is shifted to the beam's end in the case of substantial connections being present. For a simply supported beam, since the ends cannot sustain any in-plane bending moment, the major axis bending moment at the centre is always linearly related to the applied load i.e.

$$M_{centre} = \frac{1}{8} w.L^2 \tag{4.2}$$

in which w is the applied load and L is the beam's length. However, for short beams when in-plane bending is the main source of plastification and for beams with medium slendernesses which remain virtually elastic, the moments at the beam's centre will continue increasing. This is clearly shown

in figure 4.13a for $\frac{L}{r_y}$ =150 and in figure 4.13b for $\frac{L}{r_y}$ =300.

Further examinination of the geometric stiffness matrix reveals that a reduction in in-plane bending moment at the centre of the beam increases its stability since the central section is most critical. Therefore, the beam will not fail until it reaches a critical combination of material yielding and applied loads. Hence, compared with perfect beams which do not possess this 'favourable' effect, the crooked ones may sustain greater buckling loads. Furthermore, the larger the initial deflection magnitude, the more significant this 'beneficial' effect. However, for simply supported beams, there is no such effect, therefore, larger initial deflections always result in a lower buckling load; also because of the small buckling load at higher slendernesses, such beams fail basically in an elastic fashion. Therefore, the resulting pattern of buckling load variations with different initial deflections presented in Fig. 4.8a is obtained. As for the variation of the effect of the residual stress on the ultimate load of an end restrained beam, the explanation is quite straightforward. At low slenderness, complete plastification of a cross-section takes place, therefore, the effect of residual stress is negligible. With increasing the beam slenderess, the yield zone gradually decreases, consequently, the effect of residual stress increases until the maximum is reached, similar to the case of the simply supported beam with a medium slenderness; after this, the decrease in yield zone would reduce the effect of residual stress. At $\frac{L}{r_y}$ equal to approximately 150, the degree of yield penetration is minimum. At higher values of beam slenderness, the yield zone in the beam is larger, therefore, a greater effect of residual stress is produced.

4.4 Effect of Minor Axis Restraint on Beam's Ultimate Loads

Unlike the in-plane behaviour of connections, the out-of-plane responses of connections have not been thoroughly investigated, neither have their effects on the behaviour and ultimate loads of structures been examined.

Recently, Celikag[59] tested a group of flange cleats to study their out-of-plane moment-rotation relationships. Four different types of column stiffening were thought to be of practical interest, so were they tested. These ranged from no column stiffeners to stiffeners intended to eliminate both web and flange distortion of the column. Unlike the connection's in-plane response, where the column remains virtually undeformed, in the case of out-of-plane action, any point in the column undergoes significant lateral rotation which varies with its position between the two flanges of the column, because the column posseses a very small distortional rigidity. The question was therefore raised as to how the minor axis moment-rotation curves should be constructed. Four possible ways of calculating the minor axis rotation were suggested. As a result, there exist 16 minor axis moment-rotation curves for the 16 combinations under the same connection catalogue 'flange cleats'.

As observed from the study of in-plane restraint effects, more substantial restraint always leads to higher increases in a beam's ultimate loads over those for the simply supported case. The effect of five representative cases of minor axis restraint on the ultimate loads of beams are therefore compared. They are:

1. no minor axis rotational restraint;

2. type B connection arrangement with type (i) rotation calculation, which results in the most flexible minor axis moment-rotation curve among all 16 combinations;

3. type D connection arrangement with type (i) rotation calculation to represent the medium degree of minor axis restraint;

4. type D connection arrangement plus type (iv) rotation calculation, which gives the highest initial $\frac{dM}{d\phi}$ value of all combinations;

5. complete prevention of minor axis rotation.

In every case, only the initial stiffness from the moment-rotation curve is used. Although the tests were conducted on short beams ($\frac{L}{r_y}$ =50), the results are applied to a range of beam slendernesses from $\frac{L}{r_y}$ = 50 to $\frac{L}{r_y}$ =300. The in-plane moment-rotation curve from Davison's[15] test for flange cleats was adopted.

Figure 4.14 presents the result of this study. It is noticed that even for beams with infinite minor axis restraints, the maximum increase of ultimate loads over those with no minor axis restraints is approximately 20%. For type B connection arrangement, the increase is less than 5%, whereas for type D arrangement, it varies between 5% and 10%. This suggests that the minor axis rotational restraint does not affect the buckling loads of beams significantly.

Trahair[20] also investigated this effect based on elastic analysis. The increase in strengths is of the same order for slender beams, although in that analysis, as much as a 60% increase was obtained for very short beams. Since the present study is based on the ultimate strength analysis of real

beams, the minor axis restraint has an understandably negligible effect on short beams' load-carrying capacities.

A small additional study of beams under minor axis point load at mid-span indicates that the minor axis cross-sectional plastic moment capacity is always reached and that there is merely a small difference in end moments, although the beams' flexibilities are significantly reduced with the use of higher values of $\frac{dM}{d\phi}$. Therefore, only a small influence of minor axis restraint is suggested as far as the beams' strengths are concerned.

It may be recommanded that for each connection arrangement, the type (i) calculation of connection rotation, which uses the value of the difference between the rotation at the beam's end and that at the column's rear flange, be used.

4.5 Effects of End Torsional Restraints

It appears that the torsional behaviour of commonly used connections has not been fully investigated with the result that no reliable data could be utilized to assess the torsional effects of realistic connections on the behaviour of structures.

A set of $\overline{K_{tor}} = \frac{K_{tor}}{GK_T/L}$ values were thus assumed for this study. It ranges from 5 for which no strenghthening effect is to be gained from end torsional restraints to infinite.

Figure 4.15 presents the buckling load versus torsional restraint relationships for three representative slendernesses i.e. $\frac{L}{r_y}$ =50,150 and 300. The buckling load is nondimensionised by dividing it by the buckling load assuming full end torsional restraint. It can be seen from these curves that

assuming elastic behaviour (which is approximately the case for $\frac{L}{r_y}$ =150 and 300), a higher value of $\overline{K_{tor}}$ is required to produce a similar strenghthening effect for low slendernesses. For $\frac{L}{r_y}$ =50, this trend is also followed at lower values of $\overline{K_{tor}}$. However, when complete plastification takes place, the requirement is considerably reduced.

From the theoretical investigation by Trahair[20], the relationship between the elastic buckling stress (F_{ob}) ratio δ and the end torsional stiffness is given as:

$$K_{tor} = \frac{GK_T}{L}\left[\frac{A_1 + A_2B^2D^2/t_f^2L^2}{1-\delta}\right] \tag{4.3}$$

in the Australian standard[22], in which B, D and t_f are the cross-sectional width, depth and flange thickness; A_1 *and* A_2 are constants; assuming free end warping and uniformly distributed load, A_1 =1.19 and A_2 =2.12.

$$\delta = \frac{F_{ob\ for\ partial\ end\ torsional\ restraint}}{F_{ob\ for\ full\ end\ torsional\ restraint}} \tag{4.4}$$

Making use of equation 4.3, the end torsional restraint stiffness requirements for $\delta = 0.98$ and $\delta = 0.95$ are:

for $\delta = 0.98$,

$$\begin{aligned} K_{tor} &= 1586\frac{GK_T}{L} \qquad for\ \frac{L}{r_y} = 50 \\ K_{tor} &= 229\frac{GK_T}{L} \qquad for\ \frac{L}{r_y} = 150 \\ K_{tor} &= 102\frac{GK_T}{L} \qquad for\ \frac{L}{r_y} = 300 \end{aligned} \tag{4.5}$$

whereas for $\delta = 0.95$, these coeffecients are reduced to 634, 91.6 and 40.8 respectively.

This is in quite close agreement with the analytical results reported herein as shown in Fig. 4.15, although for $\frac{L}{r_y}$ =50, the requirements are significantly lower due to plastic action.

Ref.[20] recognises the fact that connections attached to the beam's flanges e.g. flange cleats are able to provide full restraint against end torsion. However, web cleats are reckoned as insufficient. This seems to be unreasonable. Celikag[59] tested a number of web cleat and flange cleat connections to study their torsional response under torque, from which an approximate value of 250,000 kN.mm/rad for the initial torsional stiffness for web cleats was obtained. This value is equivalent to $85GK_T/L$, $254GK_T/L$ and $508GK_T/L$ respectively for $\frac{L}{r_y}$ =50,150 and 300. These values are considerably higher than the requirements to ensure $\delta > 0.98$ considering plastic action at $\frac{L}{r_y}$ =50.

Figure 4.16a and 4.16b present load-deflection relationships for in-plane deflection and twisting. It is clear that different end torsional restraints have only a slight influence on the in-plane behaviour whilst the out-of-plane response of the beam is significantly affected.

This study also suggests that even the weakest connection in reality e.g. a web cleat connection, behaves virtually as a restraint of infinite stiffness torsionally in terms of its effect on the behaviour of beams. Therefore, all practical connections may be treated as providing full torsional restraints.

4.6 Effects of End Warping Restraints

Warping presents a different catalogue of problem in that it is associated with the non-uniform torsion of a member. Because of the difficulty in identification, the relationship between the warping reaction (bimoment) and the associated warping displacement (rate of axial twisting) has not been studied at all. However, it has been shown to affect the behaviour of thin-

walled structures significantly (Ojalvo and Chambers[28], Vacherajittiphan and Trahair[30] and Tam[41]).

Combinations of three representative beam slendernesses of $\frac{L}{r_y}$ =50,150 and 300 and various end warping restraint stiffnesses from freedom to warp to prevention of warping are analysed in an attempt to provide insight into the warping effect.

Fig. 4.17 presents buckling load versus end warping stiffness relationships for the three representative slendernesses on a log-linear plot. It clearly shows that for short beams ($\frac{L}{r_y}$ =50), failure is basically plastic, therefore, the end warping restraint has little effect on buckling loads. For higher slendernesses, it appears that there exists a region for end warping restraint stiffness beyond which any variation would result in a negligible effect on the load-carrying capacity of the beam, while within this region, increasing end warping restraint would considerably enhance the beam's ultimate load. This region is likely to be $0.1\frac{EI_W}{L} < K_W < 100\frac{EI_W}{L}$ (i.e -1< $log_{10}\left(\frac{K_W}{EI_W/L}\right)$ <2). As reported in this study, the percentage increases of the ultimate load at $K_W = 0.1\frac{EI_W}{L}$ over that at $K_W = 0.0$ are 1.6 and 0.7 for $\frac{L}{r_y}$ =150 and 300 respectively and the ratios of the beam's buckling load at $K_W = 100\frac{EI_W}{L}$ to that at $K_W = \infty$ are 0.98 and 0.972 for the these two slendernesses respectively.

It was pointed out in Ref.[28] that assuming elastic behaviour, the effect of warping restraints on the beam's buckling load for lower slenderness tends to be greater. This is justified if comparing results for $\frac{L}{r_y}$ =150 and 300. The increases of beam load-carrying capacities from K_W =0 to ∞ are 60.2% and 51.5% respectively. Nevertheless, if plastic action dominates the beam's failure as in the case of $\frac{L}{r_y}$ =50, this trend would not be followed.

A study of load-deflection relationships con firms that the end warping restraints affect the beam's out-of-plane responses (load-deflection about minor axis and load-axial rotation of twisting) only. The in-plane behaviour of the beam is just slightly influenced when the beam's collapse is approached as shown in figures 4.18a and 4.18b.

4.7 Comparison with the Approach of BS 5950: Part 1

Figure 4.6 shows how, with the use of more substantial connections and increases in the beam span, the ratio of the end moment to that at mid-span increases. For beams subject to non-destabilising loads,the UK code[3] recognises the effect of moment pattern on lateral stability by means of a factor n to correct the beam's geometric effective length. The calculation of this value is based on the in-plane moment distribution at failure. For uniform loading, the larger the ratio of the end moment to the mid-span moment, the smaller the value of n and the higher the lateral torsional buckling resistance.

However, for beams under destabilising loads i.e. upper flange loads in the present study, the different in-plane moment patterns cannot be allowed for when using the code and a value of unity must be given to n. Nevertheless, the effect of these favourable in-plane patterns is reflected when the following equation is used to calculate the beam's ultimate load:

$$W_b = 8.0 \times (M_e + M_{m.s.})/L^2 \tag{4.6}$$

in which M_e and $M_{m.s.}$ are moments at the beam's end and mid-span respectively.

Table 4.3 compares the beam's load-carrying capacities using the BS 5950 approach with those from the present analysis for the upper flange loading case. The representative beam slenderness of $\frac{L_E}{L}$ equal to 150 is assumed; the general pattern is typical of results for other slendernesses. The values of $\frac{L_E}{L}$ in column 2 are taken directly from the code and allow for out-of-plane restraint with a simply supported beam as the basic case. Values in column 3 are obtained assuming $\frac{L_E}{L}$ =1.2, whilst values in column 4 are obtained using $\frac{L_E}{L}$ values from column 2. Columns 5 and 6 are the $\frac{W_b}{W_p}$ values taken directly from the analytical results. In BS 5950, the section which has the largest in-plane moment is assumed to be the most critical one for which the moment resisting capacity M_b is calculated. However, in this study, the use of extended end plate and rigid joints results in greatest in-plane moments at the ends but the mid-span is most critical since out-of-plane actions are involved. Therefore, in calculating the values of W_b, the mid-span section is assumed to sustain the moment resisting capacity M_b. From the requirements in the code for $\frac{L_E}{L}$ values, it is felt that values of $\frac{W_b}{W_p}$ in columns 3 and 4 should be compared with those in columns 5 and 6 respectively. As shown in table 4.3, quite reasonable agreement with the design approach is produced.

In order to fully appreciate the beneficial effect of the favourable in-plane moment distribution patterns on the bending strengths of beams, beams of $\frac{L}{r_y}$ =150 with various connections subject to load at the shear centre have been examined. The comparison of ultimate loads with the design approach is presented in table 4.4. Extra columns of n-factors (col. 2) and $\frac{W_b}{W_p}$ using n=1 (col. 6) are given alongside the other values. It is assumed that the most critical section sustains the moment resisting capacity M_b .

Therefore, for the beam with rigid joints, since plastic hinges formed at its ends ($\frac{M_e}{M_p}$ =0.993), the end rather than the mid-span is regarded as the most critical section. Comparing values in columns 4 and 5 with those in columns 7 and 8 for the same reason as in the case of upper flange loading, table 4.4 shows that the BS 5950 method predicts the ultimate loads quite well, being slightly on the safe side. On the other hand, neglecting the beneficial effect of the favourable in-plane moment distribution patterns would unreasonably underestimate the beam's load-carrying capacities, which is clearly shown if values in column 6 are compared with those in column 5.

Considering that the basis for the n-factor of the code is elastic critical buckling, whereas the values taken from the present analysis correspond to ultimate strength, the agreement suggests that the code method provides a reasonable safe approximation.

4.8 Conclusion

The finite element computer program presented in Chapter 3 has been used to conduct a parametric study to assist in understanding the effects of various end restraints on the behaviour and strengths of beams failing by lateral-torsional buckling. Based on this investigation, the following conclusions were reached:

1. Beam strength increases and deformations decrease with an increase of the connection stiffness.

2. The effect of residual stress depends on the degree of the beams' yield penetration. The strength of a fully yielded beam or an elastic beam

will not be affected; initial lateral deflection may have a distinctly different influence on the strength of end restrainted beams from that of simply supported ones in that larger initial deflection may result in higher buckling loads at higher slendernesses for restrained beams.

3. Very accurate connection moment-rotation curves are not necessary for predicting the behaviour and strength of beams with semi-rigid connections.

4. Minor axis rotational restraints slightly modify a beam's buckling load. For web cleat or flange cleat connections, this strengthening effect may be ignored without inducing great inaccuracy in predicting the load-carrying capacity.

5. End torsional restraints have a great effect upon beam's load-carrying capacity. However, even the torsionally weakest connection - web cleats - has the ability to enhance the beam strength similar to an infinite torsional restraint.

6. Restraining end warping of a beam would considerably increase its ultimate load. The warping stiffness in the region of $0.1\frac{EI_W}{L} < K_{tor} < 100\frac{EI_W}{L}$ appears to have significant effect on the behaviour of the beam.

7. The method of allowing for non-uniform patterns of moment by means of a slenderness correction factor based on elastic critical load theory used in BS 5950: Part 1 gives acceptable results on the safe side when compared with accurately calculated ultimate strengths from the present investigation.

Table 4.1

Ultimate Beam Loads for Different Cases

	Pin joints		Web cleats		Flange cleats		Flush end plates		Extended end plates		Rigid joints	
$\frac{L}{r_y}$	EWF	EWP	EWF	EWP	EWF	EWP	EWF	EWP	EWF	EWP	EWF	EWP
40	7.95	8.15	8.40	8.55	9.10	9.45	10.15	10.30	12.53	12.25	13.33	13.33
60	3.12	3.66	3.34	3.83	3.64	4.22	4.10	4.70	5.11	5.84	6.07	6.01
80	1.47	2.01	1.59	2.15	1.76	2.38	2.00	2.63	2.46	3.39	3.46	3.47
100	0.83	1.23	0.90	1.33	1.00	1.47	1.15	1.66	1.37	2.13	1.87	2.25
150	0.255	0.424	0.285	0.468	0.323	0.526	0.379	0.602	0.440	0.764	0.532	0.875
200	0.105	0.175	0.123	0.197	0.144	0.226	0.172	0.268	0.195	0.344	0.224	0.413
300	0.031	0.046	0.043	0.056	0.056	0.073	0.071	0.087	0.083	0.120	0.081	0.128

(1) All values are in kN/cm.

(2) EWF means End Warping Free.

(3) EWP means End Warping Prevented.

Table 4.2

Percentage Strength Increase over Equivalent Simply Supported Beams

	Web cleats		Flange cleats		Flush end plates		Extended end plates		Rigid joints	
$\frac{L}{r_w}$	EWF	EWP	EWF	EWP	EWF	EWP	EWF	EWP	EWF	EWP
40	5.7	7.5	14.5	18.9	27.7	29.6	57.5	54.1	67.6	67.6
60	7.1	22.8	16.7	35.3	31.4	50.6	63.8	87.2	94.6	92.6
80	8.2	46.3	19.7	61.9	36.1	78.9	67.3	130.6	135.4	136.1
100	9.1	61.2	21.2	77.6	38.8	101.2	66.1	158.2	136.1	172.7
150	11.2	83.5	26.7	106.3	48.6	136.1	72.5	199.6	108.6	243.1
200	16.7	87.1	36.7	115.2	63.8	174.3	84.7	227.6	112.9	293.3
300	38.2	81.3	82.1	128.5	129.3	183.7	169.1	289.4	166.7	315.4

(1) EWF stands for End Warping Free.

(2) EWP stands for End Warping Prevented.

Table 4.3

Effect of End Restraint on Lateral Instability - Comparison with the Design Method of BS 5950: Part 1 for Destabilising Load

End support	$\frac{L_E}{L}$ from	W_b/W_p using code		$\frac{W_b}{W_p}$ from analysis	
	BS 5950	$L_E = 1.2L$	L_E from Col.2	E.W.F.	E.W.P.
(1)	(2)	(3)	(4)	(5)	(6)
Pin Joints	1.20	0.300	-	0.410	-
Web Cleats	1.20	0.344	-	0.458	-
Flange Cleats	1.00	0.403	0.507	0.519	0.845
Flush End Plates	1.00	0.502	0.631	0.609	0.967
Extended End Plates	0.85	0.622	0.941	0.707	1.228
Rigid Joints	0.85	0.927	1.402	0.855	1.406

E.W.F. stands for End Warping Free;

E.W.P. stands for End Warping Prevented.

Table 4.4

Effect of End Restraint on Lateral Instability - Comparison with the Design Method of BS 5950: Part 1 for Non-destabilising Load

End support	n-factor from BS 5950	$\frac{L_E}{L}$ from BS5950	W_b/W_p using code: $L_E = L$	W_b/W_p using code: L_E from Col. 3	W_b/W_p using code: n=1, L_E from Col.3	$\frac{W_b}{W_p}$ from analysis: E.W.F.	$\frac{W_b}{W_p}$ from analysis: E.W.P.
(1)	(2)	(3)	(4)	(5)	(6)	(7)	(8)
PJ	0.940	1.00	0.414	-	-	0.494	-
WC	0.929	1.00	0.475	-	-	0.561	-
FC	0.917	0.85	0.555	0.661	0.588	0.651	0.881
FEP	0.905	0.85	0.669	0.798	0.697	0.787	1.018
EEP	0.883	0.70	0.911	1.296	1.144	1.069	1.369
RJ	0.627	0.70	1.018	1.274	0.861	1.510	1.591

E.W.F. stands for End Warping Free;

E.W.P. stands for End Warping Prevented.

PJ, WC, FC, FEP, EEP and RJ stand for Pin Joints, Web Cleats, Flange Cleats, Flush End Plates, Extended End Plates and Rigid Joints respectively.

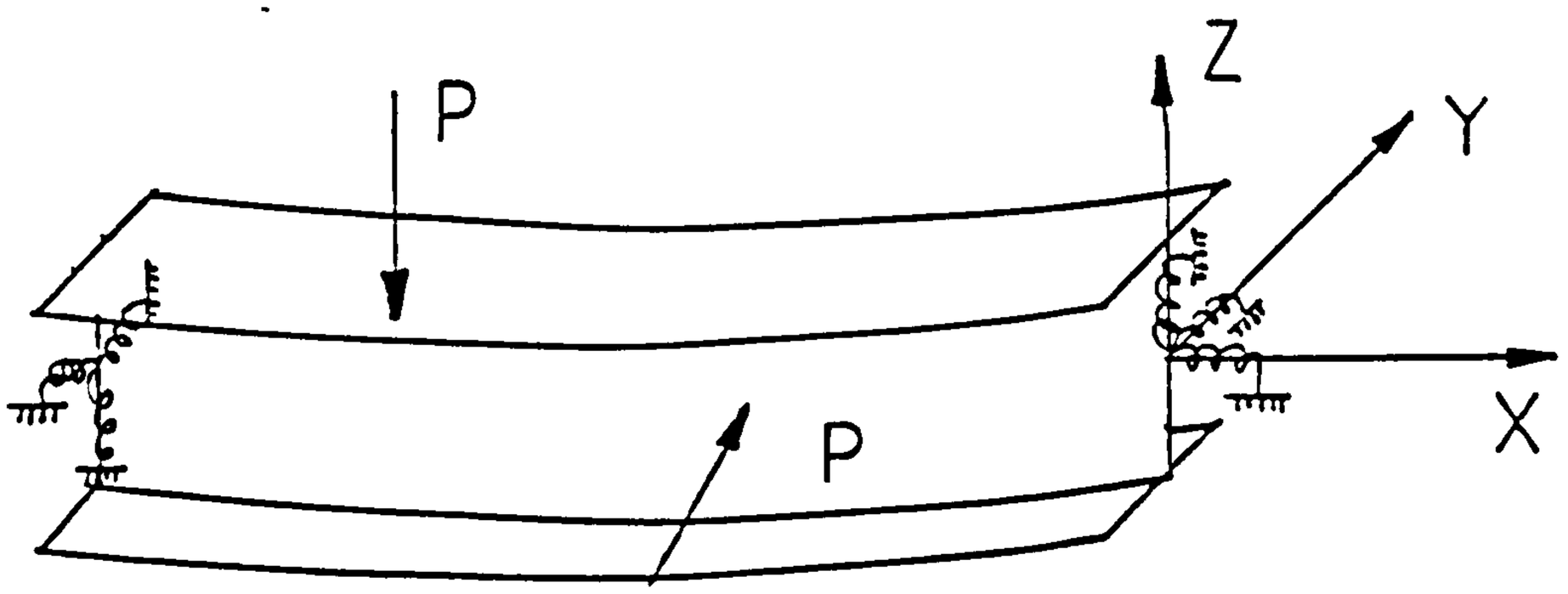

Fig. 4·1a A typical end restrained beam

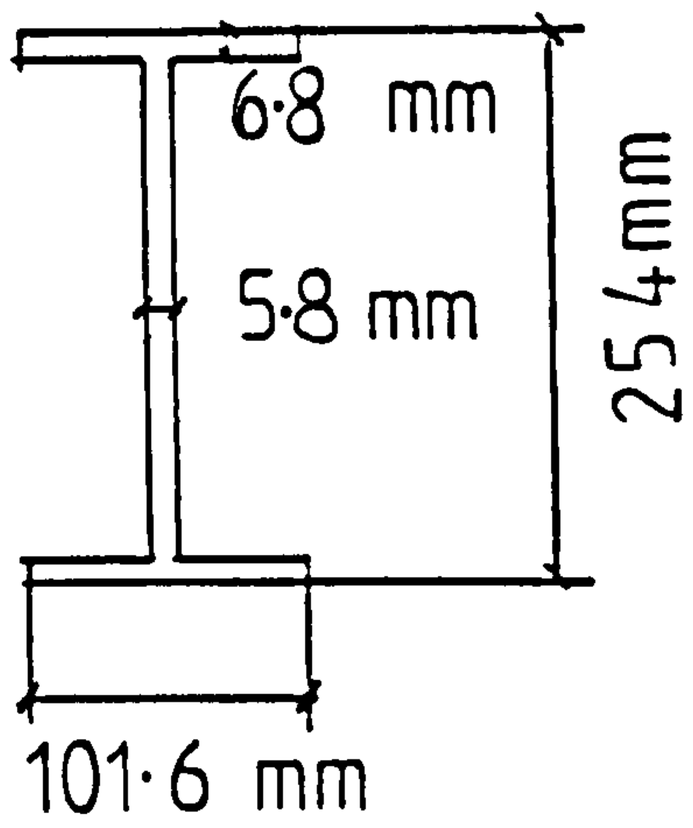

Fig. 4·1b Dimensions

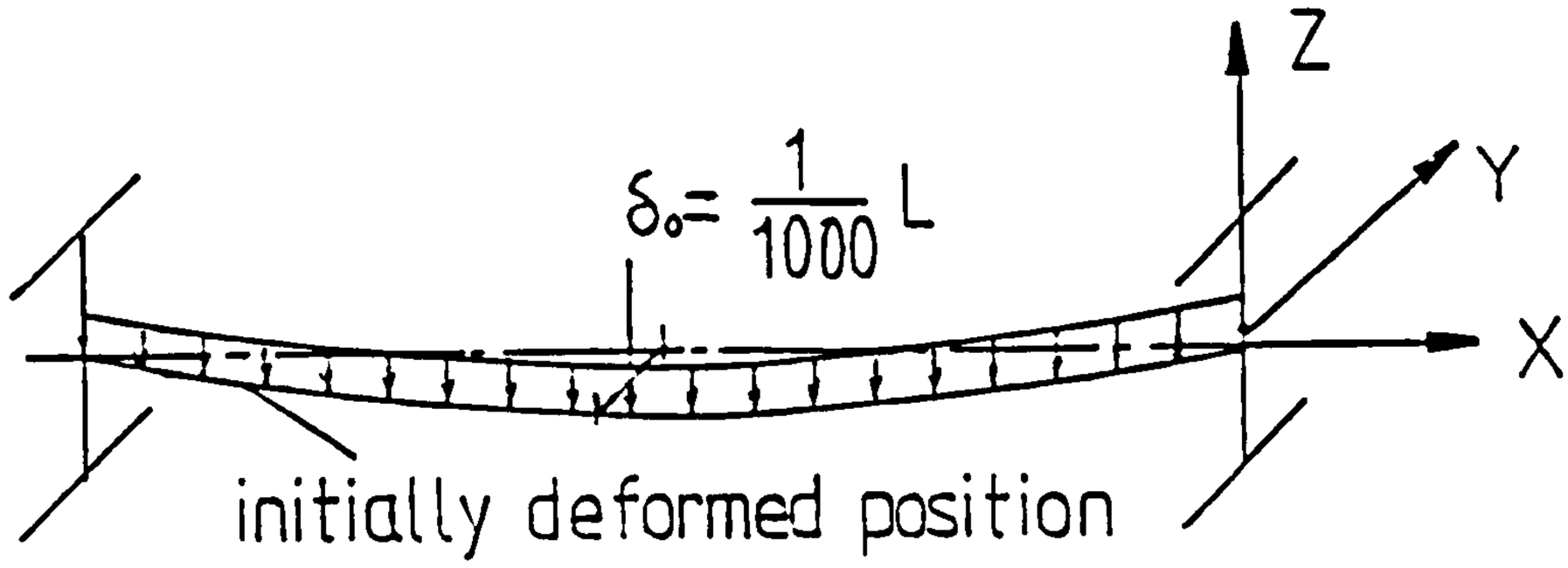

Fig 4·1c Loading condition and initial deflection

Fig. 4·1 Definition of problem under study

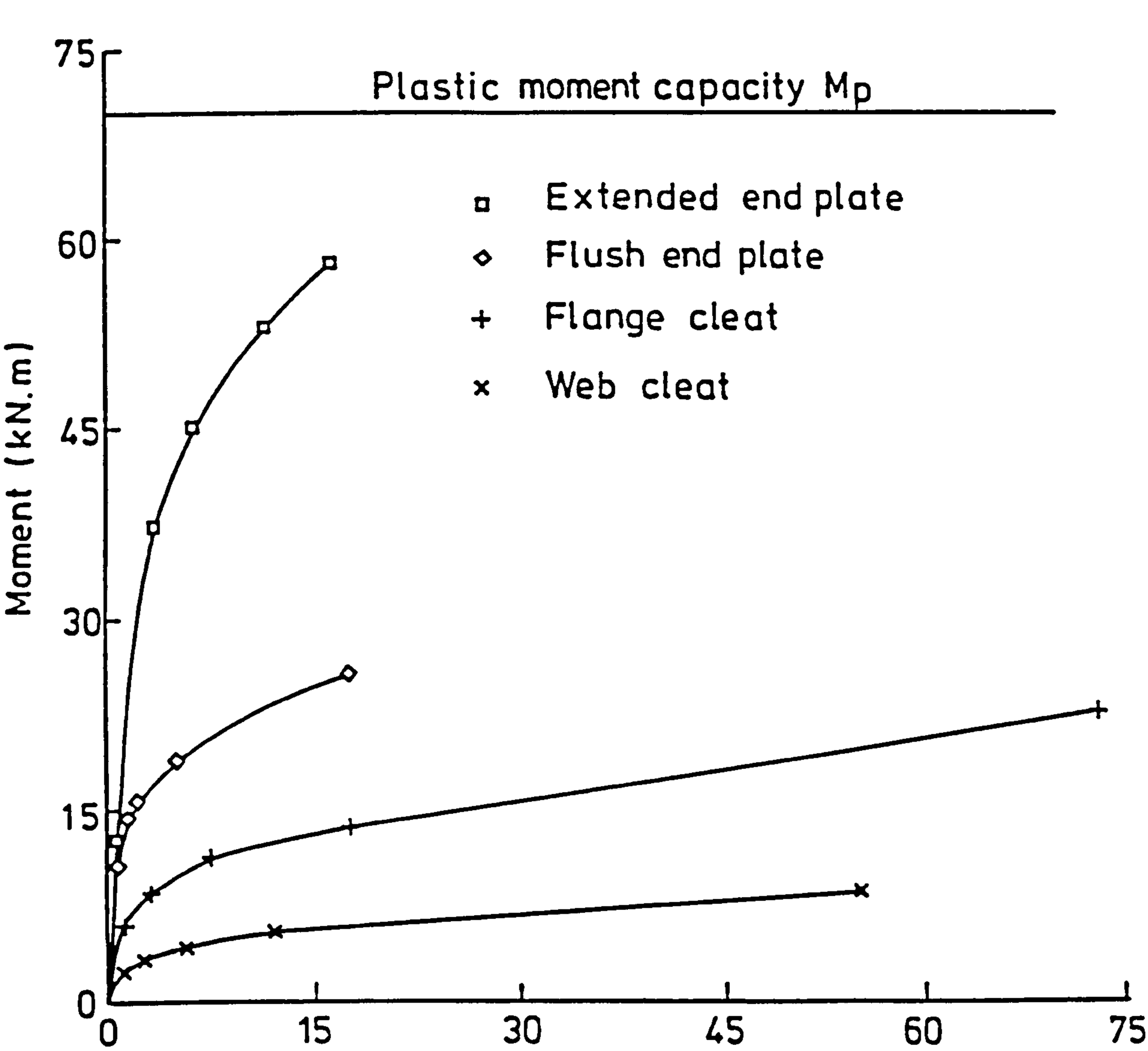

FIG. 4·2 MOMENT-ROTATION CURVES FOR DIFFERENT CONNECTIONS

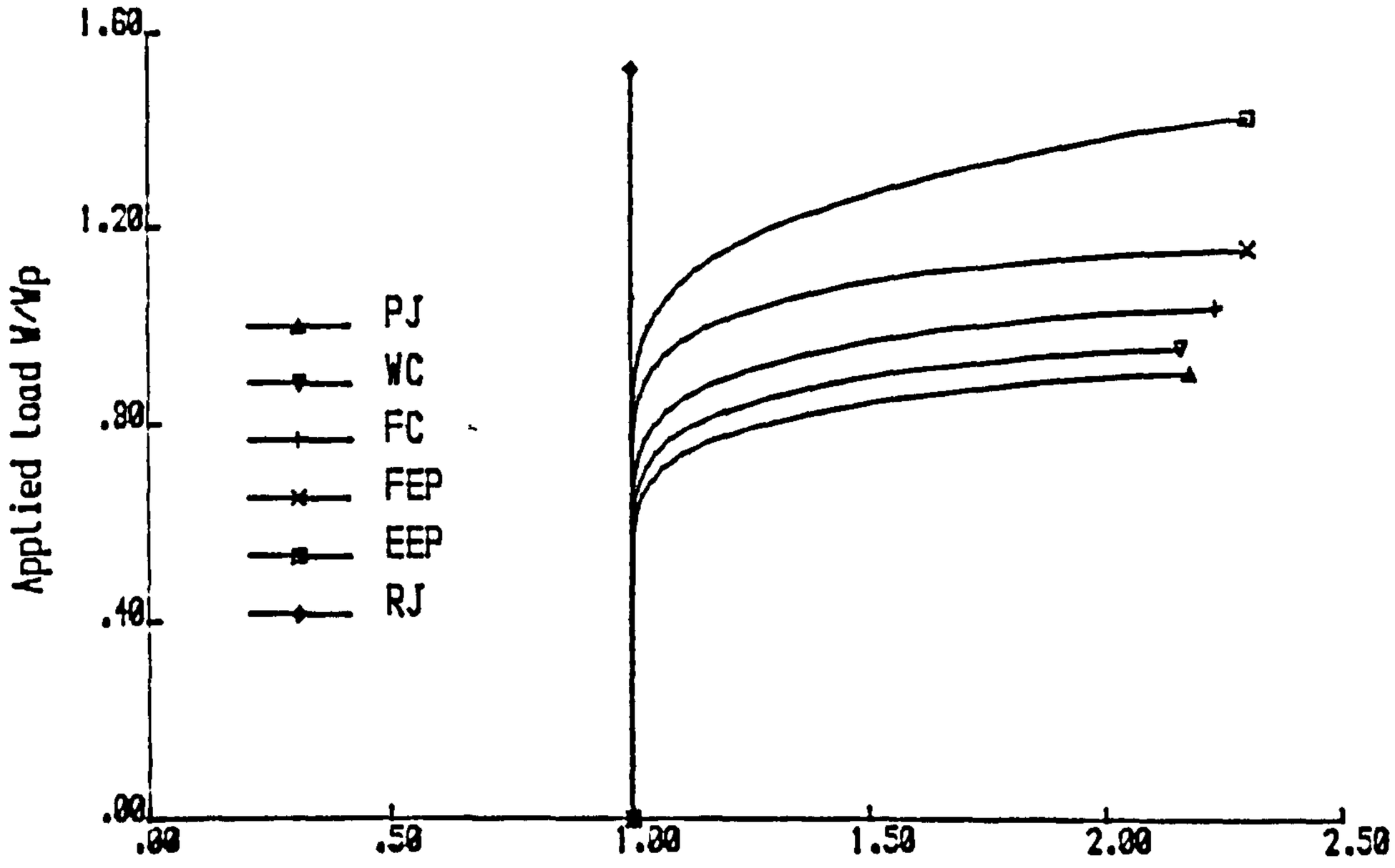

(a) Minor axis deflection at midspan/(L/1000)

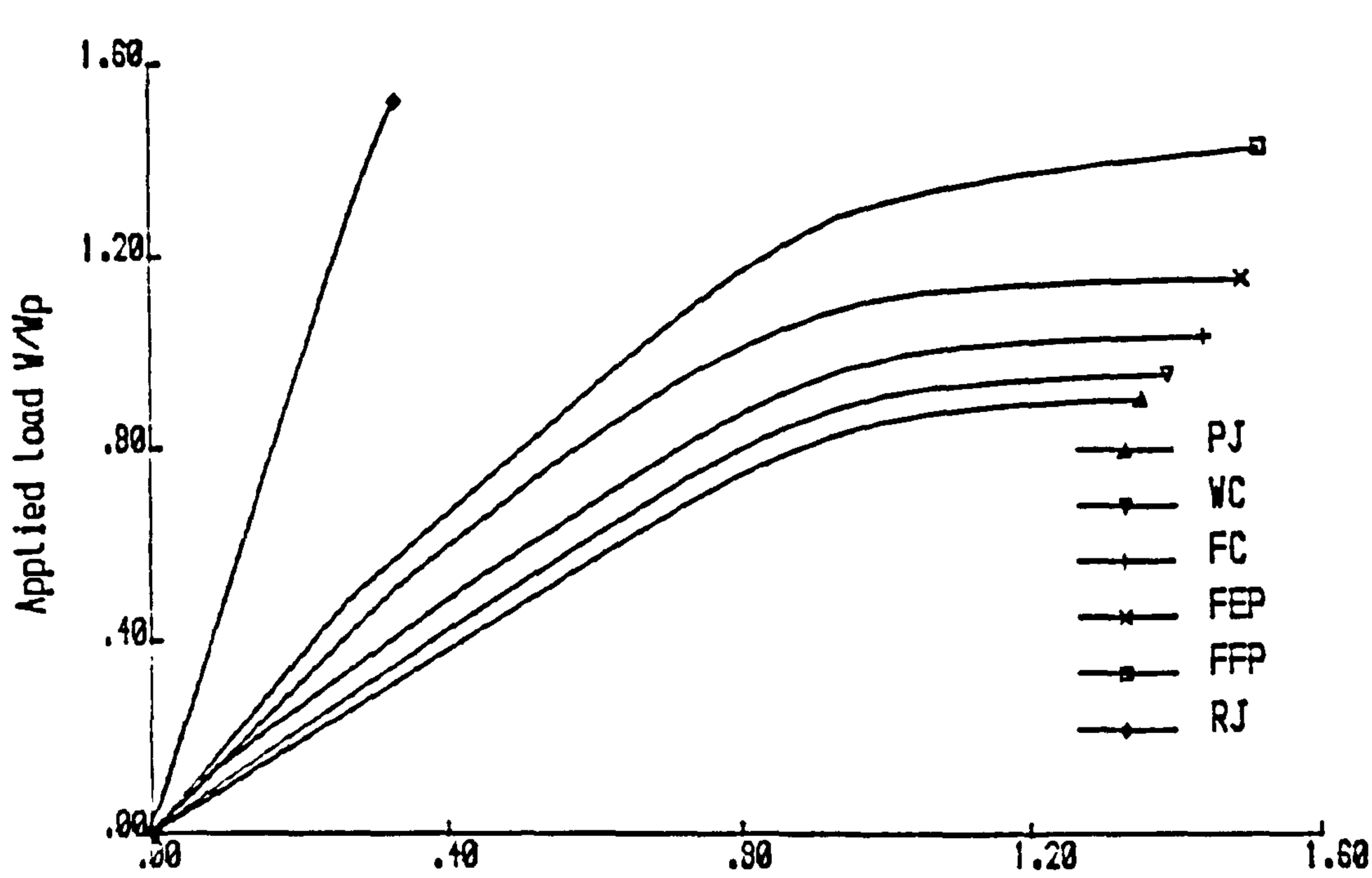

(b) Major axis deflection at midspan/(L/1000)

Fig. 4.3 Load - deflection relationships for various connections. End warping free. $L/r_y = 40$

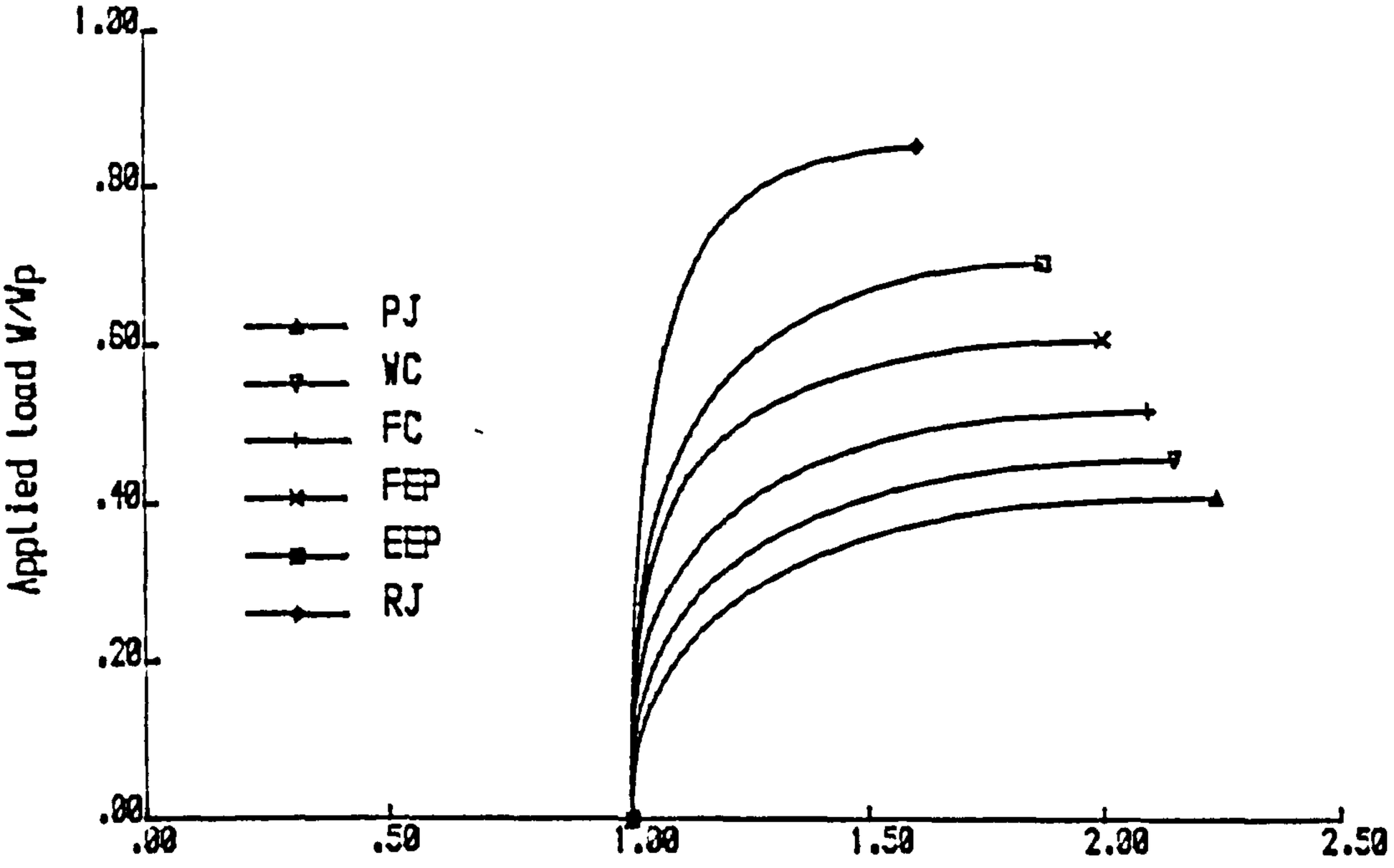

(a) Minor axis deflection at midspan/(L/1000)

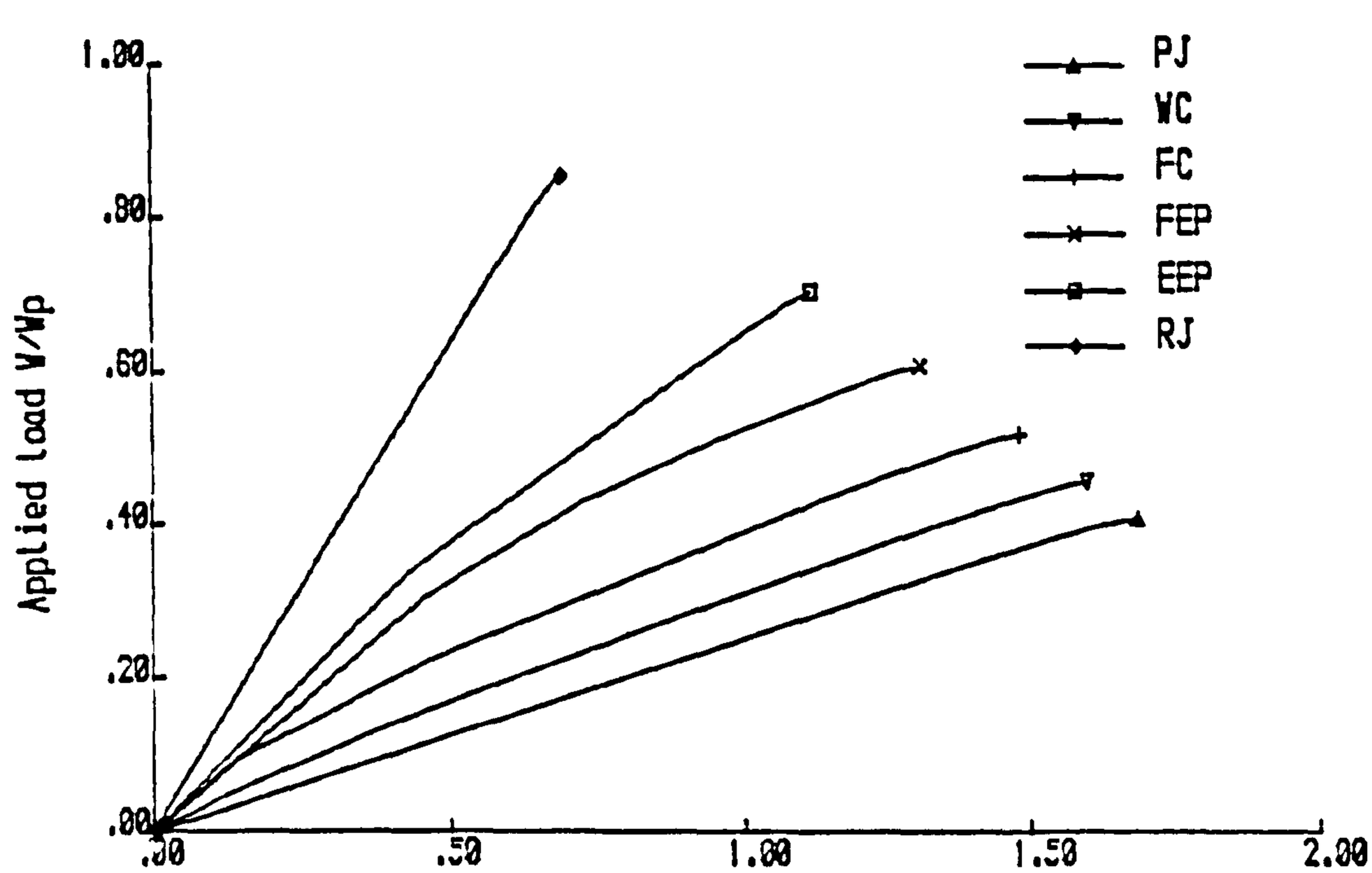

(b) Major axis deflection at midspan/(L/1000)

Fig. 4.4 Load - deflection relationships for various connections. End warping free. L/r_y=150

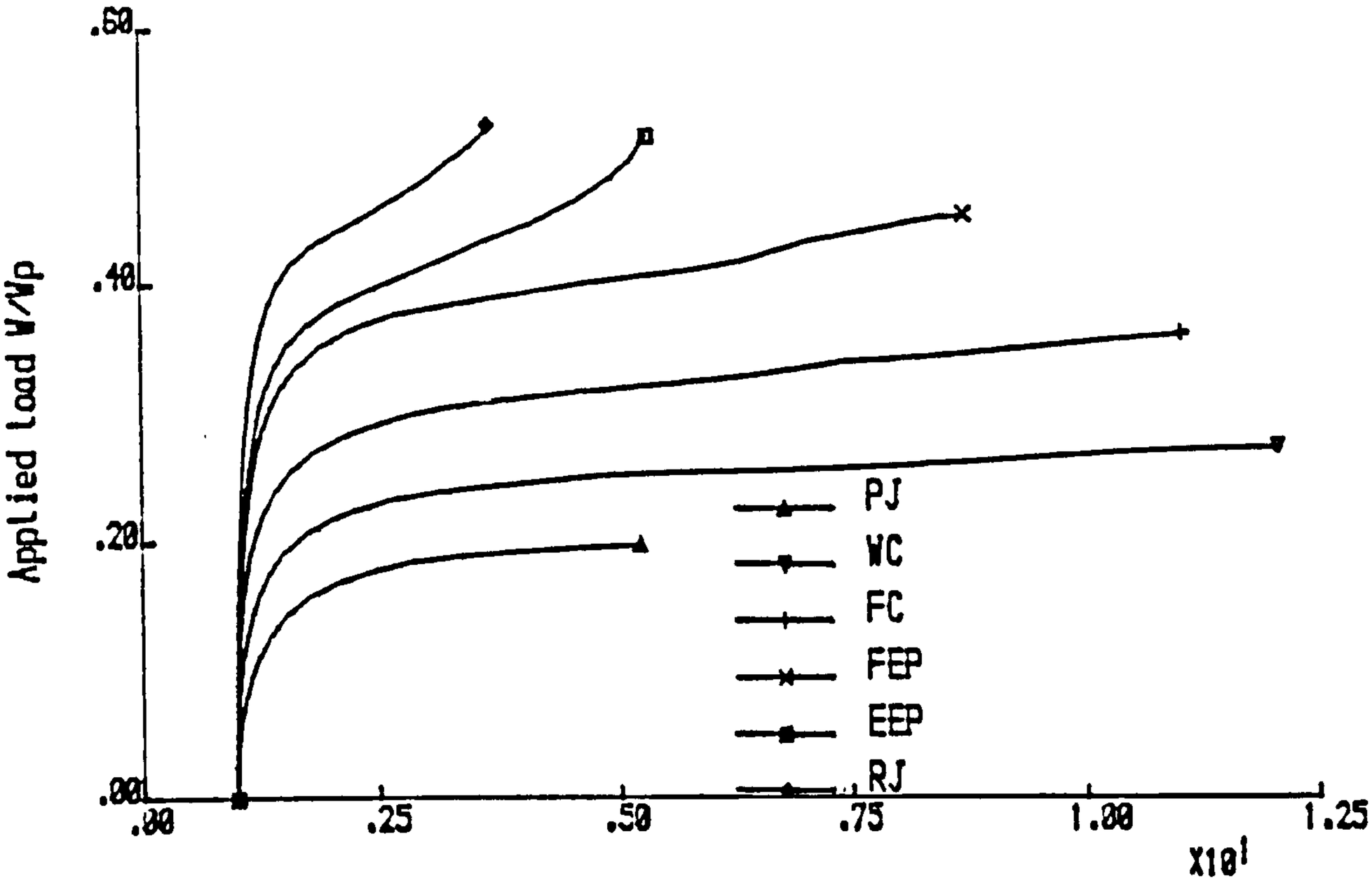

(a) Minor axis deflection at midspan/(L/1000)

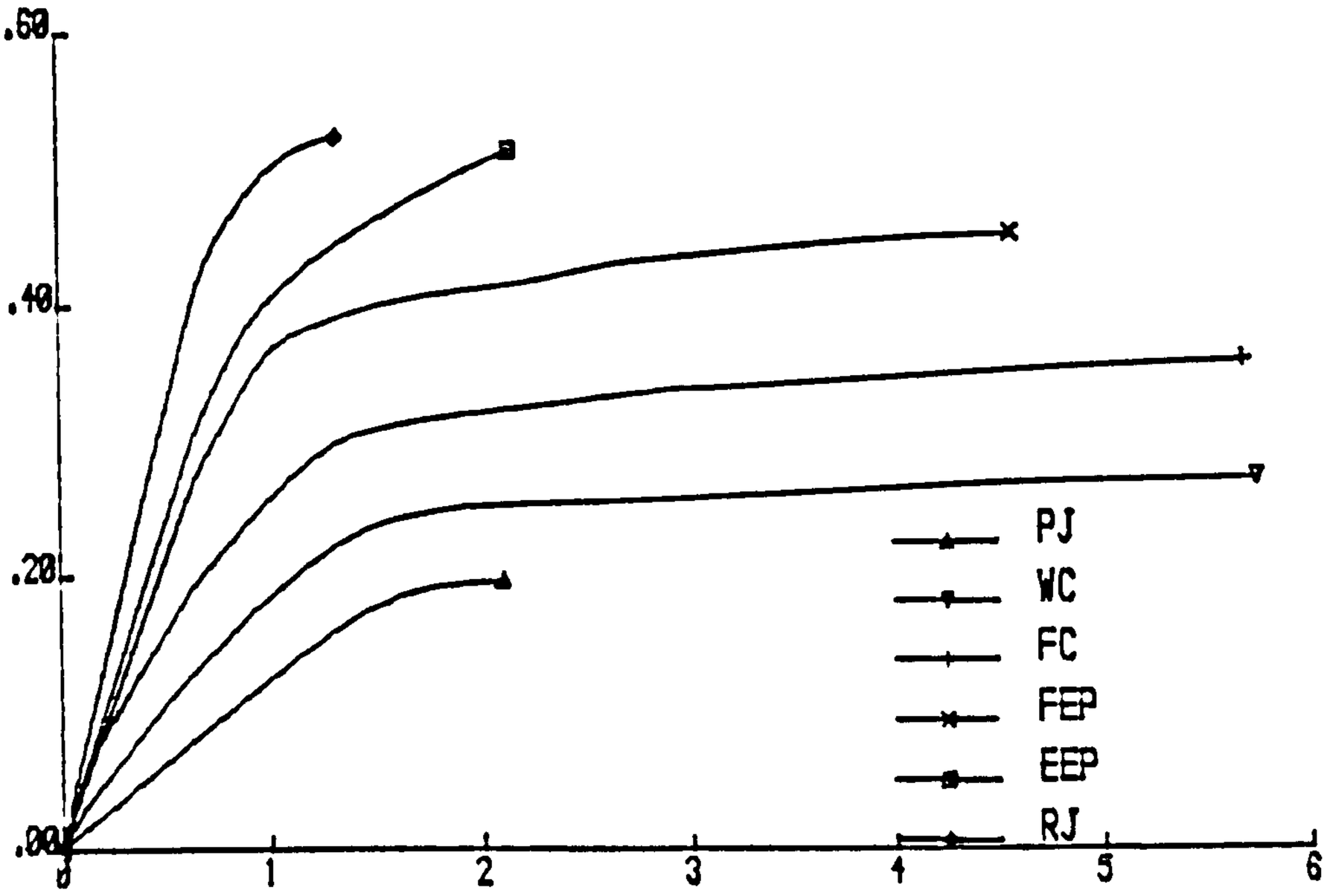

(b) Major axis deflection at midspan/(L/1000)

Fig. 4.5 Load - deflection relationships for various connections. End warping free. L/r_y=300

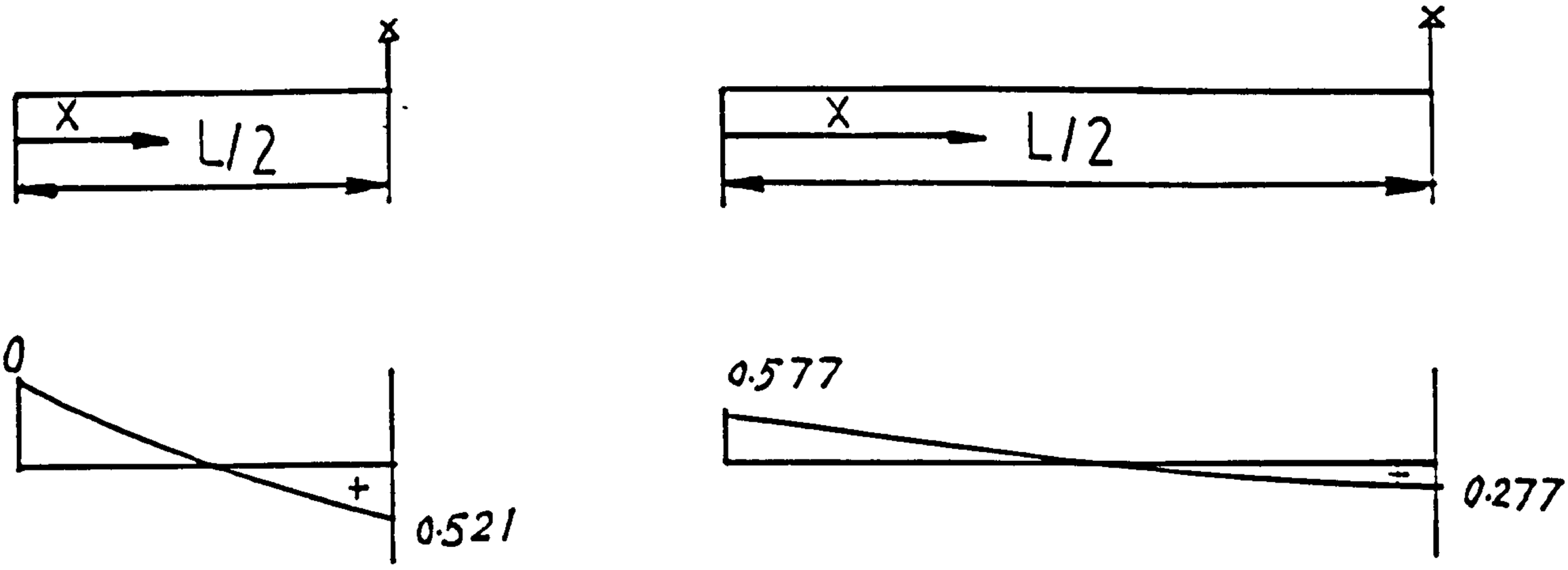

$\frac{L}{r_y} = 40$ $\frac{L}{r_y} = 150$

Fig. 4·6 In-plane moment diagrams for different connections at L/r_y=40, 150 and 300

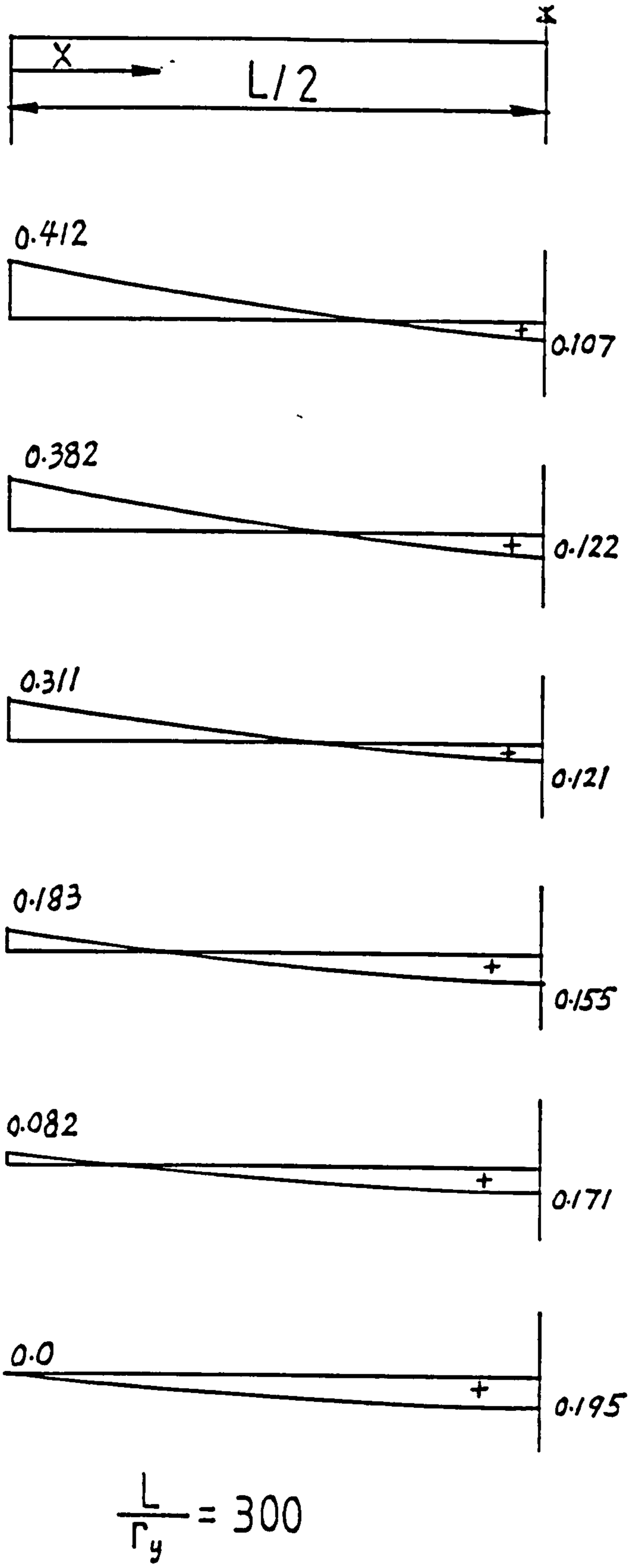

$$\frac{L}{r_y} = 300$$

Fig. 4·6 (continued)

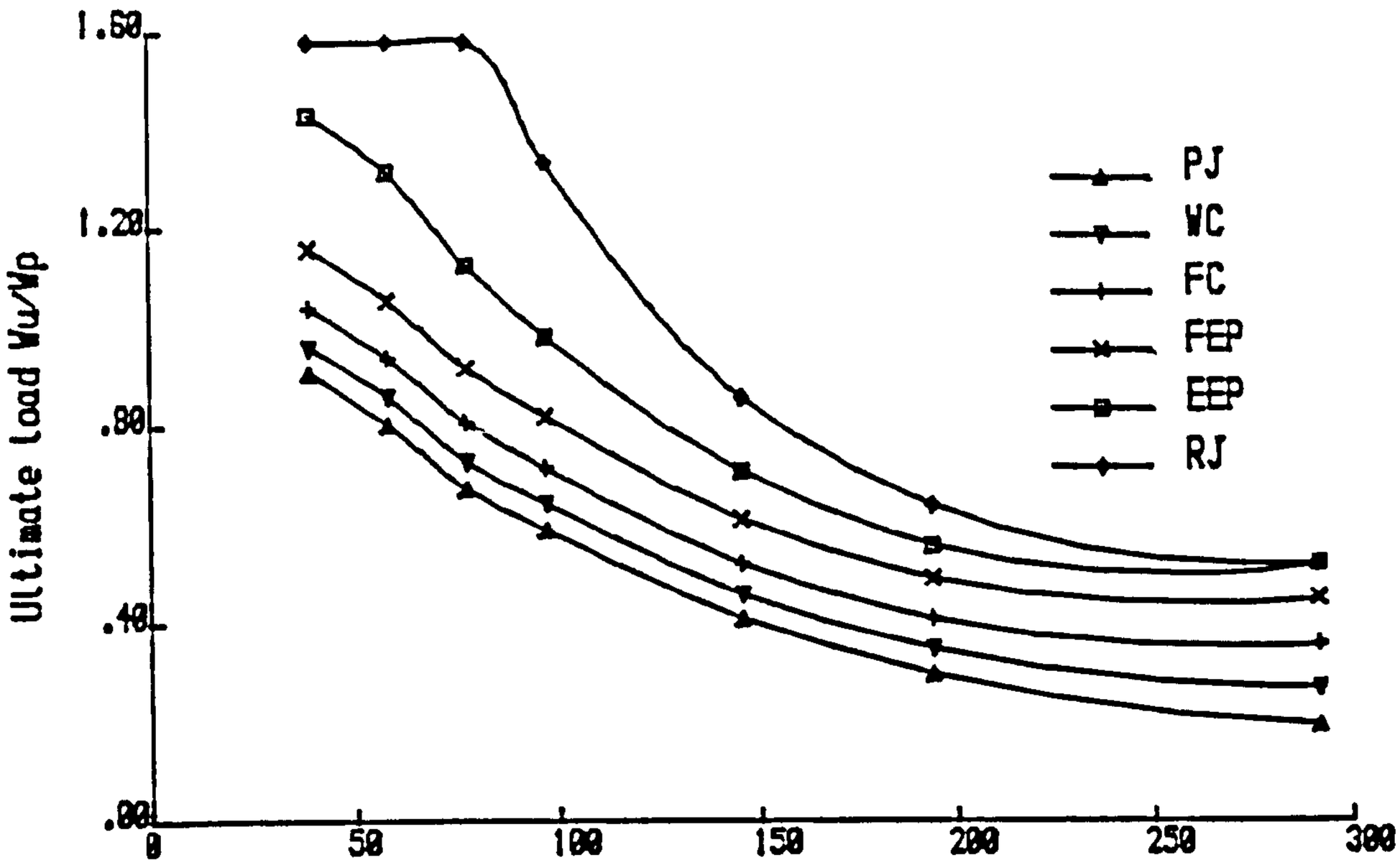

Fig. 4.7a Beam buckling curves for various connections. End warping free.

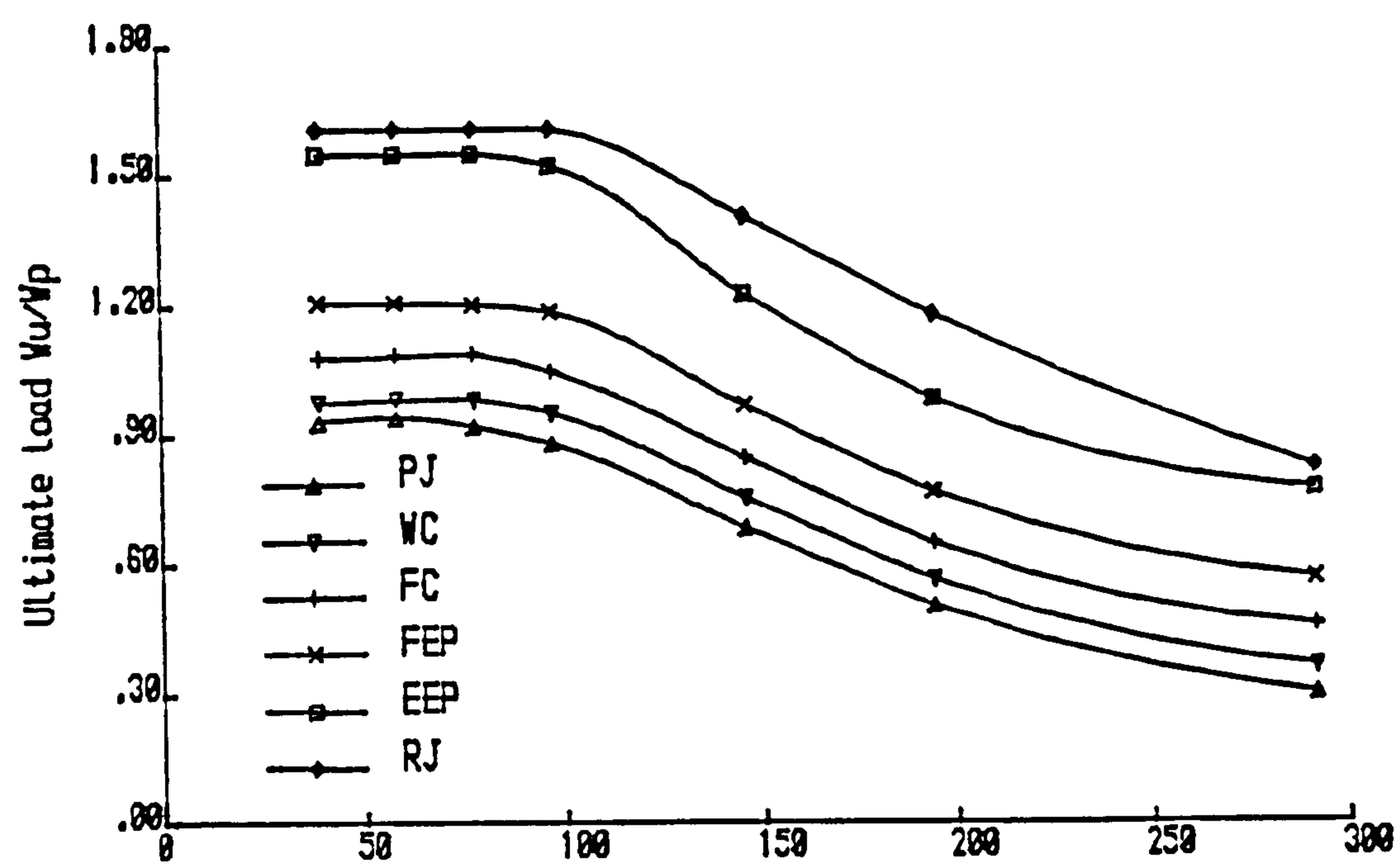

Fig. 4.7b Beam buckling curves for various connections. End warping prevented.

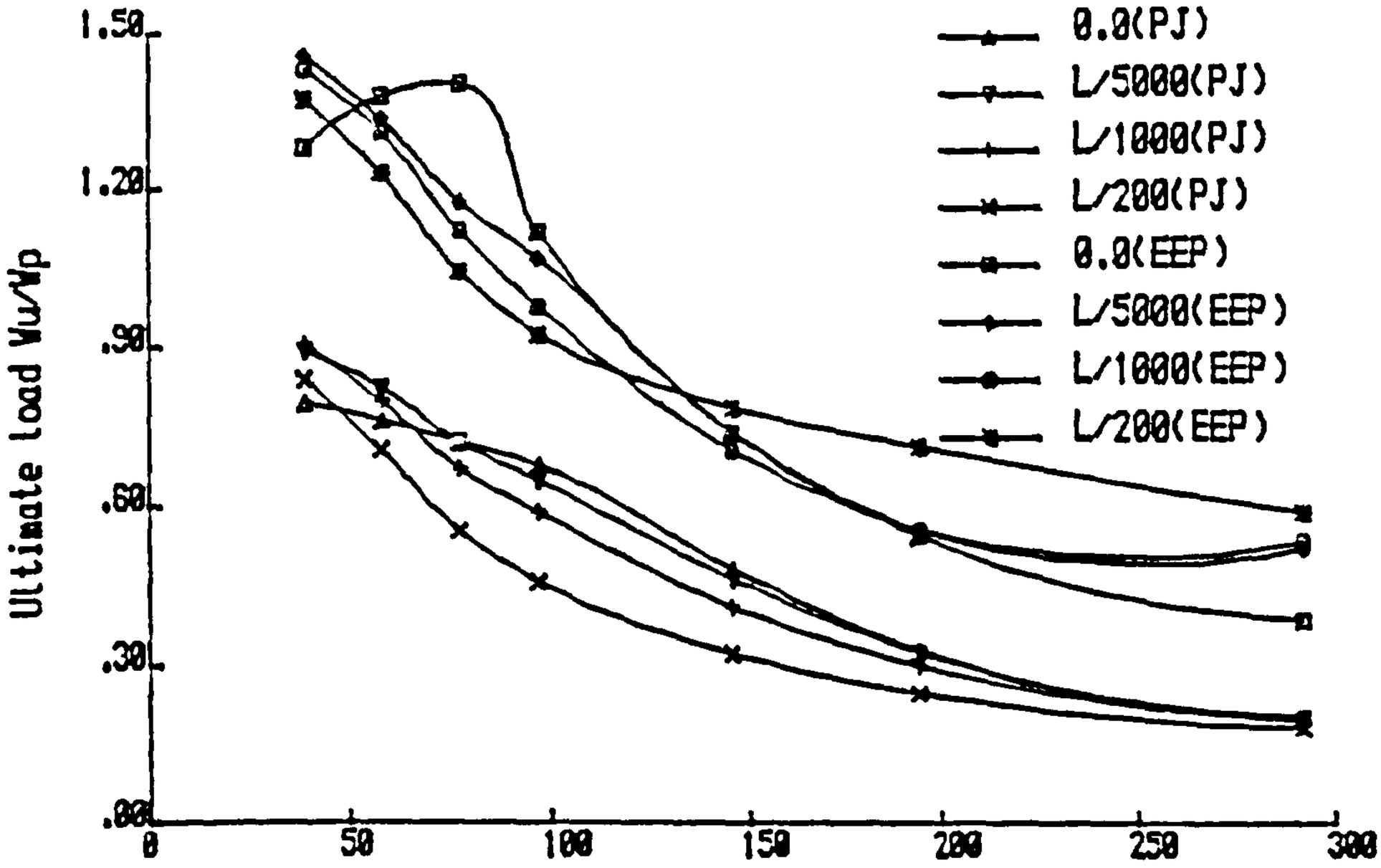

Geometrical slenderness L/r_y

Fig. 4.8a Beam buckling curves For various max. initial lateral deflections at midspan. E.W.F.

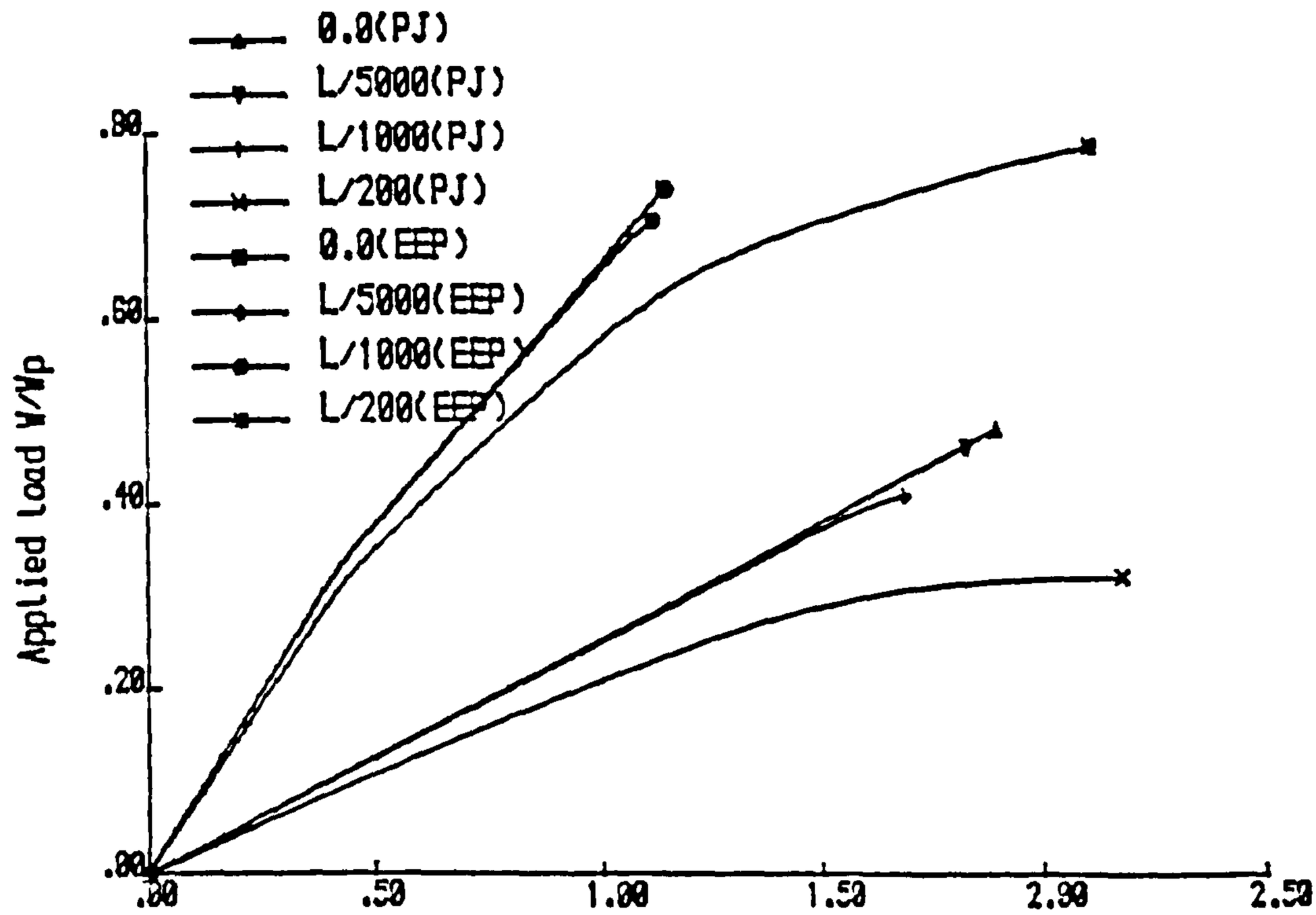

In-plane deflection at midspan/(L/1000)

Fig. 4.8b Load-deflection curves For various max. initial lateral deflections at midspan For Pin Joints (PJ) and Extended End Plates (EEP). End Warping Free (E.W.F.). L/r_y = 150

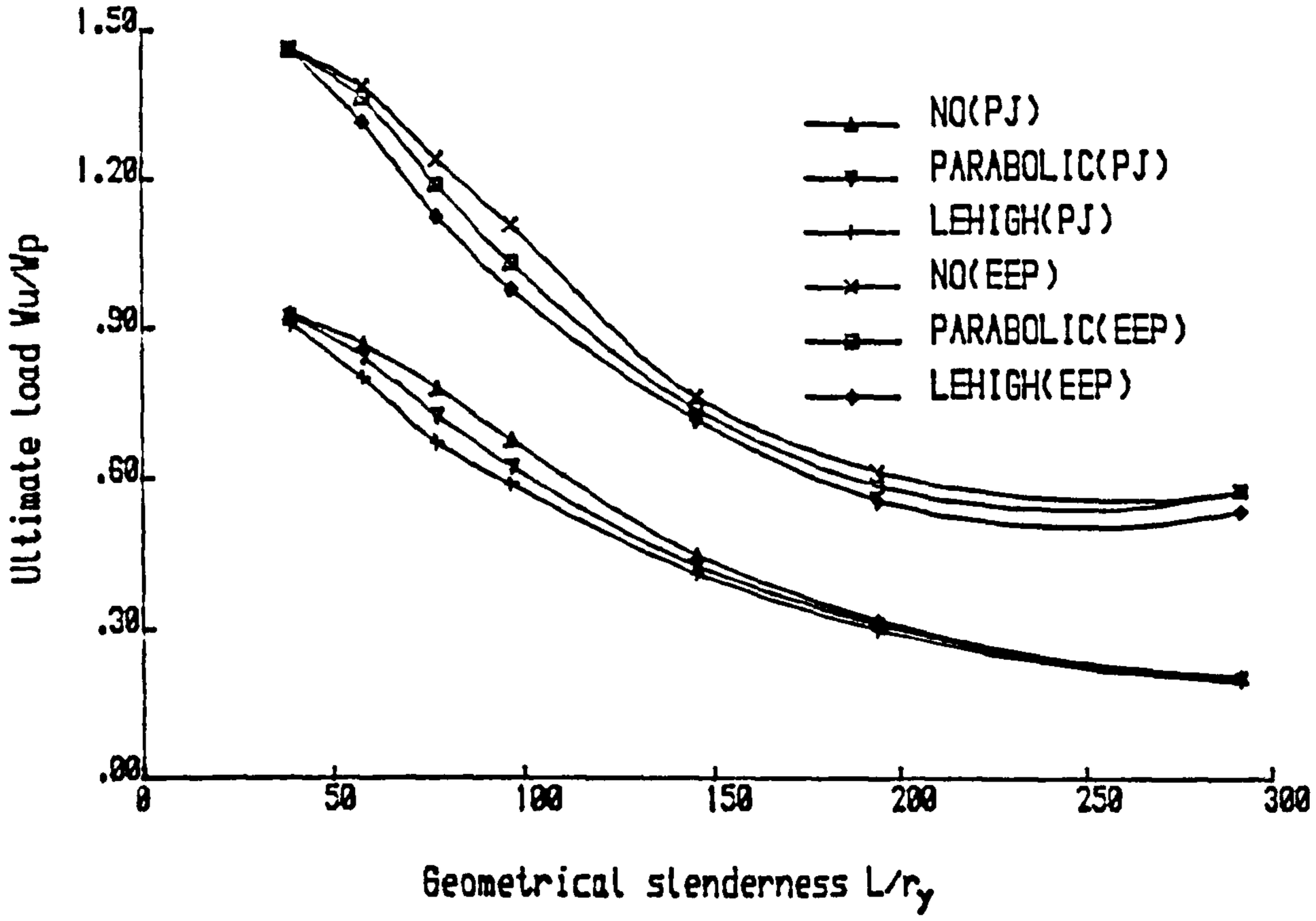

Fig. 4.9a Beam buckling curves for different types of residual stress distribution. E.W.F.

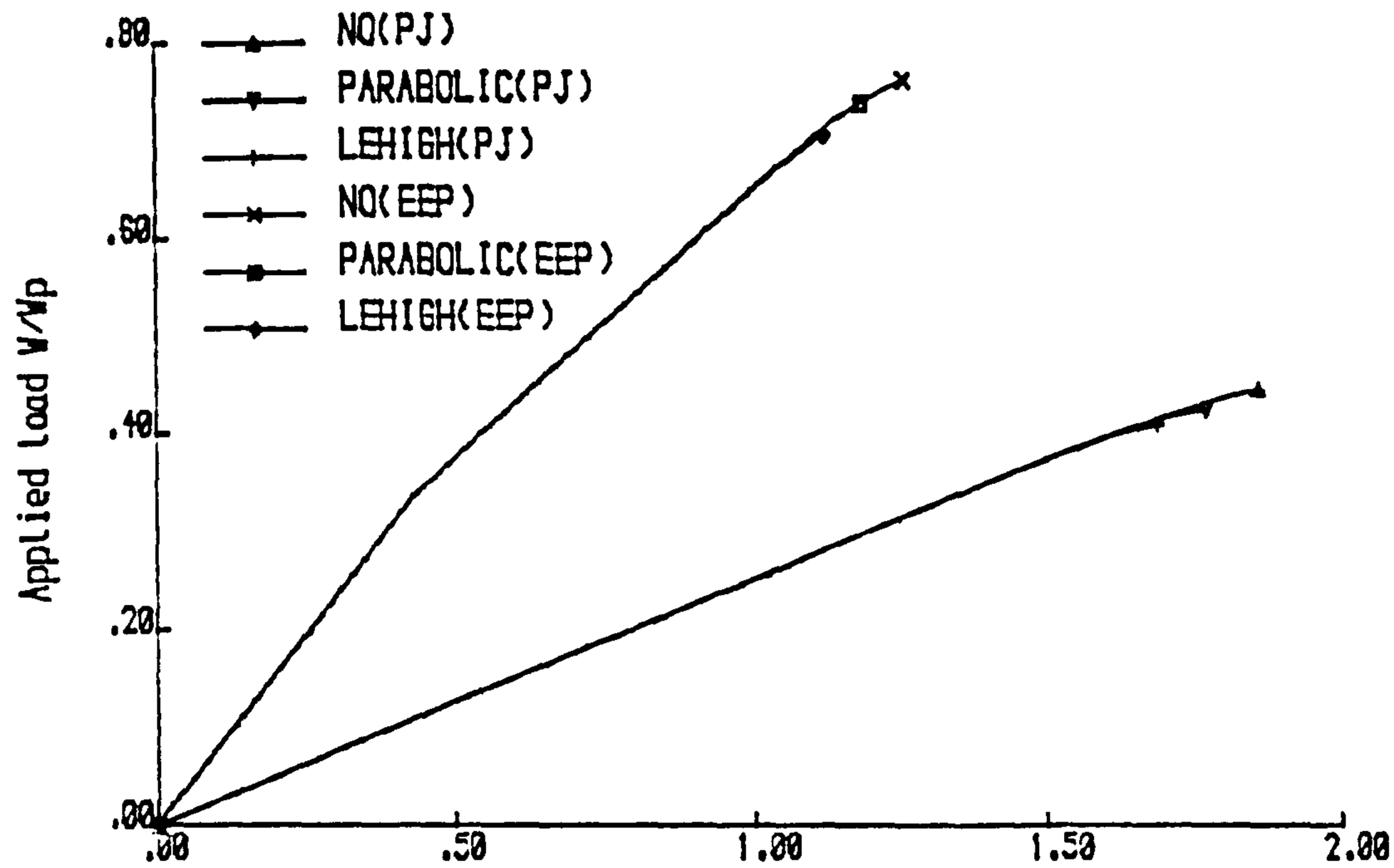

Fig. 4.9b Load-deflection curves for various types of residual stress distribution for Pin Joints (PJ) and Extended End Plates (EEP). End Warping Free (E.W.F.). $L/r_y = 150$

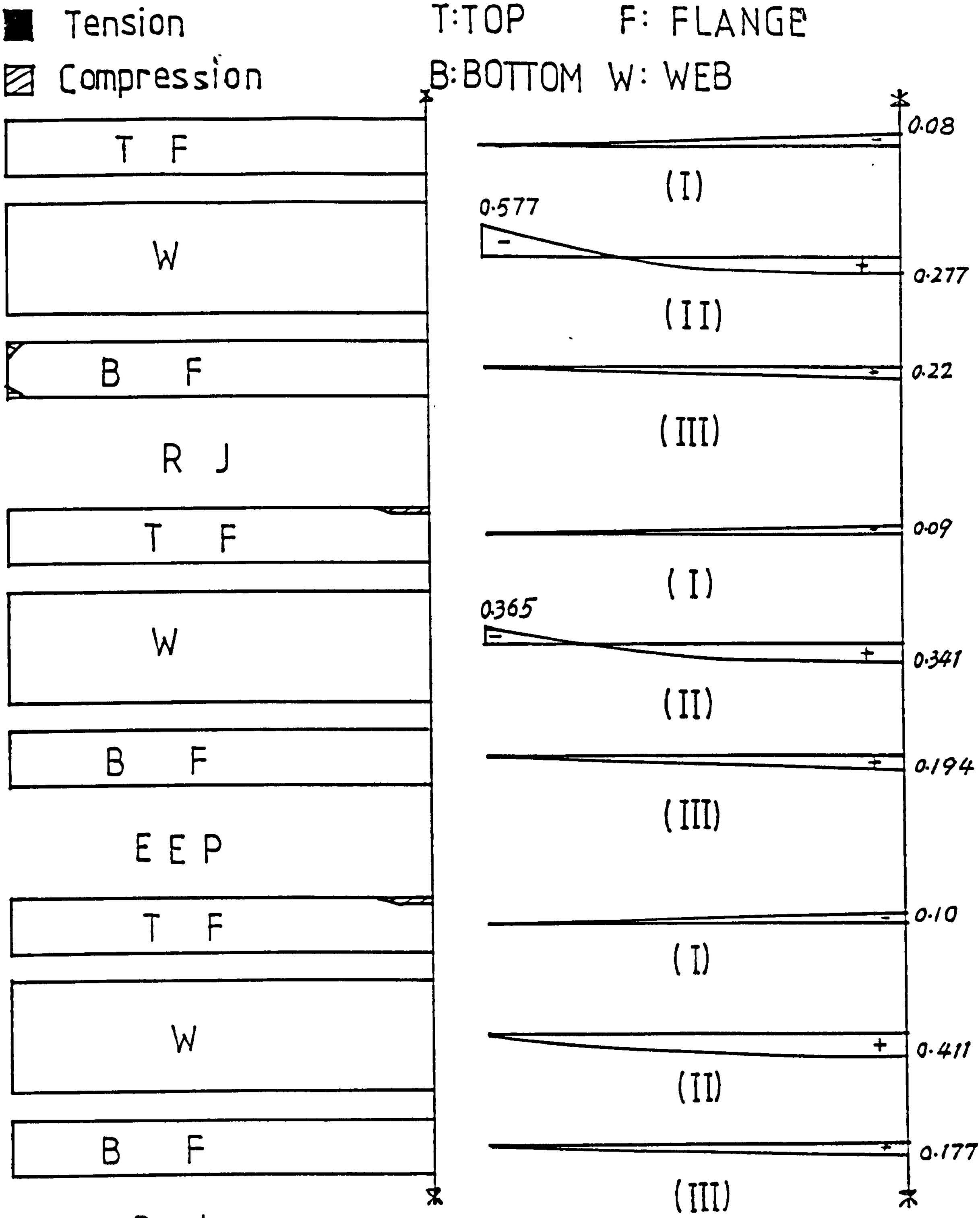

(a) yield penetration (b) moment diagram
(I) for out-of-plane moment (II) in-plane moment
(III) for bimoment

Fig. 4-10 Yield penetration and moment diagrams for different end connections, $L/r_y = 150$

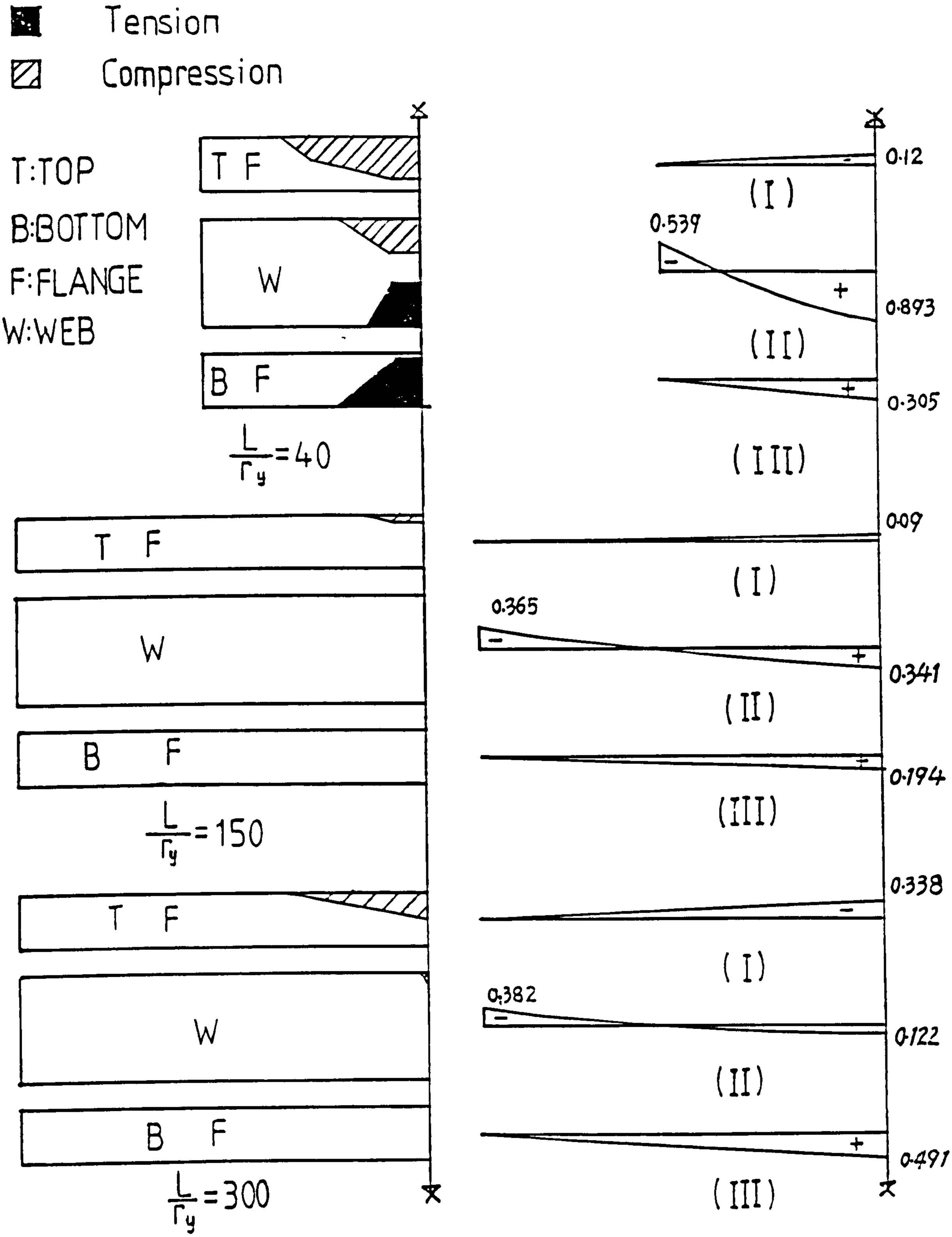

(a) yield penetration (b) moment diagram

(I) for out-of-plane moment (II) for in-plane moment

(III) for bimoment

Fig. 4·11 Yield penetration and moment diagrams for different slendernesses, Extented End Plates

Five values describing the yield status for the cross-section:

(1)	elastic moment limit about major axis:	46.67 kN.m
(2)	plastic moment capacity about major axis:	70.02 kN.m
(3)	elastic moment limit about minor axis:	7.18 kN.m
(4)	plastic moment capacity about minor axis:	10.76 kN.m
(5)	elastic bimoment limit:	0.817 $kN.m^2$

-	-	residual stress
-	+	bimoment
+	-	minor axis bending
-	-	major axis bending

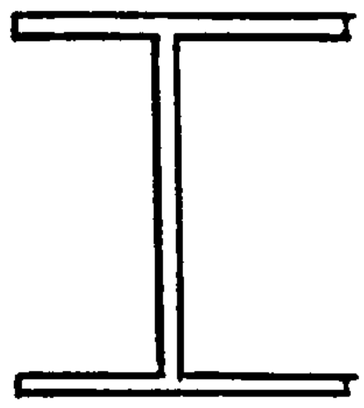

+	+	major axis bending
+	-	minor axis bending
+	-	bimoment
-	-	residual stress

Fig. 4.12a The signs of strains caused by various positive actions referring to the beam's central cross-section

-	-	residual stress
-	+	bimoment
-	+	minor axis bending
-	-	major axis bending

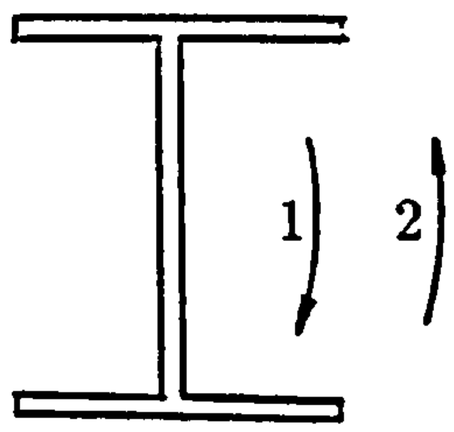

1. direction of moment from minor axis stress

2. direction of moment from major axis stress

+	+	major axis bending
-	+	minor axis bending
+	-	bimoment
-	-	residual stress

Fig. 4.12b The signs of strains in the studied beam caused by various actions referring to the beam's central cross-section

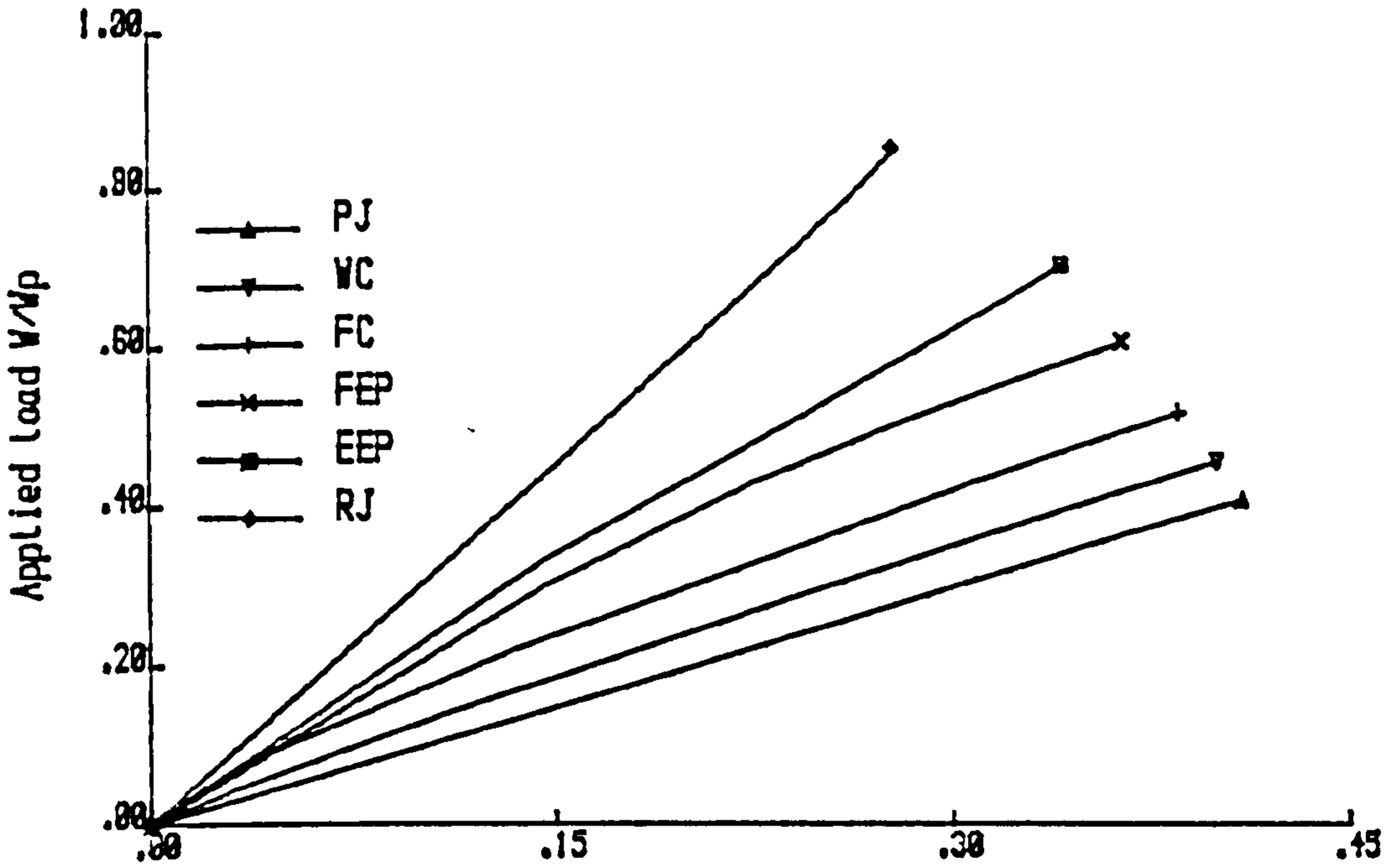

(a) Moment about major axis at midspan/Mp

Fig. 4.13a Load-moment curves for various connections. End warping free. L/r_y= 150

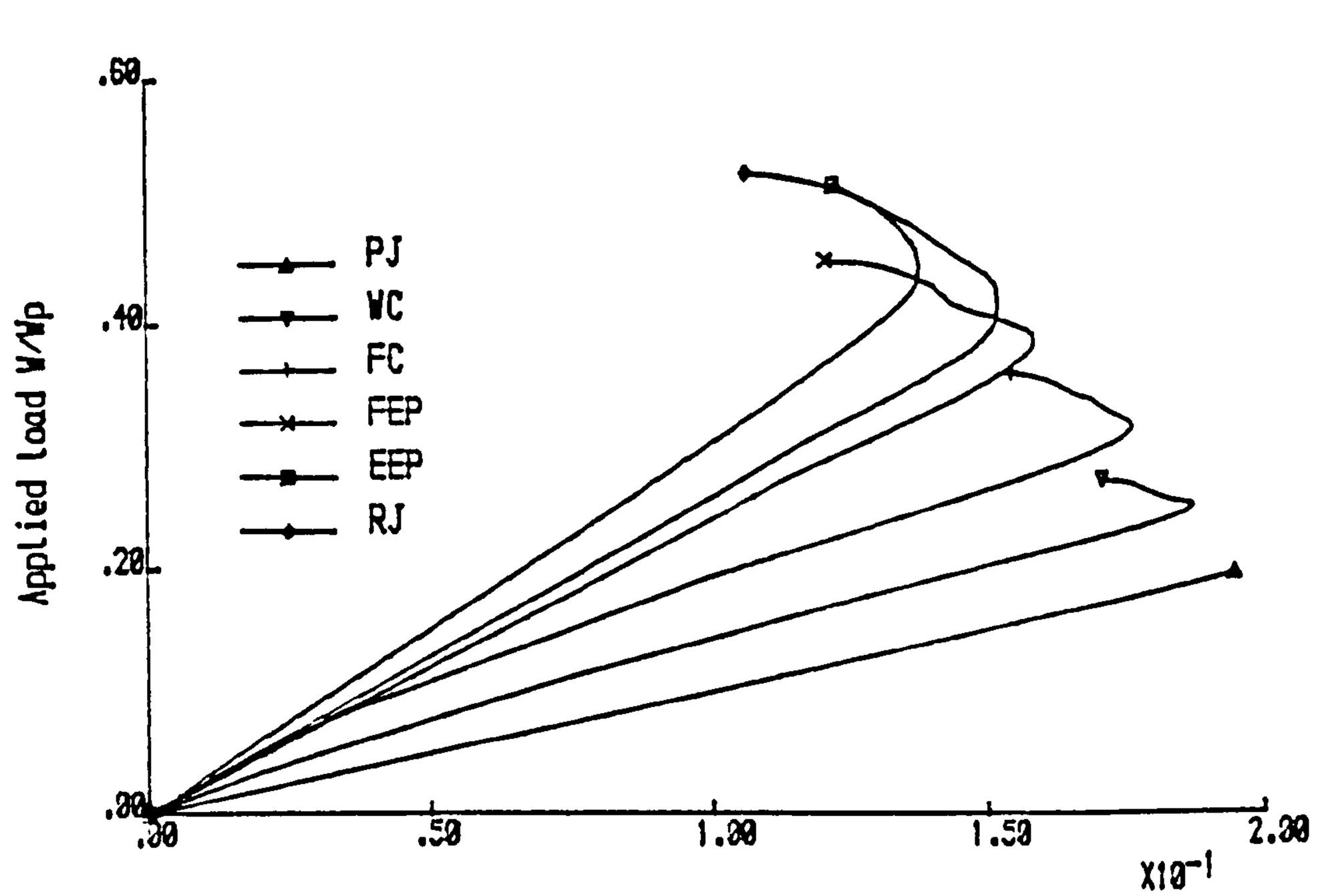

(b) Moment about major axis at midspan/Mp

Fig. 4.13b Load versus moment relationships for various connections. End warping free. L/r_y =300

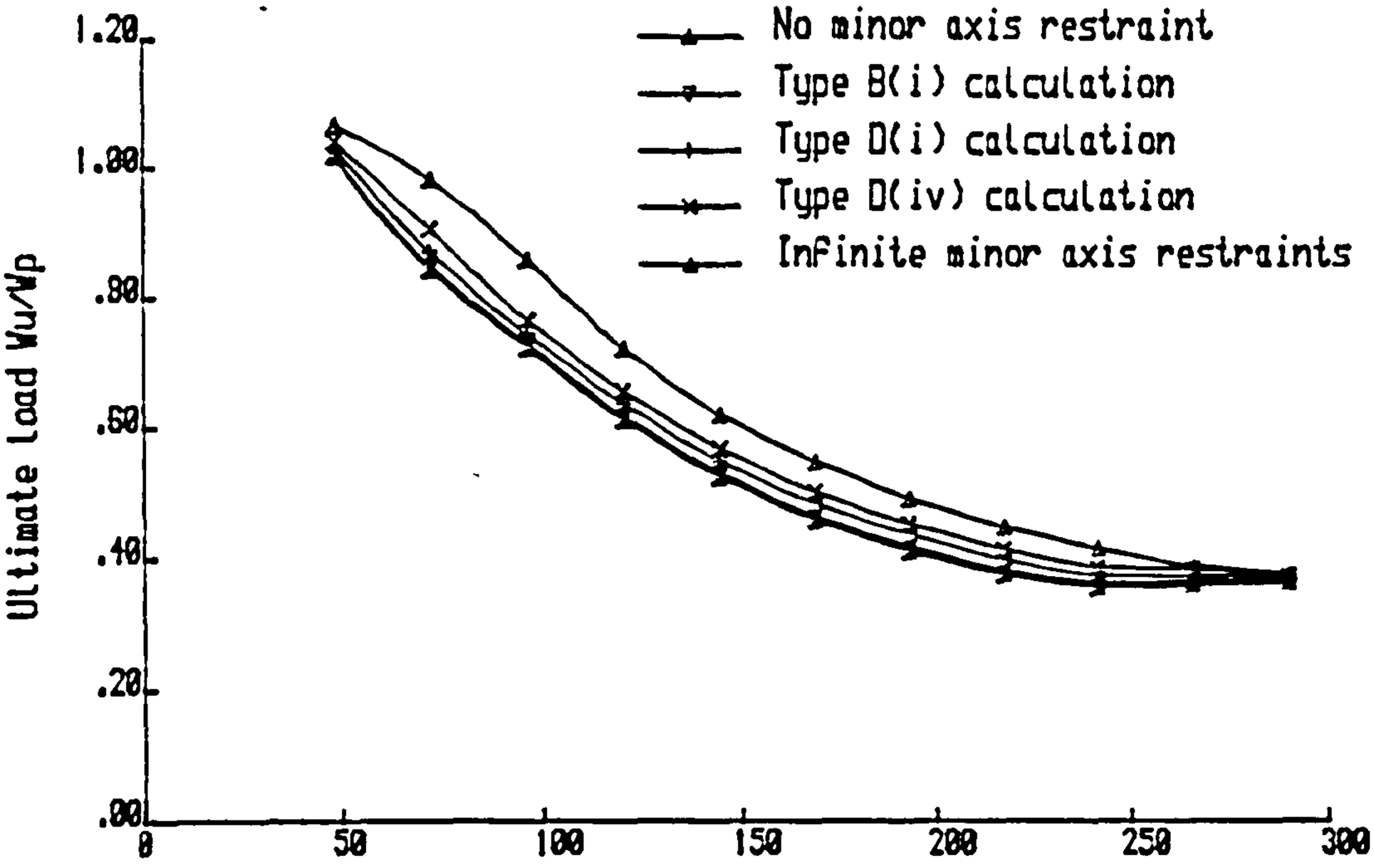

Fig. 4.14 Beam buckling curves for various minor axis stiffness calculations from Ref. 59 for flange cleat connections.

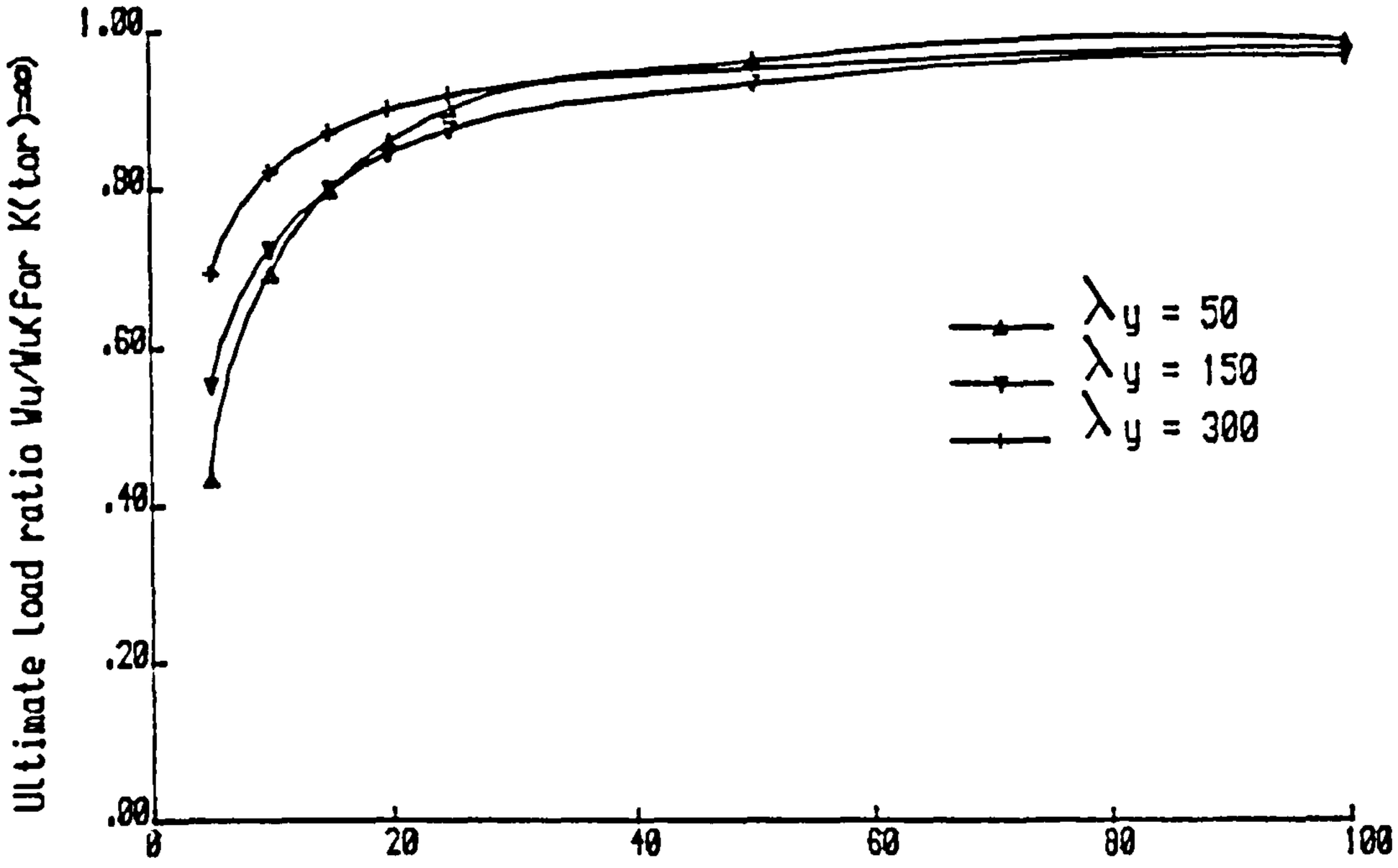

Fig. 4.15 Ultimate load ratio-end torsional stiffness relationships for various beam slendernesses $\lambda_y = L/r_y$

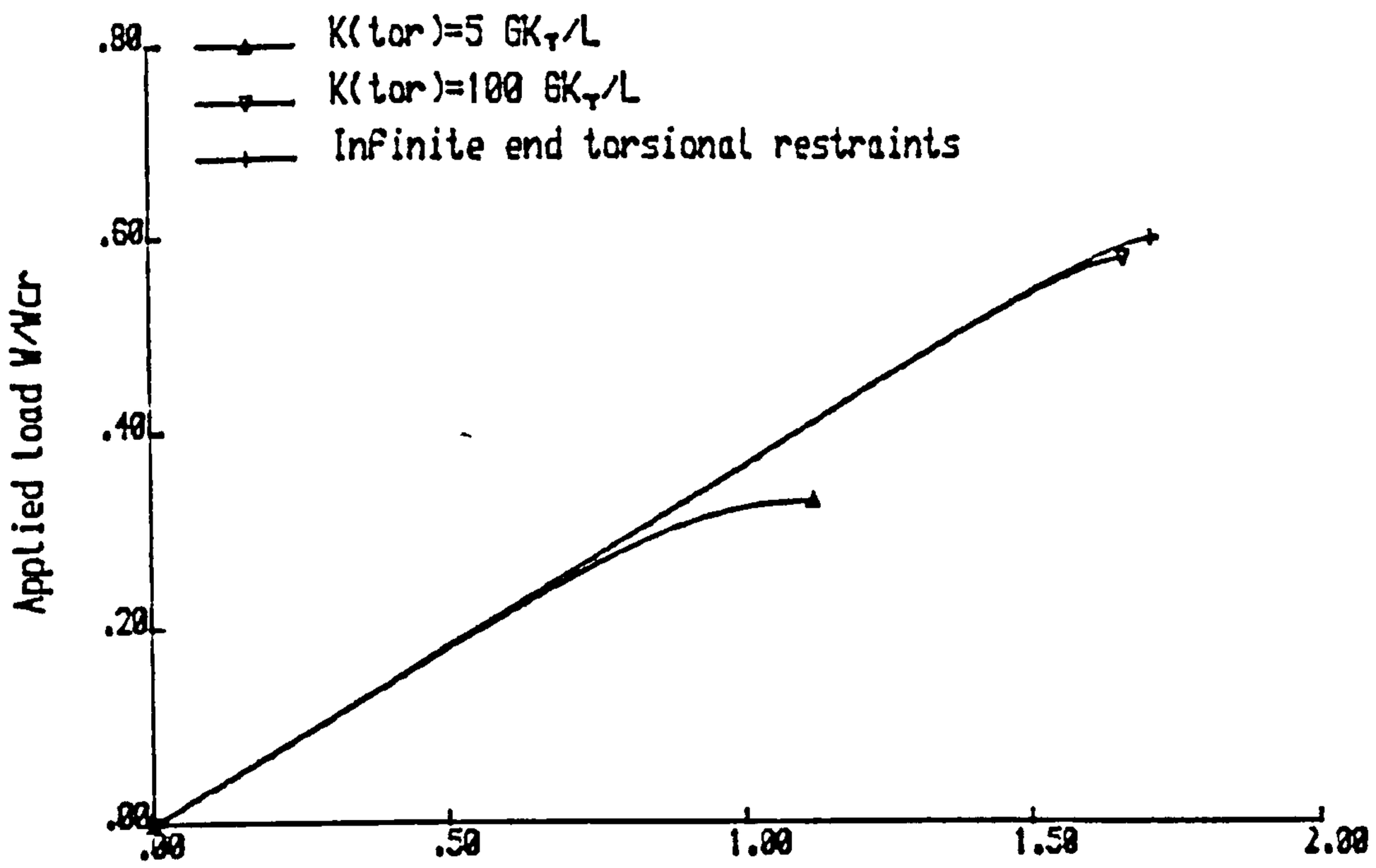

(a) In-plane deflection at midspan/(L/1000)

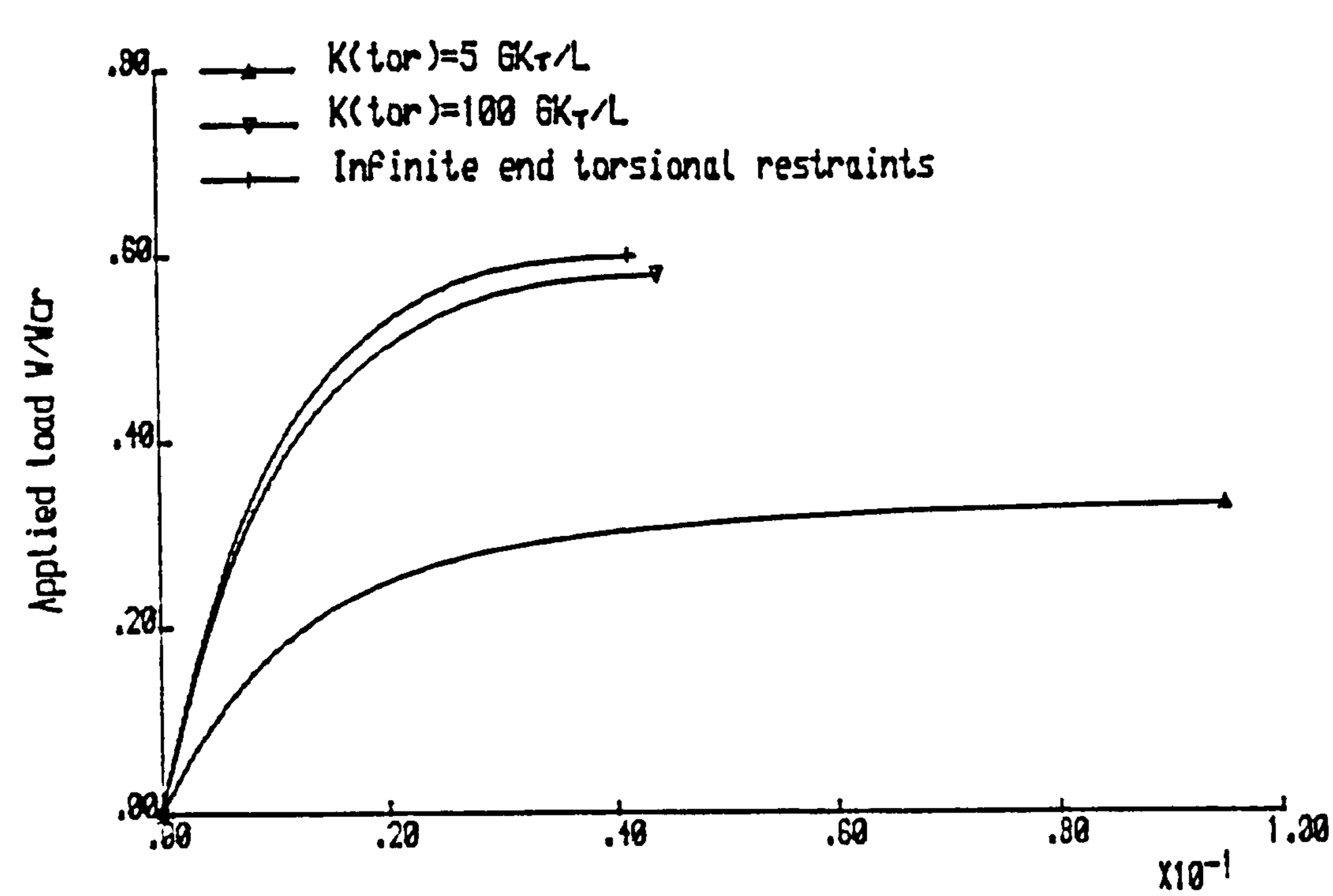

(b) Axial twisting at midspan (rad)

Fig. 4.16 Load-deflection curves for various end torsional restraints. L/r_y=150

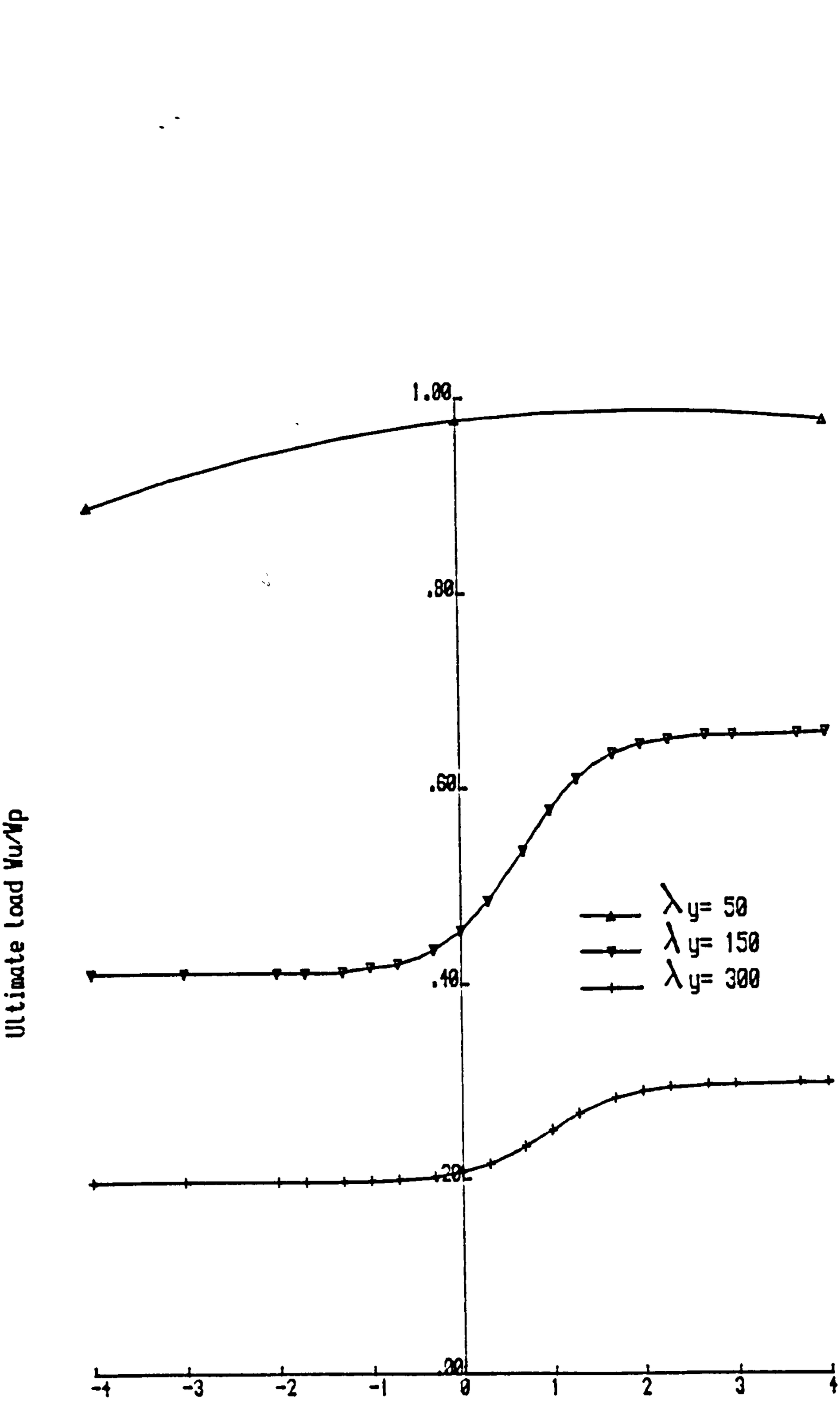

Fig. 4.17 Ultimate load-end warping stiffness behaviour for various beam stiffnesses.

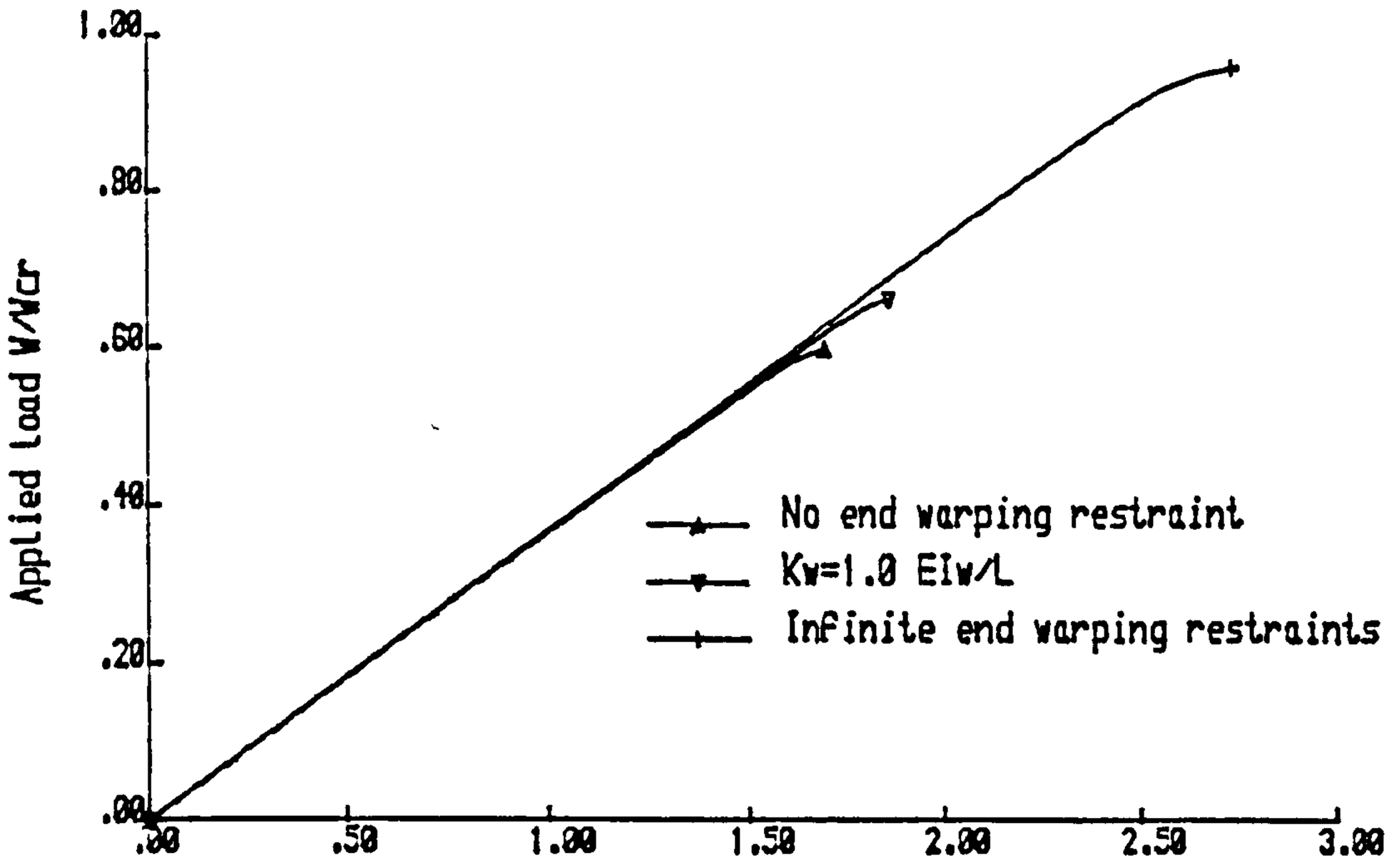

(a) Major axis deflection at midspan/(L/1000)

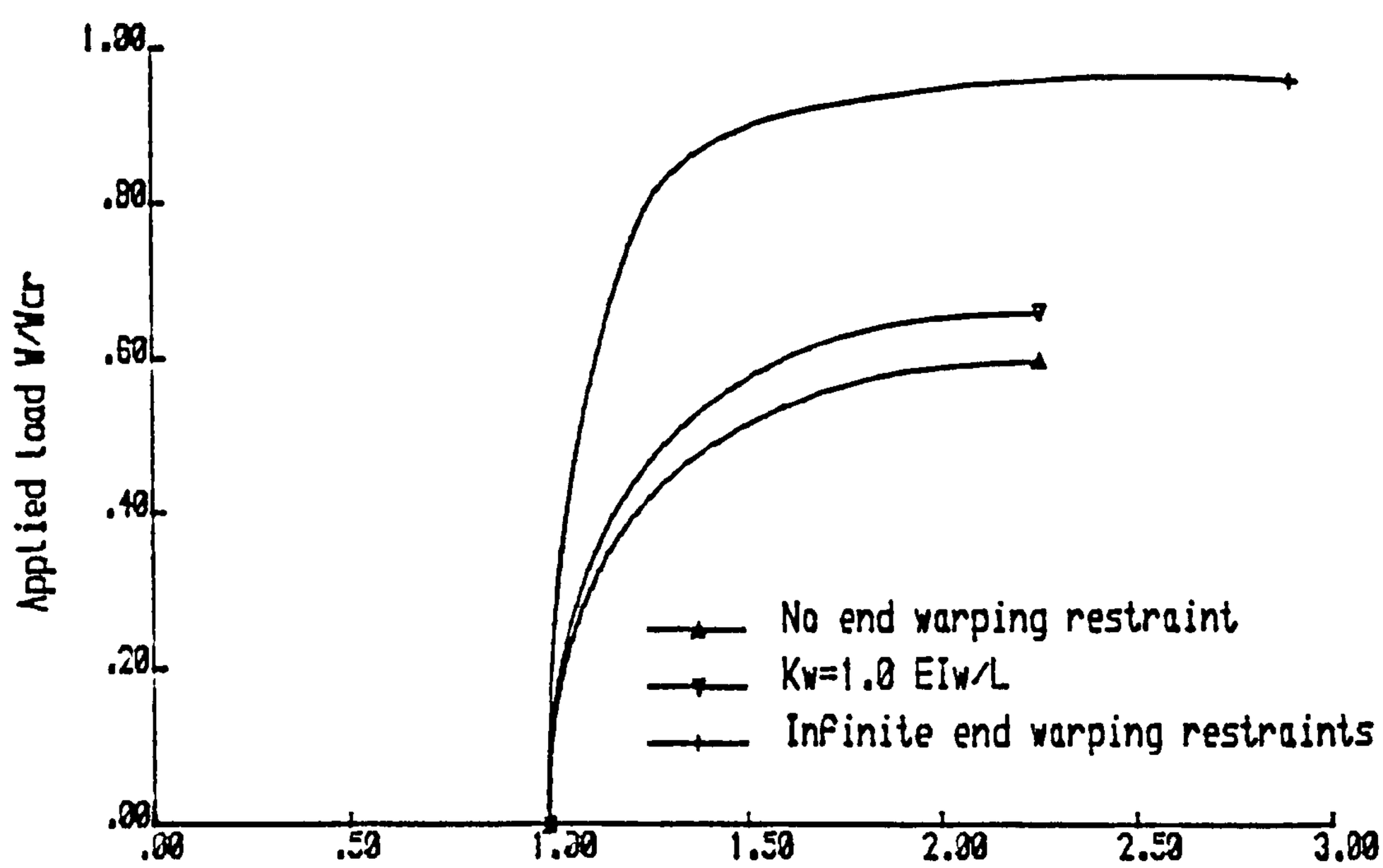

(b) Minor axis deflection at midspan/(L/1000)

Fig. 4.18 Load-deflection relationships for various end warping restraints. L/r_y=150

Chapter 5

EFFECTS OF INTERMEDIATE BRACING ON I-BEAMS

5.1 Introduction

The effects of various end restraints on the spatial behaviour of beams have been discussed in the preceeding chapter using the finite element computer program presented in Chapter 3. The effect of intermediate bracing has also been included in the program and the ability of the program to deal with the bracing problem demonstrated.

Practically, a main member is often braced by other structures e.g. floors, purlins and side-beams etc. Although the bracing effects of these secondary members on the main member have been shown to be significant by many authors (Trahair and Nethercot[31], Winter[34], Medland[42] etc), there still exists a gap between the understanding of the bracing action and

the common use of braces in practice, especially the strength required of a brace to ensure its effectiveness in improving the performance of the main member.

This chapter reports the study of the inter-relationship between bracing stiffness, main member ultimate load and bracing force for a series of representive cases using the computer program presented in Chapter 3. Two types of bracing system - single bracing and multiple bracing - have been addressed. Results are presented in sections 5.2 and 5.3.

In this study, the following parameter are taken as basic values:

Cross-section UB 254 × 22 as given in Fig. 5.1a

Residual stress Lehigh type of distribution, see figure 5.1b

Initial deflection type 1 and δ_0 =L/1000 (fig. 5.1c)

Beam length L=6.0m corresponding to $\frac{L}{r_y} = 300$

Location of braces single brace at midspan

Multiple braces equally spaced

End restraints allowing for lateral rotations and warping

5.2 Single Bracing System

Fig. 5.2a and 5.2b give the general load-deflection and load-bracing force relationships for a beam with a midspan brace of stiffness of $1.0\frac{EI_y}{L^3}$ located at its upper flange (**UF** bracing). The load was also applied at the upper flange (**UF** loading), whilst the deflection shown is that of the shear centre.

It can be seen that both curves are highly non-linear. Fig. 5.2a shows a tendency for the deflection to change sign with increasing load, because initially the brace resists top flange lateral deflection sufficiently that the shear centre is forced to move slightly in the opposite sense. At higher loads, however, lateral deflections increase rapidly and the shear centre moves in the expected direction. For stiffer braces, this effect is more pronounced with the result that a greater deflection in the opposite sense is produced with the increase of bracing stiffness, leading to slight reductions of the ultimate load as will be presented later. Fig. 5.2b indicates that the bracing force increases more sharply with the increase of applied load, particularly when the applied load approaches the ultimate value. Bracing forces at different load levels near failure are marked on this figure and a list of $\left(\frac{F_b}{F_d}\right) / \left(\frac{P_u}{P_p}\right)$ values for a set of bracing stiffnesses is given in table 5.1. These illustrate clearly the importance of relating bracing strength requirements to both the level of main member capacity required and the level of bracing stiffness provided. An obvious point is the benefit of using bracing that is rather stiffer than that required to just ensure 'complete support', a point that has been observed previously in a more limited study of columns[35].

Fig. 5.3-5.4 present the relationships between ultimate load or the corresponding ultimate bracing force and bracing stiffness for translational braces at the upper flange or shear centre (SC bracing) and for torsional braces. For each bracing arrangement, two loading positions - upper flange and shear centre (SC loading) - were considered. The applied load and the ultimate load are nondmensionised as $\frac{P}{P_p}$ and $\frac{P_u}{P_p}$ respectively, whilst the bracing rigidity is shown as $S_b / \left(\frac{48EI_y}{L^3}\right)$ for the case of translational bracing or $S_b / \left(\frac{GJ}{L}\right)$ for torsional bracing. The ultimate bracing force F_u or moment

M_u is nondimensionised as $\frac{F_u}{F_d}$ if translational bracing is considered or as $\frac{M_u}{M_d}$ if the beam is torsionally braced. P_p, F_d and M_d are respectively the plastic collapse load of the beam, one percent of the axial capacity of a fully stressed beam flange and the moment corrsponding to F_d given by:

$$P_p = \frac{4M_p}{L} \tag{5.1}$$

$$F_d = 0.01\sigma_y t_f b_f \tag{5.2}$$

$$M_d = F_d h \tag{5.3}$$

in which h is the distances between the two flange centroids.

It can be seen from these figures that for the beams braced on their upper flange or for beams with torsional bracing, there exists a distinct value of bracing stiffness $\overline{S_{bl}}$ corresponding to which both the ultimate load and the bracing force against bracing stiffness curves attain their respective peak values. In the case of the ultimate load curves, the peak value may be retained or may reduce very slightly at higher bracing stiffnesses, whereas for the bracing force curves, a sharp decrease of values is obtained once bracing with a stiffness in excess of $\overline{S_{bl}}$ is employed.

Applying the load to the upper flange results in a potentially more unstable arrangement leading to a higher value of bracing stiffness being required for complete bracing. Taking translational bracing as an example, the critical values of bracing stiffness are shown in Fig. 5.3a as being approximately 2.5 and 5.0 for shear centre loading and upper flange loading respectively. However, for torsional bracing, since both flanges are braced, the height of the load will not significantly affect the behaviour of the beam, except at very low value of bracing stiffness.

For translational bracing placed at the shear centre, see Figs 5.3a and 5.3b, the state of complete bracing is not reached for the bracing stiffness range shown due to the inability of the bracing system to restrain the twisting of the beam. For the case of upper flange loading, the greater amount of twisting associated with the buckled shape results in an almost steady lateral deflection and thus a continuous increase in the ultimate bracing force with increases in the bracing stiffness. For shear centre loading, however, a peak value of bracing force is present in Fig. 5.3b, although Fig. 5.3a indicates that complete suppport has not actually been attained (Fig. 5.3a indicates that a value of $\overline{S_b}$ of at least 200 was actually found to be necessary to produce the full beam strength). However, as indicated in Fig. 5.3b bracing forces for this case are much larger; even at a bracing stiffness $\overline{S_b}$ of 200 the force is approximately 3 per cent (see figure 5.5b), although further increases in bracing stiffness will cause this to continue to reduce. A value of 2 percent for the bracing force for this case with $\overline{S_b} = \infty$ was produced by Zuk[33] using elastic analysis.

Taking the case of top flange bracing and noting that the beam's ultimate load corresponds to about 80% of M_p being reached in the critical cross-section, the force in one flange at failure is about 80% of F_d or the equivalent couple is about 80% of M_d. Scaling up the non-dimensional ultimate bracing force by 1.25, provided the bracing stiffness exceeds, say, 2.0 S_{bl}, a value of 1.0 percent of flange force may be taken as the bracing strength requirement. This bracing strength requirement compares quite closely with the value in the British Standard[3] for lateral and torsional restraints, although the standard does not link the force reqirement to any particular bracing stiffness level.

From the study by Trahair and Nethercot[31], the estimated critical value for complete bracing of a perfect elastic beam is approximately 15 for shear centre bracing and shear centre loading. Clearly this value needs to be higher when the presence of geometrical imperfections in the beam is allowed for as illustrated in Figs 5.5a and 5.5b. If $\delta_0 = \frac{L}{10000}$, the bracing stiffness requirement is about 25 as indicated in fig. 5.5a, whilst for $\delta_0 = \frac{L}{1000}$, complete bracing is not quite achieved for the range of stiffnesses considered. This phenomenon has been observed previously for braced columns in Ref.[34].

The relationship between the bracing strength requirement and initial deflection has been studied for this case, assuming the bracing stiffness to be infinite. Bracing force values at different applied load levels approaching beam failure - $\frac{P}{Pu}$ = 0.90,0.95,1.0 - are plotted against initial deflection values in fig. 5.5c on a log-log scale, from which it can be seen that an approximately linear relationship is suggested on this form of plot. Fig. 5.5c also indicates that the bracing forces at $\frac{P}{P_u}$ =0.90 or 0.95 are much lower than those at failure. Nevertheless, it is not possible to reach any general conclusion for relating the bracing strength requirement to the values of the applied load level and initial deflection.

5.3 Multiple Bracing Sysptm

Fig. 5.6-5.9 present the relationships between ultimate load, ultimate bracing force and bracing stiffness for different numbers of braces. The load is assumed to act at the upper flange in all cases. A similar pattern of results may be observed from these figures as for the case of a single brace, noting that the ultimate bracing force is taken as the value obtained by summing

the contributions of each individual component.

Use of a multiple bracing system appears to increase the bracing stiffness required for complete bracing, as pointed out previously by Trahair and Nethercot[31]. Since the slenderness of the main member used for these studies is modest if thought of in terms of distance between braces, the ultimate loads for different arrangements of full bracing shown in figure 5.6a are quite close regardless of the number of top flange braces. Moreover, Fig. 5.6b shows that only a small difference exists in the bracing force-stiffness curves for these cases.

The comparative ineffectiveness of shear centre bracing for this beam is shown in figures 5.7a and 5.7b. Both the ultimate load and the bracing force at failure continue to increase with increasing bracing stiffness and only a relatively modest increase in the ultimate load for infinite bracing stiffness over the case of zero bracing stiffness is found compared with other types of bracing. Once again this is due to the inability of shear centre lateral bracing to prevent the twisting (and thus top flange lateral movement) associated with top flange loading.

The most striking result of this study of multiple braces is that the number of braces seems to have little effect on the total bracing strength requirement of the bracing system. If the ultimate bracing forces are scaled up for a factor $\frac{P_p}{P_u}$ in line with the procedure for a single brace, the value of 1% on average or conservatively 2% as an upper limit of the flange force at failure may be proposed as the bracing strength requirement in design for the majority of multiple bracing systems. The exceptions are those forms of bracing which are not capable of approaching the condition of complete support e.g. systems with very low stiffnesses or those for which the arrangement

itself is unable to prevent the main buckling type displacements.

This conclusion also holds for different type of initial deflection as shown in figs 5.9a and 5.9b. The shapes of the initial lateral deflections are given in figure 5.1c and a maximum value of $\delta_0 = \frac{L}{1000}$ was assumed for both cases. It is clear that the first type is rather more severe than the second if the bracing stiffness is less than the critical value for complete bracing. However, figure 5.9b shows that when both the ultimate load and the ultimate bracing force stabilise, the influence of different types of imperfection becomes negligible.

So far, only beams with a practical upper limit on their original (unbraced) slenderness of $\frac{L}{r_y} = 300$ have been investigated. However, since the failure is always at moments quite close to M_p, the difference in the ultimate load of a beam braced by different numbers of multiple braces may not be fully appreciated. For this purpose, a beam with an original slenderness of 600 has been studied. This is sufficiently slender that if complete bracing is obtained through the use of a single brace, the beam buckles in a mode approaching double curvature at a moment of $0.416M_p$, which compares well with the theoretical elastic critical moment using half the length of the beam of $0.402M_p$. For multiple braces and assuming the beam to buckle into multiple half waves between braces, the theoretical value for the elastic buckling moment of an interbraced length is higher than M_p. Thus, failure occurs by inelastic buckling as indicated in fig. 5.10a.

For this beam, since the original slenderness is very high, a large amount of lateral and/or torsional displacement is expected. However, as shown in fig. 5.10b a value of 2% of the flange force at failure is still sufficient as the bracing strength limitation, providing sufficiently stiff bracing is

employed.

In order to confirm that these conclusions hold for beams with practical slendernesses, a beam of $\frac{L}{r_y}$ =100 with 3 upper flange braces has been studied. Fig. 5.11a and 5.11b show the main member strength - bracing stiffness and bracing reaction - bracing stiffness relationships respectively. Although the bracing force is reduced, a value of 1% of the flange force is still required for the strength requirement of the bracing system to retain its effectiveness in restraining the main member.

Although the bracing strength requirement for the whole bracing system is quite steady, the bracing requirement for each individual component varies considerably according to the initial deflection patterns and the location of each brace. Figs 5.12-5.14 give the bracing force in each brace for different values of bracing stiffness.

Fig. 5.12 compares different initial deflection types. As expected for type 2, since the initial deflection is antisymmetrical, whilst the applied load is symmetrical, the brace at midspan will only deform slightly and as a result a negligible bracing force is developed. Therefore the other two braces may be assumed to equally share the total bracing force. For type 1 the brace at midspan suffers the largest displacement thus most of the bracing force (approximately 80%) is sustained by this brace. It is also noticeable that the other two braces deform in the opposite direction, although this is not significant.

Fig. 5.13 deals with a system of 5 braces for a beam having a slenderness $\frac{L}{r_y}$ of 300. A similar pattern of results is indicated as for the 3 brace case (figure 5.12) with the same initial lateral deflection i.e. $F_{u(3)}$ is far greater than either $F_{u(2)}$ or $F_{u(1)}$ and there is a tendency towards a multiple half

wave buckling mode. The same type of result was also obtained for more slender beams ($\frac{L}{r_y}$ =600) with 5 braces.

Figure 5.14a gives the relationship between ultimate bracing couple in a torsional brace and bracing stiffness for 5 braces. Since no initial twist was assumed, the bracing couple in each individual component seems to depend solely on the position of the brace. Considering the symmetry of the beam, a linear relationship between the bracing couple and the distance of the brace from the end is suggested. Repeating this analysis for a beam with initial axial rotation of twisting of 0.01 radian produces very similar results in terms of the bracing force - bracing stiffness relationship as shown in fig. 5.14b which is related to shear centre loading.

5.4 Conclusions

Based on the study reported herein, the following conclusions may be drawn:

1. The forces induced in a restraint depend on the inter-relationship between load level in the main member, load type, main member initial deformation, bracing stiffness, bracing type, number of restraints and position of the restraint. Bracing force levels are generally lower and more consistent for arrangements that are capable of inducing buckling between restraints.

2. For a beam of practical slenderness, a value of 1 percent of the force in a flange at failure may be taken as the bracing strength requirement for a single brace providing it possesses adequate stiffness. For multiple brace systems, 1% may be unconservative in certain instances, particularly as bracing forces are not shared equally. A value of 2% is

considered more appropriate as a total figure with 1% for each individual restraint.

3. A linear relationship appears to exist between the bracing strength requirement and the magnitude of the initial deflection in the main member.

Table 5.1

Non-dimensional ultimate bracing force

$S_{ty}/\frac{48EI_y}{L^3}$	ratio of applied load to failure load			
	0.90	0.95	0.98	1.00
(1)	(2)	(3)	(4)	(5)
0.0	0.0	0.0	0.0	0.0
1.0	0.81	1.08	1.29	2.01
5.0*	1.39	2.00	2.67	3.54
10.0	0.73	0.84	0.92	0.98
25.0	0.58	0.63	0.67	0.69
∞	0.52	0.55	0.57	0.59

*: approximate stiffness value for complete bracing

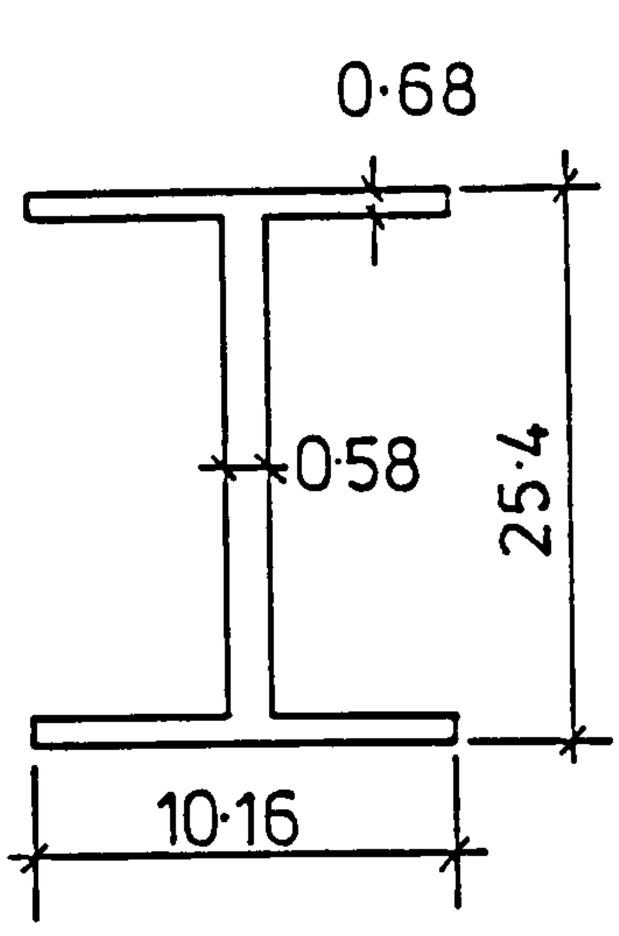

(a) Dimensions in cm

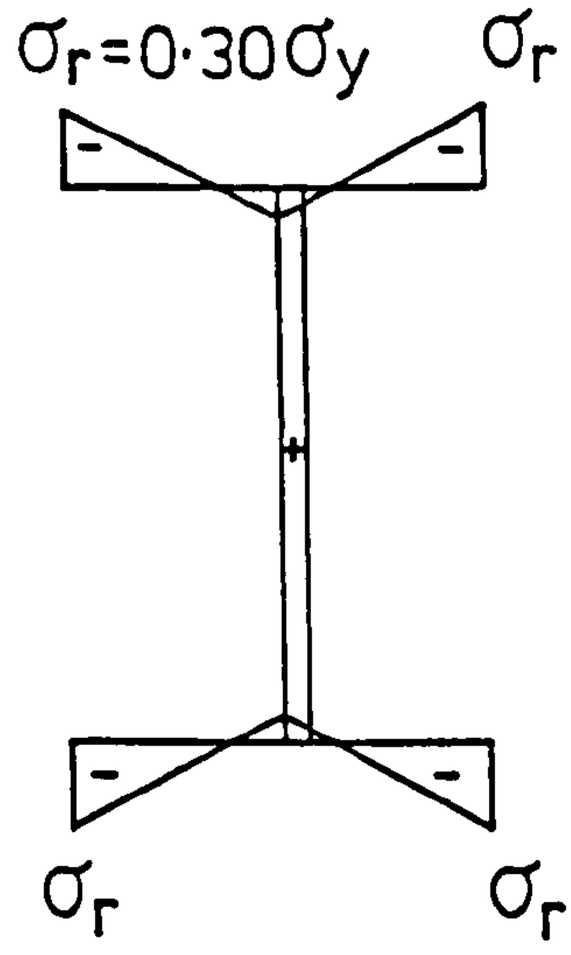

(b) Residual stress

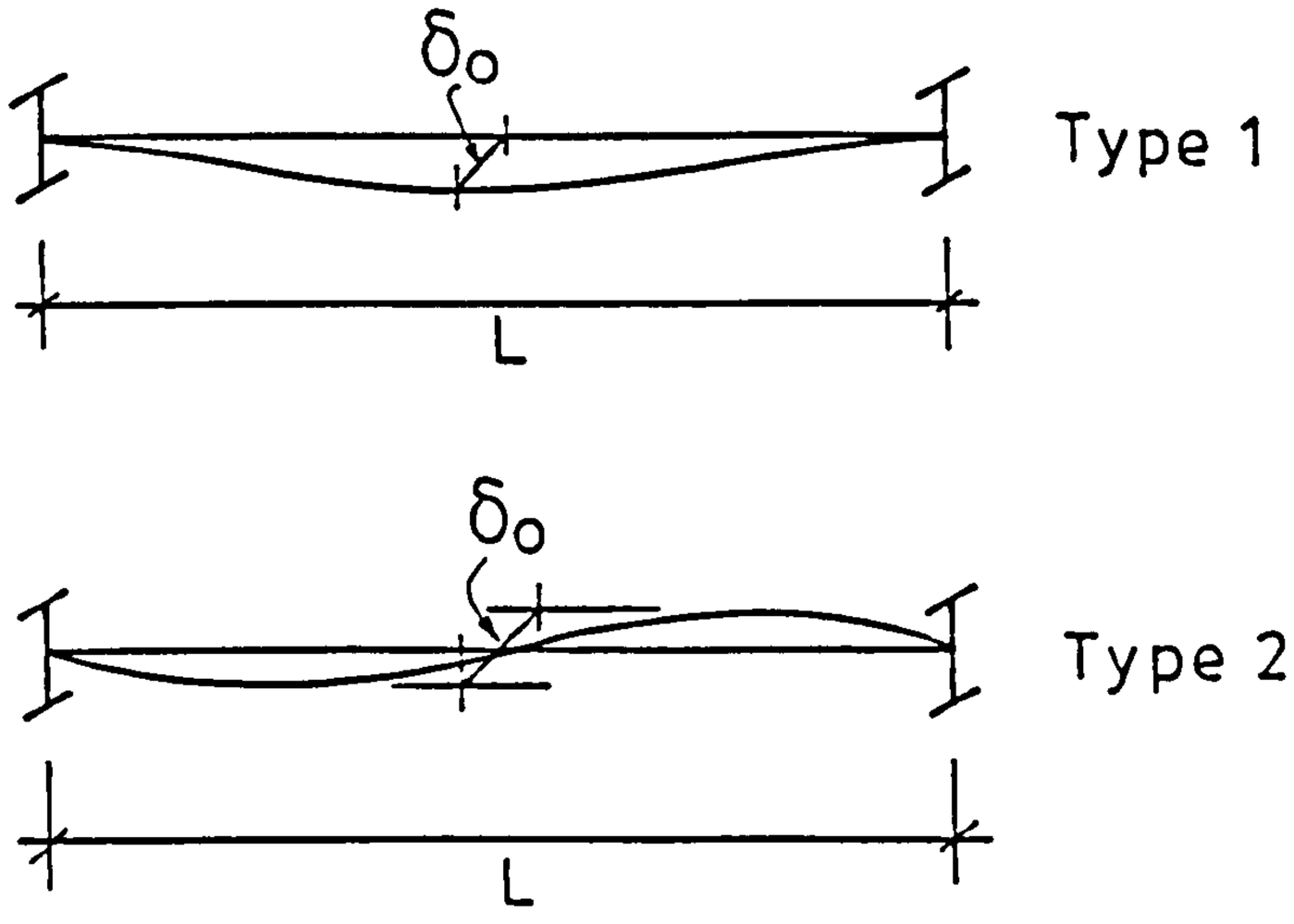

(c) Two types of initial lateral deflection

FIG 5·1 BASIC DATA FOR STUDY

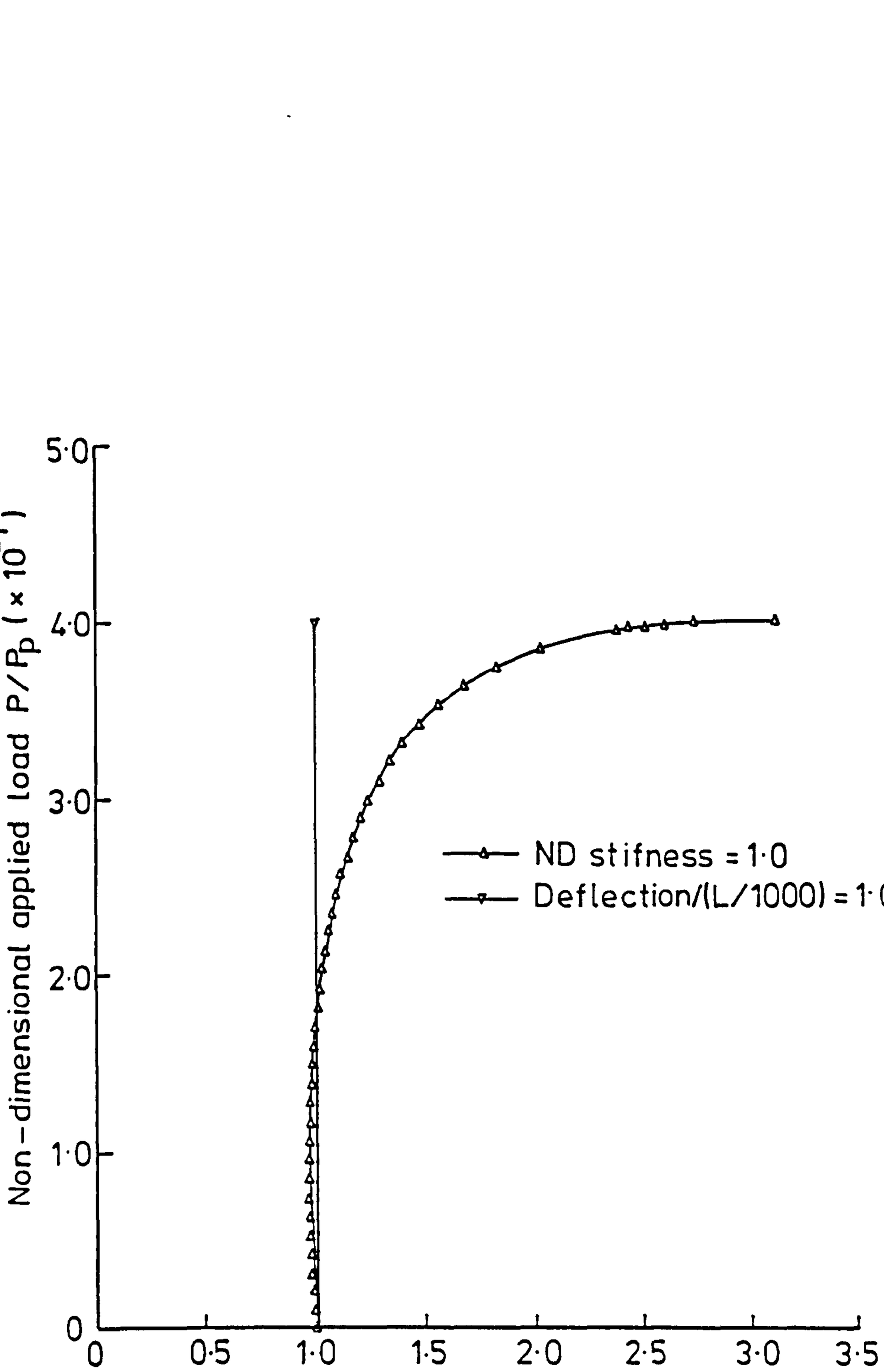

FIG 5·2a LOAD-DEFLECTION RELATIONSHIP FOR UPPER FLANGE BRACING, UPPER FLANGE LOADING. $\overline{S_b} = 1·0$

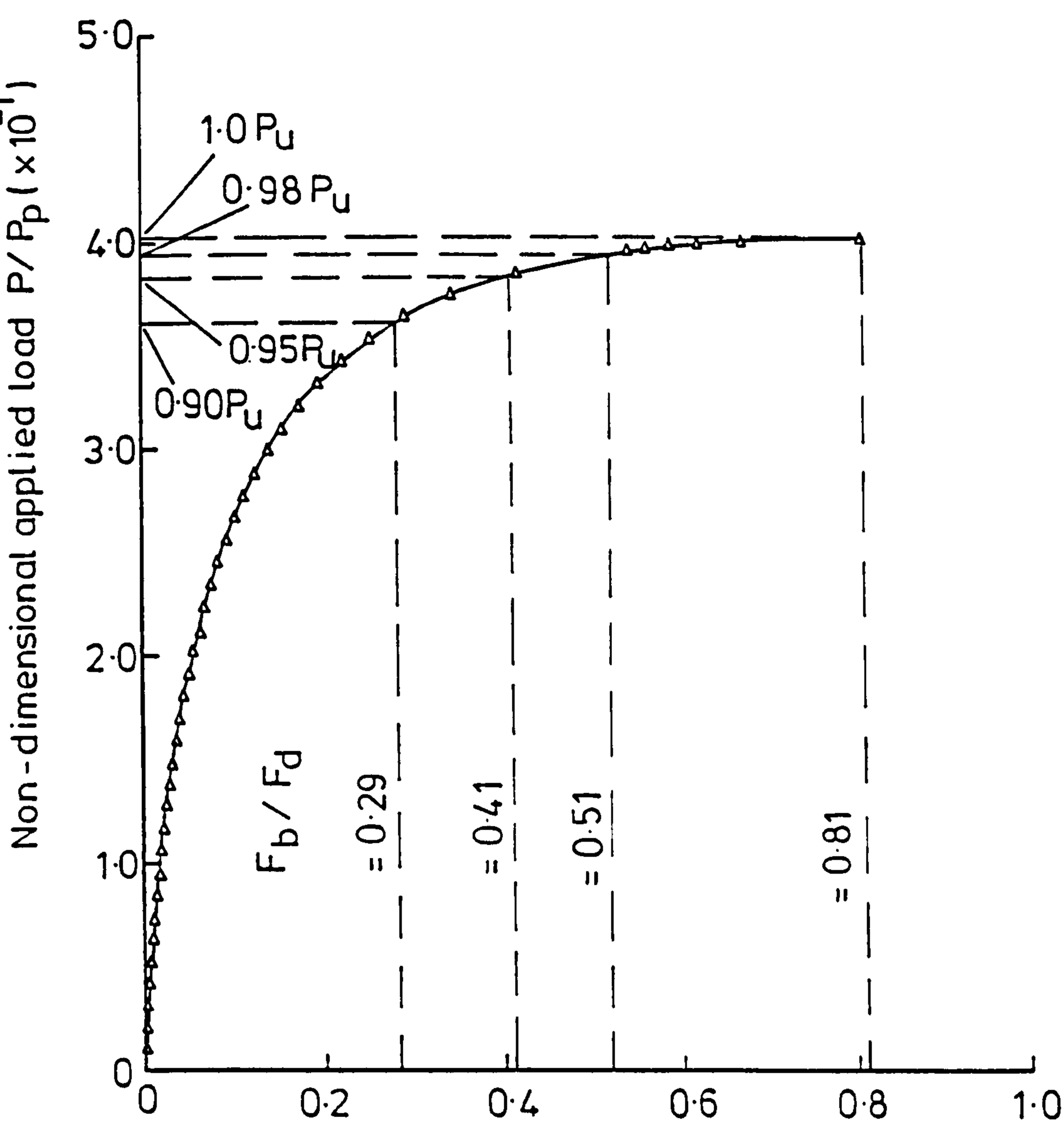

FIG. 5·2b LOAD VERSUS BRACING FORCE RELATIONSHIP FOR UPPER FLANGE LOADING, UPPER FLANGE BRACING.
$\overline{S_b} = 1{\cdot}0$

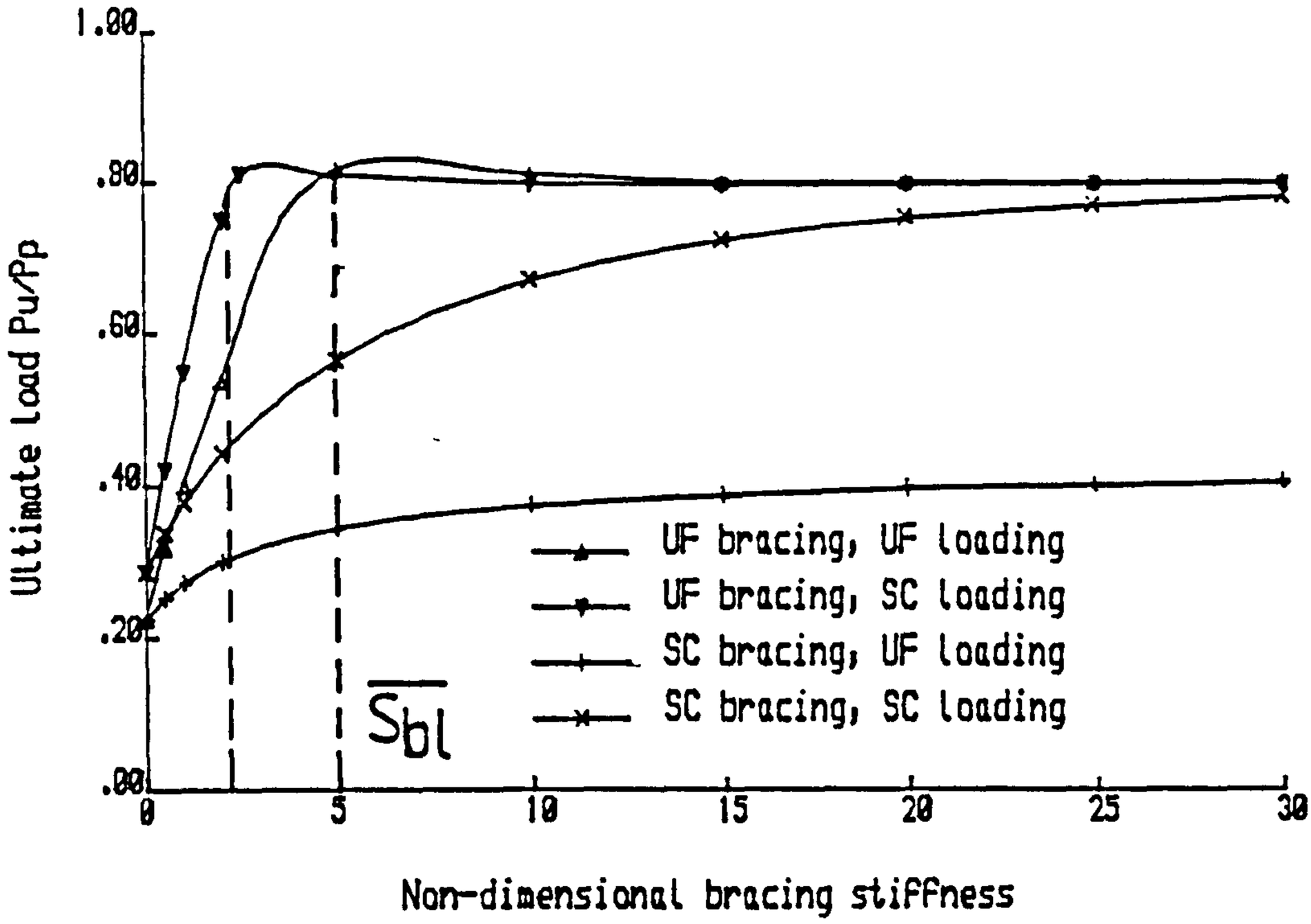

Fig. 5.3a Ultimate load-bracing stiffness curves for translational bracings. Maximum Initial Lateral Deflection (ILD) at midspan =L/1000

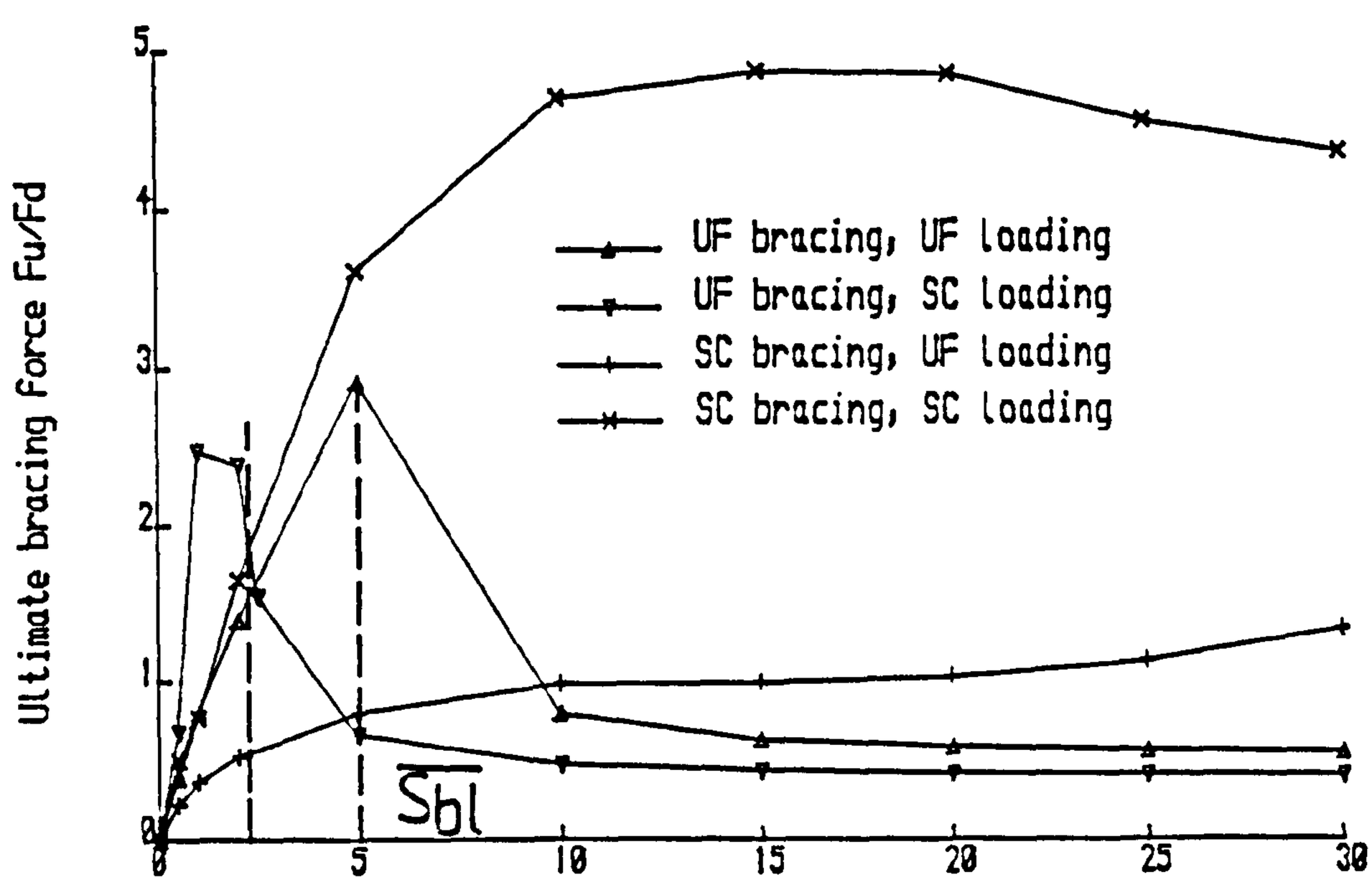

Fig. 5.3b Bracing force-bracing stiffness curves for translational bracings. Maximum Initial Lateral Deflection (ILD) at midspan =L/1000

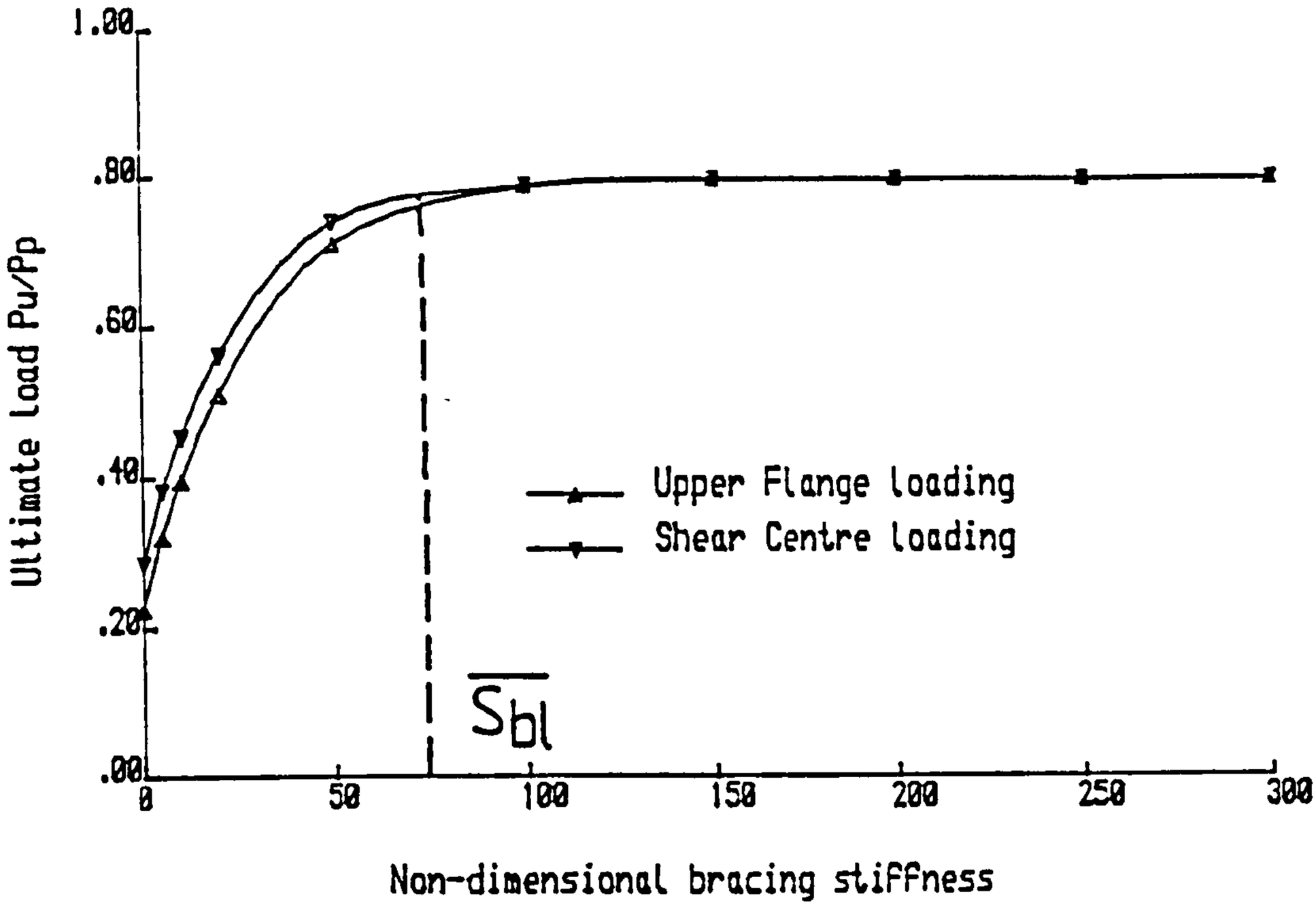

Fig. 5.4a Ultimate load-bracing stiffness curves
For torsional bracing. Maximum ILD =L/1000.

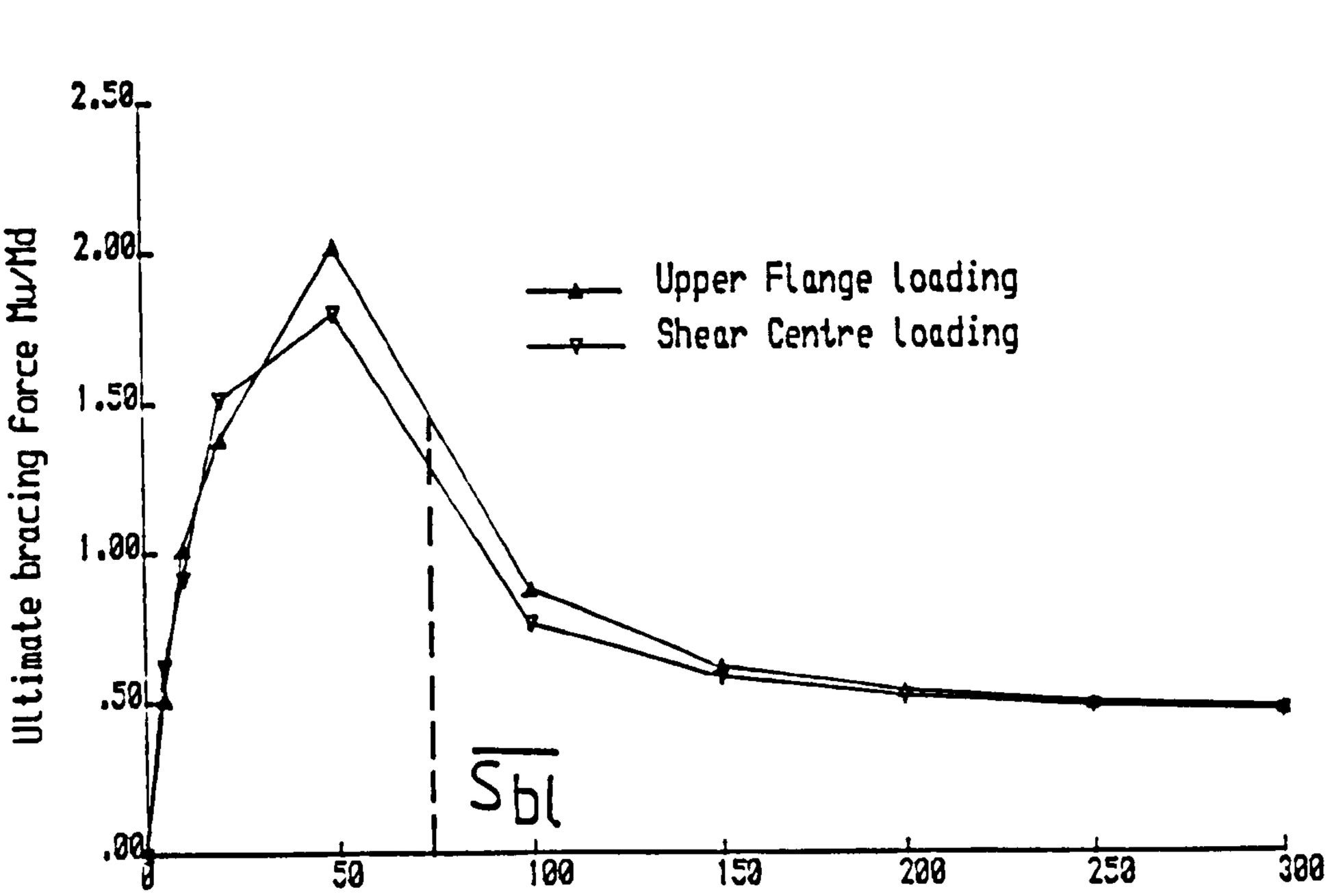

Fig. 5.4b Bracing force-bracing stiffness curves
For torsional bracing. Maximum ILD =L/1000.

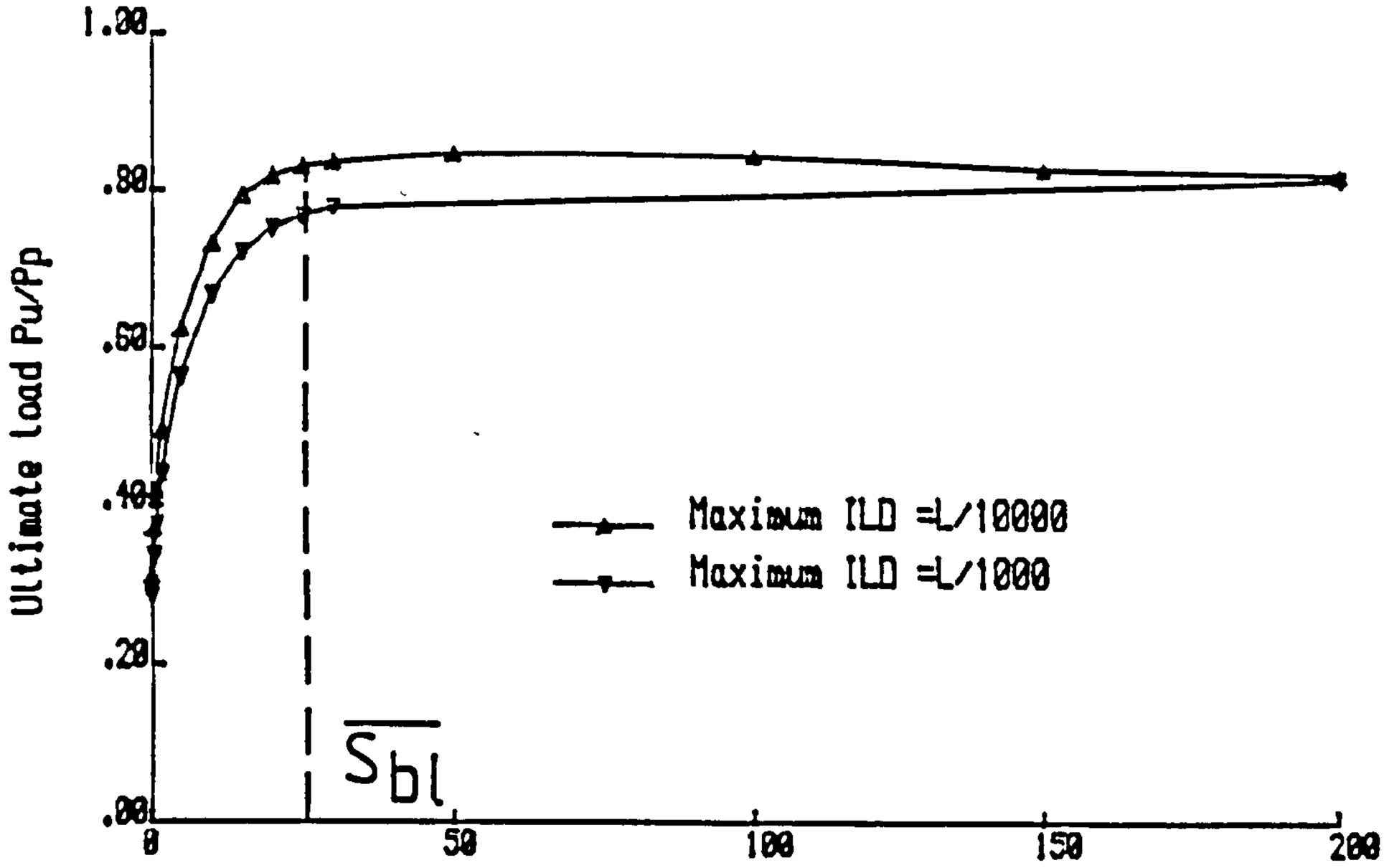

Fig. 5.5a Ultimate load-bracing stiffness curves For two maximum Initial Lateral Deflection (ILD) magnitudes at midspan. SC bracing. SC loading.

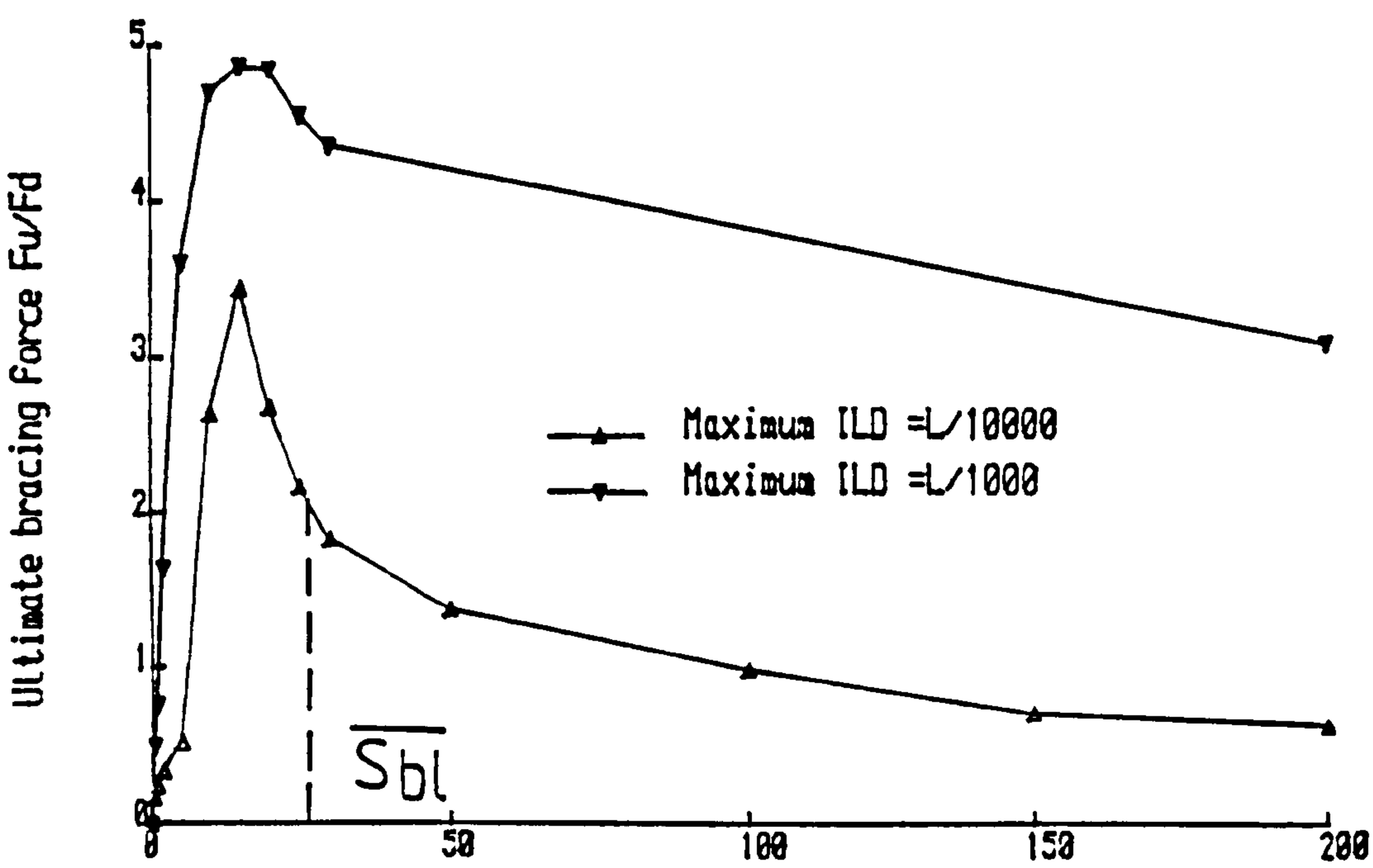

Fig. 5.5b Bracing force-bracing stiffness curves For two maximum Initial Lateral Deflection (ILD) magnitudes at midspan. SC bracing. SC loading.

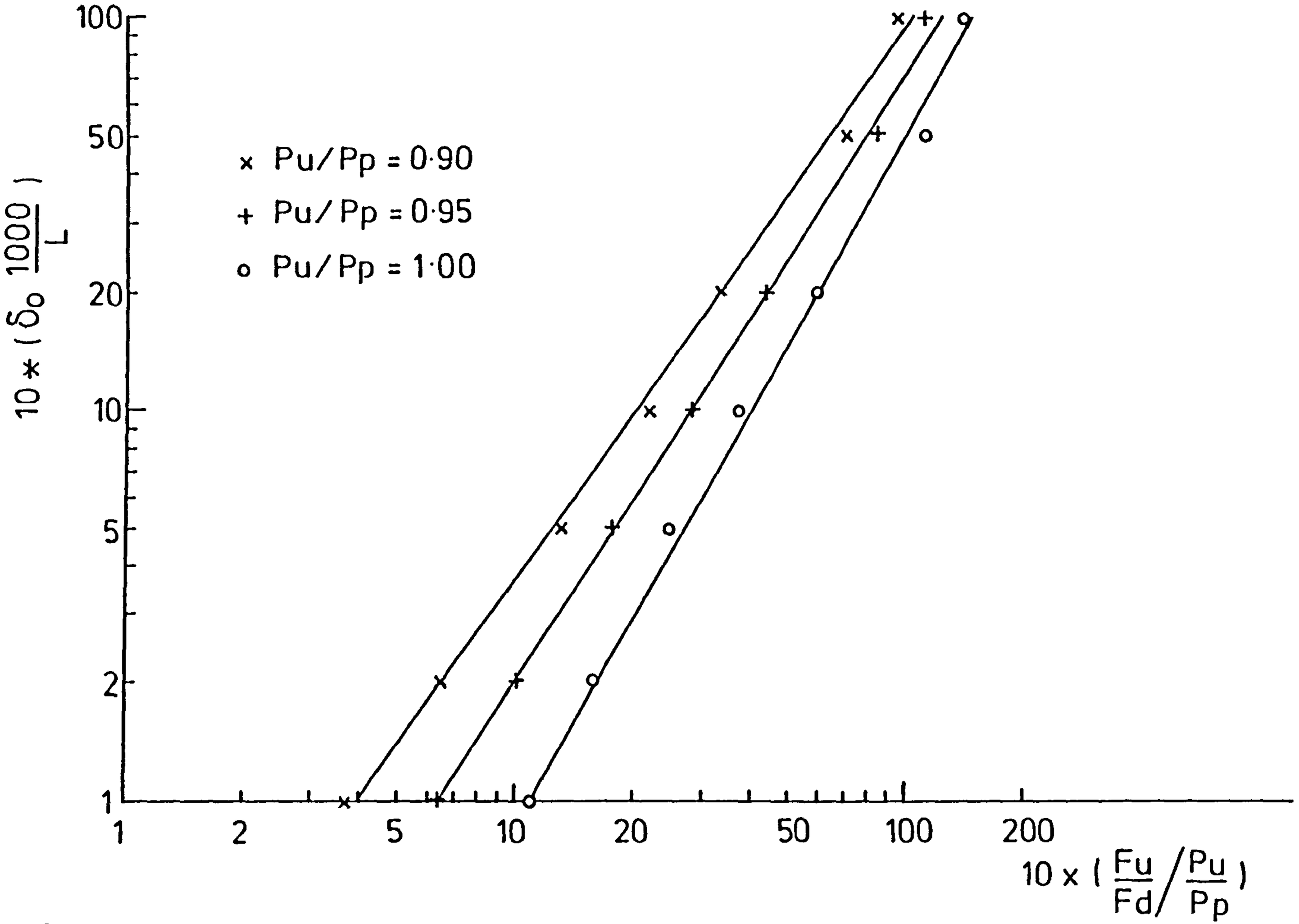

FIG.55C BRACING FORCE – INITIAL DEFLECTION BEHAVIOUR FOR DIFFERENT APPLIED LOAD LEVELS. SHEAR CENTRE LOADING, SHEAR CENTRE BRACING. $L/r_y = 300$

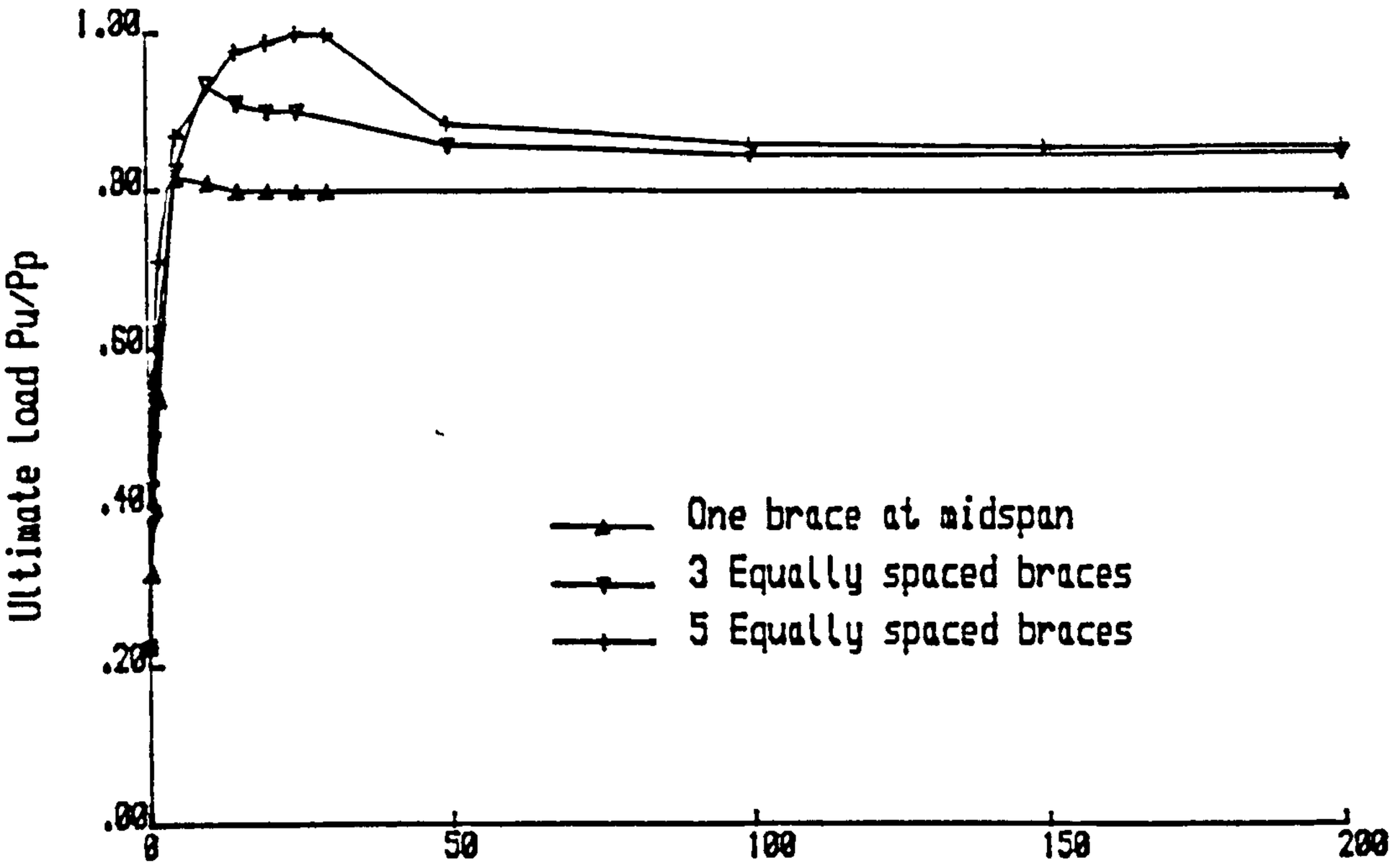

Fig. 5.6a Ultimate load-bracing stiffness curves
for different number of UF braces. ILD type 1.

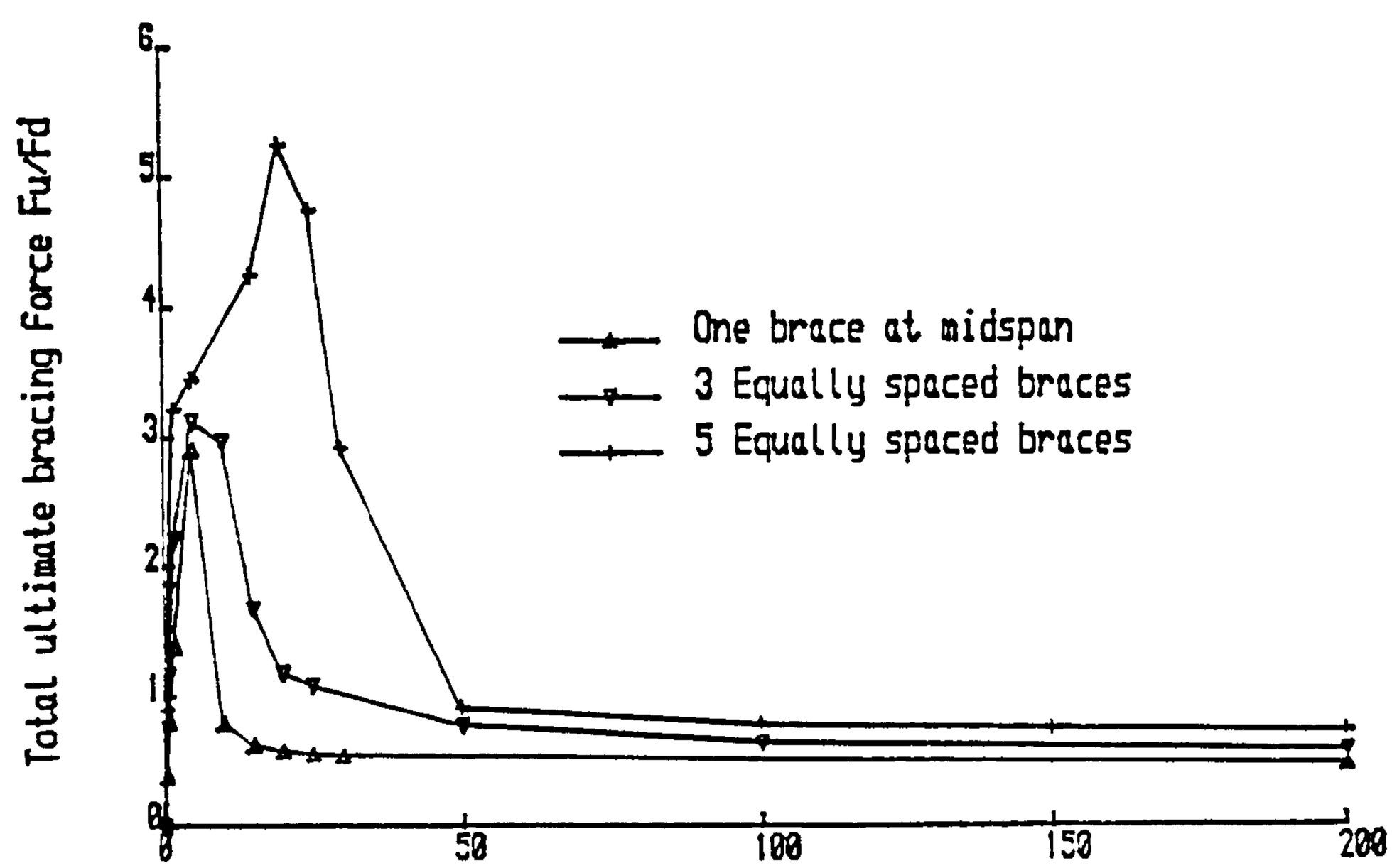

Fig. 5.6b Bracing force-bracing stiffness curves
for different number of UF braces. ILD type 1.

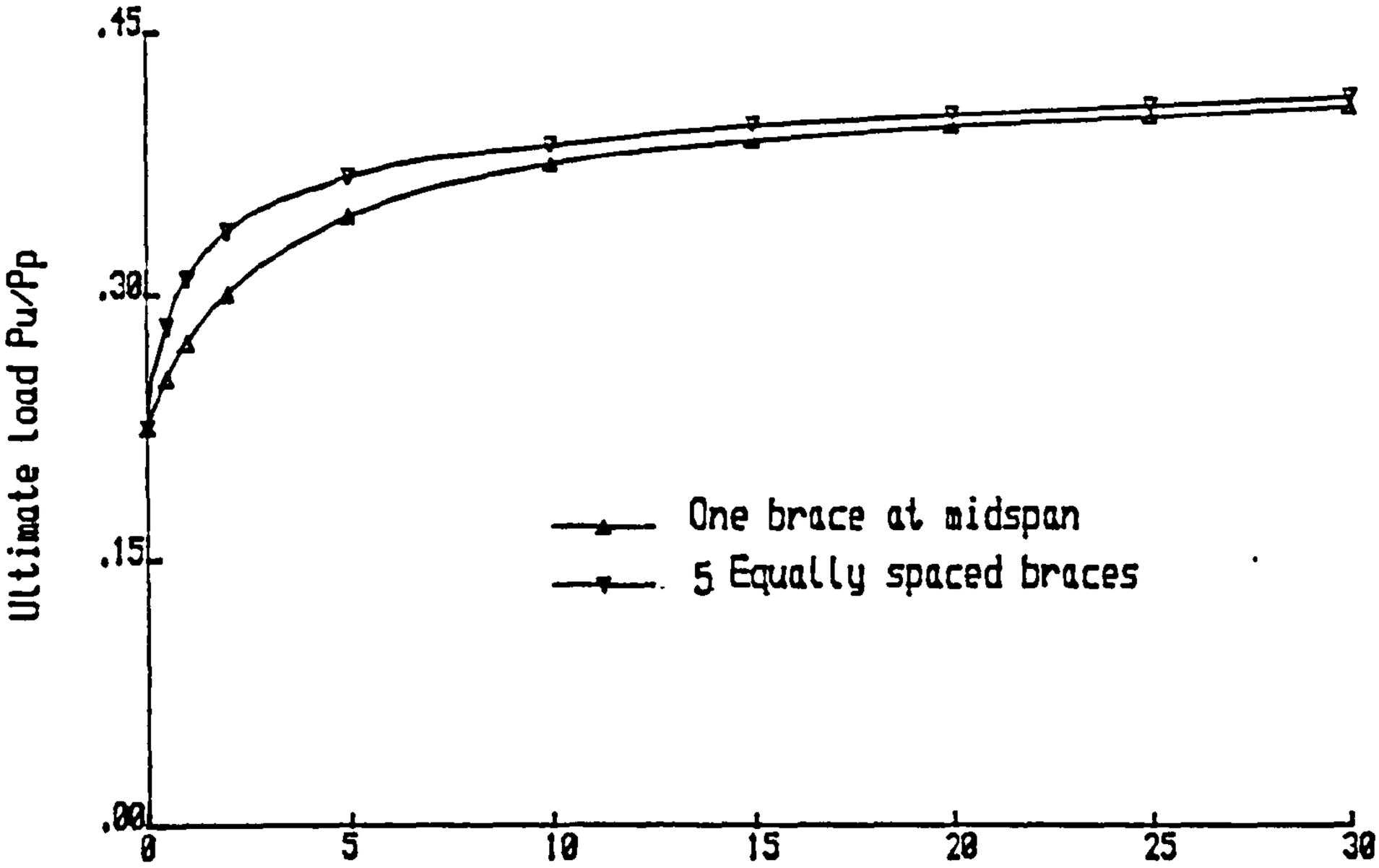

Fig. 5.7a Ultimate load-bracing stiffness curves
for different number of SC braces. ILD type 1.

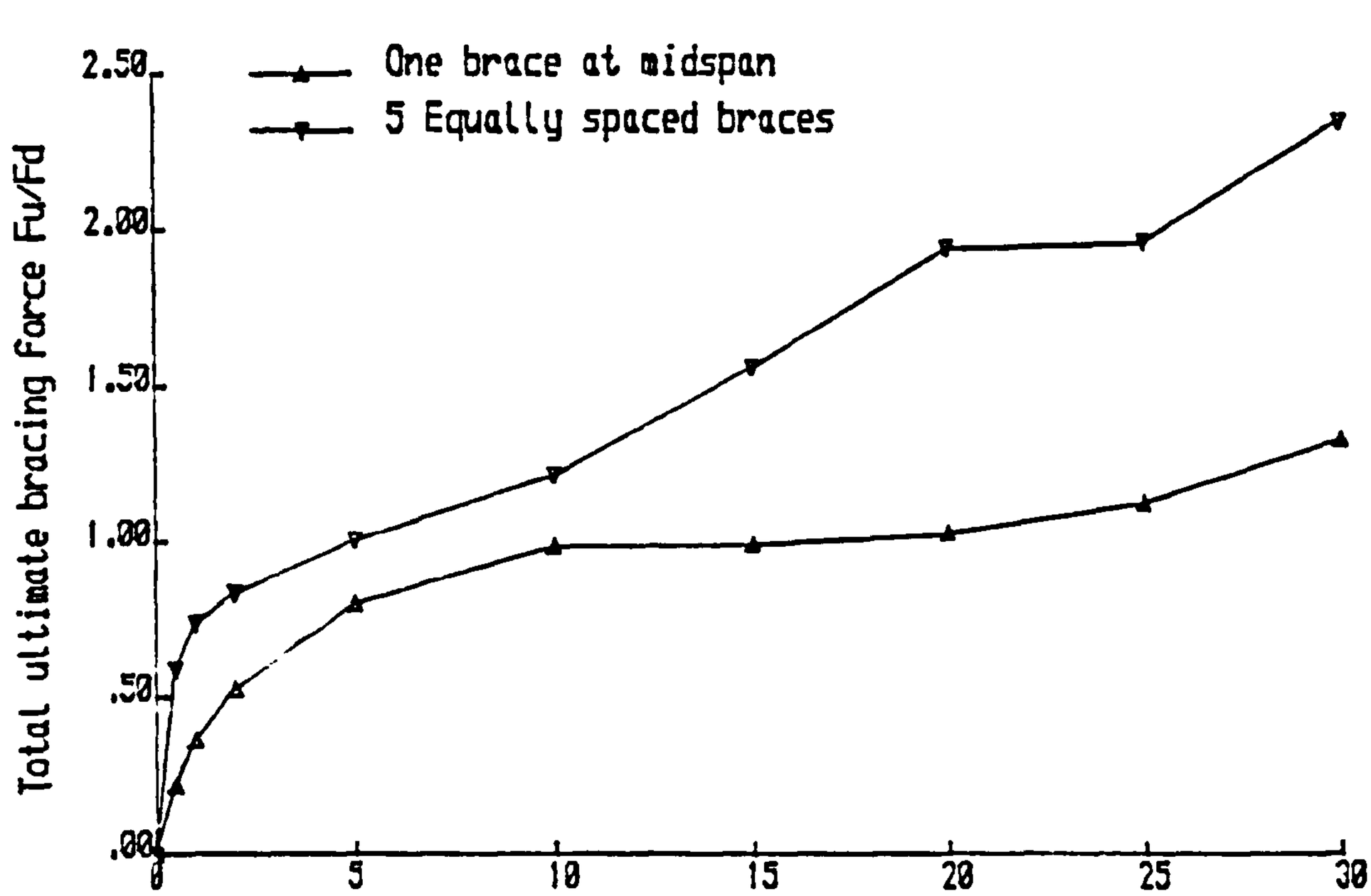

Fig. 5.7b Bracing force-bracing stiffness curves
for different number of SC braces. ILD type 1.

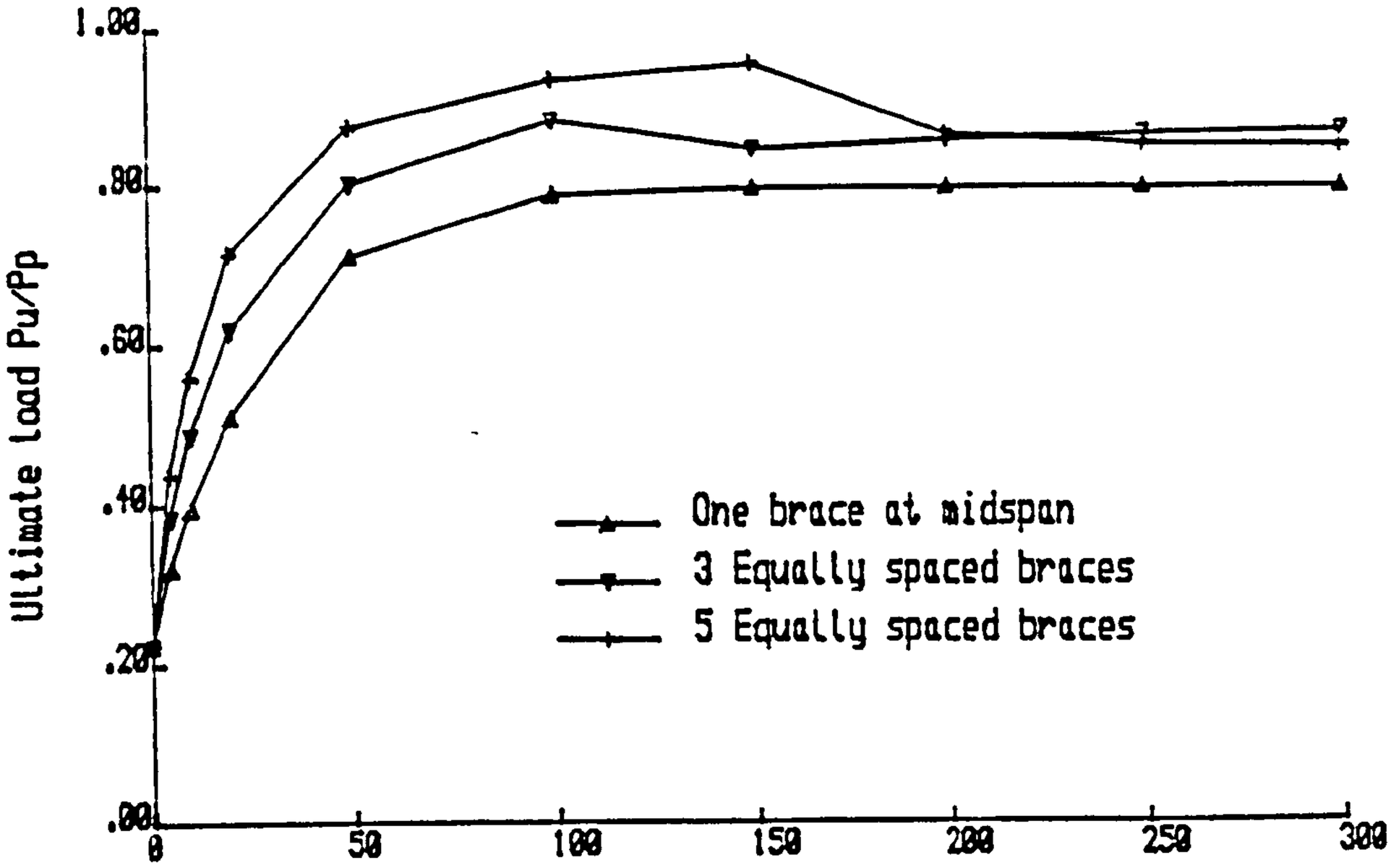

Fig. 5.8a Ultimate load-bracing stiffness behaviour for different number of torsional braces. ILD type 1.

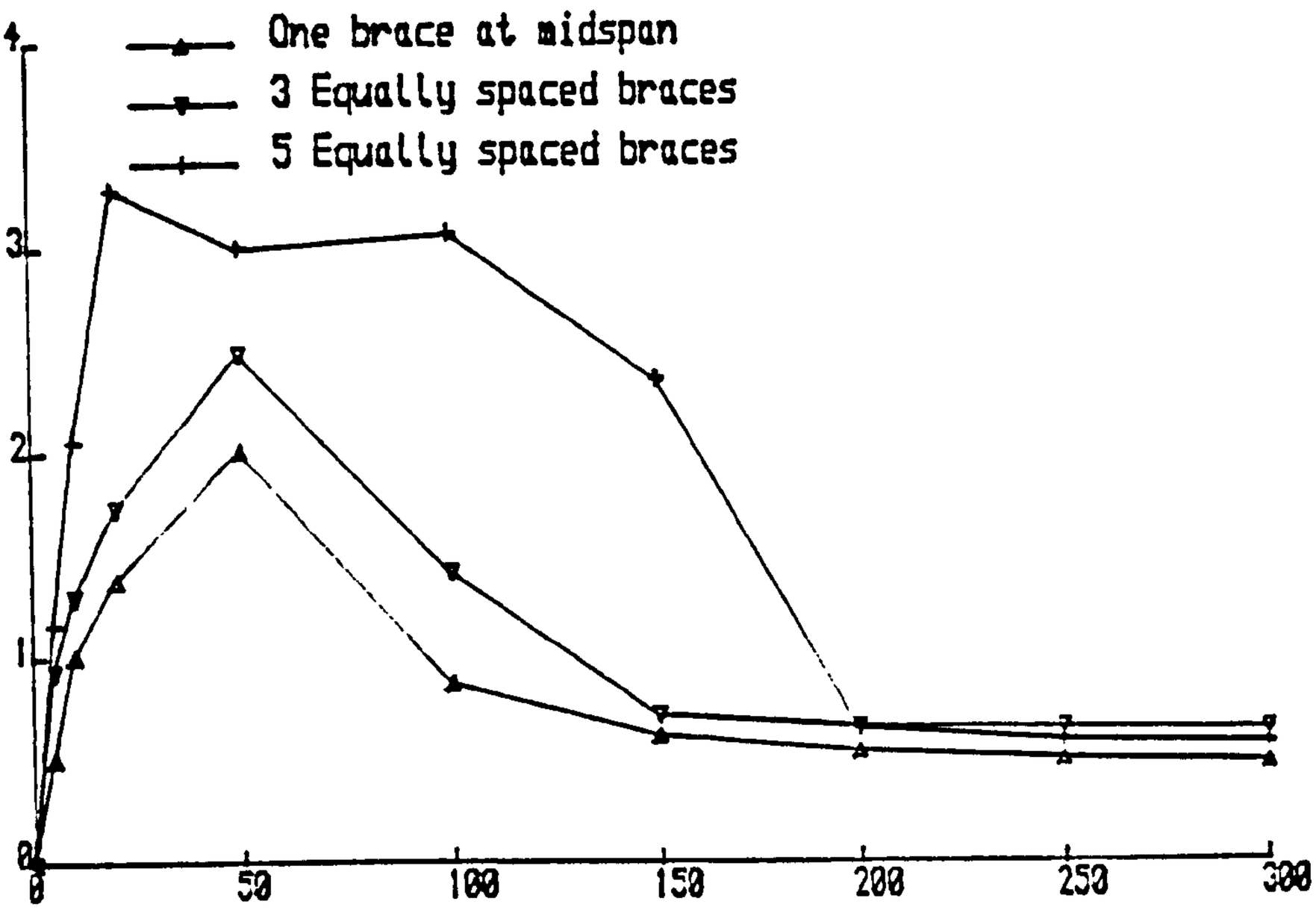

Fig. 5.8b Bracing force-bracing stiffness behaviour for different number of torsional braces. ILD type 1.

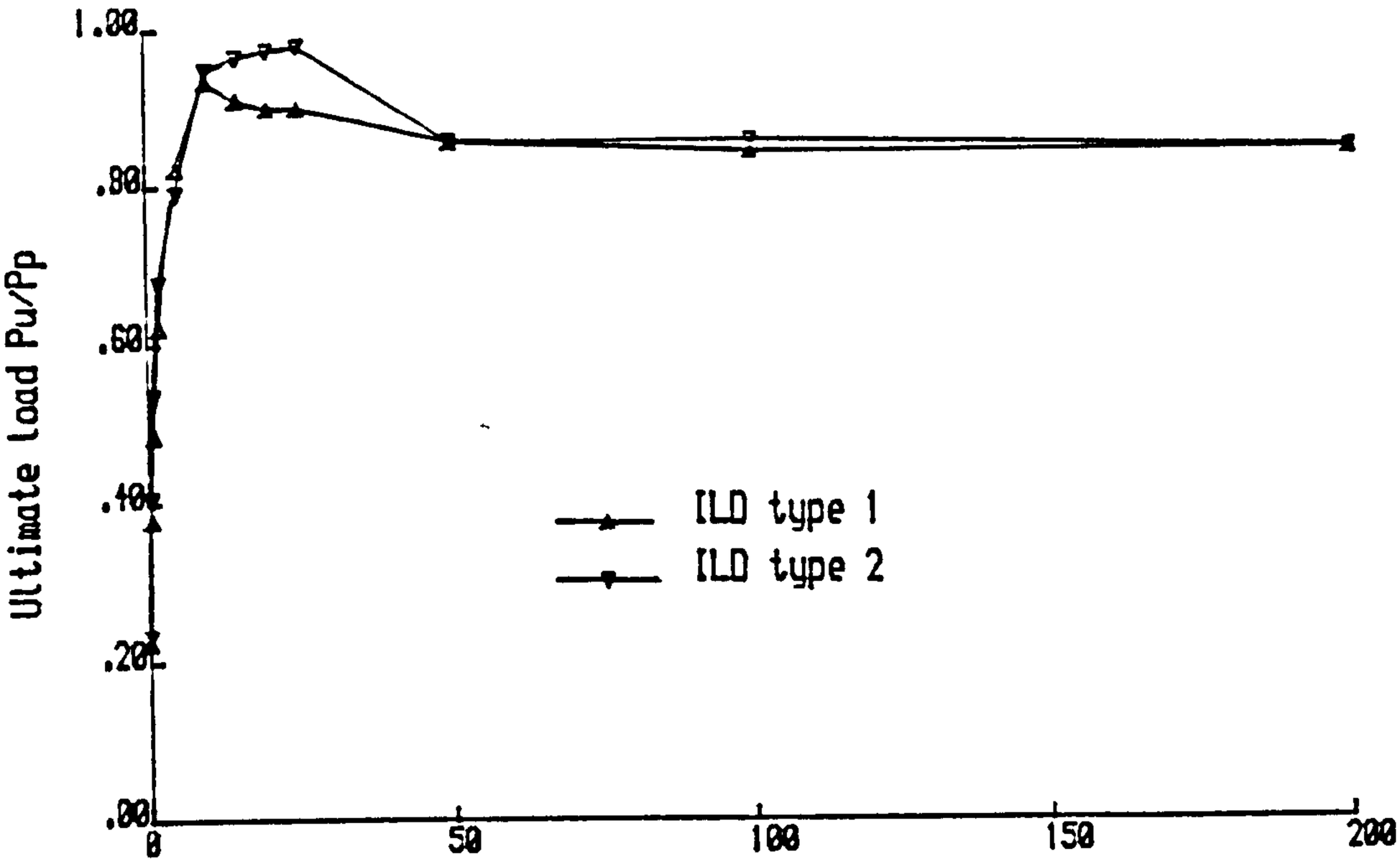

Fig. 5.9a Ultimate load-bracing stiffness curves for different Initial Lateral Deflection(ILD) types. 3 Equally spaced upper flange braces.

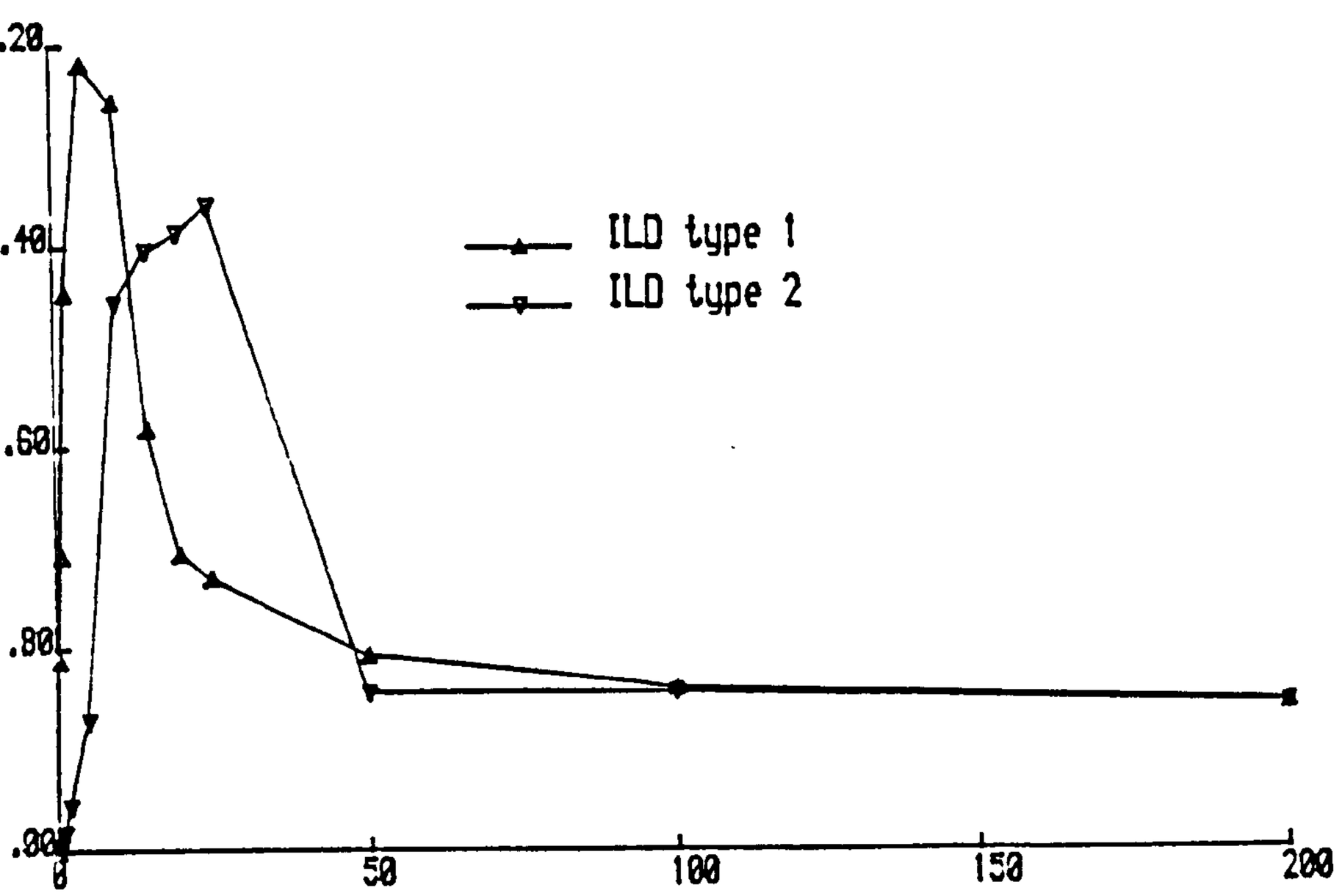

Fig. 5.9b Bracing force-bracing stiffness curves for different Initial Lateral Deflection(ILD) types. 3 Equally spaced upper flange braces.

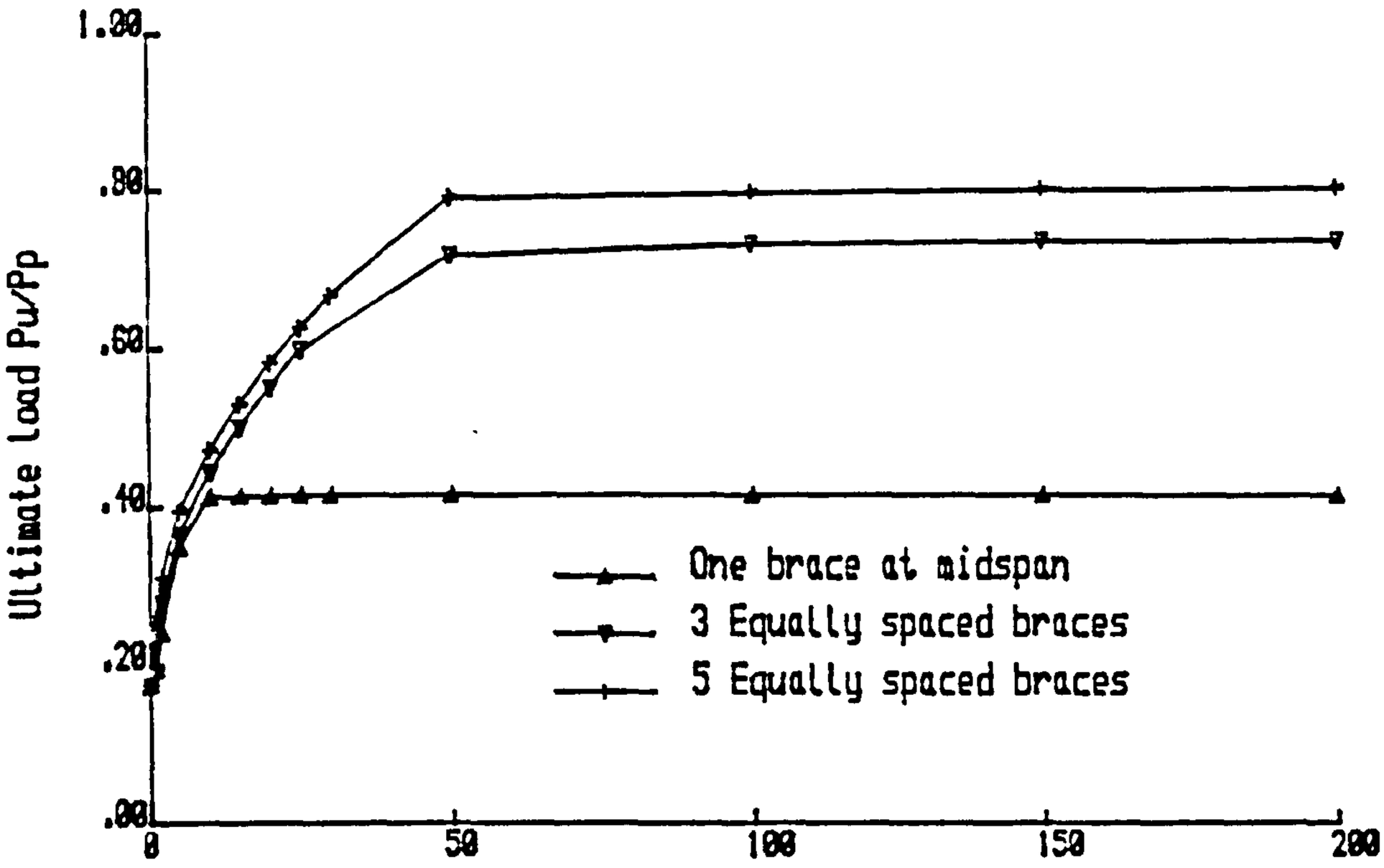

Fig. 5.10a Ultimate load-bracing stiffness curves For beam slenderness=600 (L=12 m). UF bracing, UF loading. ILD type 1, max. value at midspan=L/1000

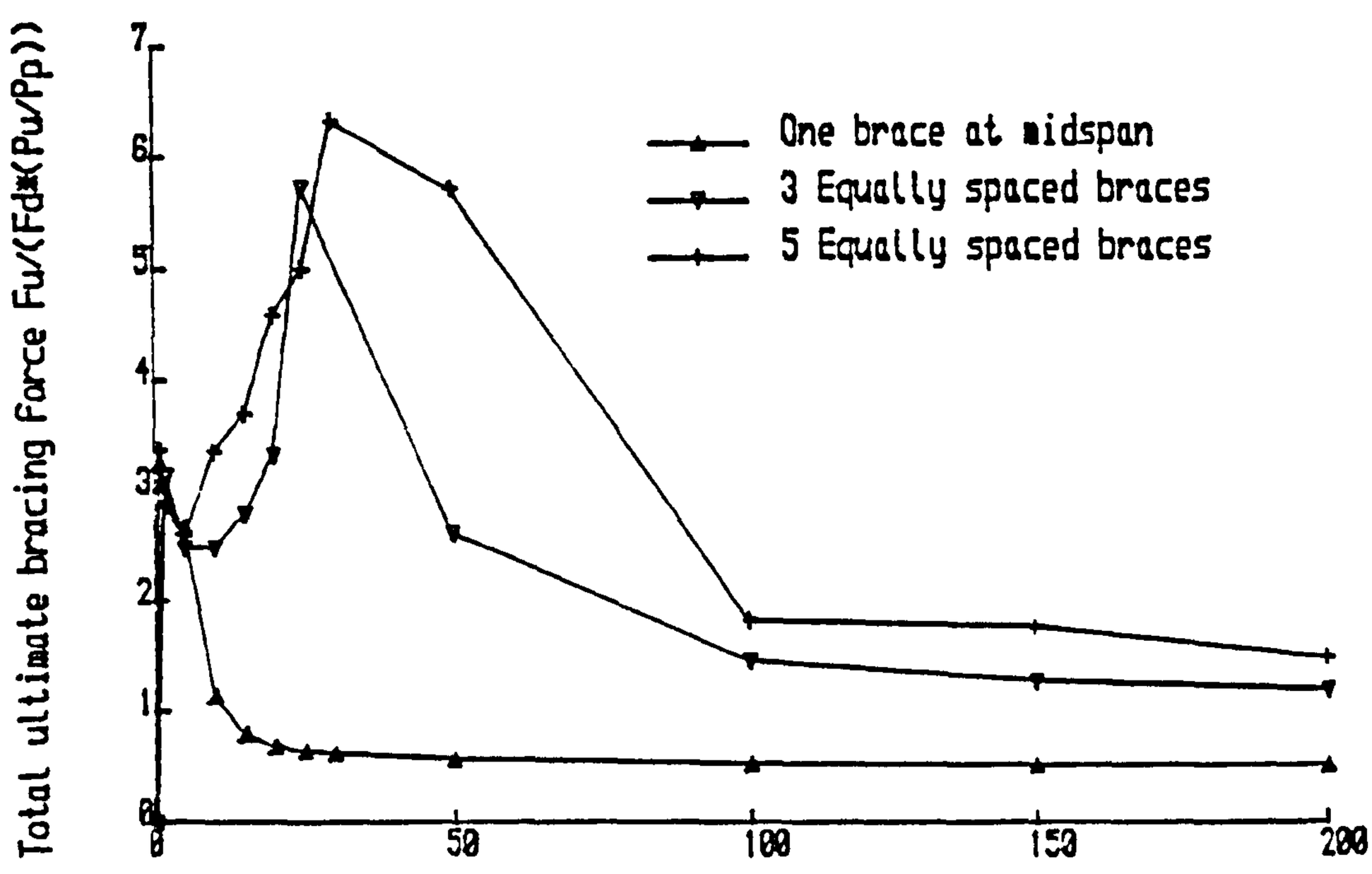

Fig. 5.10b Bracing Force-bracing stiffness curves For beam slenderness=600 (L=12 m). UF bracing, UF loading. ILD type 1, max. value at midspan=L/1000

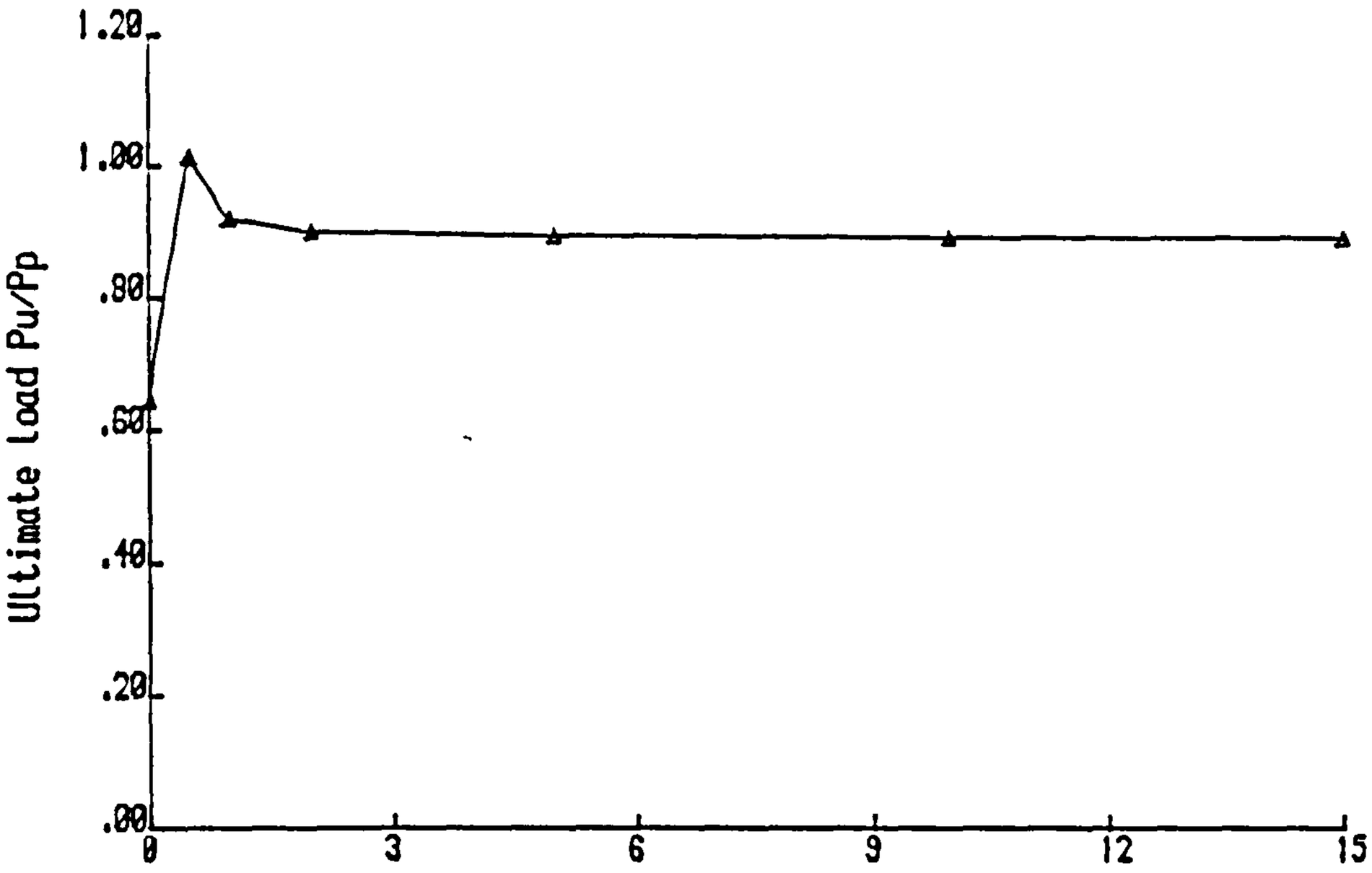

Fig. 5.11a Ultimate load-bracing stiffness curves for beam slenderness =100 (Lb=2m). UF bracing, UF loading. ILD type 1, max. value at midspan=L/1000

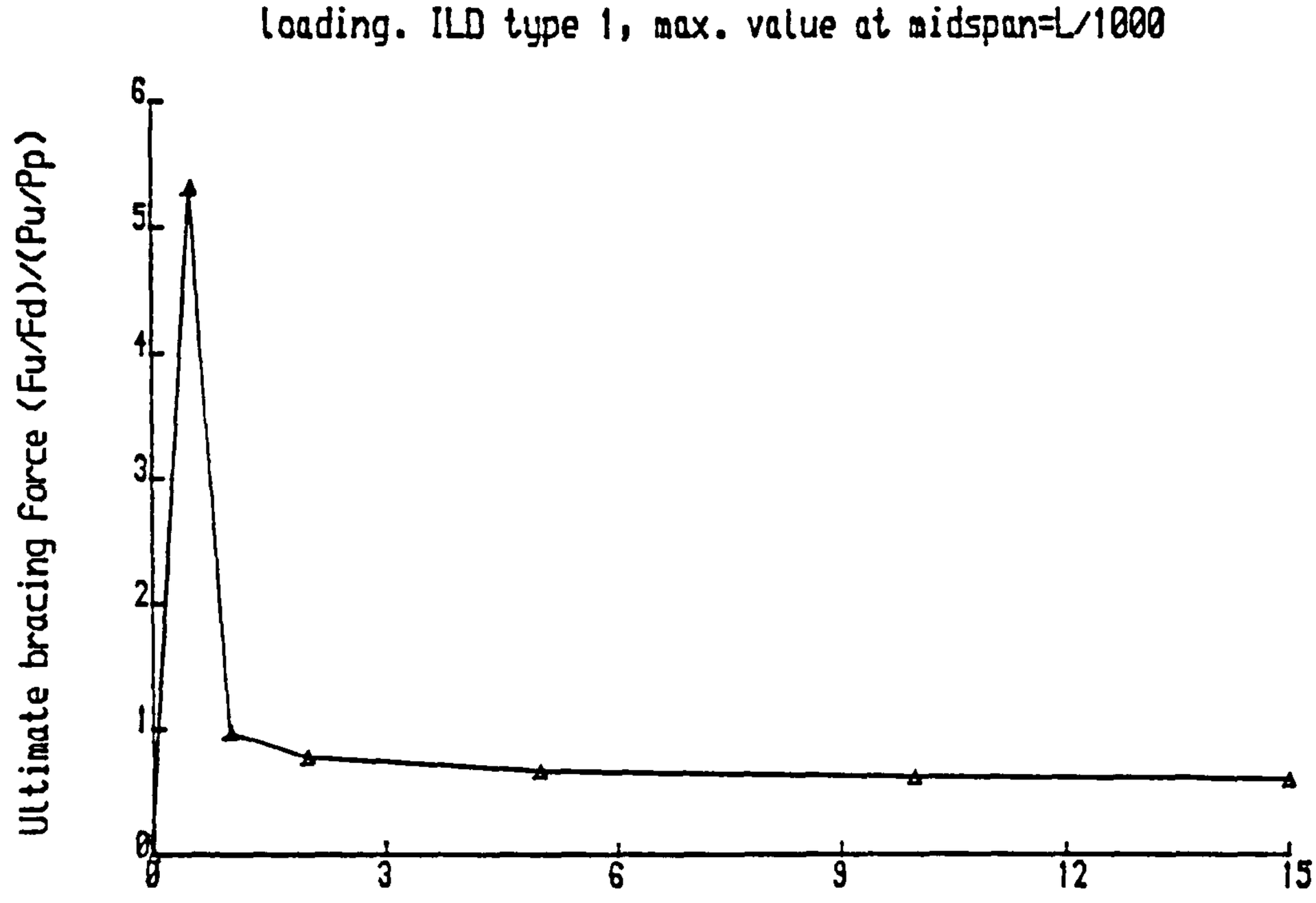

Fig. 5.11b Bracing force-bracing stiffness curves for beam slenderness =100 (Lb=2m). UF bracing, UF loading. ILD type 1, max. value at midspan=L/1000

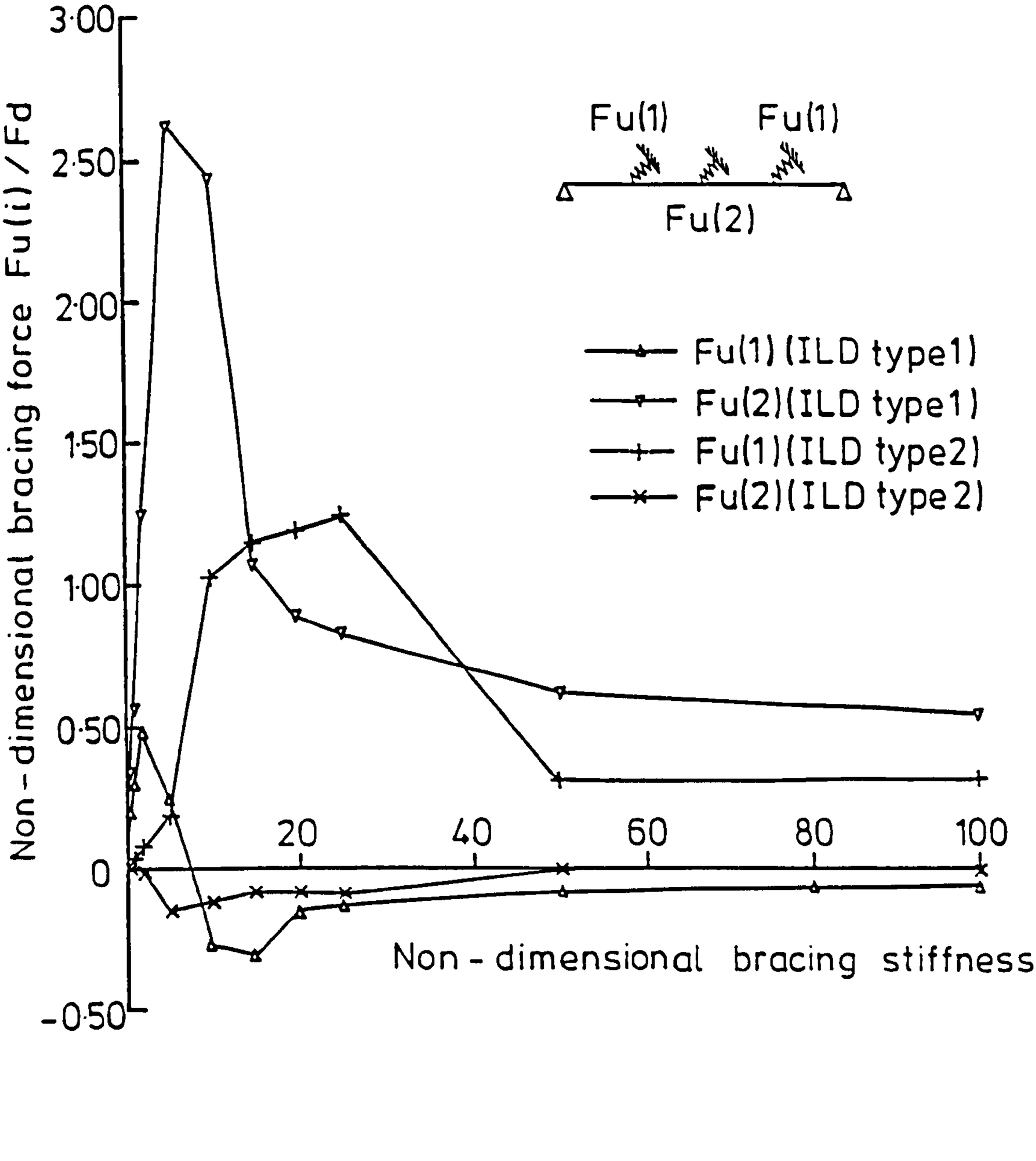

FIG.5·12 BRACING FORCE VERSUS BRACING STIFFNESS RELATIONSHIP FOR DIFFERENT BRACING COMPONENTS FOR DIFFERENT INITIAL LATERAL DEFLECTION (ILD) TYPES. UPPER FLANGE LOADING, UPPER FLANGE BRACING.

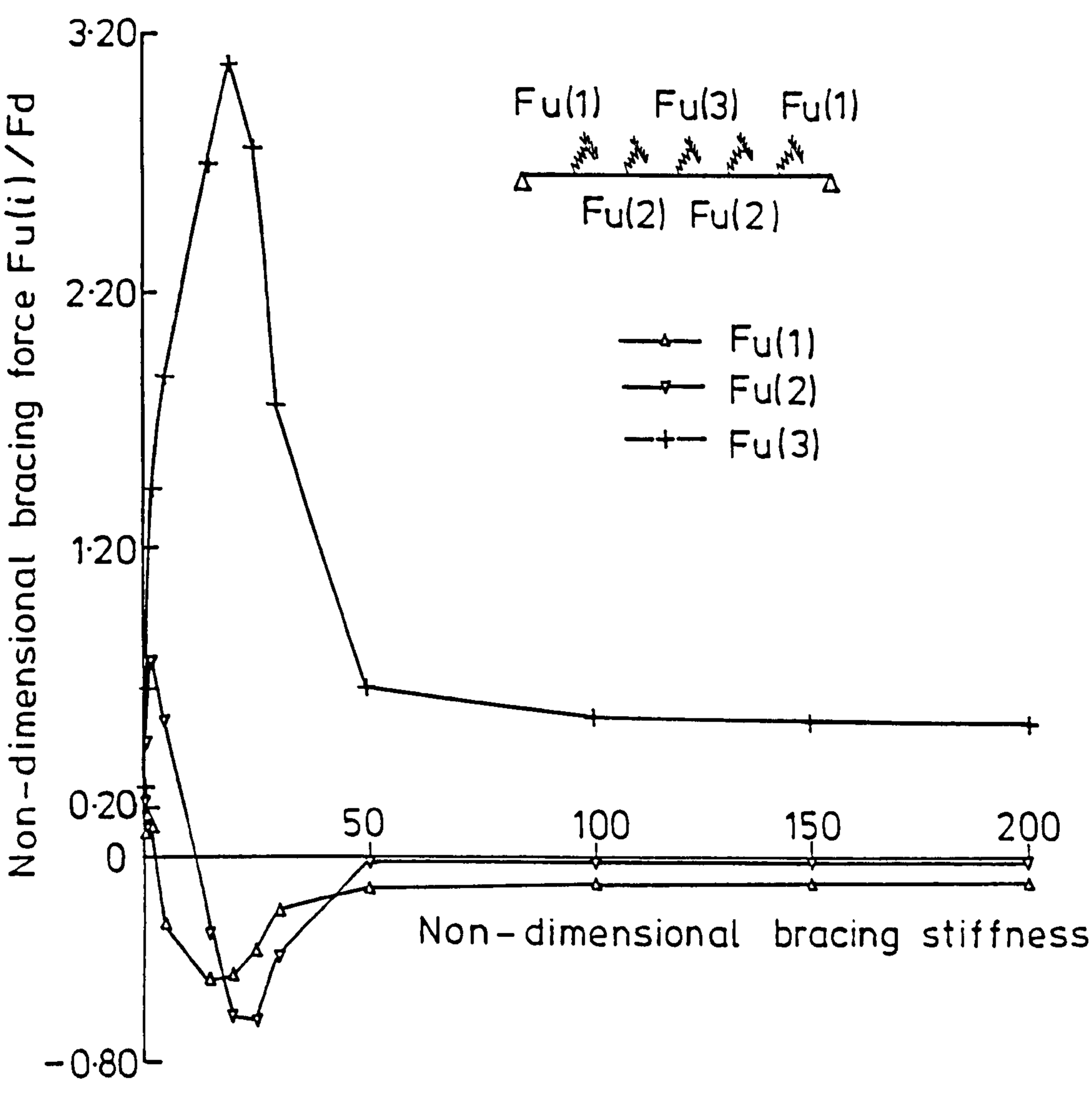

FIG. 5·13 BRACING FORCE VERSUS BRACING STIFFNESS RELATIONSHIP FOR DIFFERENT BRACING COMPONENTS UPPER FLANGE LOADING. UPPER FLANGE BRACING

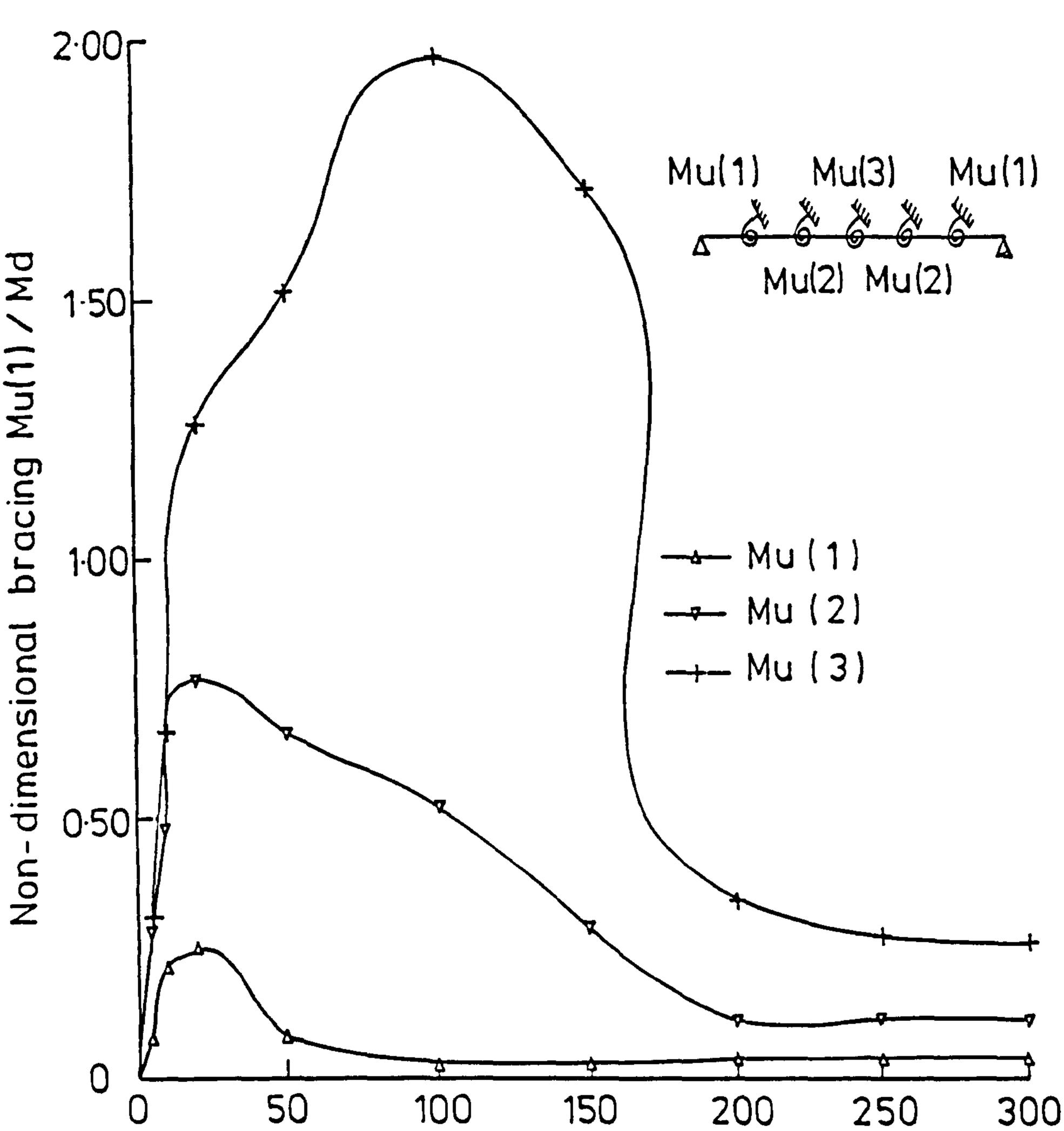

FIG. 5-14a BRACING FORCE VERSUS BRACING STIFFNESS RELATIONSHIP FOR DIFFERENT BRACING COMPONENTS UPPER FLANGE LOADING. ROTATIONAL BRACING

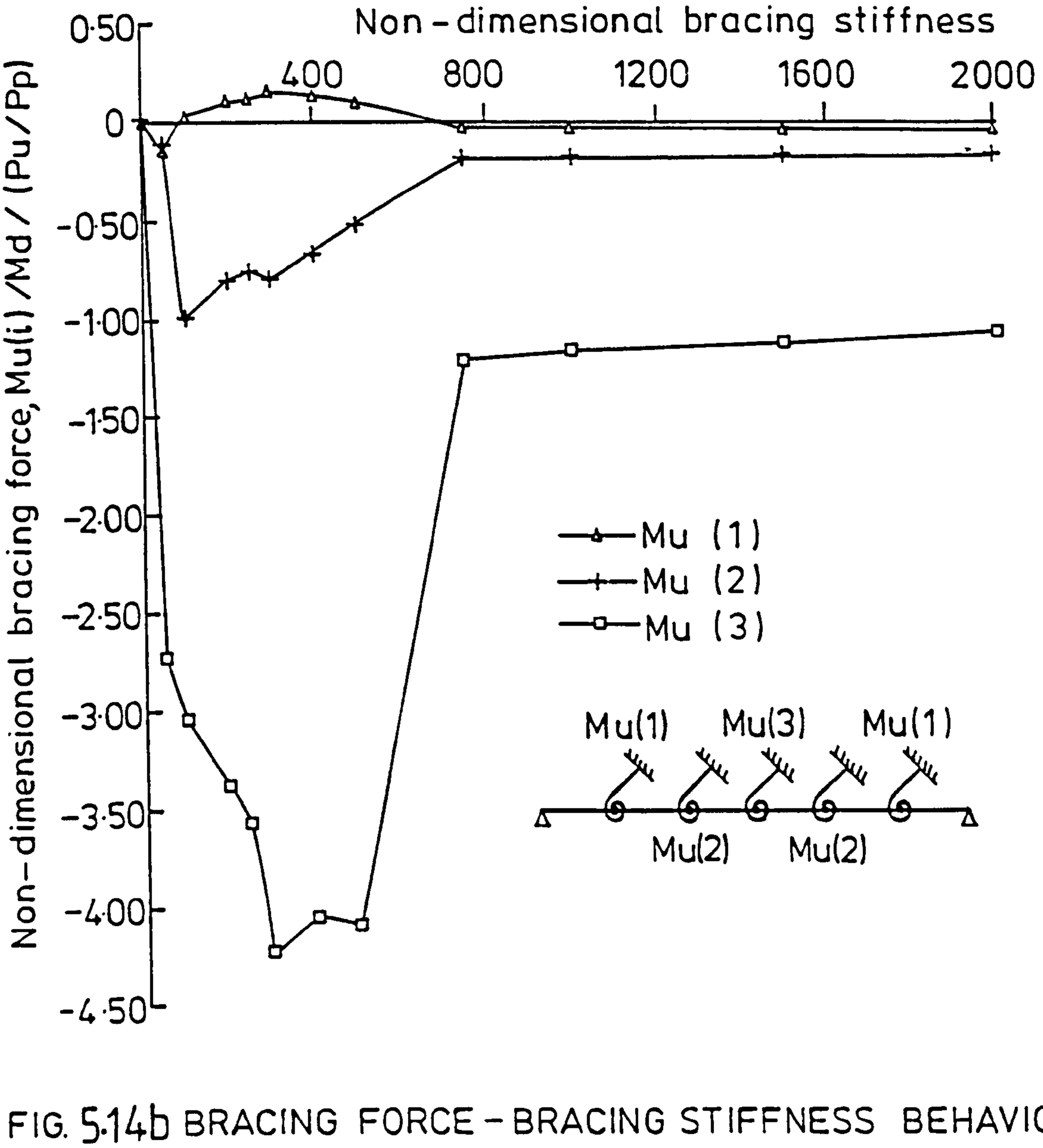

FIG. 5.14b BRACING FORCE - BRACING STIFFNESS BEHAVIOUR FOR INDIVIDUAL COMPONENTS. WITH INITIAL TWISTING, 5 TORSIONAL BRACING, SHEAR CENTRE LOADING

Chapter 6

ULTIMATE STRENGTH ANALYSIS OF FLEXIBLY CONNECTED THREE DIMENSIONAL COLUMN SUBASSEMBLAGES

6.1 Introduction

In Chapter 3, an analogy for including various restraints into the conventional analysis of thin-walled beam-columns has been presented. A finite element program has been written based on this method. Utilising this program, the effects of flexible end connections and intermediate bracings on heams bave been investigated and these studies have been reported in Chapter 4 and Chapter 5 respectively.

Although the behaviour of isolated beam-columns has been extensively studied both experimently and analytically by many previous authors, research into the detailed behaviour of three dimensional frames is rare due to the much greater degree of complexity involved. In those studies of 3-D behaviour that have been reported (Milner and Gent[46], Lightfoot and LeMessurier[53], Ang and Morris[54] etc.), various simplifications concerning connection behaviour, material and geometrical properties were introduced; therefore, the accuracy of these studies was limited.

With the progressive improvement in understanding of joint behaviour and the recognition of connection flexibility for an actual joint as well as the availability of large computer facilities, it is now practical that research into the influence of joint flexibility on the behaviour of 3-D frames be conducted.

The analysis of Chapter 3 has been extended to study the behaviour of 3-D subassemblages with semi-rigid connections and various bracings. Although the same method may be used for complete frames or column subassemblages (a typical example of which consists of a column and a number of beams framed into it at both ends about both axes), this study is focused on the behaviour of column subassemblages due to the smaller requirement for computing storage. Figure 6.1 shows the column subassemblage that has been considered. This chapter presents the extension of the analytical procedure of Chapter 3 and its verification against available results.

6.2 General Description of the Analytical Procedure

In this study, only one flexible connection is assumed to be present at one end of a member, the other end being either simply supported or fixed or rigidly jointed to another member. If a member is flexibly connected to other members at both ends, it is divided into two members. Since the main concern of this investigation is the effect of different types of beam-column connections, a linear force-deformation relationship is assumed for any boundary connection, although nonlinearity of the support may be incorporated as in the case of an isolated beam-column.

Each member of the subassemblage may be divided into a number of segments. The formation of the stiffness matrix for each of these segments and the procedure for assembling these to generate the overall stiffness matrix for the member in its own coordinate system are the same as desribed in Chapter 3 for a beam-column member. In order to save computing storage, the internal degrees of freedom within each member are condensed out employing the static condensation technique[60].

As mentioned in Chapter 3, three sets of coordinate systems are used for a beam-column member. In this analysis, an additional set of coordinates which is fixed in space for the whole subassemblage is adopted. The member stiffness matrix after static condensation is then transferred from its local coordinate axes to the system directions for the subassemblage by a geometric transformation matrix $[T_3]$ which depends on the relative position of the member and the main column. The terms in the matrix for ordinary transverse deflections and rotations can be obtained by taking the direction

cosine between the member direction and the system direction about every axis. The transformation for the 7th variable, which is the deriative of the axial rotation of twisting, is treated following the method proposed in Ref.[56]. The transformation matrices for 4 frequently used combinations of beam-column framing are provided in Appendix B1.

6.3 Inclusion of Semi-Rigid Joints

In the analysis, the connection is regarded as a member. It is assumed to possess the same orientation as that of the member it is attached to. Its stiffness matrix in the local system is obtained as follows:

$$\begin{aligned} K_{i,i} &= C_i \qquad (i = 1,14) \\ K_{i,i+7} &= -C_i \qquad (i = 1,7) \\ K_{i-7,i} &= -C_i \qquad (i = 8,14) \\ K_{i,j} &= 0.0 \qquad (otherwise) \end{aligned} \tag{6.1}$$

in which C_i is the tangent to the force-deformation curve of the connection for the appropriate degree of freedom.

As explained in Chapter 3, the connection tangent stiffness at the begining of each load increment remains unchanged throughout the loading step. The same multi-linear representations for the connection's force-deformation characteristics are adopted.

From various analytical[16] and experimental work[25], it has been realised that unloading is likely to occur at some connections under most loading sequences; the unloading path of the connection is therefore included. Fig. 6.2 shows the typical loading and unloading paths for a connection.

An offset of the connection from the column centreline will often be present, depending on the way in which the beam is framed into the column. This is accounted for by a rigid bar transformation, the simplified version of which in 2-D column subassemblage analysis is given in Ref.[16]

Following the established procedure for a beam-column member, the stiffness matrix of the connection member is transferred to the global axis system using the same transformation matrix for the member to which it is attached.

6.4 Inclusion of Intermediate Bracing

The inclusion of bracing terms in the stiffness matrix of a member is carried out following the procedure described in Chapter 3 for an isolated member in the local coordinate system prior to the transformation of the member stiffness matrix from the local system to the subassemblage system direction. Because the static condensation technique has been used to form the stiffness matrix for the member, braces are assumed to be located at the ends of the member. In other words, a bracing point is treated as a node.

6.5 Verification of the Analysis

The computer program in Chapter 3 was modified to reflect the different nature of the problem from that of an end restrained beam-column member. In order to check the accuracy of the program, comparisons with available experimental results were made.

6.5.1 Comparison with Tests by Gent and Milner

Gent and Milner[25] tested a series of H-columns under biaxial bending. These tests were conducted on rigidly jointed column subassemblages only. Unfortunately so for as the author could ascertain, no experimental data on 3-D flexibly connected column subassemblages are available.

In the tests, the column was first bent about both axes by beam loads applied through a pair of turnbukles. These loads were then kept unchanged by clamping the turnbukles rigidly and the direct column axial load was applied up to failure of the column. No residual stress or initial deflection data were reported in ref.[25].

Table 6.1 gives the comparison for the ultimate load values between the author's analytical method and the tests. The ratio of $(P/P_s)_{ana.}$ to $(P/P_s)_{test}$ has been used to judge the accuracy of the analytical results so the likely error due to slightly different cross-section dimensions and material properties may be minimized. P_s is the squash load of the column and is calculated from

$$P_s = \sigma_y \times A \tag{6.2}$$

where A is the cross-sectional area of the column.

It can be seen that the analytical values for specimens A2,A4,B1,B3 and B4 agree well with the test results i.e. difference being within 5% of the experimental failure loads. However, serious underestimates have been found for specimens A1,A3 and B2. This situation agrees precisely with the experience of Gent and Milner, who found in their analytical paper[46] about the same percentage of underestimation for each of these specimens.

The relationship between axial load and column midheight deflections

and axial load versus moments at the column top have been plotted for specimen B4 in figure 6.3; only slight differences between theory and test were found until very close to failure of the subassemblage.

6.5.2 Comparison with Tests by Dooley and Locke

Dooley and Locke[39] publised results of tests conducted on 49 braced columns with different slendernesses ($\frac{L}{r_y}$ = 154.7,231.8 and 309.4), different major and minor axis end eccentricities and varying pitches of attachment to an axis offset from one flange. These tests were also analysed by Harung and Millar[40].

Because of the peculiarity of the existence of a pair of reinforced segments at both ends of the test beam, the present program rather than that in Chapter 3 was used for the comparison.

Table 6.2 compares the author's analytical results with the test results from Ref.[39] and analytical results by Harung and Millar[40] for a selection of columns. It was reported in Ref.[39] that the offset of the attachment from the centroid was rather larger than the initial value of 9in due to the movement of the columns. The real values reported in Ref.[39] were therefore used in the present analysis. It was also noticed that the torsional constant varied from column to column. However, a constant value was used in the author's analysis. No geometrical or material imperfections were reported; it was therefore assumed that the columns were free of residual stress and that a bow of $\frac{L}{1000}$ was used for column slendernesses of 154.7 and 231.8 and $\frac{L}{2000}$ for $\frac{L}{r_y}$ =309.4. The yield stress reported for each speciman was used. A cross-section of $305mm \times 101.6mm \times 25kg/m$ was given, however, its real dimensions for each column were not provided.

Table62 clearly shows that the author's analysis is much more accurate than that of Harung and Millar[40] and a reasonable agreement with the tests is obtained. Due to the inevitable differences in cross-sectional properties and imperfections, some discrepencies are bound to exist and no attempt was made to duplicate the test results.

In Ref.[39], the load-deflection curve, including post-buckling region for each column was provided. However, only the ascending part is of interest herein, since the present analysis can only trace the load-defelction curve until the attainment of the ultimate load. The comparisons of load-deflection behaviour are shown in Figs 6.4a, 6.4b and 6.4c for column slenderness $\frac{L}{r_y}$ of 154.7,231.8 and 309.4 respectively. These curves clearly show that the program can trace the load-deflection curves quite accurately.

Although the comparison is limited, it is thought that the present analysis has sufficient ability to cope with the problem under current investigation.

6.6 Conclusion

The analytical method for a restrained beam-column member has been extended to include the effects of semi-rigid connections and flexible bracings on the beha viour of beam-column subassemblages. A limited comparison with other studies con firms the ability of the method to solve this class of similar problem.

Table 6.1 Comparison of present analysis with Ref. 25 for ultimate loads

Speciman No. (1)	Test load(kN) (2)	$\frac{P}{P_s\ test}$ (3)	Analytical load(kN) (4)	$\frac{P}{P_s\ ana.}$ (5)	$\frac{Col.5}{Col.3}$ (6)
A1	36.94	0.96	24.44	0.61	0.64
A2	37.38	0.97	36.31	0.94	0.97
A3	34.71	0.95	26.70	0.73	0.77
A4	32.93	0.90	30.80	0.85	0.94
B1	14.29	0.80	14.42	0.81	1.01
B2	15.26	0.90	12.31	0.72	0.80
B3	14.91	0.87	14.60	0.85	0.98
B4	9.97	0.59	9.99	0.59	1.00

Table 6.2 Comparison of present analysis with Ref. 39 for ultimate loads

Speciman No. (1)	Test load kN, Ref.39 (2)	Present Analysis (3)	$\frac{Col.3}{Col.2}$ (4)	Analysis Ref. 40 (5)	$\frac{Col.5}{Col.2}$ (6)
1	355.0	351.0	0.989	-	-
4	208.0	205.0	0.986	238.0	1.15
5	196.0	171.0	0.872	221.5	1.13
6	192.0	176.0	0.917	-	-
7	182.0	171.0	0.940	-	-
8	111.0	118.5	1.068	133.3	1.20
9	110.0	115.5	1.041	124.5	1.13
12	74.0	87.3	1.179	99.0	1.37
17	64.0	67.3	1.051	71.25	1.20
21	236.0	218.0	0.924	-	-
22	231.0	194.5	0.842	-	-
23	161.0	150.0	0.932	169.5	1.06
24	153.0	140.5	0.918	157.8	1.03
27	77.0	80.75	1.049	81.2	1.20
30	54.0	56.5	1.046	61.7	1.15
32	42.0	44.0	1.048	44.1	1.05
33	40.0	42.3	1.056	44.1	1.10
37	145.0	141.0	0.972	-	-
39	125.0	113.0	0.904	139.2	1.11
41	70.0	74.4	1.063	-	-
43	60.0	63.5	1.058	-	-

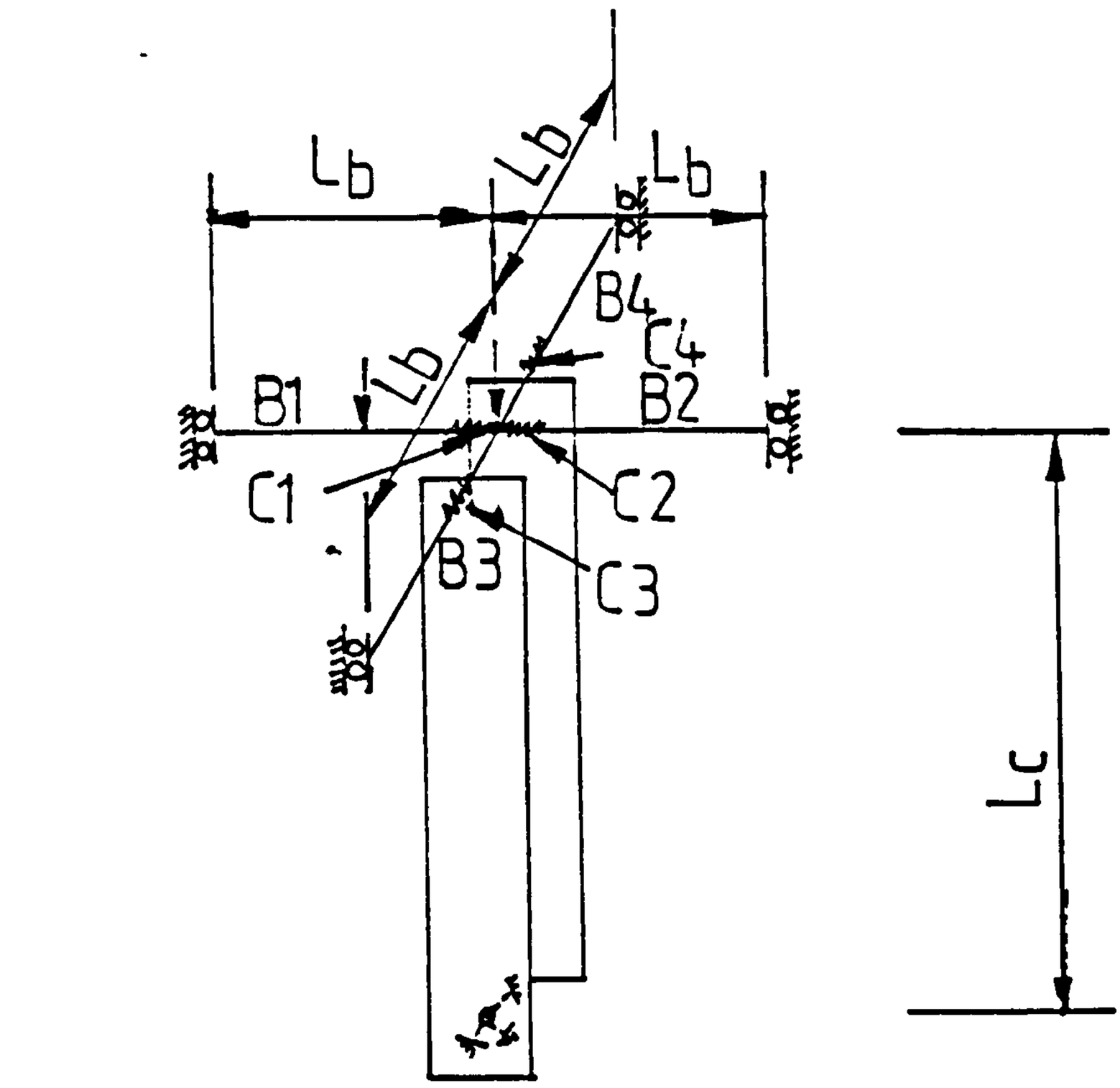

Fig. 6·1 Problem under consideration

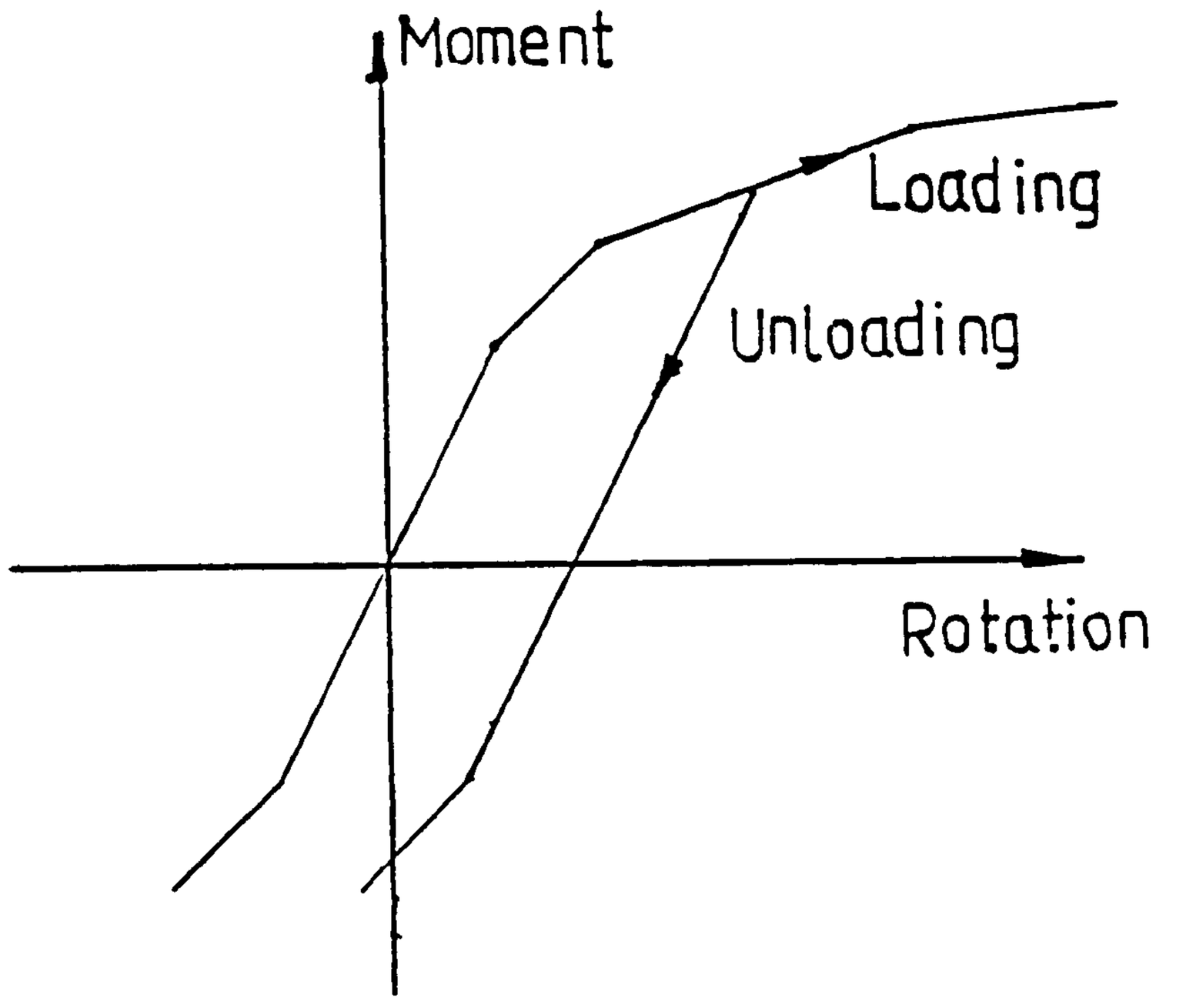

Fig. 6·2 Typical loading-unloading behaviour of a semi-rigid connection

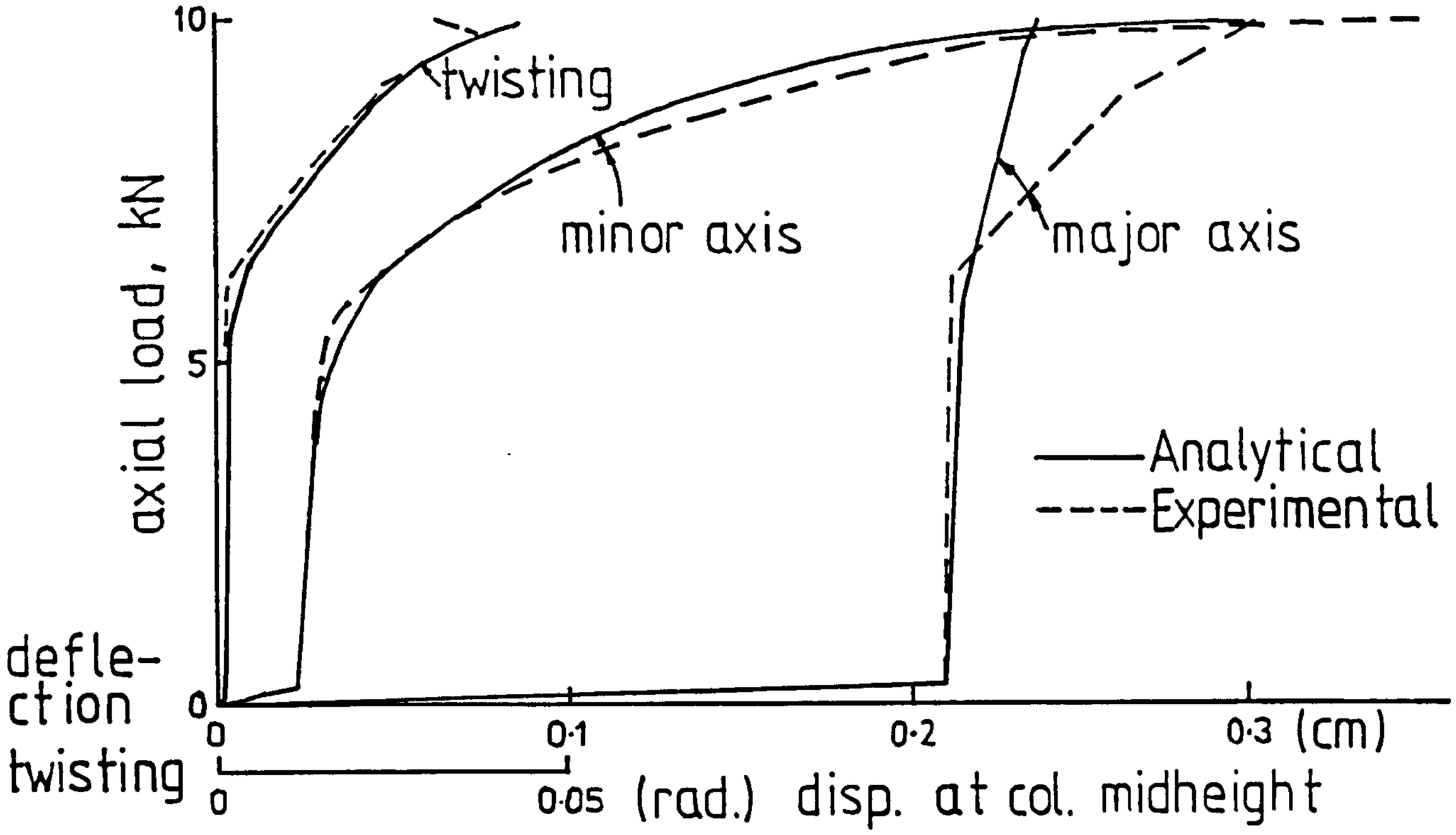

Fig. 6·3a Load Vs deflection behaviour

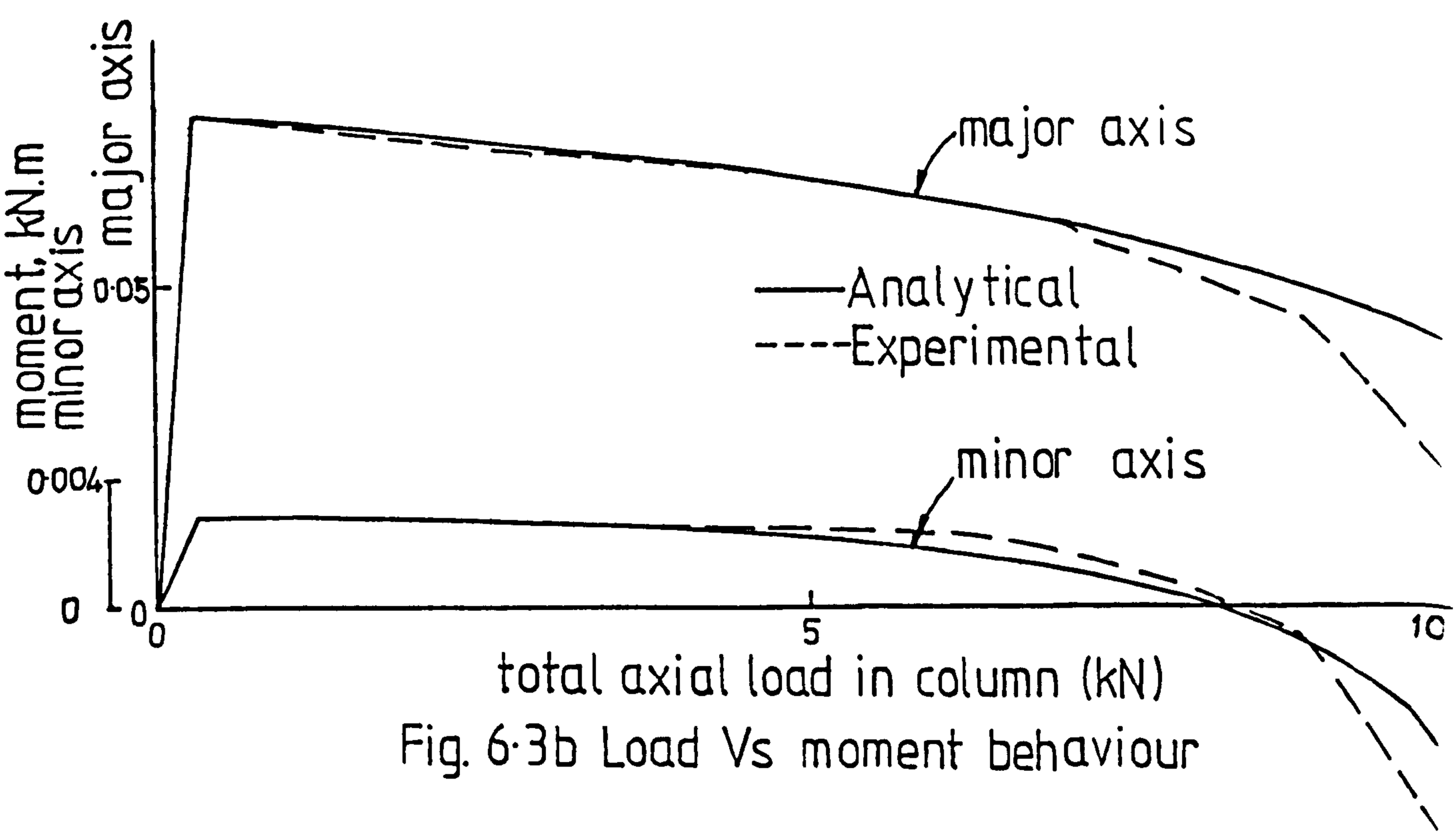

Fig. 6·3b Load Vs moment behaviour

Fig. 6·3 Comparison with experimental results (Ref: 25)

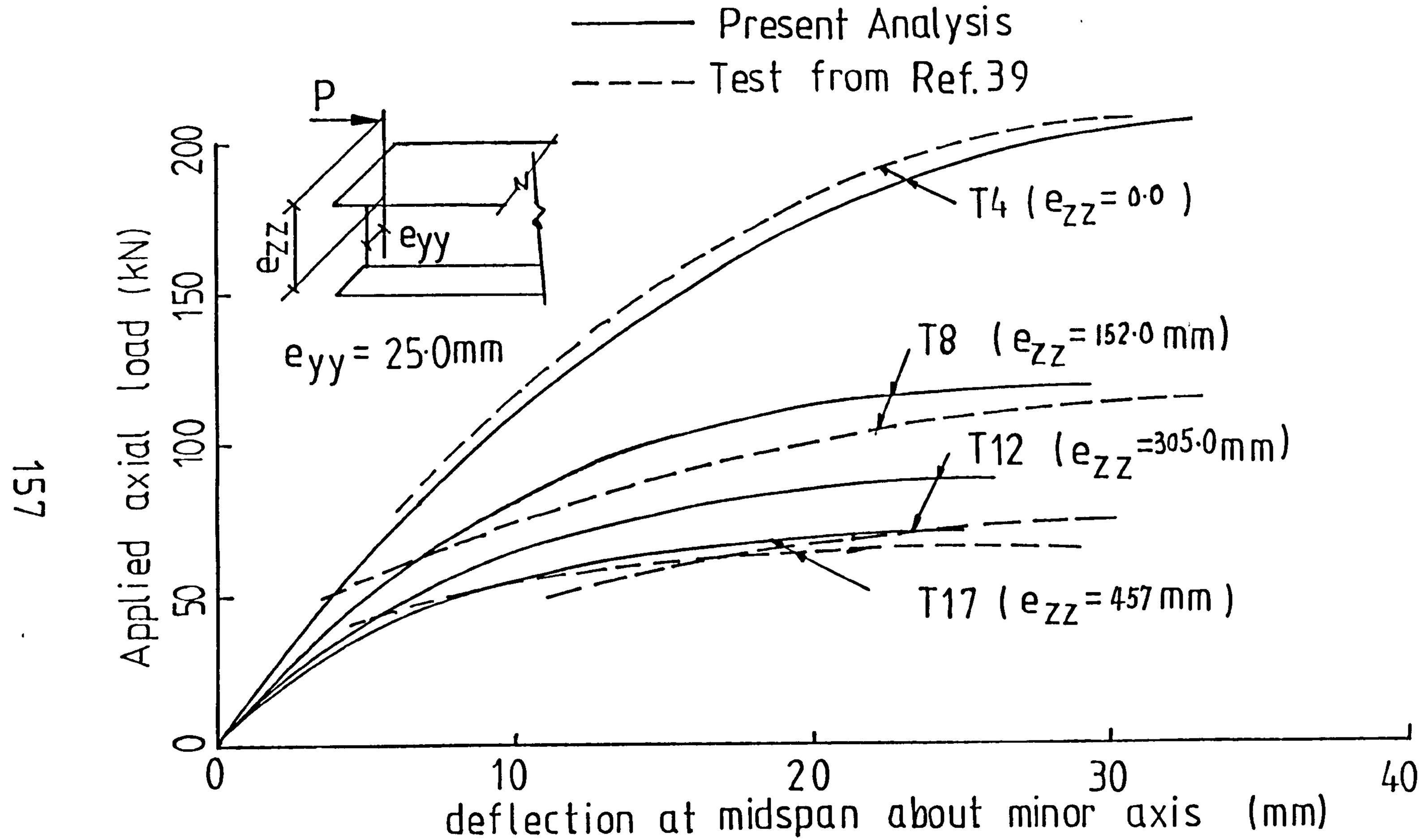

Fig. 6·4a Load-deflection curves for column slenderness =154·7- Comparison with test of Ref. 39

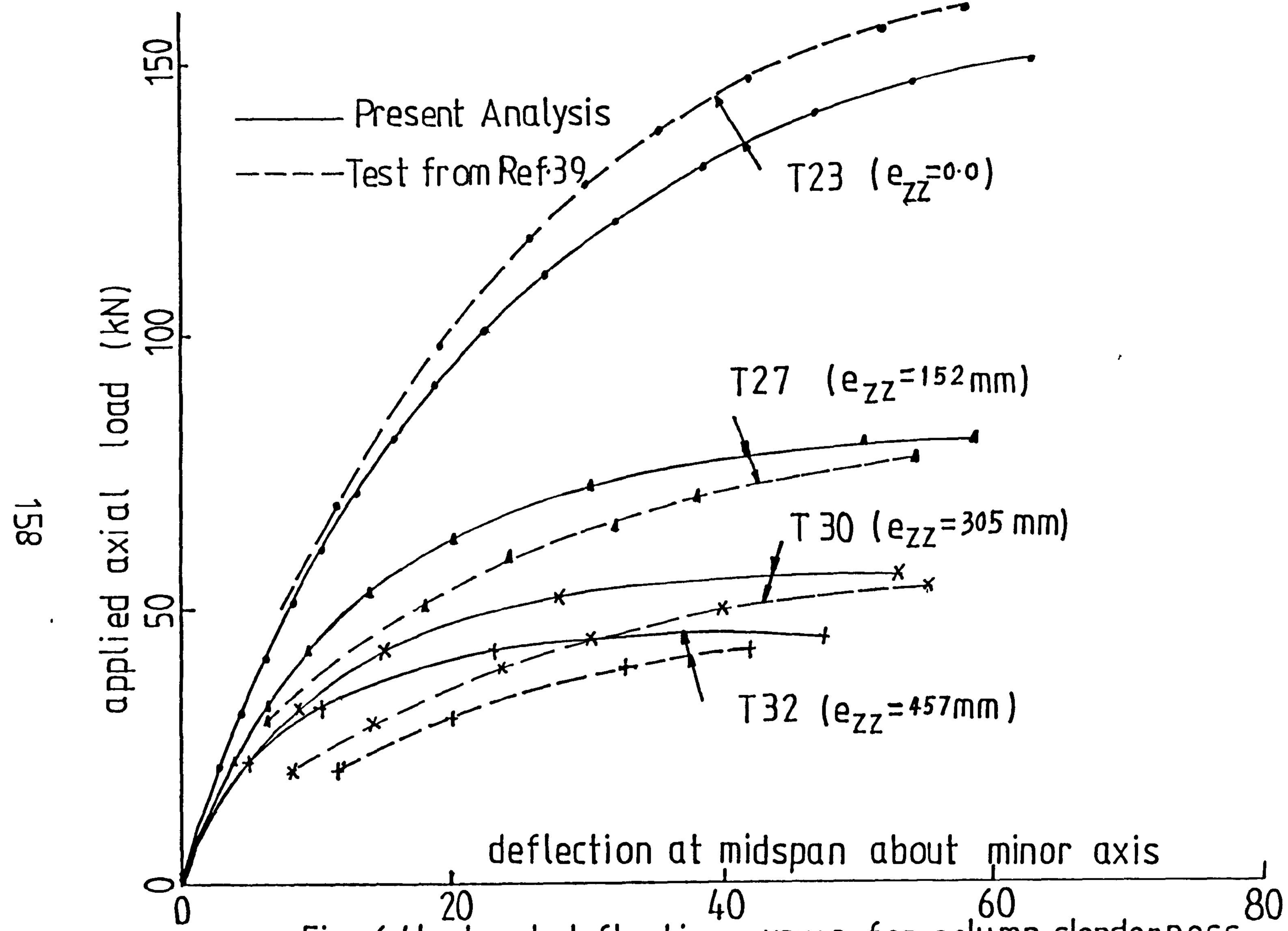

Fig. 6·4b Load-deflection curves for column slenderness = 231·8 -Comparison with test of Ref. 39

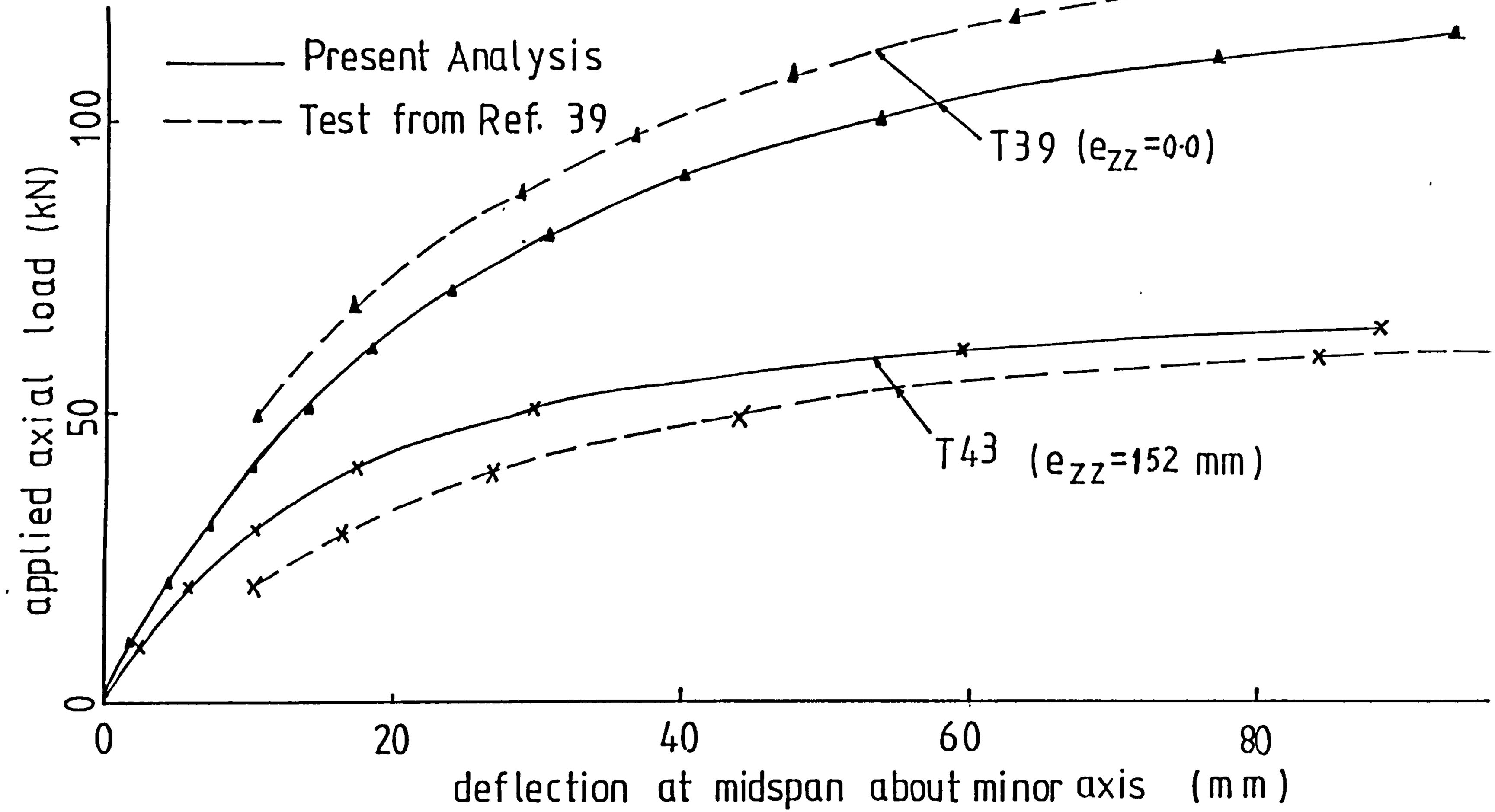

Fig. 6·4c Load-deflection curves for column slenderness = 359·4 - Comparison with test of Ref. 39

Chapter 7

EFFECTS OF SEMI-RIGID CONNECTIONS ON THE BEHAVIOUR OF THREE DIMENSIONAL COLUMN SUBASSEMBLAGES

7.1 Introduction

A method of tracing the ultimate loads of column subassemblages allowing for the effects of beam-column joint flexibility and bracings has been presented in Chapter 6. Test results for rigidly jointed column subassemblages were compared with the analysis and the close agreement obtained accepted as validation of the performance of the method for similar problems.

In order to better understand the influence of joint flexibility on the

behaviour and load carrying capacity of column subassemblages, a limited parametric study has been conducted using the program metioned above. The main parameters are the flexural stiffness of the connection referred to the major axis of the beam to which it is attached (including the beam itself) and the amount of moment transferred from the beams to the column. Consideration is also given to the effect of the connection's out-of-plane i.e. torsional and out-of-plane flexural restraints. This chapter discusses the results from this study and presents the assessment of these results against the prediction methods of the U.K. steelwork code[3] and Wood[63].

7.2 Description of Basic Parameters

A column subassemblage shown in Fig. 6.1 has been used for this study. The connections investigated herein are rigid joints, extended end plates, flange cleats, web cleats and pin joints. Due to the lack of information on the moment-rotation curves of connections attached to the web of the column, [1] the same major-axis in-plane moment-rotation curve is used for both major and minor axes (referred to the column). Nevertheless, the influence of the joint flexibility on the behaviour of the subassemblage should follow qualitatively the same general pattern no matter what data are used. Moment-rotation curves (fig.4.2) used in Chapter 4 for the study of flexibly restrained beams are adopted. Twisting of the column is assumed to be completely prevented by the end connections which are also assumed to offer no restraint against warping.

[1] since this work was started some data on the behaviour of weak axis column connections have become available[65].

The beam and column dimensions as well as the beam and column lengths are all given in table 7.1, together with the second moments of area and areas for the beam and column cross-sections and the geometric slendernesses for the various column lengths. The material properties are: Young's modulus E=200,000 N/mm^2, shear modulus G=80,000 N/mm^2, Poisson's ratio $\nu = 0.25$ and yield stress σ_y =285N/mm^2.

Beam loads are applied first and then the column load is applied while the beam loads remain unchanged until failure of the column. Referring to the beam loads, four different load arrangements are included in the study; these are shown in figure 7.1. The maximum beam load T is 100kN, which acts 37.5 cm away from the top of the column in every case. No residual stress was included due to its small effect on the load-carrying capacity of structures responding in a 3-D fashion(Chapter 4). A half sine wave with a bow of $\frac{L}{1000}$ was assumed for the column initial shape about both axes.

7.3 Results and Dicussion

7.3.1 Results

Fig. 7.2-7.6 present the relationships of (1) axial load against deflection about the major axis at the centre of the column; (2) axial load against deflection about the minor axis at the centre of the column; (3) axial load against twisting at the centre of the column; (4) axial load against connection moments on both sides of the weak axis of the column; (5) axial load against column moments at the top and the centre of the column for various connections. The load case is 'TT' and the column slenderness used is $\frac{L}{r_y}$ =81.

The complete list of ultimate loads for all the cases is given in table 7.2, whilst tables 7.3 and 7.4 give the ultimate loads for various connection arrangements. Figures 7.7 and 7.8 show the load against column midheight deflection behaviour about the major and minor axes for different load cases with web cleat connections and $\frac{L}{r_y}$=81.0. The load-deflection relationship for a range of beam lengths with no beam load, web cleat connections, and $\frac{L}{r_y}$ =81.0 is given in figure 7.9. The load against column top moment behaviour about the minor axis for column slendernesses of 81,121 and 162 with web cleat connections and load case TT is shown in figure 7.10. The marks on these curves indicate the points at which the direct column load is applied.

7.3.2 Behaviour of the Subassemblage

Several interesting points may be observed in these figures and tables:

1. From figures 7.2-7.4, it can be observed that the deformation of the column is composed of large minor axis deflections, considerably smaller major axis deflections and very little twisting. This is due partly to the large difference between the minor axis and major axis bending stiffnesses of the column, and partly to the absence of any direct torsional loading i.e. twising only occurs due to the end loads acting through the column deformations. It was also observed in running the computer program that the failure of the subassemblage always occurred by minor axis instability unless a heavy major axis load (load case '0T') was applied. In no case, was torsional instability the failure mode. Figure 7.4 indicates that the twisting of the column only really becomes perceptible when the subassemblage approaches failure, by which stage

large losses of stiffness will have occurred due to spread of yield. It is of interest that this form of behaviour closely accords with that observed in the BRE rigid jointed frame test[50].

The behaviour of other types of column cross-section , ranging from beam type to wide flange column type has been found to be of the same general form i.e. even when I_x *and* I_y are closer, minor axis failure always dominates the response.

2. The load carrying capacities, which are defined as the total axial load in the column at failure, for the case of rigid connections and each type of semi-rigid connection do not vary significantly as was observed previously for a single beam-column(see Chapter 4). For instance, for 'TT' load and $\frac{L}{r_y}$ =81.0, the values are 650.0kN, 652.0kN, 670.0kN, 684.0kN and 608.0 kN for rigid joints, extended end plate connections, flange cleat connections, web cleat connections and pin joints respectively. (The seemingly surprising result that the largest increase is obtained for the weakest semi-rigid connection type is discussed later in paragraph (5).) However, even the web cleat connections are able to increase the ultimate load of the subassemblage very significantly as compared with the equivalent pin jointed case e.g. for '00' load, the increases of ultimate load for web cleat connections over the pin jointed case are 21.4%, 60.4% and 80.2% for $\frac{L}{r_y} = 81.0$, 121.5 and 162.0 respectively. Similar noticable increases of ultimate strength for cases involving web cleats over equivalent pin-jointed cases were also obtained in the analyses of two dimensional frames conducted by Rifai[16]. For these reasons, further discussion will concentrate mainly on rigid joints,

web cleat connections and pin joints.

3. A small study of the effect of residual stress confirms the observations for an isolated member. Firstly, the residual stress reduces the ultimate load most when the degree of yield penetration across a cross-section is modest e.g. the reductions of ultimate load for 'TT' load case, web cleat connections with $\frac{L}{r_y}$ =81.0, 121.5 and 162.0 are 7%, 8% and 5% respectively in the presence of a parabolic pattern of residual stress with the maximum value at the flange tips being $0.30\sigma_y$ in compression; secondly, the behaviour of the structure is not affected until the initiation of yield of the material. The comparison of the total axial load in the column against the column central deflection about the minor axis for $\frac{L}{r_y}$ =121.5, web cleat connections and load 'TT' is shown in figure 7.11, which clearly reveals the influence of residual stress. In no case was the reduction of ultimate load particularly significant due to the presence of residual stress.

4. For cases of unbalanced beam loading, the connection between the loaded beam and the column (C1 or C3) starts to unload once the direct column load is applied, while the connection (C2 or C4) between the unloaded beam and the column continues to load (see figure 7.5). This can readily be explained by the different directions of beam rotations required under beam loading and direct column loading (see figure 7.14). Comparisons of typical loading-loading and loading-unloading moment -rotation curves for a web cleat connection extracted from the subassemblage analysis and the originally input data are plotted in figures 7.12 and 7.13. The reason for the former being slightly higher

follows from the way in which the program operates i.e. the stiffness of the connection will remain unchanged within each loading step. If the loading step becomes very small, the analytical curves will follow the input characteristics exactly. These figures also show that the connection rotations are quite noticeable, being about 0.004 radians. For web cleat connections, the loading stiffnesses in these regions are normally insignificant[15].

The variation of moment at the top of the column follows the trend of loading-unloading, whilst that of the centre continues to increase but at different rates. This result accords with previous analytical and experimental work ([16],[25]). The reason is that the moment at the column top is the balance of the connection moments on the two sides of the column and consists of two parts, namely the moment transferred to the column due to pure beam loading (M_t^1) and that resulting from column top rotation (M_t^2), see figure 7.15b. These two moments act in opposite directions. However, the moment from beam loading (M_c^1) and that from column deflection (M_c^2) are in the same direction at the centre of the column, see figure 7.15c.

5. For every column length, the use of stiffer connections produces a higher buckling load in the case of the '00' load case, but for loading 'TT', this will reverse for low slenderness and high slenderness. This is explained by the two-fold role played by the connection in influencing the behaviour of the subassemblage. Firstly, the stiffer connection will provide more restraint and so reduce the column deflection; secondly it transfers more bending moment from the beam to the column, which

tends to reduce the stability of the column. These two effects tend to cancel one another and the net effect of a change in connection will therefore depend on their relative influence.

For short columns, the squash load could be reached by the subassemblage even if the column was not provided with any restraint (i.e. in the case of pin joint) were it not for the moments produced as a result of column flexure due to initial deflection. That is to say, the difference in the restraining effect of different connections will not be particularly significant. Since the failure of the subassemblage will be controlled by the development of plasticity, the effect of the connection transferring more moment from the beam to the column is the more significant effect and the greater moment transferred by the stiffer connection will cause the subassemblage to fail at a lower load. This negative effect of the 'overstiff' connection has also been pointed out in other studies ([61],[62]).

In the case of the '00' load, it is the more flexible connection which will be associated with the greater moment within the column due to larger column deflections since it provides a small degree of restraint. Therefore, lower load carrying capacities will result for the more flexible connections.

For slender columns, the failure of the subassemblages is mainly due to instability of the column about the weak axis. The buckling load is therefore sensitive to the change of connection restraint (see table 7.2 for the ultimate load for '00' case for different lengths). However, as the column is very flexible in this case, the moment transferred to

the column from pure beam loading (M_t^1) is insignificant and does not change very much for different connections, but the moment resulting from the column deflection depends to a much greater extent on differences in the connections. As a result, subassemblages with stiffer connections always have higher load carrying capacities regardless of the beam loading patterns.

6. Figure 7.10 gives some explanation for column strength variation with column slenderness. From this figure it is clear that the top of the column starts to unload before the commencement of direct column load for higher slendernesses $\frac{L}{r_y}$ =121.5 and 162.0). This is because the M_t^2 values are larger than M_t^1 values at higher slendernesses even within the beam loading phase due to the large column top rotation. The small value of M_t^1 only slightly affects the ultimate load of the structure and may be neglected. Therefore, the ultimate load variation follows the same pattern as '00' load for other load cases, whilst for low slenderness $\frac{L}{r_y}$, M_t^1 is very influential and is proportional to the change of connection restraint.

7. The interaction between major axis bending, minor axis bending and twisting is not very noticeable. Figure 7.8 shows that the minor axis deflection alters slightly for loading cases '00' and '0T'; figure 7.7 suggests no noticeable change in the deflection for loading cases '0T' and 'TT'; while the small contribution of major axis and minor axis bending to the twisting of the column is clearly illustrated in figure 7.4.

7.4 Actions of the Connection

In order to clarify the two effects of end restraint and moment transfer, the following investigation has been carried out in which both effects have been varied separately.

7.4.1 End Restraint

For this study, the moment transferred from the beam to the column by the connection has been kept approximately unchanged and the stiffness of the connection (including the beam) varied in different ways, so that the effect of the connection in providing the subassemblage with different degrees of restraint may be assessed.

Different arrangement of connections

In this case, five of the above mentioned connections were connected in turn to the weak axis of the column so as to produce different degrees of restraint, a web cleat connection was used about the strong axis. Table 7.3 lists the ultimate loads for this study and clearly shows the improvement with the use of stiffer connections.

Variation of beam length

Subassemblages provided with web cleat connections about both axes of the column without beam loading were studied for the five beam lengths 150cm, 300cm, 600cm, 1200cm, 2400cm. Figure 7.9 plots the axial load versus deflection about the minor axis at the centre of the column and gives the ultimate load values for each case. The behaviour and the ultimate strength of the

equivalent pin jointed subassemblage is also given in this figure. The longer the beam length, the smaller the stiffness of the connection plus beam relative to that of the column, and therefore the lower the restraining effect of the connecton. Figure 7.11 clearly illustrates the trend. Theoretically, an infinite beam length would make the stiffness of the beam zero, so providing no restraint to the column, corresponding to the case of the pin jointed subassemblage.

7.4.2 Moment Transfer

For this study, the restraint about the weak axis of the column has been kept unchanged, but the moment transferred to the column was varied through the use of different arrangements of the connection.

In contrast to the case of 7.4.1.1, the web cleat connection is used to provide restraint about the minor axis so that the restraining effect is the same for every case. The load is applied to the beam attached to the major axis of the column so that the moment transferred to the column is changed. Clearly, the effect of the stiffer connection is to transfer more bending moment to the column and thus to reduce the strength of the subassemblage. The complete list of ultimate load values for this type of connection arrangement with different column slendernesses under different loading arrangements is given in table 7.4. This suggests that the stiffer connection does not necessarily always increase the load carrying capacity of the structure.

As discussed above, the strength variation of a column subassemblage with different connections, column slendernesses and under different loading cases cannot be predicted quantitatively as simply as for the case of an isolated beam-column. This is due to the two opposite effects of the connection

as discussed earlier in section 7.3. When the restraining effect dominates, the strength of the subassemblage will be increased with the use of stiffer connections; whilst in the case of the moment transfer effect being dominant, the use of stiffer connections may result in a reduction in the strength of the subassemblage.

7.5 Effects of Out-of-plane Restraints

As discussed in the last two sections, the connection's in-plane restraint has a great effect on both the behaviour and ultimate load of the column subassemblage. A small additional study has been conducted to evaluate the effects of the connection's out-of-plane restraints.

Web cleat connections and load case '00' were assumed. The column slenderness was taken to be 162 in order to show the greatest variation of the connection's effects. Table 7.5 lists the ultimate strength values of various studies for the connection's torsional restraint. It clearly shows that reducing the beam length would increase the ultimate load of the structure and for the beam length of the previous study, the improvement in the subassemblage's strength for infinite stiffness over zero stiffness is negligible.

Examining the directions of various restraints of the connection referred to the column will reveal that the torsional restraint of the connection referred to the beam adds to the perpendicular connection's in-plane stiffness. The connection's torsional restraint (including the beam) is very small compared with the flexural restraint provided to the column by the perpendicular connection's in-plane restraint. Therefore, a very small strenghthening effect is produced as shown in table 7.5, which shows that the greatest

increase in strength from $K_{tor} = 0.0$ to $K_{tor} = \infty$ is approximately 10 per cent. Furthermore, increasing the length of the beam will reduce the ratio of the connection's torsional restraint to the in-plane restraint. Consequently, smaller increases in strength from K_{tor} =0 to $K_{tor} = \infty$ will be generated with the use of more slender beams.

Figure 7.16 clearly shows that the subassemblage's load-deflection behaviour is just slightly affected for a beam length of 5 cm. Bearing in mind that the beam length of 5 cm represents a case of academic interest only and even the weakest connection possesses a certain degree of torsional restraint as described in Chapter 4, the prevention of the connection's twisting may be justified.

The problem under current investigation is basicaly of a column type. Because of the dominance of lateral (flexural) buckling, the torsional restraint provided to the column by the connection has an imperceptible effect on its behaviour. This torsional restraint is from the out-of-plane flexural bending restraint of the connection; therefore, it implies that the behaviour of the subassemblage is not influenced by the connection's minor axis bending restraint, which was exactly the conclusion reached from such case studies.

7.6 Comparison with Design Methods

7.6.1 Comparison with the BS 5950 Approach

In order to predict the design load of a rigidly connected column subassemblage, the British design code[3] includes a set of charts from which the effective length ratio of the column may be obtained and thus the compressive

strength of a column provided with restraint from the adjacent beams may be assessed. Using equation 4.8.3.3.1, the overall buckling of the subassemblage can be checked.

The incorporation of connection flexibility into the design approach is made possible by calculating an equivalent beam stiffness. Following the equation proposed by Wood[63], the general form of beam effective stiffness is:

$$K_b' = \frac{M}{4E\phi} = \frac{Applied\ moment}{4E\ (Resultant\ rotation\ if\ far\ end\ is\ fixed)} \tag{7.1}$$

in which M and ϕ are the applied moment and resulant rotation respectively of the beam end near the column.

Considering the supporting condition at the far end of the beam and the connection stiffness C, the effective stiffness of the beam is:

$$K_b' = \frac{3/4K_b}{1 + \frac{3EK_b}{C}} \tag{7.2}$$

where $K_b = \frac{I_b}{L_b}$ is the effective stiffness when the far end of the beam is fixed and the near end is rigidly connected to the column. In determining the connection stiffness, the secant stiffness is used when both connections are loading-loading. In the case of unbalanced loading, when the applied load is high and the connection is flexible, the initial stiffness (unloading stiffness) of only one connection is considered as effective, neglecting the stiffness of the loading-loading connection so as to compensate for the loss of stiffness of the loading-unloading connection before the commencement of the column load phase. The stiffness of connections attached to the weak axis of the column is used because the failure of the column is always about the minor axis of the column.

Since the moments on the column are dependent on the applied axial load, the axial load should be calculated by trial and error. In this study, the moments in the subassemblage are found by a simple elastic method (Appendix C1) at each load level (including P- δ effect) which is suitable for micro-computer use. In the calculation, the major and minor axis bending are decoupled because of the negligible interaction observed and discussed previously. The virtual work principle is applied and the column central deflection, connection moments and hence column moments are calculated. The comparison of this calculation and the 'exact' computer analysis is shown in figure 7.17 and 7.18. The simple method is of sufficient accuracy for the moment calculation bearing in mind the low sensitivity of the design load to the variation of the flexural bending moments.

The design load calculated using this approach is compared with the applied load. If the applied load is lower, it is increased until the design load equals the applied load.

To demonstrate the application of this method, an example is given: In this example, the connections are assumed to be web cleats; the load case is 'TT' and the slenderness $\frac{L}{r_y}$ =81.0. According to the method, the following variables are: for beam B1 (associated with connection C1), K_b' =3.094; for beam B2 (related to the connection C2) K_b' =0.0; then at the top of the column:

$$K_1 = \frac{K_c}{K_c + \sum K_b'} = 0.3022 \tag{7.3}$$

and since the bottom of the column is pinned, K_2 =1.0

From the formula in Ref.[47],

$$\frac{L_e}{L_c} = 0.5 + 0.14(K_1 + K_2) + 0.055(K_1 + K_2)^2 = 0.77588$$

Using appendix C in the design code, the compressive strength $p_c = 200.3N/mm^2$, Z_y =52.95cm^2, $m_x = m_y$ =0.57.

Suppose at the end of beam loading, the applied axial load in the column is 200kN, the moments calculated from the simple elastic method at the top of the column are M_x =2.85kN.m, M_y =1.68kN.m.

Using the design method, the design load is F = 527kN, which is higher than the applied load i.e. the subassemblage is able to sustain a higher load. Increasing the applied load until the two loads are equal, the coincident value is the required design load. In this case, the value is 536kN. The reason for this value being higher than the previous one (527kN) is due to the column top starting to unload when the direct column axial load is applied. Table 7.6 gives various values required at a typical iteration. Figure 7.19 plots the relationship between the total axial load in the column and the design load at each step as calculated above, comparing the results with both simple moment calculations and the 'exact' calculation.

Table 7.7 lists the design values of ultimate load for rigid joints, web cleat connections and pin joints with different column slendernesses under different load types.

Comparing the results in table 7.7 and those in table 7.2, the above method appears to be quite satisfactory, although in the case of '0T' load for high slendernesses, the relative strength of rigid joints to the flexibly connected arrangement is not quite in accord with the analytical prediction. This has arisen because of difficulty in modelling connection stiffness. In this case, the secant stiffness of the connection was used. However, the moment from the analytical values with initial deflection is higher than that from simple calculation without initial deflection (initial deflection is not included

due to the consideration of this in the code values of compressive strength p_c). Therefore, high results were obtained for flexibly connected subassemblages.

In conclusion, the BS 5950: Part 1 method incorporating joint flexibility in the way described above gives conservative but reasonable predictions of the ultimate load for the subassemblages.

7.6.2 Comparison with Wood Method

Another possible design method would be a modification of Wood's 'variable stiffness' approach[63] for columns in rigid jointed frames.

In this method two coefficients are used : the first is R'_x which considers the major axis bending moment and the effect of axial load; the second is C' which is the ratio of the collapse load to the reduced Euler load ($R'_x \times P_{Euler}$) and accounts for the existence of restraints.

The basic steps involved in this procedure are as follows:

Knowing the bending moment values in the column, starting from a trial value of ultimate load ratio F

$$F = \frac{P_{collapse}}{P_{squash}} \tag{7.4}$$

the values of R'_x and C' are calculated.

$$\begin{aligned} R'_x &= R_x(1 - F^2) \\ &= \left(1 - \frac{M_{max}}{M_{ax}}(0.4 - 0.2m)\right)(1 - F^2) \end{aligned} \tag{7.5}$$

where M_{max} *and* M_{ax} are respectively the maximum bending moment about the major axis in the column and the allowable moment; m is the end moment ratio, $\mid m \mid \not> 1$.

$$M_{ax} = 1.08 Z_x \sigma_y (1 - F) \tag{7.6}$$

in which Z_x is the cross-sectional plastic modulus and σ_y is the yield stress.

C' is obtained graphically depending on the values of the stiffness distribution coefficients to the column at its top k'_t *and bottom* k'_b.

$$K' = \frac{R'_x K_c}{R'_x K_c + R'_x K_{other\ columns} + \sum K_{minor-axis\ beams}} \tag{7.7}$$

The ultimate load ratio F is obtained from

$$F = \frac{C' R'_x}{\lambda^2} \tag{7.8}$$

in which

$$\lambda = \frac{L/r_y}{\pi\sqrt{E/\sigma_y}} \tag{7.9}$$

It is obvious that to obtain F, an iterative approach has to be employed, which makes the calculation of the ultimate load rather onerous for the present column subassemblage, since the moments in the column are functions of the applied axial load ratio F.

In order to show the capacity of the design approach, some simplifications are introduced. Column length L=3m corresponding to $\frac{L}{r_y}$ =81 with rigid connection and web cleat connection arrangements are taken as examples. λ^2 =0.9455. Assuming F=0.75, M_{ax} =13.9 kN.m results. From the author's ultimate strength analysis, M_{max} equal to 6.13 kN.m and 3.80 kN.m are generated for rigid connections and web cleats respectively at failure. Hence:

R_x = 0.82 *for rigid connections*

R_x = 0.89 *for web cleats*

For rigid connections, assuming F=0.75, R'_x =0.359, hence, K'_t =0.0132 and K'_b =0.0 and C' =2.02, therefore, F=0.766. Assuming $F = 0.5\times(0.750+0.766)$

=0.758 and repeating the above procedure produces F=0.749. Averaging these two values gives F=0.753 which is taken as the final value. Therefore, $P_{collapse} = F \times P_{squash}$ =626 kN.

Starting from F=0.76 for web cleat connections, R'_x =0.376, $\sum K_b$ =3.094 (only one connection with initial stiffness is included to keep in line with the assumption for the comparison with BS 5950: Part 1.) C' =1.90, a value of F of 0.756 is obtained, thus F=0.758 is accepted. $P_{collapse}$ =631 kN.

Compared with the analytical values of 650 kN and 684 kN for rigid connections and web cleats respectively, it may be concluded that the Wood method presents a quite reasonable prediction for the ultimate load of the column subassemblage.

Using this approach may be time consuming in this case. However, when the applied moments in the column are fixed, this method could be more suitable than the BS 5950 approach.

7.7 Conclusion

The method for including the effect of joint flexibility when analysing the behaviour and strength of column subssemblages has been used to conduct a limited parametric study for the understanding of this effect, based on which the following observations were made:

1. The connection's in-plane flexibility has two opposite effects on the ultimate load of the subassemblage, namely providing restraint (thereby reducing deflections) and transferring moment.

2. When the first effect is dominant, the use of stiffer connections will give higher ultimate loads.

3. When the latter controls, the weakening effect of the overstiff connection will be observed.

4. The connection's torsional restraint has a negligible effect on the ultimate load of the subassemblage; the out-of-plane flexural restraint has no effect on the behaviour of the column subassemblage.

5. The joint flexibility may be incorporated into the column design procedure of BS 5950 : Part 1 to predict the maximum load of subassemblages by including the connection stiffness in the determination of the effective beam stiffness.

	cross-section dimensions (cm)				2nd moments of area (cm^4)		area (cm^2)	length (cm)	$\lambda_y = L/r_y$
	D	B	t_f	t_w	Iy	I_x			
Beam	10.16	25.4	0.68	0.58	119.3	2783.0	27.76	150.0	72.36
Column	15.24	15.24	0.68	0.61	401.4	1235.0	29.19	300.0, 450.0, 600.0	80.95, 121.4, 161.9

Table 7.1 Basic data for parametric study

Table 7.2 Summary of ultimate axial loads for same connections about both axes of the column

Loading condition	$\frac{L}{r_y}$	Axial load (kN)		
		connection		
		righd	web cleat	pin
00	81.0	748	738	608
	121.4	562	526	328
	161.9	360	328	182
0T	81.0	700	726	
	121.4	542	522	
	161.9	352	326	
TT	81.0	650	684	
	121.4	484	464	
	161.9	312	284	

Table 7.3 summary of ultimate axial loads for unchanged connection (web cleat) about major axis and different connections about minor axis of the column

Loading condition	$\frac{L}{r_y}$	Axial load (kN)		
		connection		
		rigid	web cleat	pin
00	81.0	744	736	610
	121.4	558	524	330
	161.9	356	326	184
0T	81.0	726	718	602
	121.4	546	514	328
	161.9	352	324	182
TT	81.0	656	666	602
	121.4	468	452	328
	161.9	302	270	182

Table 7.4 Summary of ultimate axial loads for unchanged connection (web cleat) about minor axis and different connections about major axis of the column

Loading condition	$\frac{L}{r_y}$	Axial load (kN)		
		Connection		
		rigid	web cleat	pin
00	81.0	736	736	724
	121.4	524	524	522
	161.9	326	326	324
0T	81.0	674	718	724
	121.4	502	514	522
	161.9	322	324	324
TT	81.0	622	666	678
	121.4	442	452	456
	161.9	266	270	274

Table 7.7 Summary of ultimate axial loads for same connections about both axes of the column using design method

Loading condition	$\frac{L}{r_y}$	Axial load (kN)		
		Connection		
		rigid	web cleat	pin
00	81.0	619	602	475
	121.4	446	429	282
	161.9	308	296	177
0T	81.0	561	581	
	121.4	411	415	
	161.9	284	285	
TT	81.0	511	536	
	121.4	402	389	
	161.9	283	269	

Column axial load (kN)	$M_{x\,(top)}$ (kN.m)		$M_{y\,(top)}$ (kN.m)		m_x	m_y	M_b	Z_y
	Simple	"Exact"	Simple	"Exact"			kN.m	(cm^2)
200	2.85	2.81	1.68	1.62	0.57	0.57	45.0	52.95

L_E/L	P_c N/mm^2	Design load from BS 5950 (kN) Simple	"Exact"	Ultimate design load (kN) Simple	"Exact"	Ultimate Load (kN)
0.77558	200.3	527	529	536	539	684

Table 76 Various values required in a typical iteration when using modified BS 5950 approach to calculate design load.

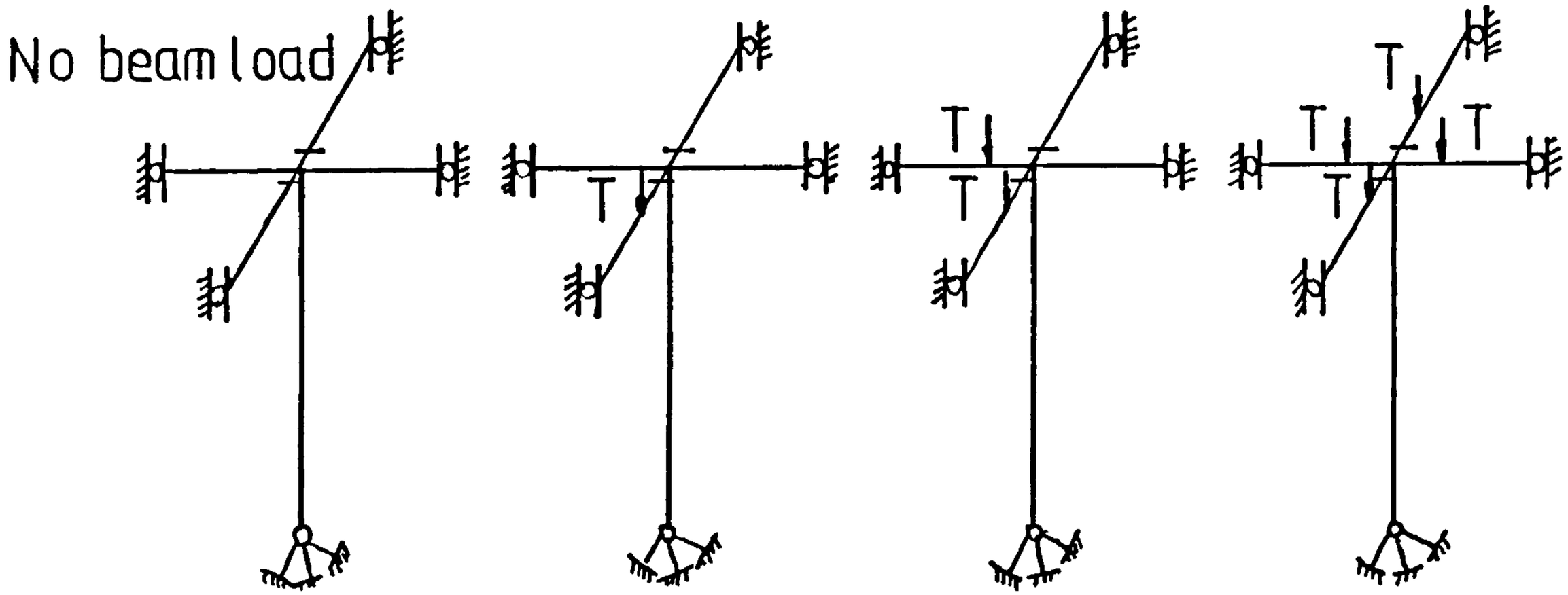

Case 00 Case 0T Case TT Case BTT

Fig. 7·1 Four beam loading cases

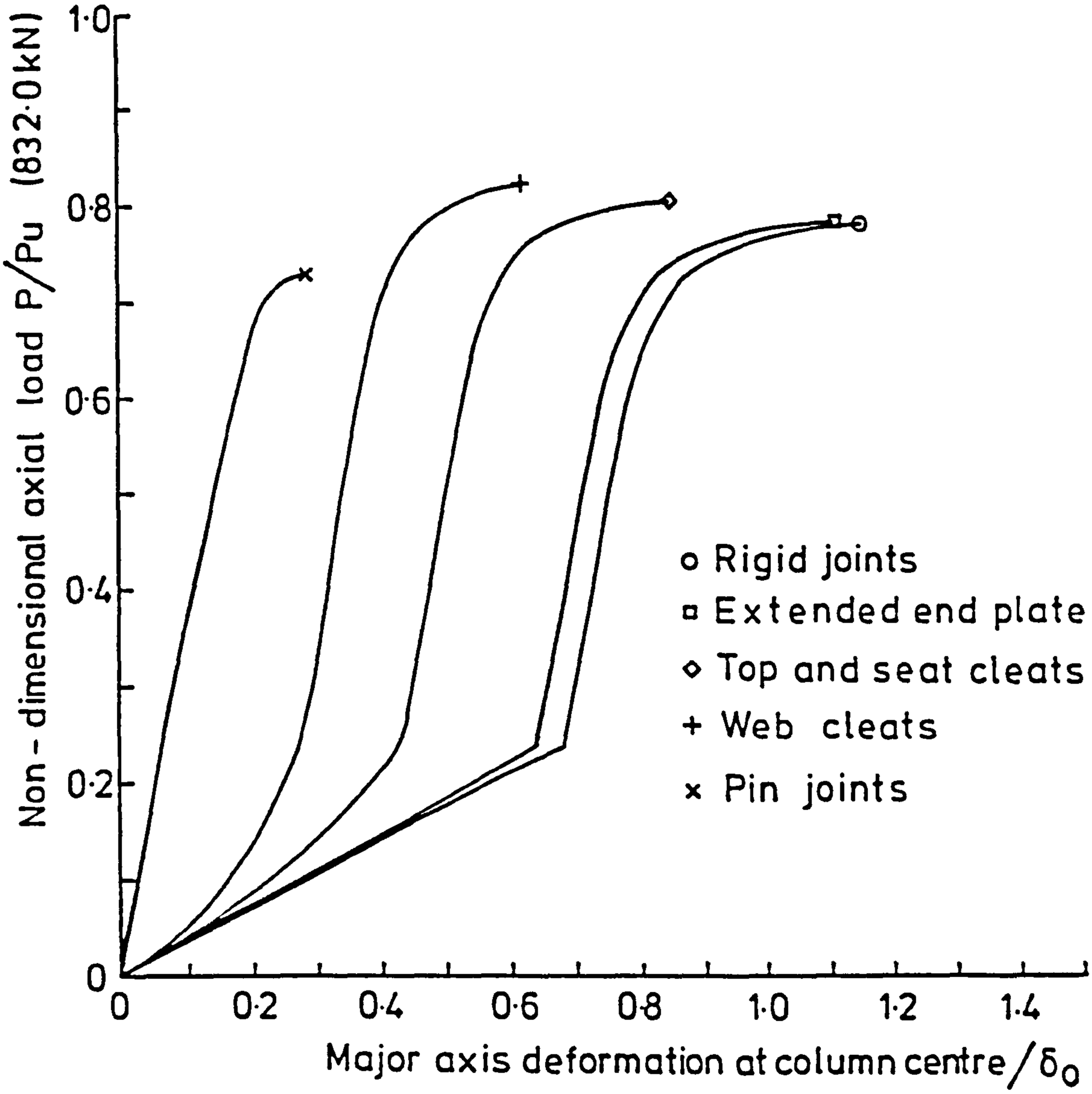

FIG.7·2 AXIAL LOAD Vs MAJOR AXIS DEFLECTION BEHAVIOUR FOR VARIOUS CONNECTIONS, LOAD CASE TT, $\lambda_y = 81$

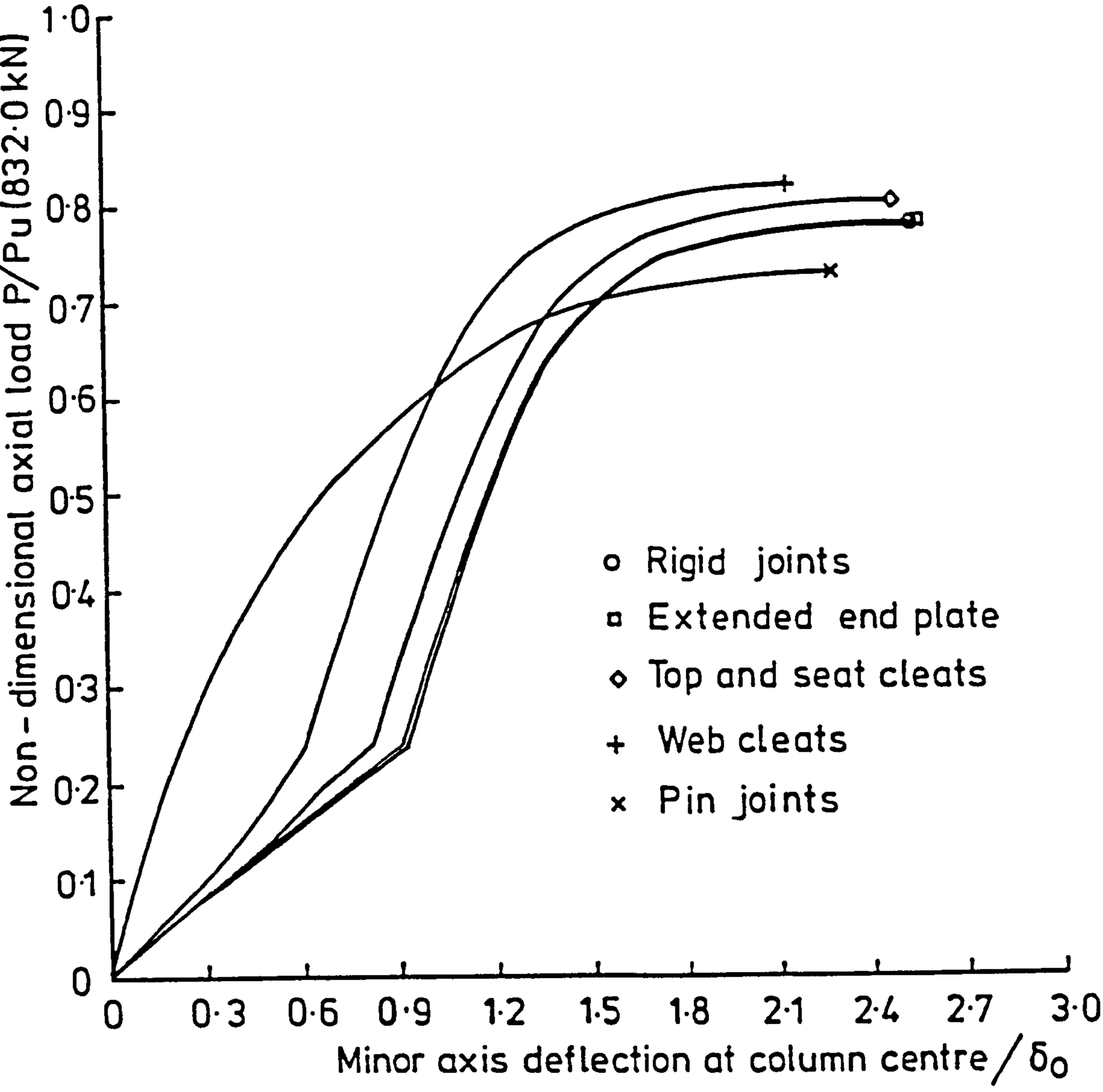

FIG. 73 AXIAL LOAD Vs MINOR AXIS DEFLECTION BEHAVIOUR FOR VARIOUS CONNECTIONS, LOAD CASE TT $\lambda_y = 81$

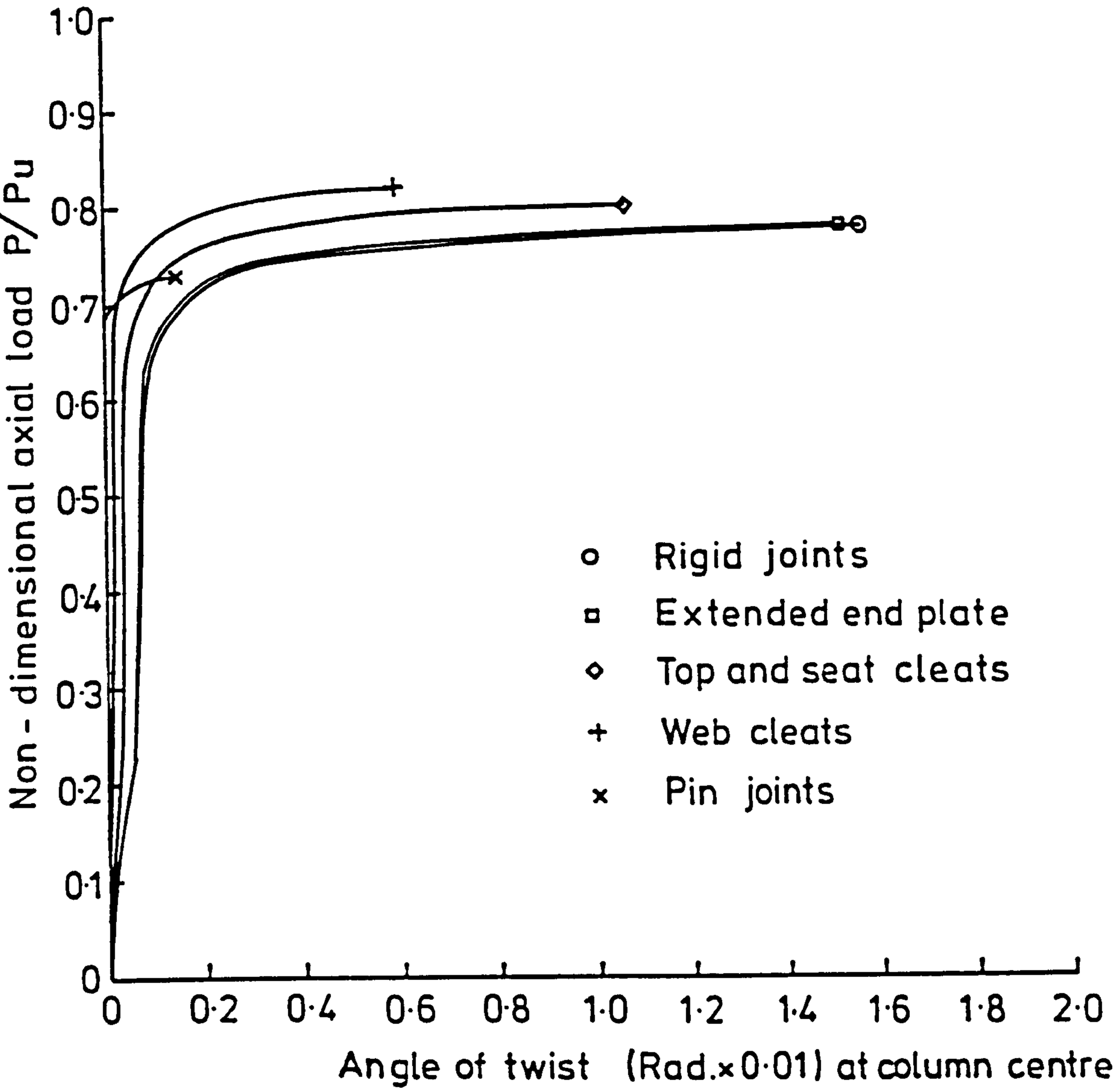

FIG. 7·4 AXIAL LOAD Vs TWISTING BEHAVIOUR FOR VARIOUS CONNECTIONS, LOAD CASE TT, $\lambda_y = 81$

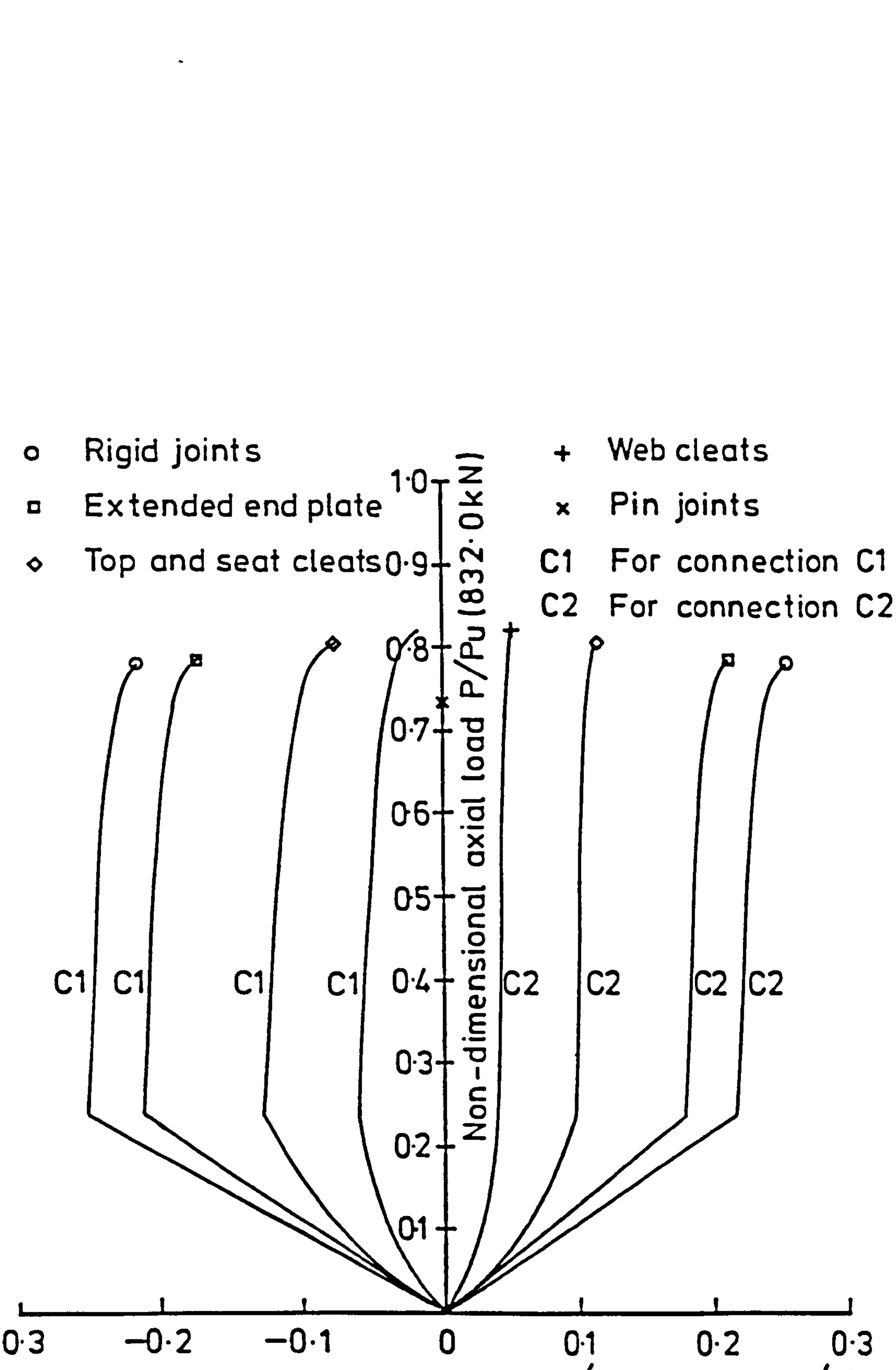

FIG. 7·5 AXIAL LOAD Vs CONNECTION MOMENTS BEHAVIOUR FOR VARIOUS CONNECTIONS, LOAD CASE TT, $\lambda_y = 81$

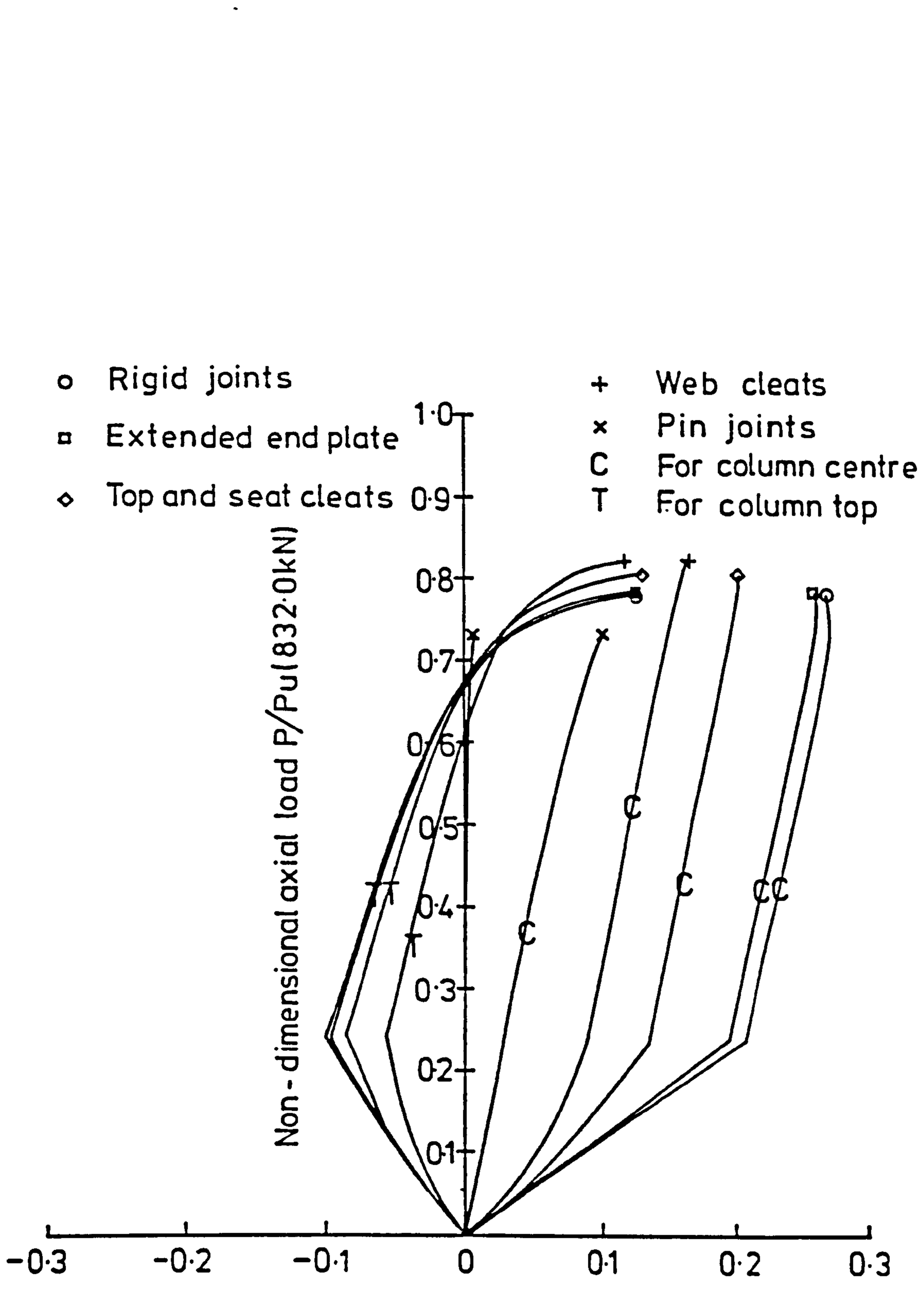

FIG. 76 AXIAL LOAD Vs COLUMN MOMENTS BEHAVIOUR FOR VARIOUS CONNECTIONS, LOAD CASE TT $\lambda_y = 81$

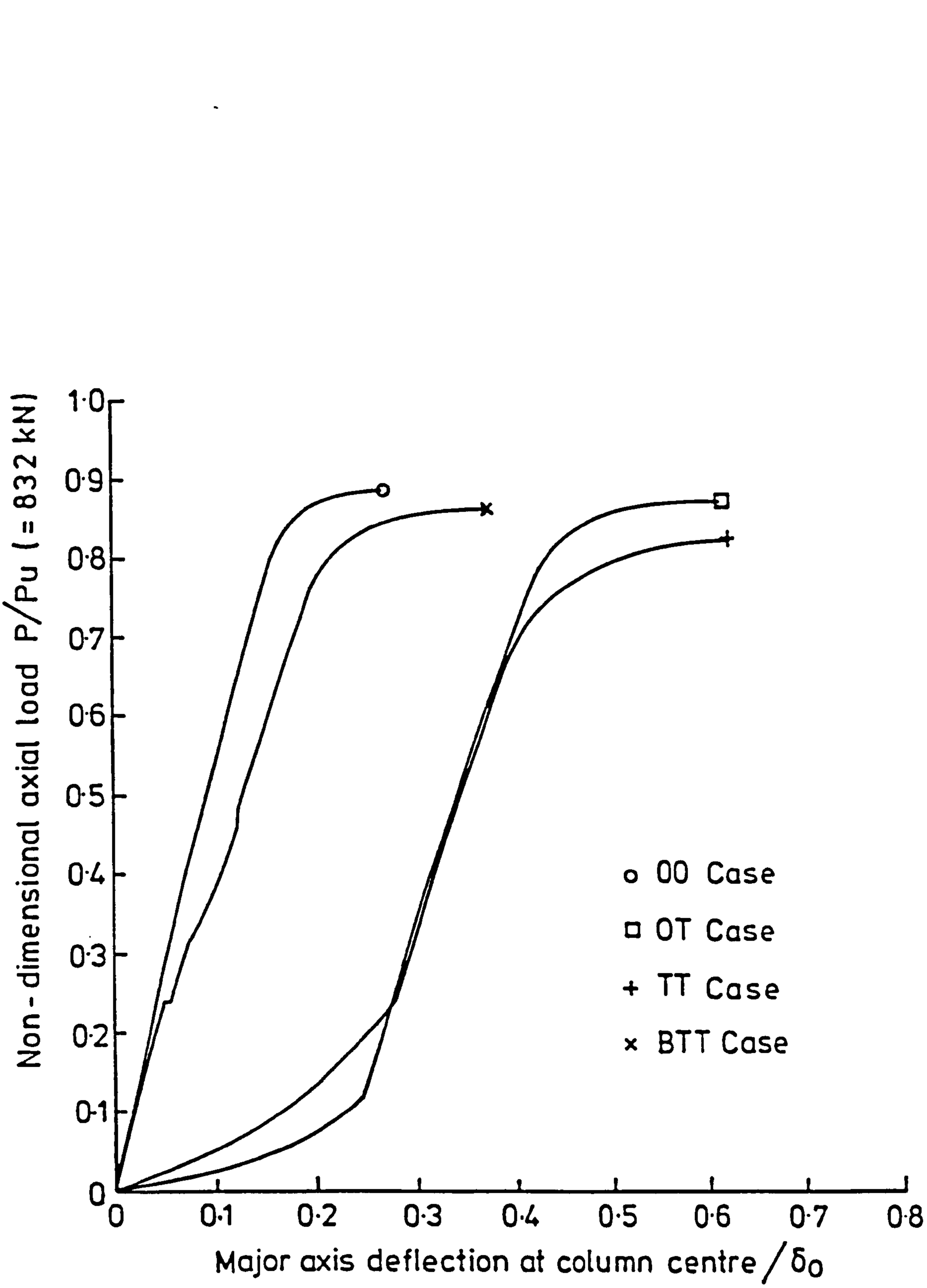

FIG. 7·7 AXIAL LOAD V_s MAJOR AXIS DEFLECTION BEHAVIOUR FOR DIFFERENT LOAD CASES, WEB CLEATS, $\lambda_y = 81$

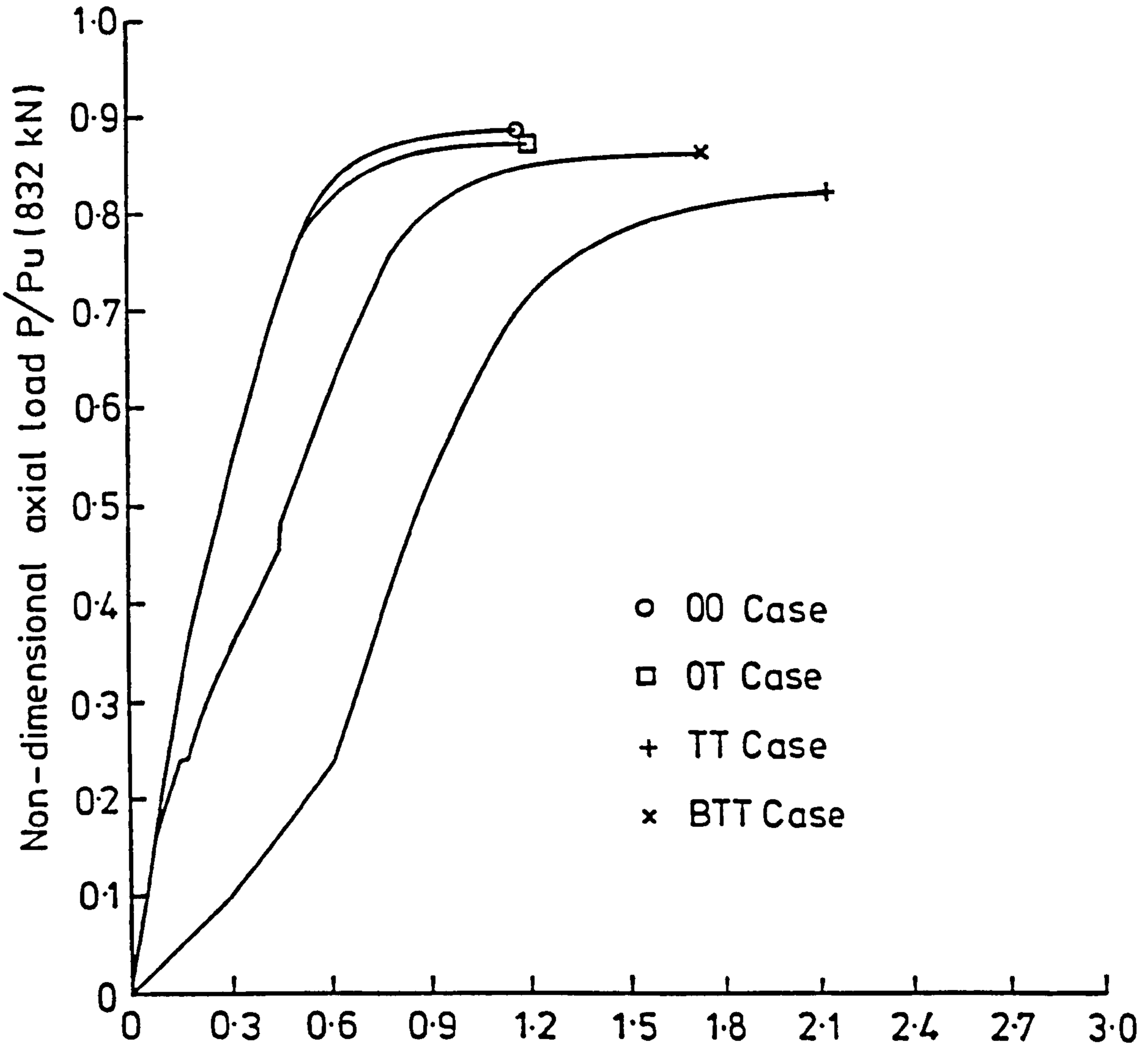

FIG 78 AXIAL LOAD Vs MINOR AXIS DEFLECTION BEHAVIOUR FOR DIFFERENT LOAD CASES, WEB CLEATS, $\lambda_y = 81$

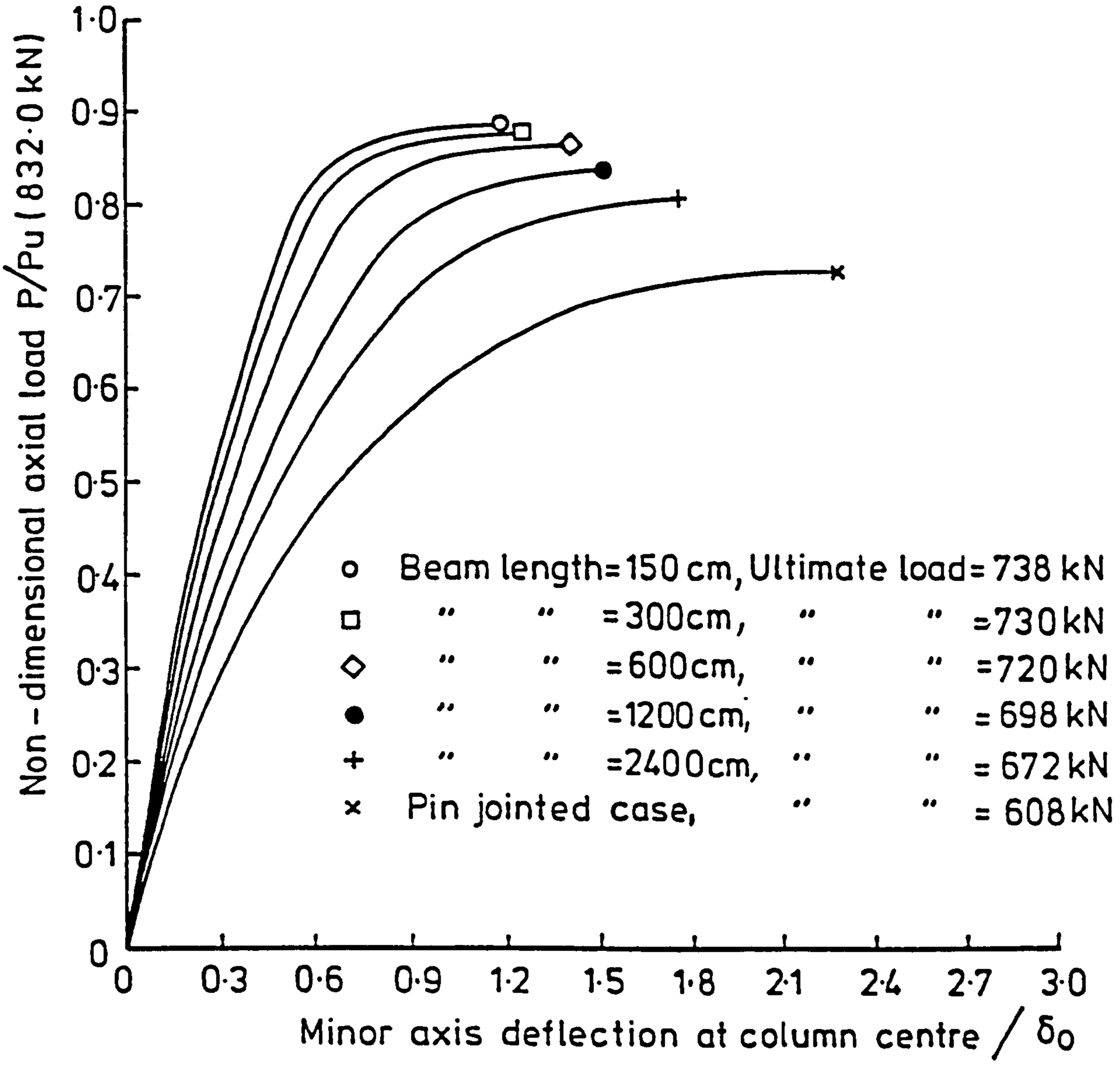

FIG. 7·9 AXIAL LOAD Vs MINOR AXIS DEFLECTION BEHAVIOUR FOR DIFFERENT BEAM LENGTHS, WEB CLEATS, LOAD CASE 00, $\lambda_y = 81$

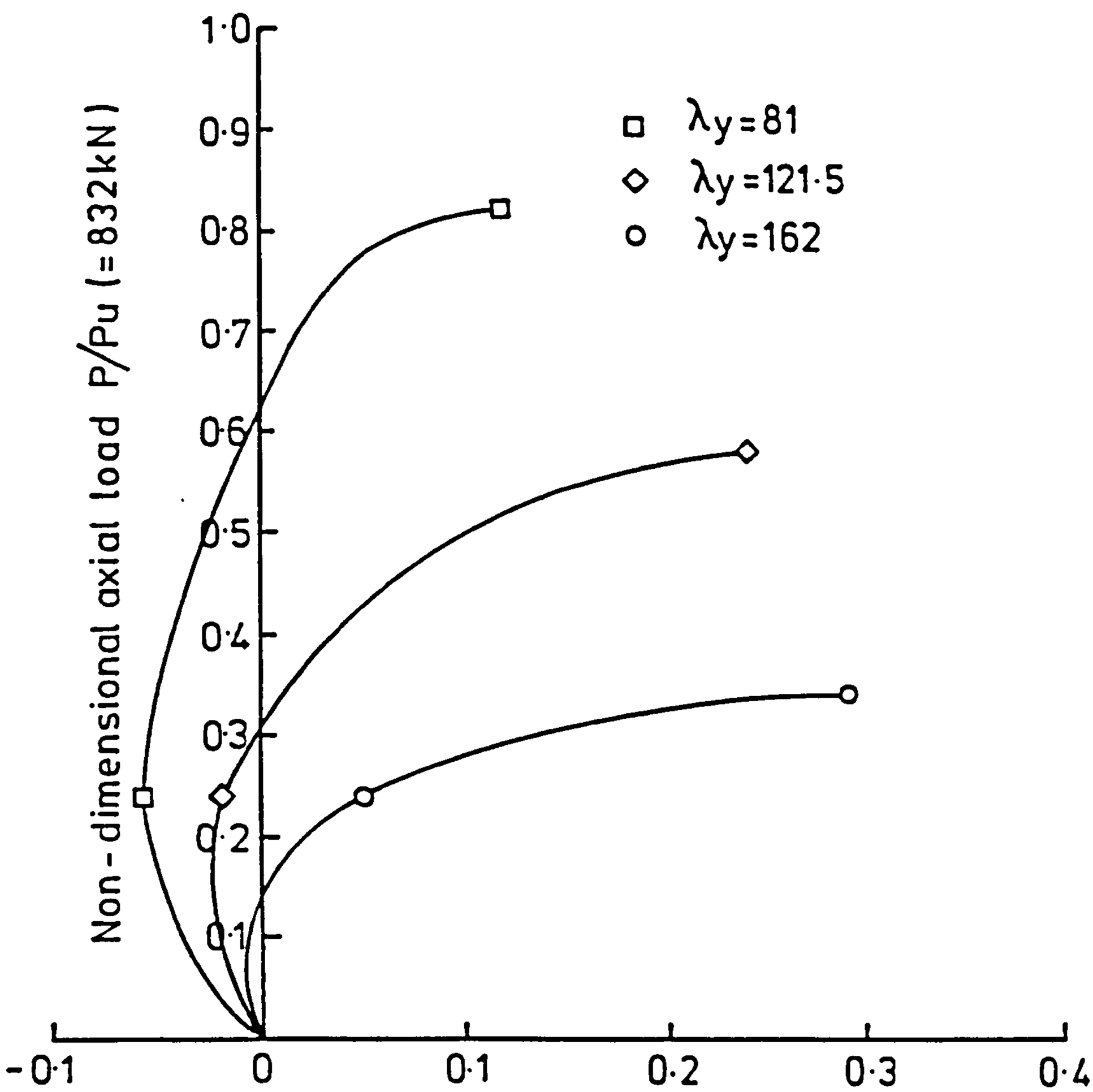

FIG. 7·10 AXIAL LOAD Vs COLUMN MOMENTS BEHAVIOUR FOR DIFFERENT COLUMN SLENDERNESS, WEB CLEATS, TT LOAD CASE

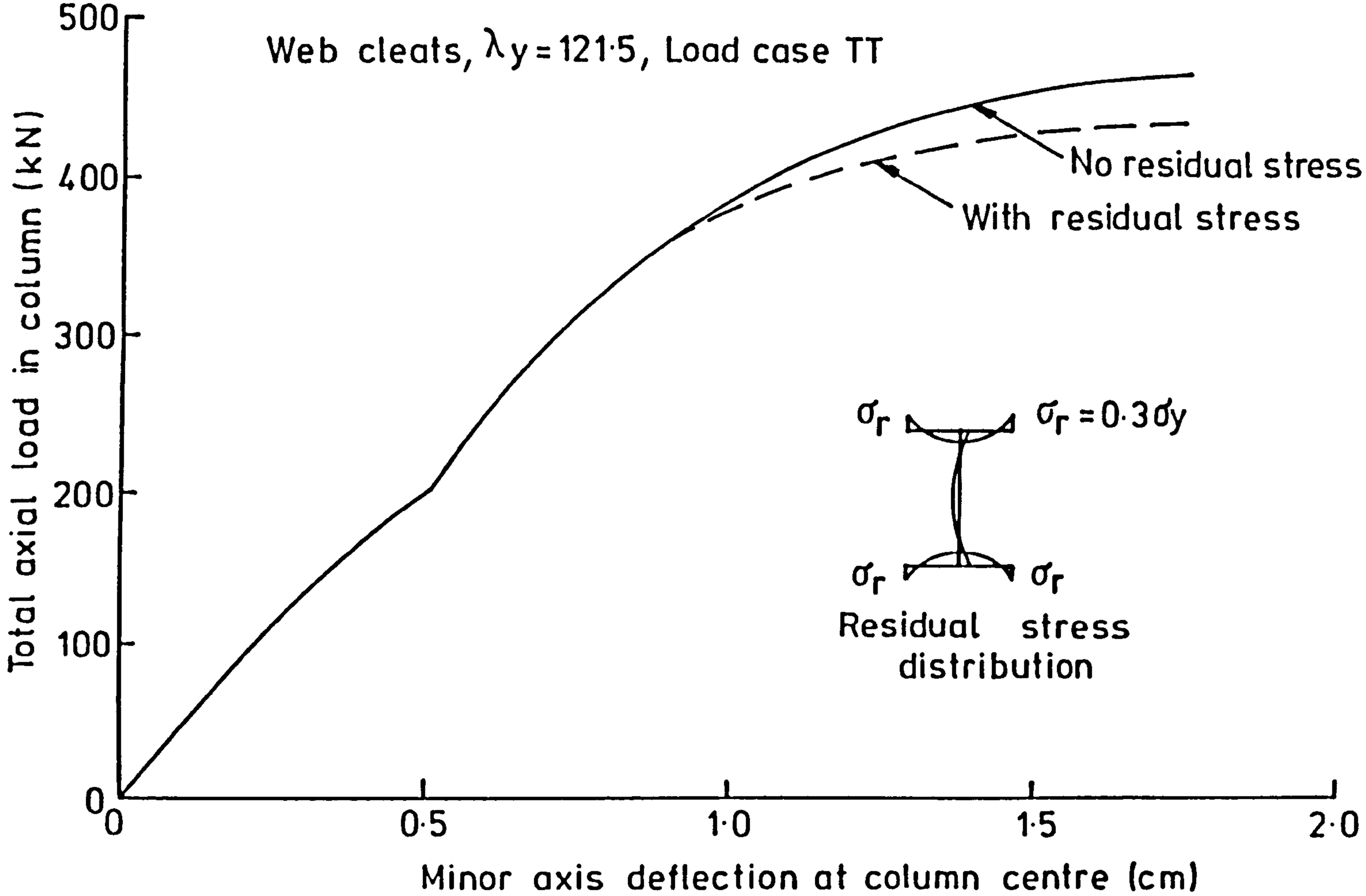

FIG. 7·11 EFFECT OF RESIDUAL STRESS ON LOAD-DEFLECTION CURVE

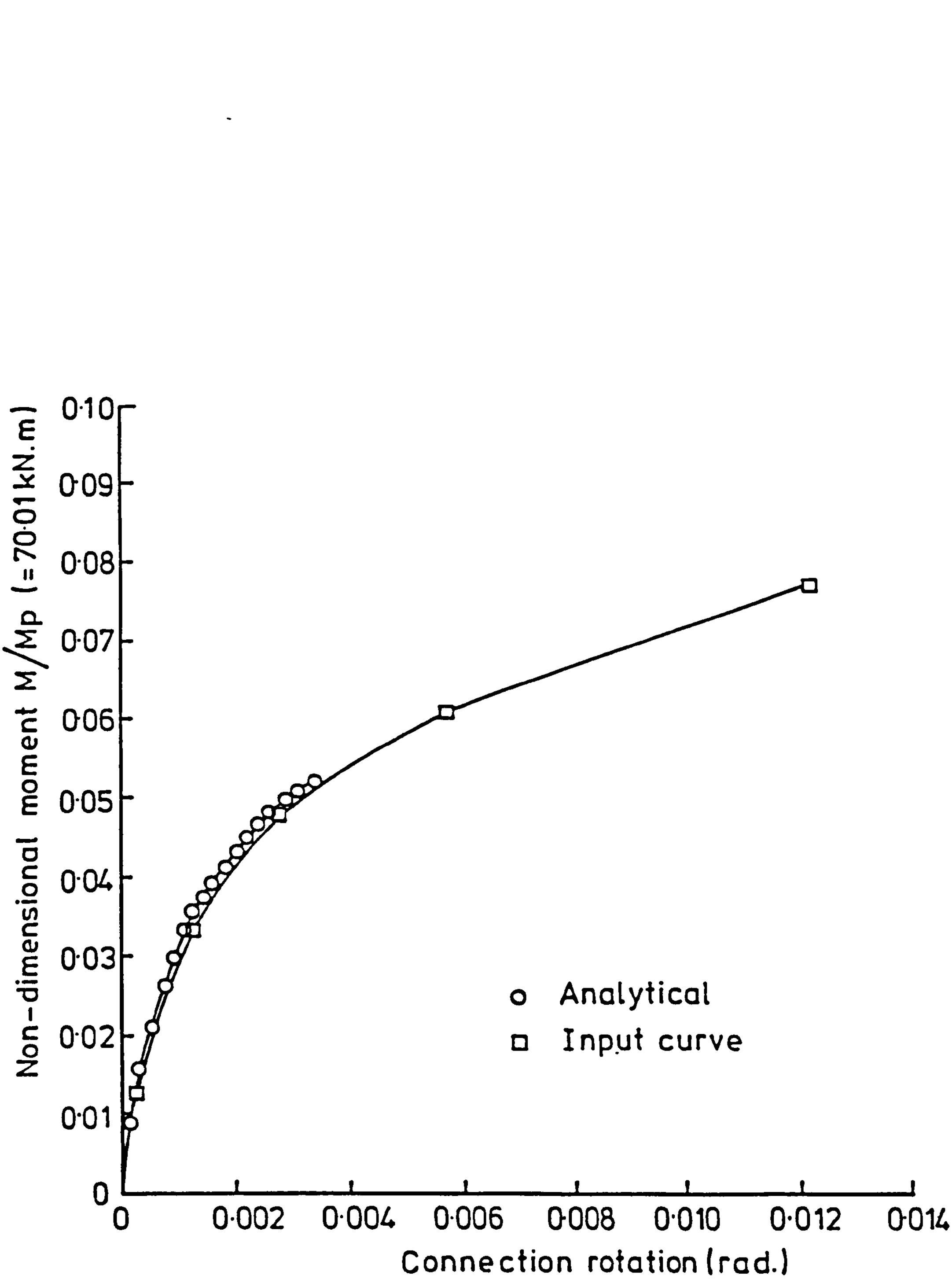

FIG. 7·12 COMPARISON OF MOMENT-ROTATION CURVES FOR TYPICAL LOADING-LOADING, WEB CLEATS

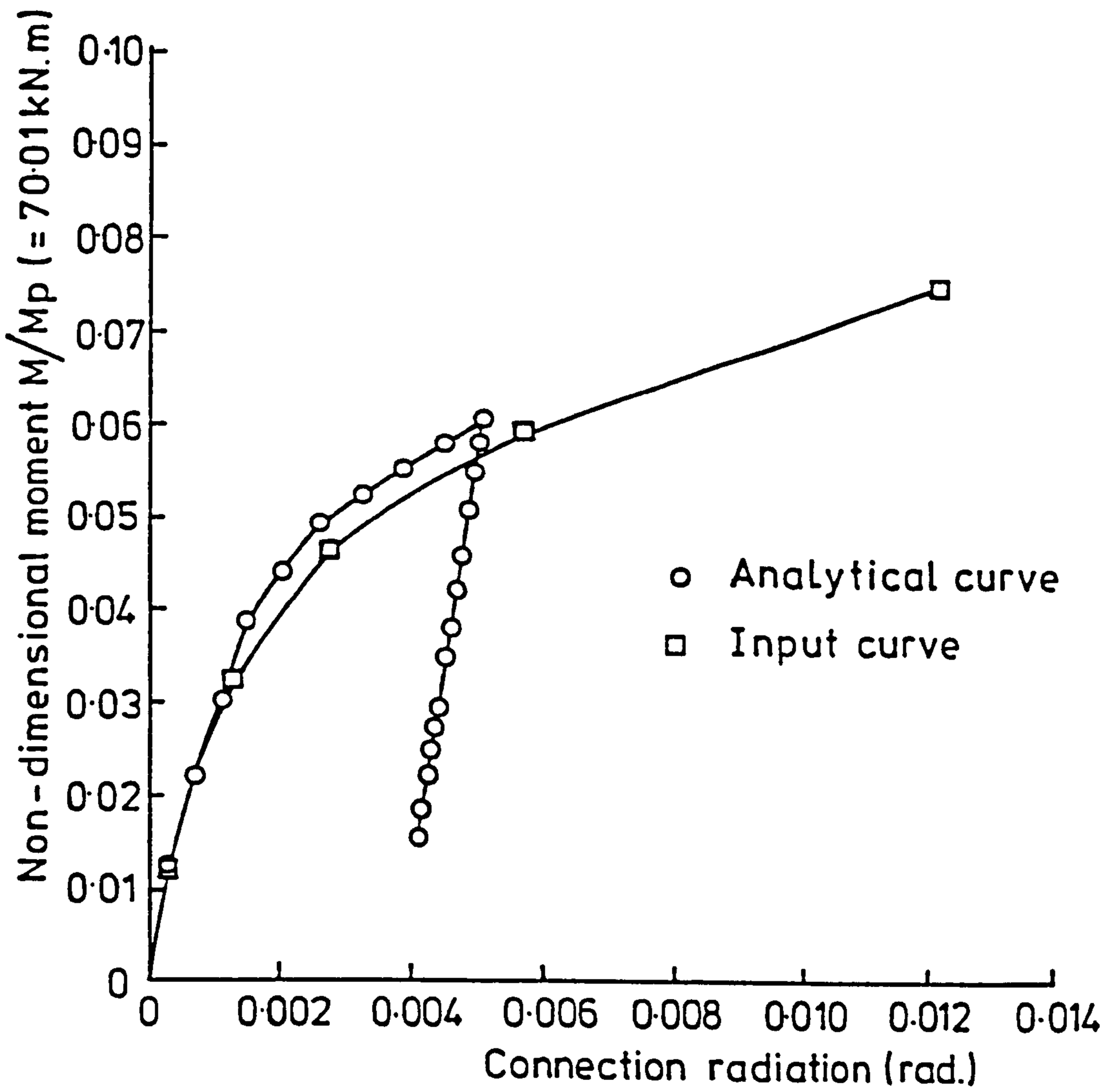

FIG. 713 COMPARISON OF MOMENT-ROTATION CURVES FOR TYPICAL LOADING-UNLOADING WEB CLEATS

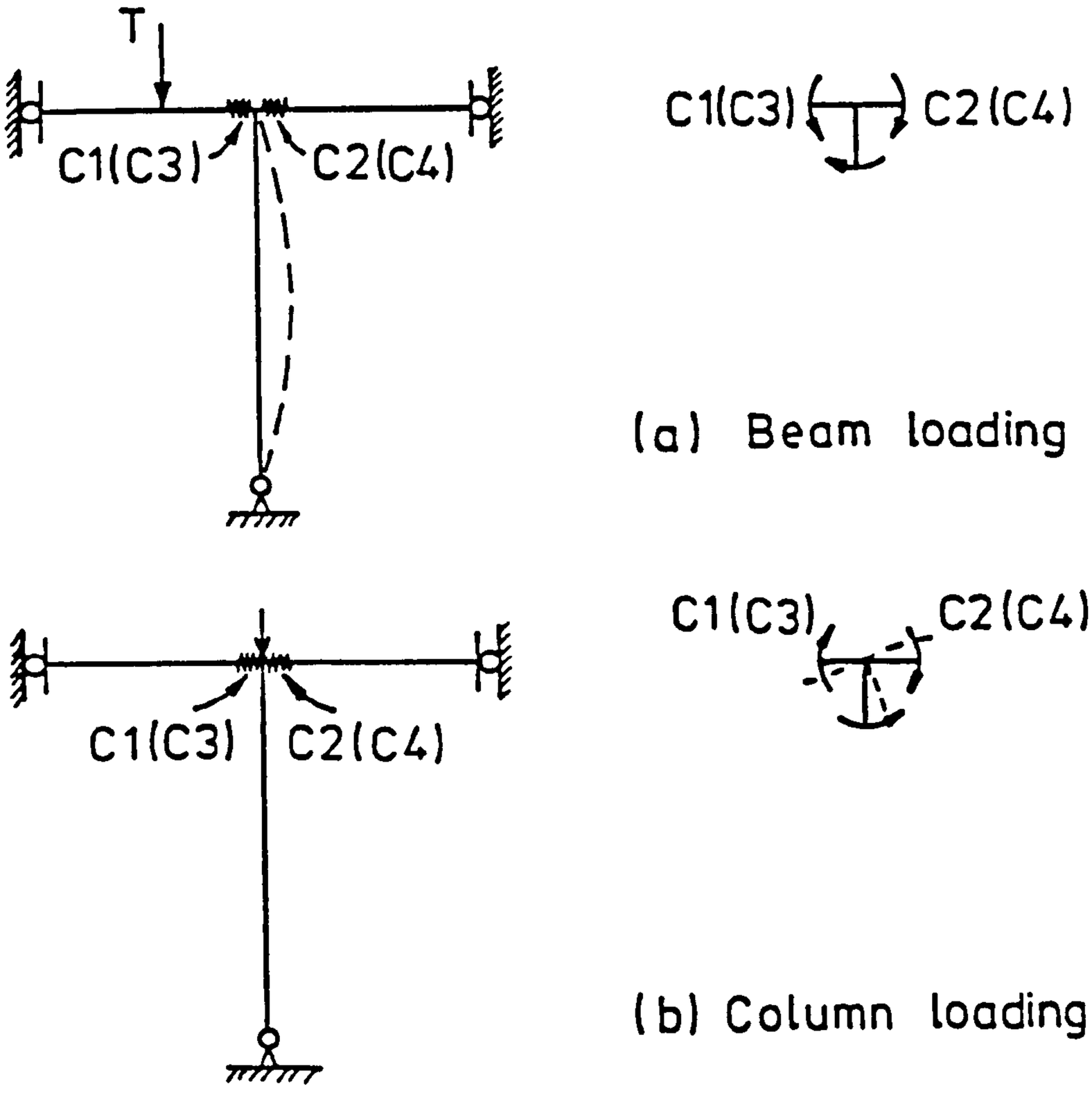

(a) Beam loading

(b) Column loading

FIG. 7·14 CONNECTION MOMENT DIRECTIONS UNDER DIFFERENT LOADS

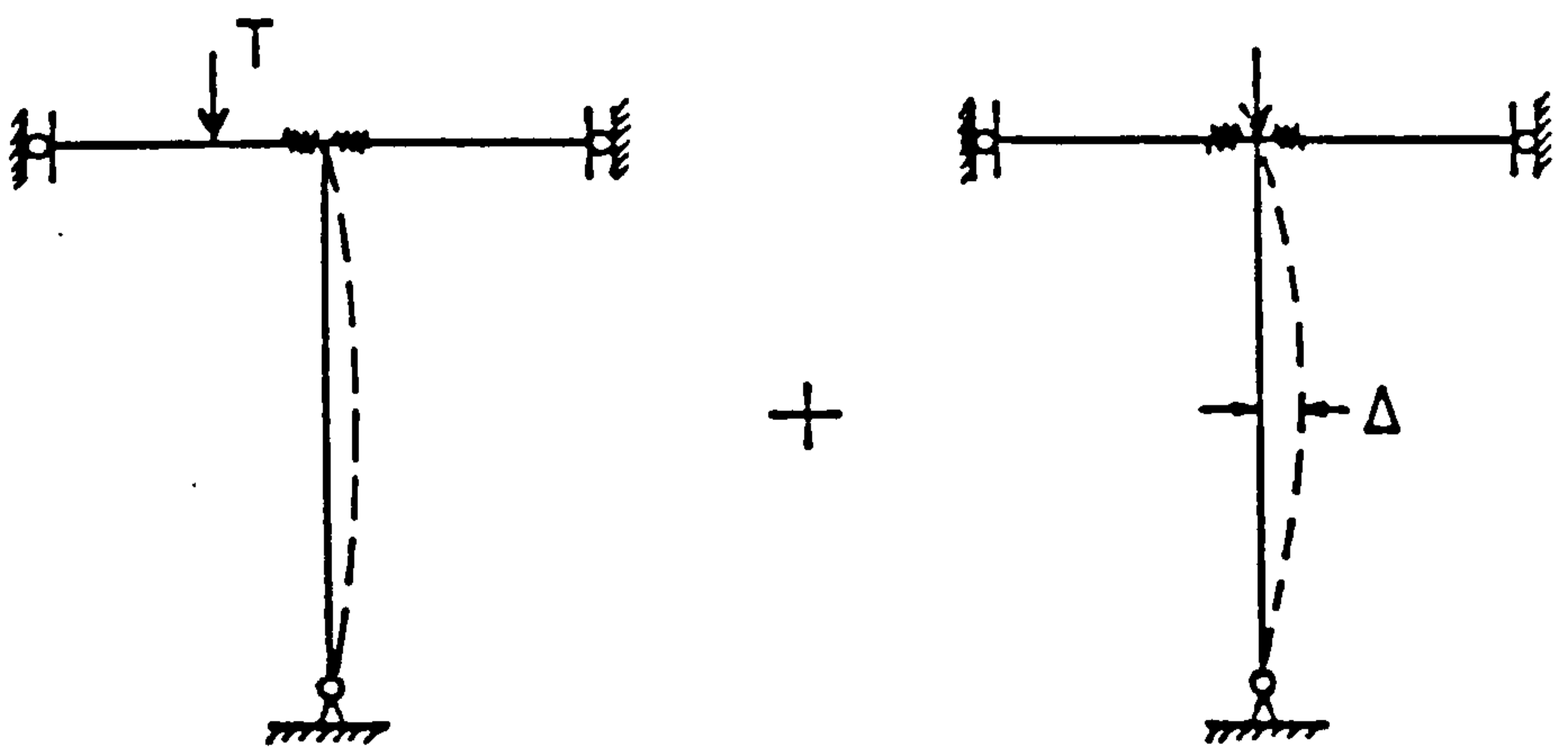

(a) Loading sequence

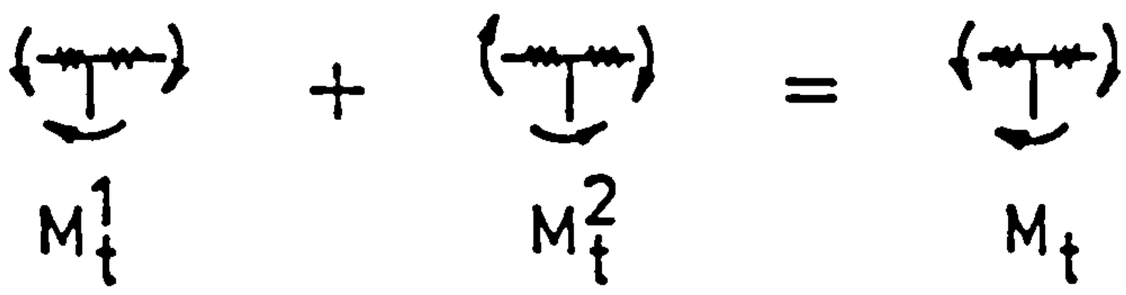

(b) Column top moments

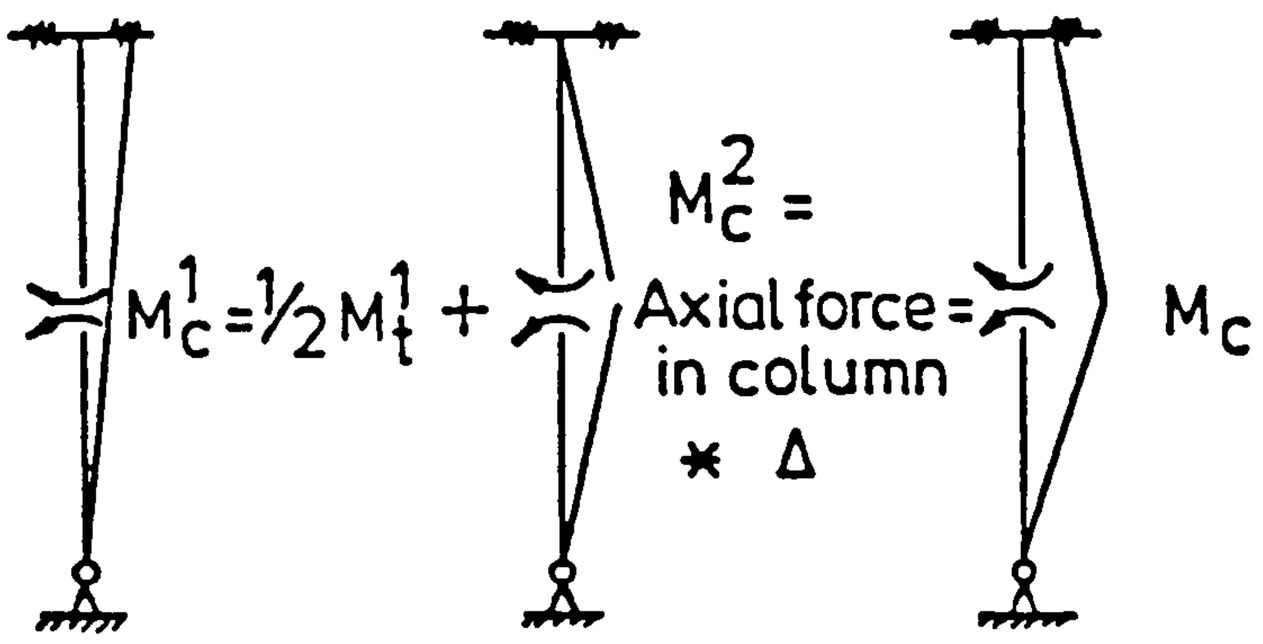

(c) Column centre moments

FIG.715 MOMENTS IN THE COLUMN UNDER DIFFERENT LOADS

Table 7.5 Ultimate loads for different arrangements of beam length and connection torsional stiffness

Beam length (mm)	Ultimate load (kN)		$\frac{Col.3}{Col.2}$
	$K_{tor} = 0$	$K_{tor} = \infty$	
(1)	(2)	(3)	(4)
1500	327	328	1.003
500	331	343	1.042
50	337	372	1.104

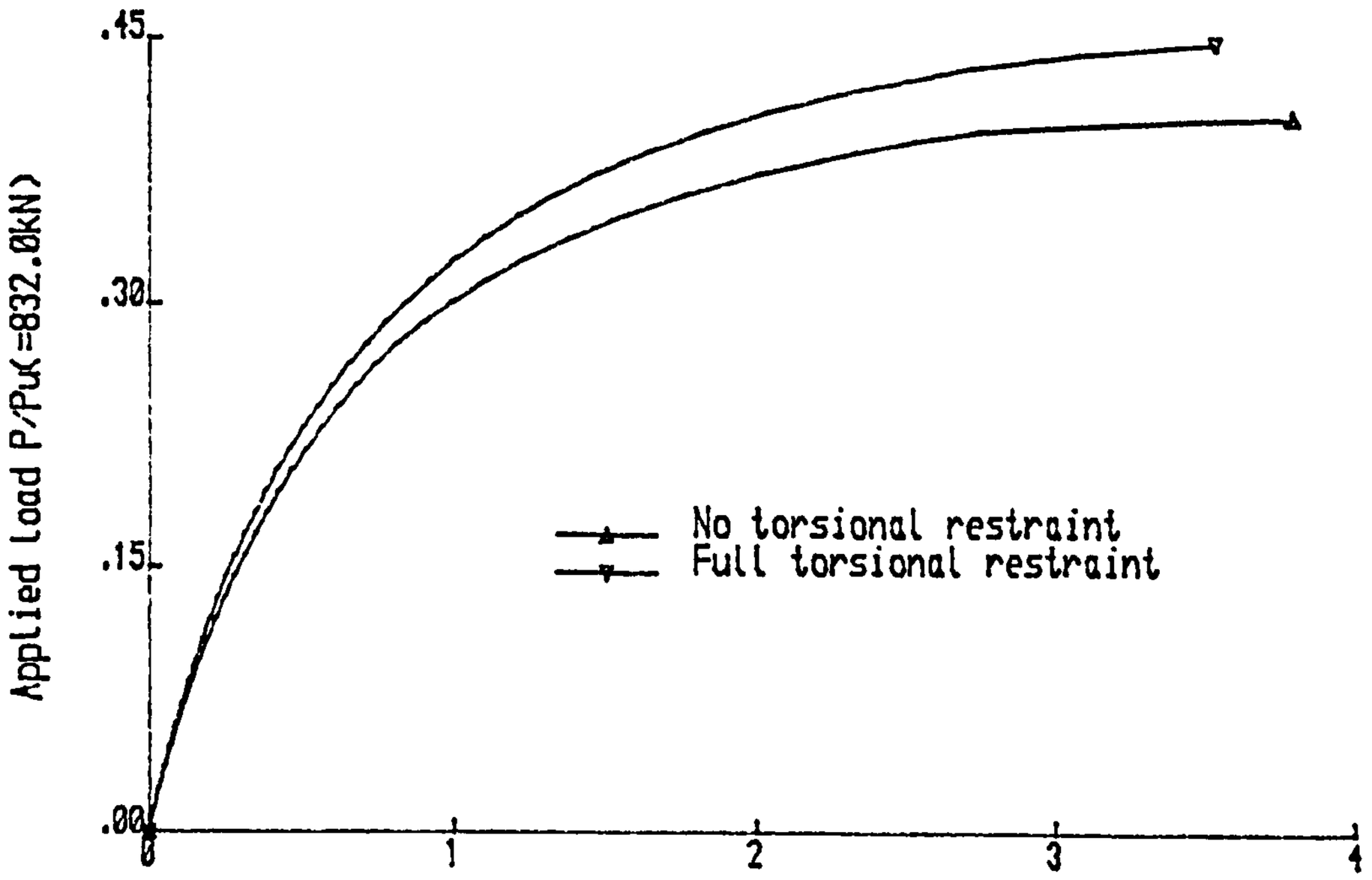

Fig. 7.16 Load - deflection behaviour for two cases of connection torsional restraint. Beam length = 50 mm. Column slenderness = 162.

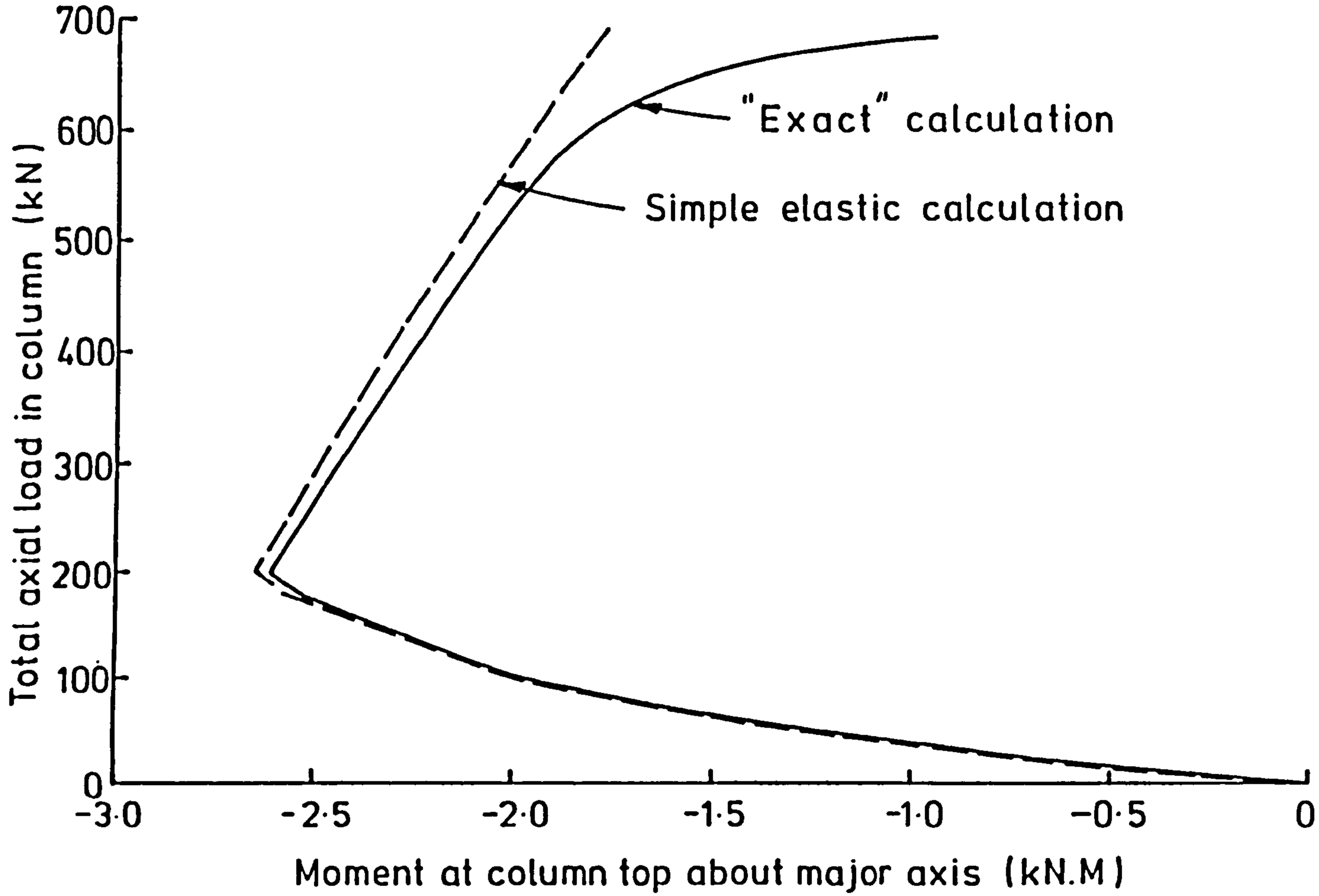

FIG 7·17 COMPARISON FOR LOAD-MOMENT BEHAVIOUR, WEB C., λ_y =81, LOAD CASE TT

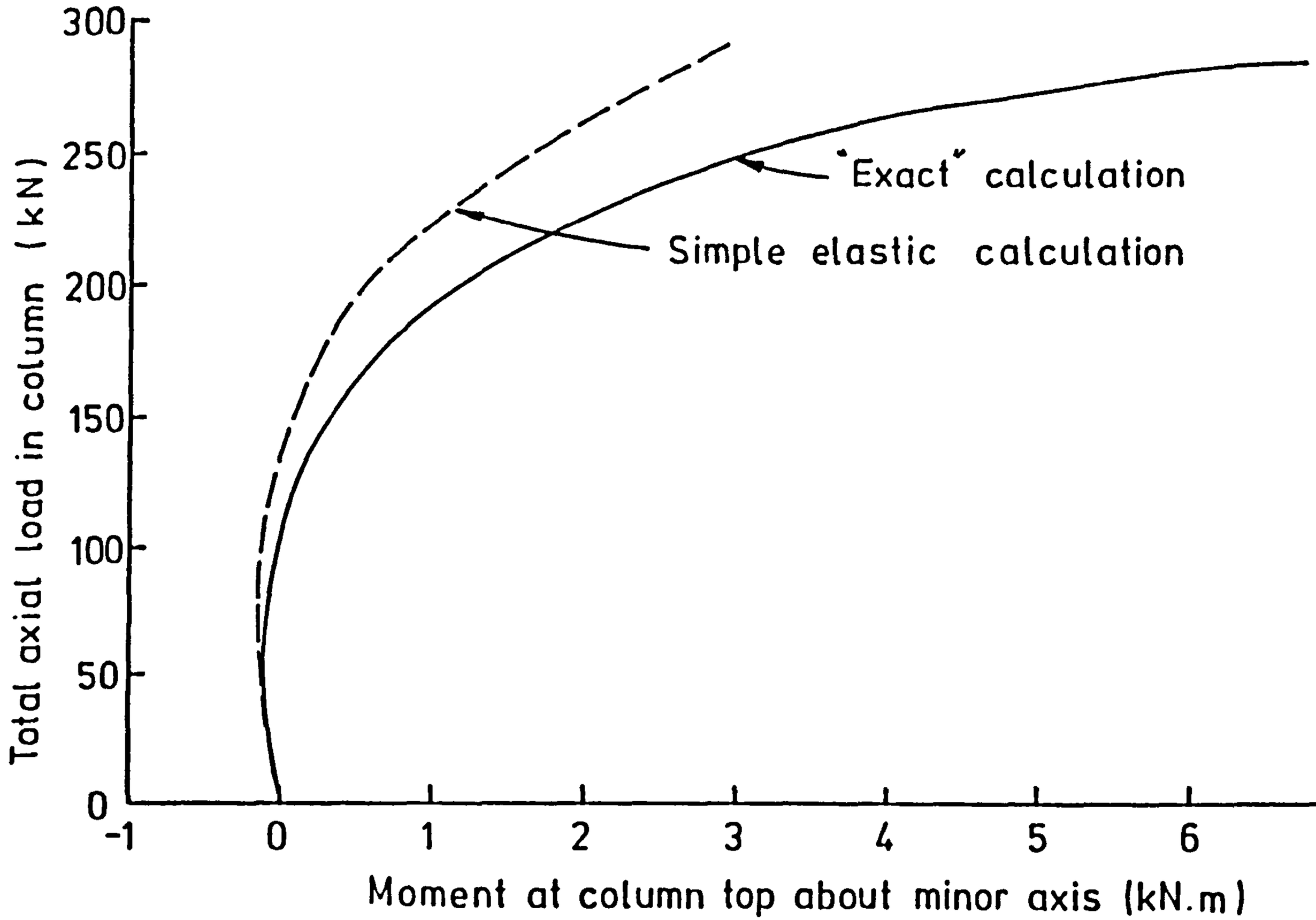

FIG. 7·18 COMPARISON FOR LOAD-MOMENT BEHAVIOUR, WEB C., $\lambda_y = 162$, LOAD CASE TT

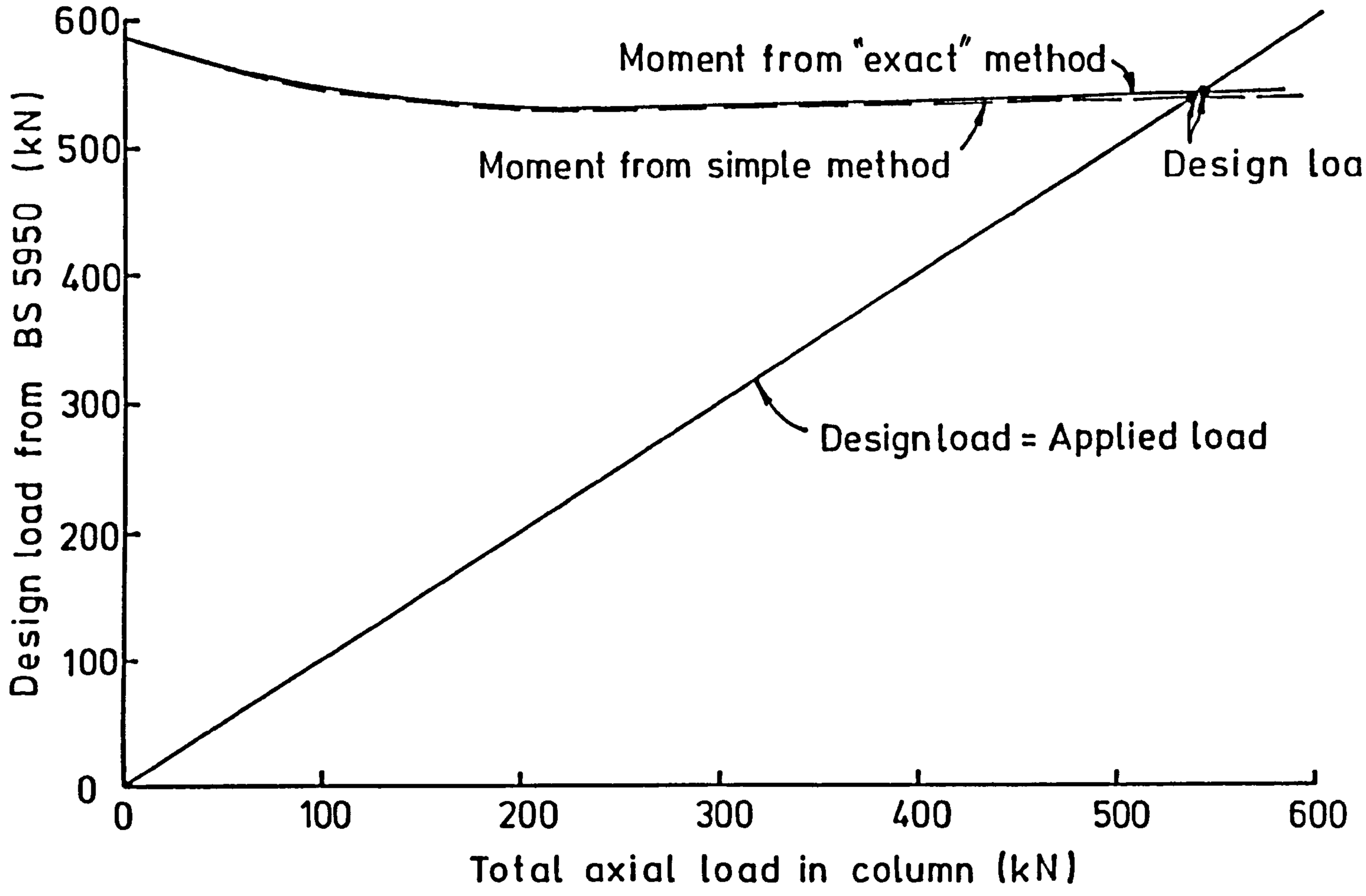

FIG. 7·19 CALCULATION AND COMPARISON OF DESIGN LOAD USING BS 5950

Chapter 8

EFFECTS OF BRACING ON 3-D COLUMN SUBASSEMBLAGES

8.1 Introduction

Chapters 4,5 and 7 presented the studies of the effects of flexible end connections and intermediate bracings on isolated beams and semi-rigid beam-column connections on column subassemblages. To complete the study on 3-D structures, it is necessary to conduct a study on the bracing effects on column subassemblages.

Previous investigations by other authors (Trahair and Nethercot[31], Zuk[33], Medland[42] etc.) were restricted to isolated columns. The interaction between the bracing and other members as parts of a frame was overlooked due to its relative complication. Using the analytical procedure in chapter 6, this difficulty is easily overcome. This chapter reports the re-

sults of this study. The main parameter is the bracing stiffness. Various arrangements of bracing, connections, loading conditions, column and beam slendernesses as well as column initial lateral deflections are examined.

8.2 Choice of Basic Parameters

As pointed out in Chapter 6, a node is always assumed at the bracing point; therefore, if the column is braced by a number of braces, the computing storage will be profoundly increased. Due to the limited available quota of computing storage, the subassemblage shown in figure 8.1a has been adopted. If not specially specified, the beam length $L_b = 2m$ and the column length $L_c = 4m$, so that the effects of single bracing and multiple bracing on the ultimate load may be distinguished.

For a practically proportioned H-column, the ratio of major axis rigidity I_x to the minor axis rigidity I_y is approximately 3. If an unyielding shear centre brace is applied at the column centre, a double curvature buckling mode is likely to develop; therefore, the column will most likely fail by major axis buckling, which is unexpected since the present study is for the understanding of bracing effects. A beam profile has therefore been chosen for the column to ensure that the column fails about the minor axis.

As indicated in chapter 7, even web cleats were able to increase the ultimate load of a subassemblage significantly and the use of stiffer connections was not proportionally reflected by its effect on the strength of the main structure. As a result of this, either pin joints (**PJ**) or rigid joints (**RJ**) are assumed in this study.

Two types of initial lateral deflection (**ILD**) for the column have been

assumed in the study of multiple bracings. Type 1 is a half sine wave with the magnitude $\delta_0 = \frac{1}{1000}L_c$; where type 2 is shown in figure 8.1b with $\delta_0 = \frac{1}{1000} \times \frac{L_c}{4}$. For a single bracing system, the first type has always been used. Lehigh type residual stress distribution with $\sigma_{r1} = 0.30\sigma_y$ is assumed.

Only translational bracings i.e. shear centre (SC) bracing and flange (F) bracing have been considered since it was pointed out in chapter 7 that the behaviour of column subassemblages was not affected by torsional restraints.

The same Young's modulus E, shear modulus G, Poisson's ratio ν and cross-section dimensions as in chapter 4 have been adopted.

8.3 Results and Discussion

Figure 8.2 presents the results for various cases of a single bracing system. The ultimate load P_u is nondimensionised by dividing it by the elastic buckling load P_{cr} for the simply supported column with the same geometric slenderness without bracing, i.e. $P_{cr} = \frac{\pi^2 E I_y}{L_c^2}$, whilst the nondimensional bracing strength requirement is obtained by dividing the bracing reaction at failure P_b by one percent of the load-carrying capacity of the column subassemblage ($\frac{P_u}{100}$). It is clearly shown in figure 8.2a that for column loading (CL) cases, with increasing bracing stiffness, the difference in the ultimate loads between rigidly jointed and pinned column subassemblages decreases, since the column effective length is reduced and thus the relative stiffness of the beam plus connection to the column weakened. Doubling the beam length in the case of a rigid joint arrangement results in a very small change in the ultimate load of the subassemblage and the bracing force. As pointed out in

chapter 7, if the beam length reaches infinity, the structure is equivalent to a pin jointed subassemblage.

Applying the load at the minor axis beam (which is connected to the web of the column) will remarkedly reduce the load-carrying capacity of the subassemblage. An interesting phenomenon for this loading case (**BL** for beam loading) is that there exists a peak value in the ultimate load versus bracing stiffness curve at a certain value of bracing stiffness. This arises from the fact that the combined action of flexural bending (mainly about minor axis) and axial loading in the column causes the subassemblage to fail almost fully plastically. The use of stiffer bracing brings more moment to the column, therefore, the subassemblage fails at a lower load (which is equal to the applied beam load).

Placing the brace at the column's flange is apprently not as effective as at the shear centre. It is not capable of inducing the double curvature buckling mode as happened for shear centre bracing, therefore, the ultimate load is much lower.

Examining figure 8.2b, which shows the relationship between the bracing reaction at failure and the bracing stiffness for different cases of one bracing system, indicates that for shear centre bracing without direct bending from the beam about the minor axis, a value of one percent of the buckling load of the subassemblage (approximately 0.6% as given by Zuk[33]) is necessary for the brace to provide fully restraint to the main structure provided it possesses adequate stiffness. If beam load is applied, a much higher value of bracing reaction will be generated in the brace since it is acting as a member sustaining primary action. Again, the effect of different beam slendernesses is imperceptible. For subassemblages with substantial connection stiffnesses,

the column centre is not the neutral point for the double curvature buckling mode, a noticable drop of bracing reaction once 'complete bracing' is exceeded could not be observed as in the case of the pin jointed structures. In the case of flange bracing, the force generated in the brace actually increases with increasing the bracing stiffness although the rate is very low. This results from the fact that the flange bracing is unable to resist the small torsion from biaxial flexural actions.

The effect of bracing on the behaviour of column subassemblages with different column slendernesses is as expected. As shown in figure 8.3a, the values of $\frac{P_u}{P_{cr}}$ for $\frac{L}{r_y}$ =400 are higher than those for $\frac{L}{r_y}$ =200, which is understandable since a relatively high degree of restraint is provided to the column at higher column slendernesses. Figure 8.3b shows that the bracing strength requirement in terms of the buckling load of the subassemblage is higher for the more slender column subassemblage. This comes from the fact that more bending moment is generated from the more slender column at the same load level from the $P-\Delta$ effect; therefore, larger deflections leading to higher bracing reactions will be generated. However, the use of one percent of the buckling load of the subassemblage for the bracing strength requirement is still reasonable.

In cases of column subassemblages with multiple bracing systems and under column loading, the bracing effect on the performance of the main structure is negligible since almost full plastification from axial load and flexural bending (resulting from $P-\Delta$ effect) occurs. However, the bracing strength requirements for rigid joint arrangements are higher than those for pin jointed cases. This is mainly due to the difference in bracing force produced in the brace near the top of the column. In cases of rigidly jointed

subassemblages, a flexural bending moment will be developed at the column top (which is equal to the connection moment) because of the rotation from the $P-\Delta$ effect. This moment contributes to the difference in bracing forces of this brace from the others. As shown in figure 8.5, P_{b1} is much higher than either P_{b2} or P_{b3}. However, for the simply connected subassemblage, the distribution of bracing force is nearly symmetrical if the flexural restraint provided to the column from the torsional stiffness of the connection is ignored. The bracing force in the top brace is much smaller than for the rigidly jointed case.

Figure 8.4b also indicates that for type 2 initial lateral deflection, the bracing strength requirements are approximately two times those for the first type of ILD, although no difference in the subassemblage load-carrying capacities may be observed due to complete plastic action. As pointed out by Winter[34], the shape of this form of initial deflection is affine to the likely buckling shape under the bracing system, in other words, this shape is most 'unfavourable' in terms of its effect on the bracing strength requirement. Zuk[33] graphically showed that in this case, the bracing strength requirement for the one bracing system should be adopted for each brace of the multiple bracing system. As shown in figure 8.5, significant forces are developed in each brace in the case of type 2 ILD. It may thus be suggested that a value of one percent of the ultimate load in the column be taken as the bracing strength requirement for a single bracing system, whilst in cases of multiple bracing system, Zuk's conclusion be followed, i.e. assuming the most severe shape of initial lateral deflection for the sake of safety.

If the column is under flexural bending from the beam, the effect of different initial deflections is of little significance. Figure 8.6a illustrates

the variation of subassemblage strength; figure 8.6b gives the relationship between bracing force and bracing stiffness; whilst figure 8.7 is the bracing force behaviour in each brace. Figure 8.7 clearly shows that the bracing force in the top brace is great because of the significant moment it has resisted. Due to the continuous increase in bending moment with the use of stiffer bracings, the bracing force increases continuously. The pattern of the bracing force for a single brace is produced because of the low level of flexural moment at failure following moment unloading with applied beam load for slender columns as explained in chapter 7. Therefore, the subassemblage behaves to some extent as if without beam loading, although the bracing reaction is much greater.

The variation of column top flexural bending moment about the minor axis M_z against applied beam load is given in figure 8.8 for infinite bracing stiffness, which is typical of other bracings provided adequate stiffness is present. For 1 brace, the moment shedding is observed. However, for subassemblages with 3 braces, the moment increases continuously until approaching failure when the column's stiffness deteriorates significantly. Also because of the enhenced column rigidity from multiple bracing, the moment for this case is much higher than that for 1 brace at the same load level. It is clearly shown that the moment for a multiple bracing system approaches the cross-sectional plastic moment capacity about the minor axis M_{pz}, which indicates that the column subassemblage fails fully plastically since the elastic buckling load of the column effective length between the braces and supports (P_E) is much higher than the column's squash load P_{squash}. Whilst for one bracing system, the failure of the subassemblage is due to the combined action of axial load and flexural bending since $P_E < P_{squash}$.

The results of the studies on column subassemblages with flange bracing agree with the observation by Dooley[38] i.e. the pitch of intermediate restraints does not have significant effect on the performance of the restrained structures. As can be seen in figure 8.9a, for the same type of initial lateral deflection, the load-carrying capacity against bracing stiffness curves for 1 brace and 3 braces are quite close. This figure also shows that the type 2 ILD is less severe for flange bracing and a slightly higher value of load-carrying capacity is obtained and in figure 8.9b, a lower value of bracing reaction developed. This is expected since the column subassemblage fails inelastically and the bending moment generated in the column is lower due to the smaller magnitude of type 2 initial lateral deflection. Figure 8.9b exhibits an increase in bracing force, which results because of the inability of flange bracing to resist the torsion of the column from the $P - \Delta$ effect, although this variation in bracing force is quite small.

8.4 Conclusion

A limited study has been conducted to gain an understanding of bracing effects on the behaviour of column subassemblages. Based on this investigation, the following conclusions may be drawn:

1. If axial loading is the main action on the column subassemblage, the interaction between joint type and bracing effects is small;

2. A value of one percent of the column subassemblage buckling load may be taken as the bracing strength requirement for each brace regardless of the number of braces;

3. If the brace sustains primary actions, the bracing reaction will be great and the subassemblage will fail basically plastically. In this case, the form of initial deflection will have little effect on both the performance of the main structure and the bracing reaction.

4. The conclusion made by Dooley[38] regarding the effects of offset bracings is validated.

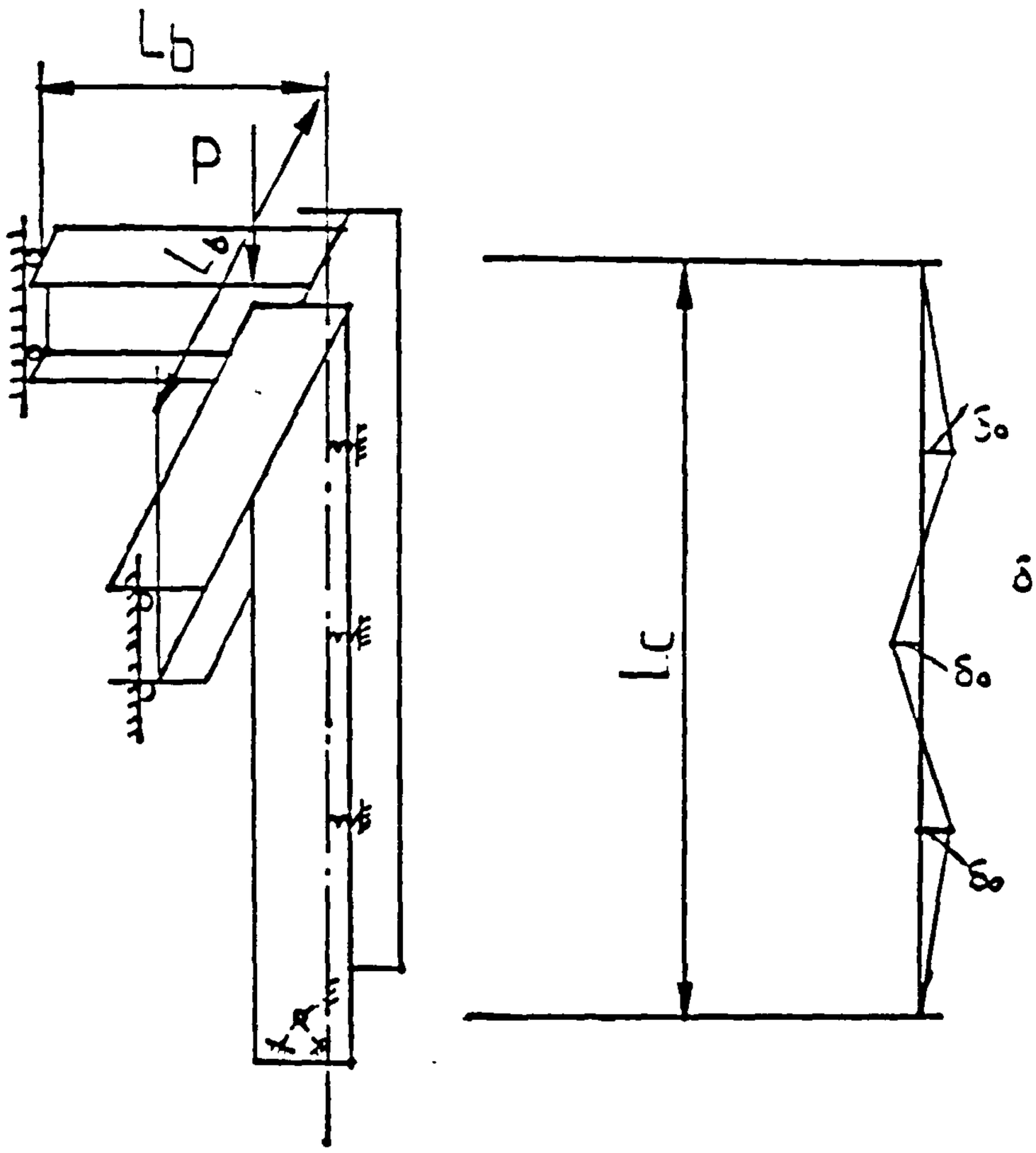

(a) General view of a braced Column subassemblage

(b) Type 2 Initial Lateral Deflection (ILD)

Fig. 8: Problem under consideration

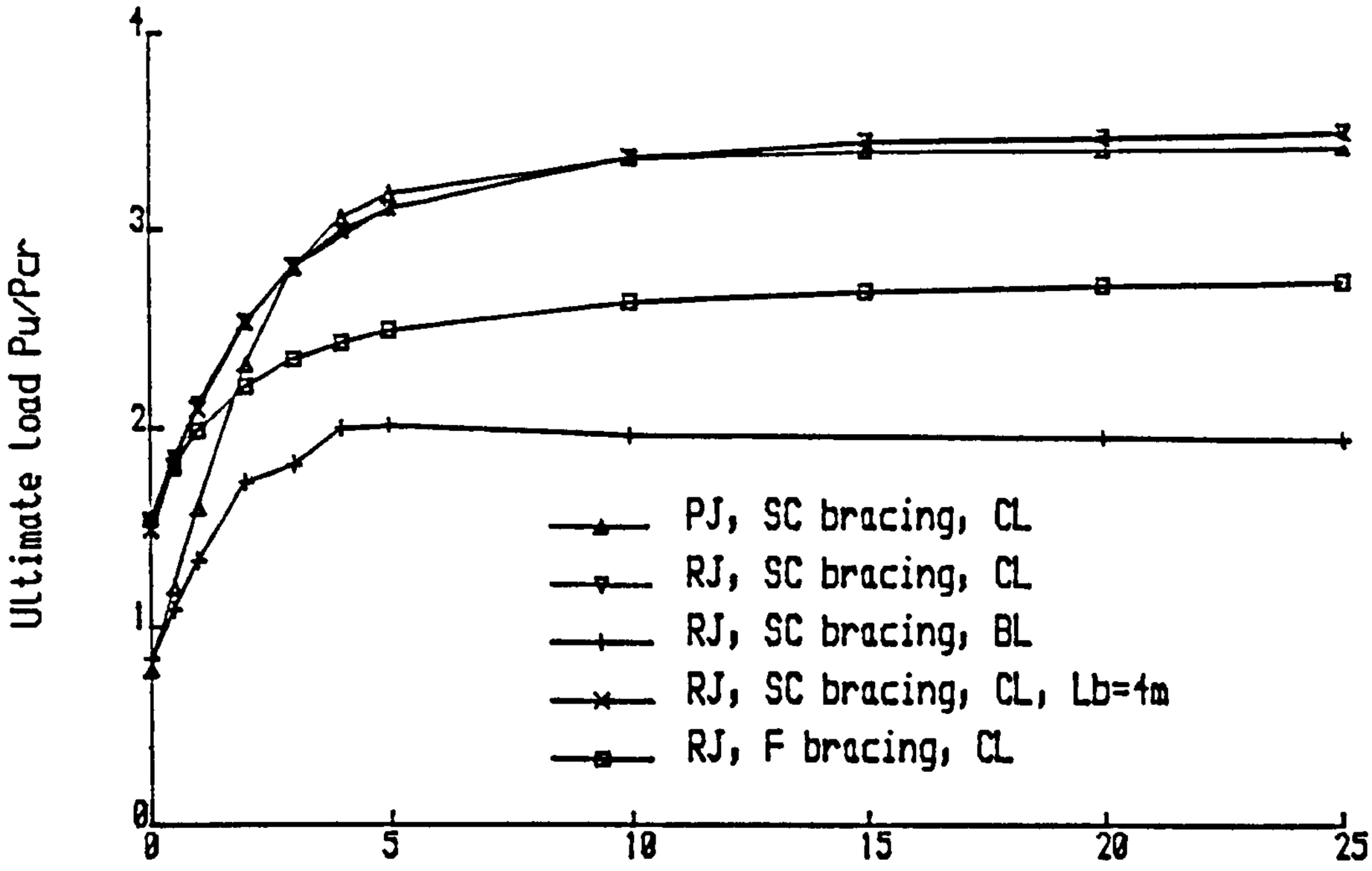

Fig. 8.2a Ultimate load-bracing stiffness behaviour for various cases of one brace at column centre. Column slenderness=200.

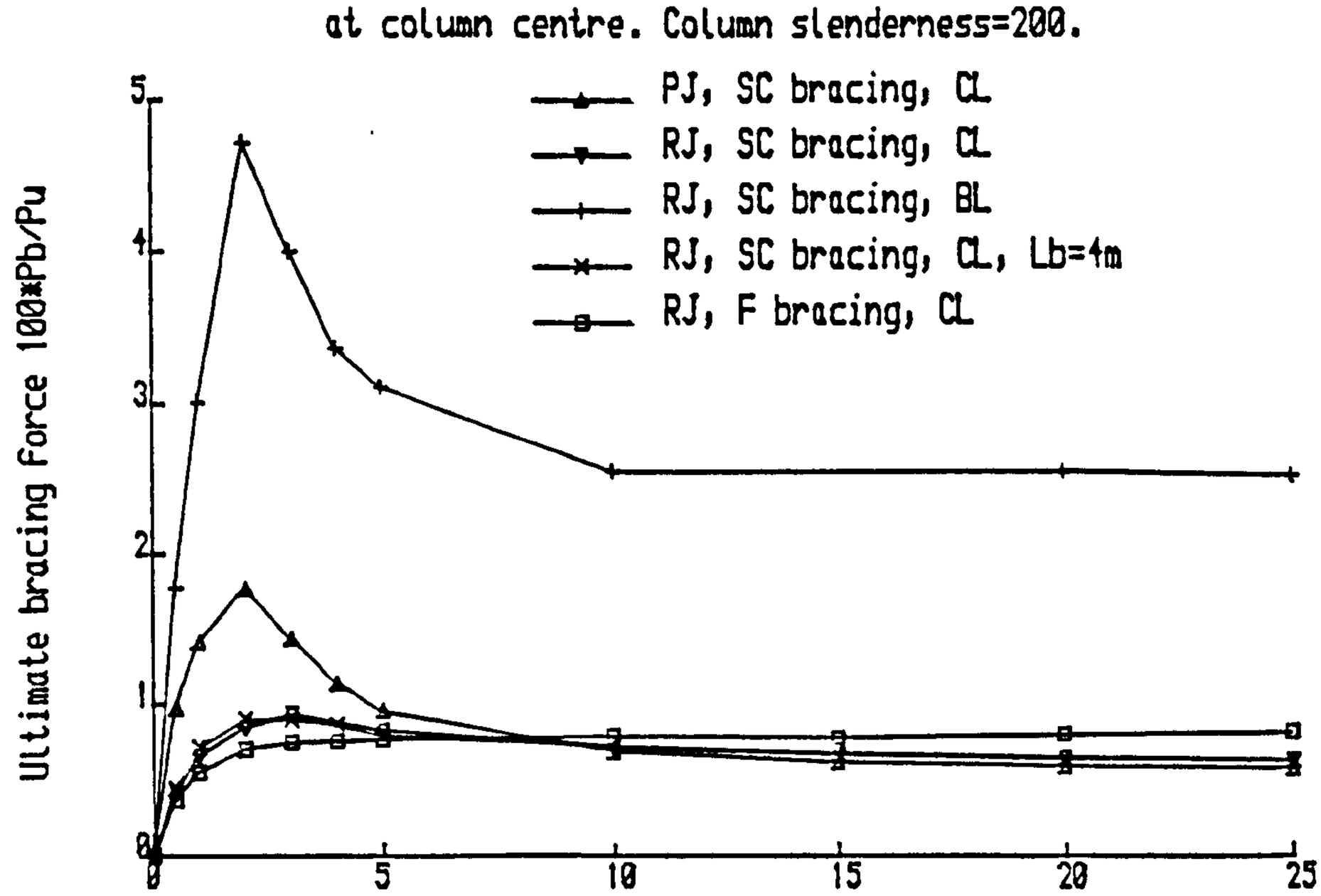

Fig. 8.2b Bracing force-bracing stiffness behaviour for various cases of one brace at column centre. Column slenderness=200.

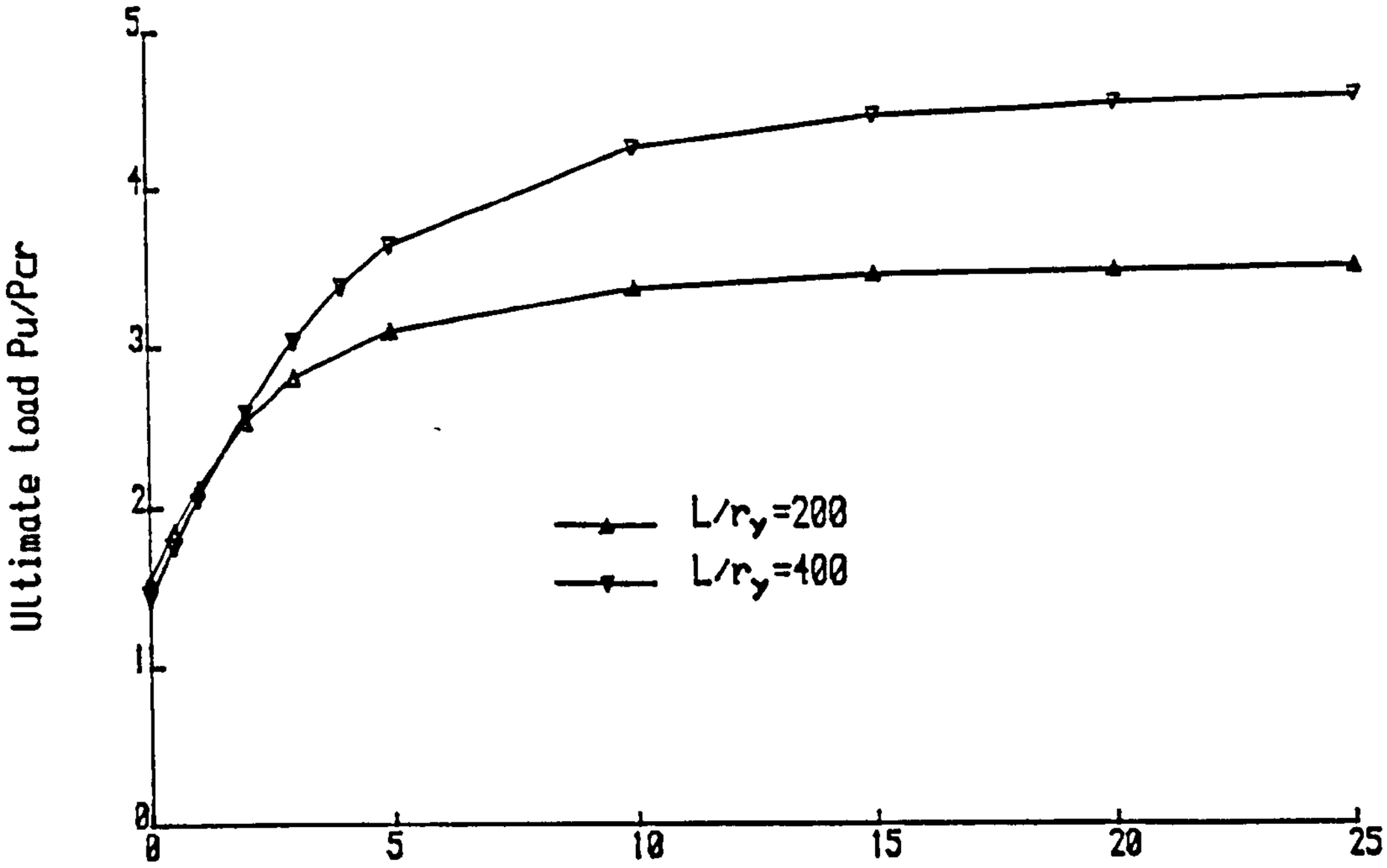

Fig. 8.3b Ultimate load-bracing stiffness behaviour for two column slendernesses. Rigid joints. Column loading.

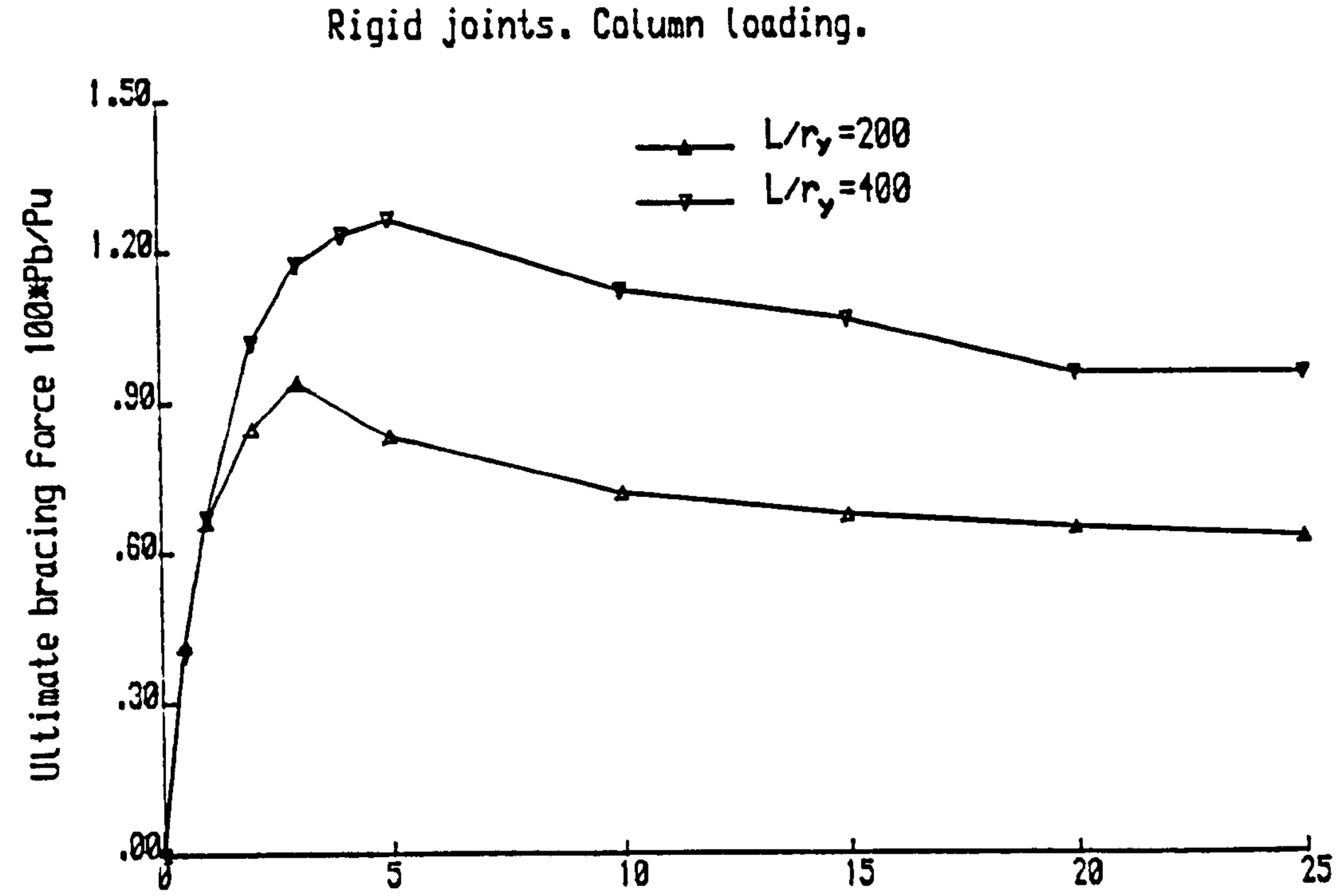

Fig. 8.3b Bracing force-bracing stiffness behaviour for two column slendernesses. Rigid joints. Column loading.

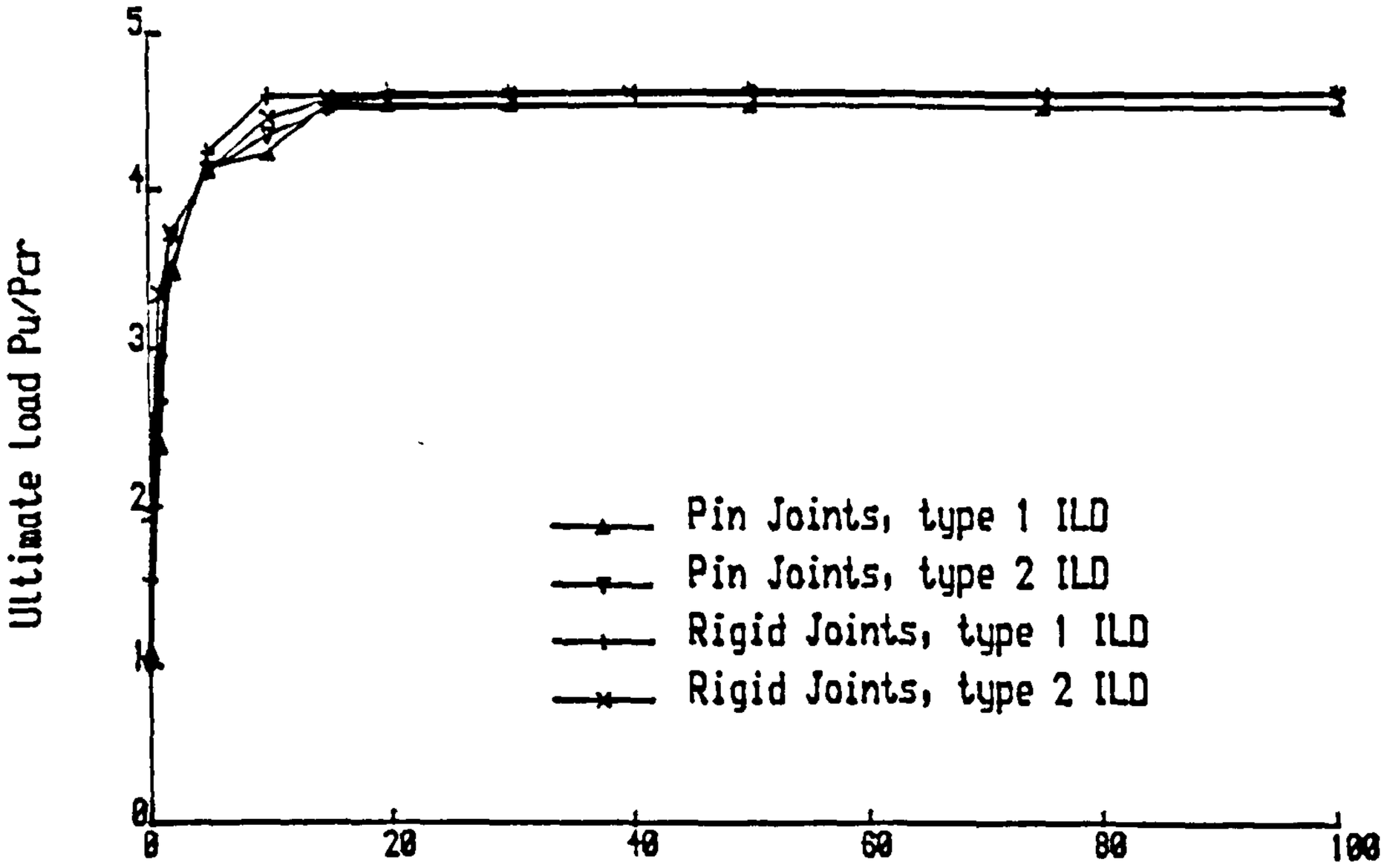

Fig. 8.4a Ultimate load-bracing stiffness behaviour for Column Loading (CL) and Shear Centre (SC) bracing

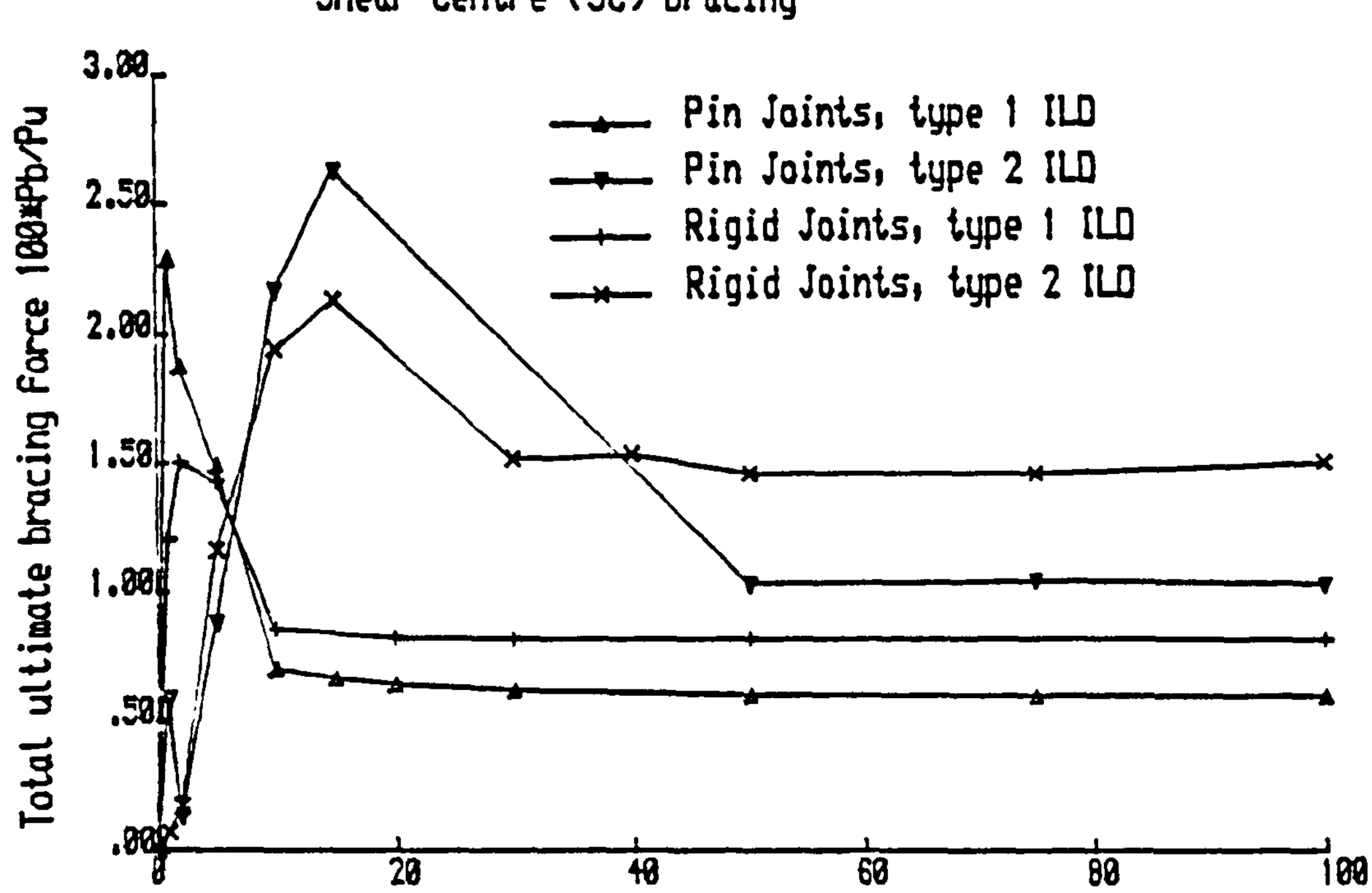

Fig. 8.4b Bracing force-bracing stiffness behaviour for Column Loading (CL) and Shear Centre (SC) bracing

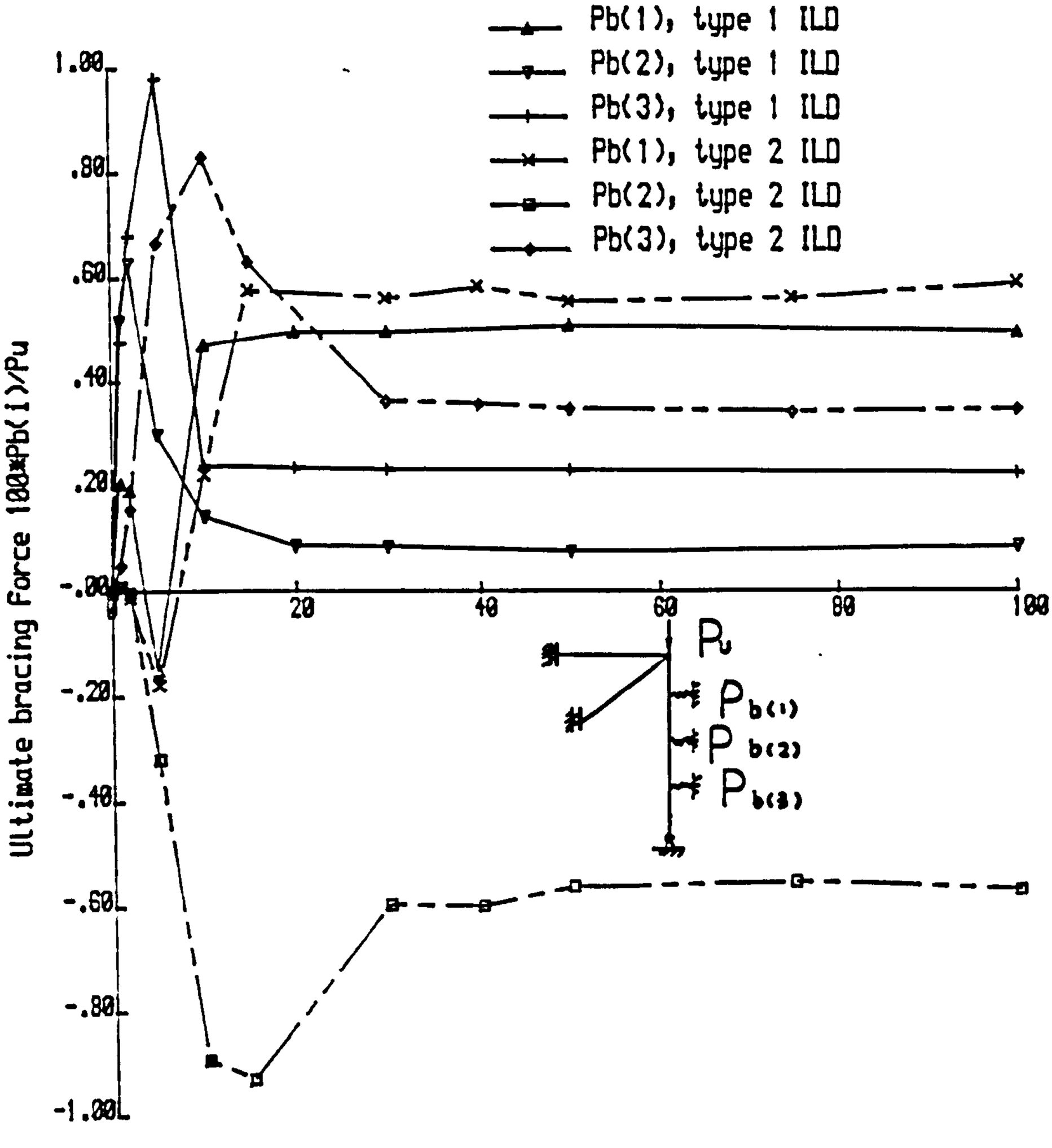

Fig. 8.5 Bracing Force-bracing stiffness behaviour
for each brace. Rigid joints. Column loading.

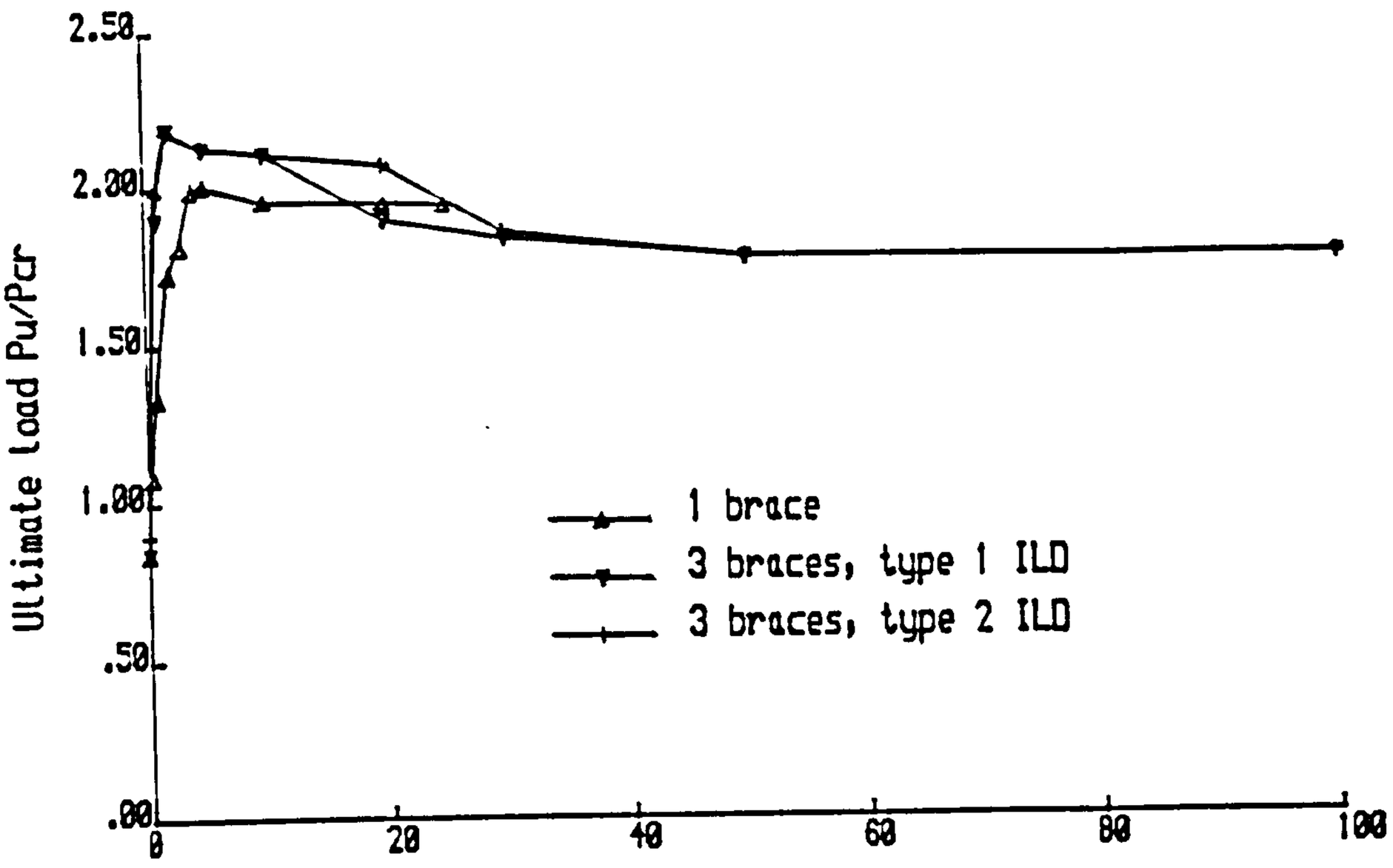

Fig. 8.6a Ultimate load-bracing stiffness curves
For Beam Loading (BL), Shear Centre (SC) bracing

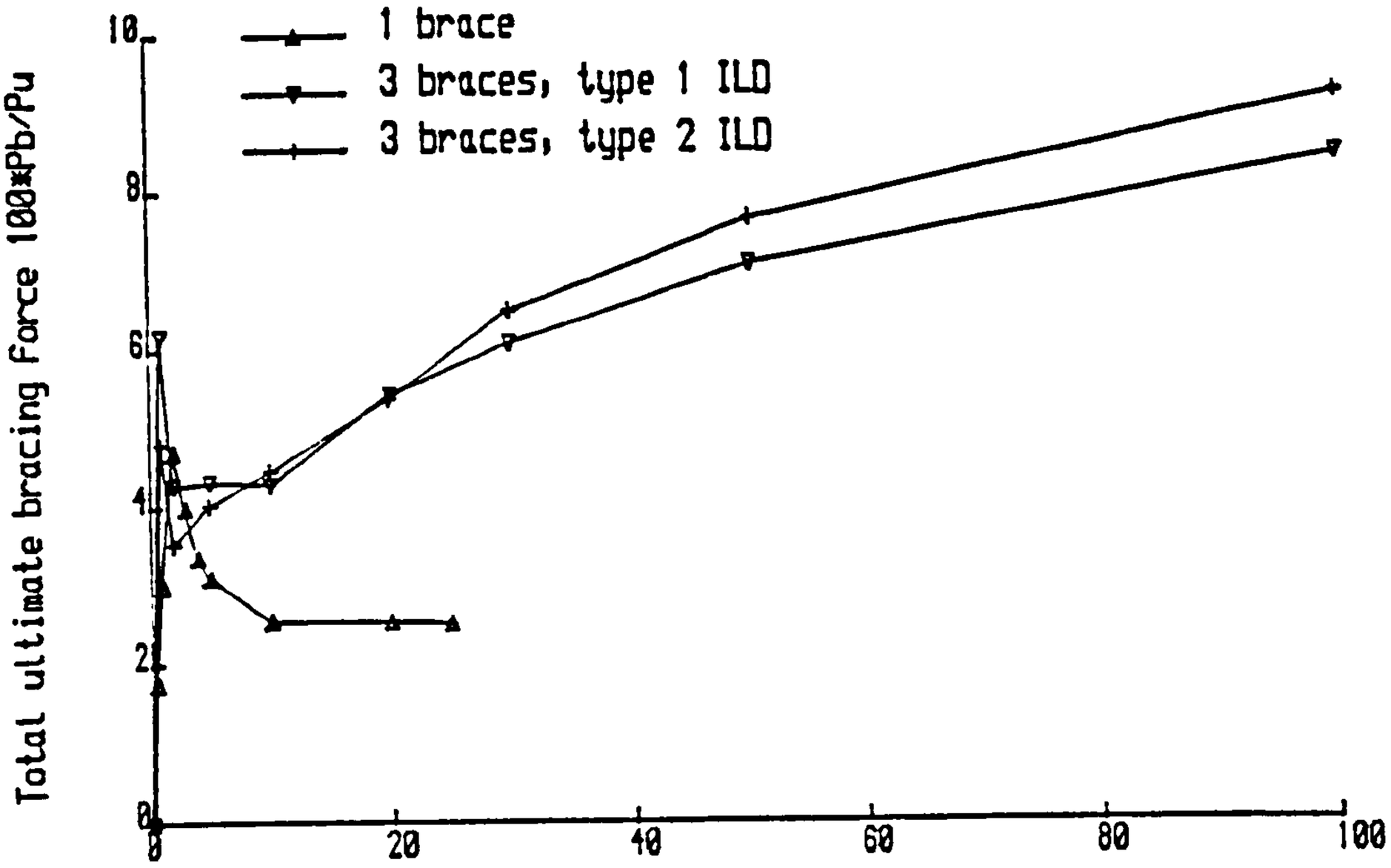

Fig. 8.6b Bracing Force-bracing stiffness curves
For Beam Loading (BL), Shear Centre (SC) bracing

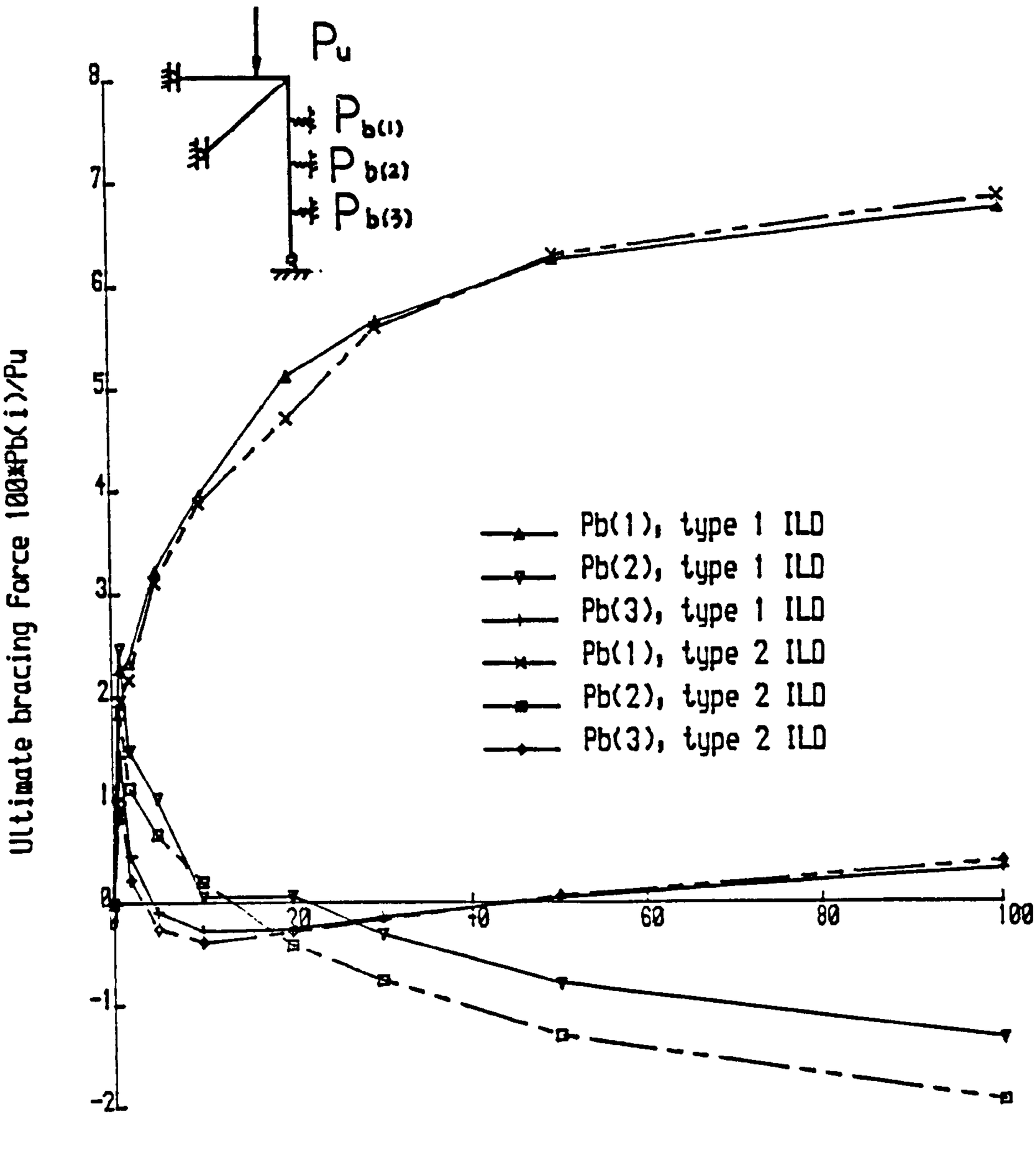

Fig. 8.7 Bracing force-bracing stiffness behaviour
for each brace. Rigid joints. Beam loading.

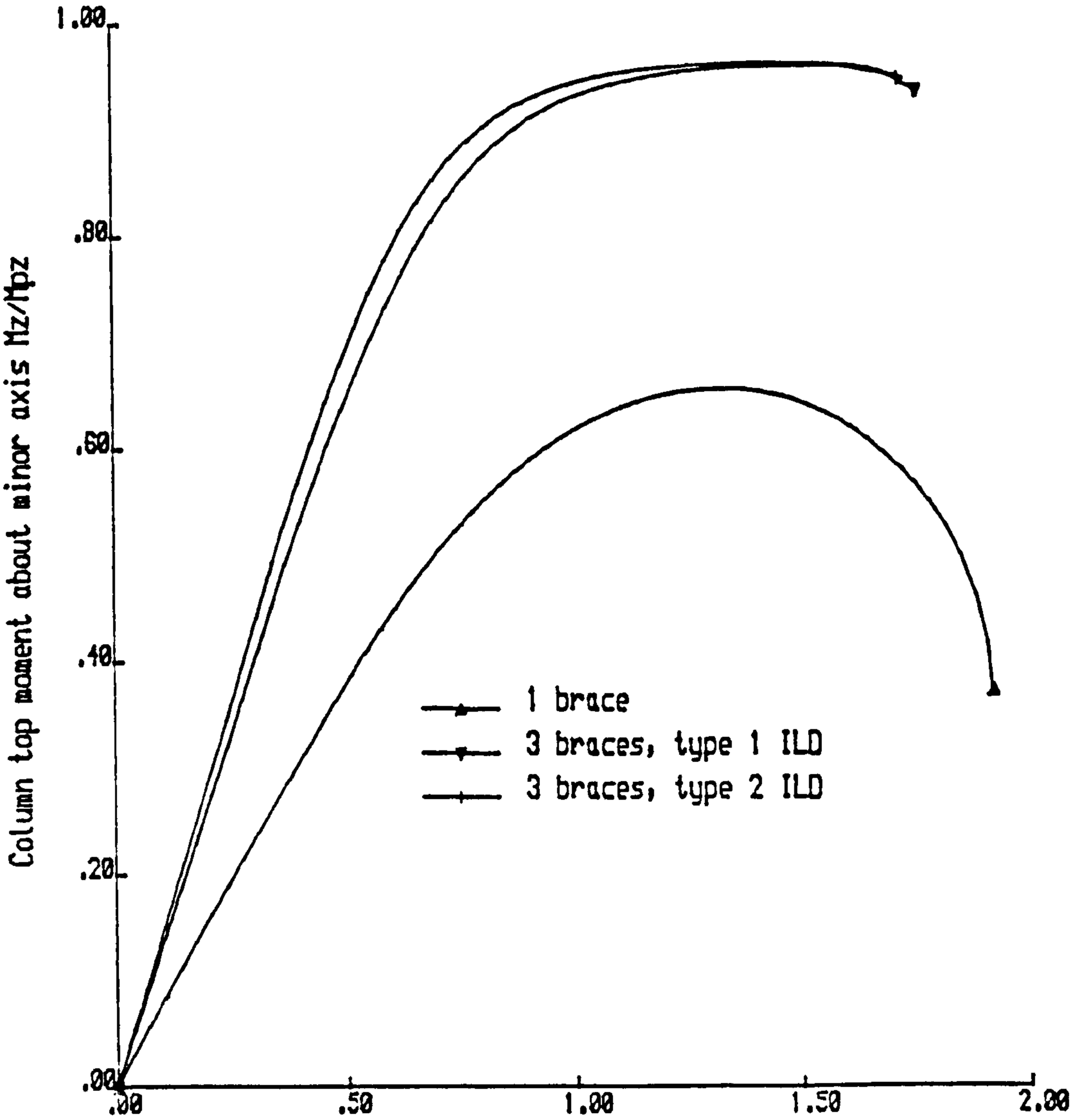

Fig. 8.8 Load - moment behaviour for different cases of beam loading and shear centre bracing

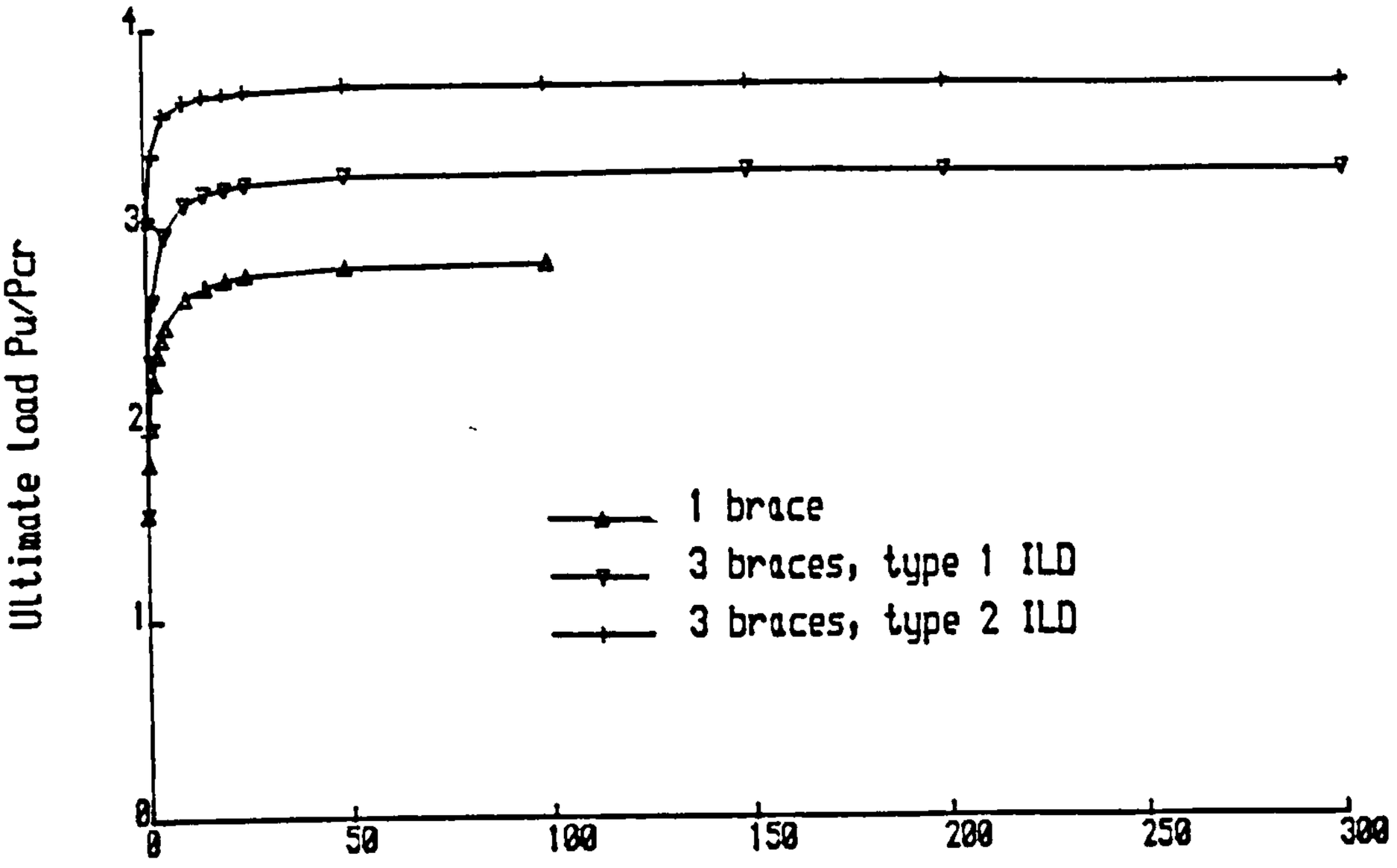

Fig. 8.9a Ultimate load-bracing stiffness curves
for Column Loading (CL) and Flange (F) bracing

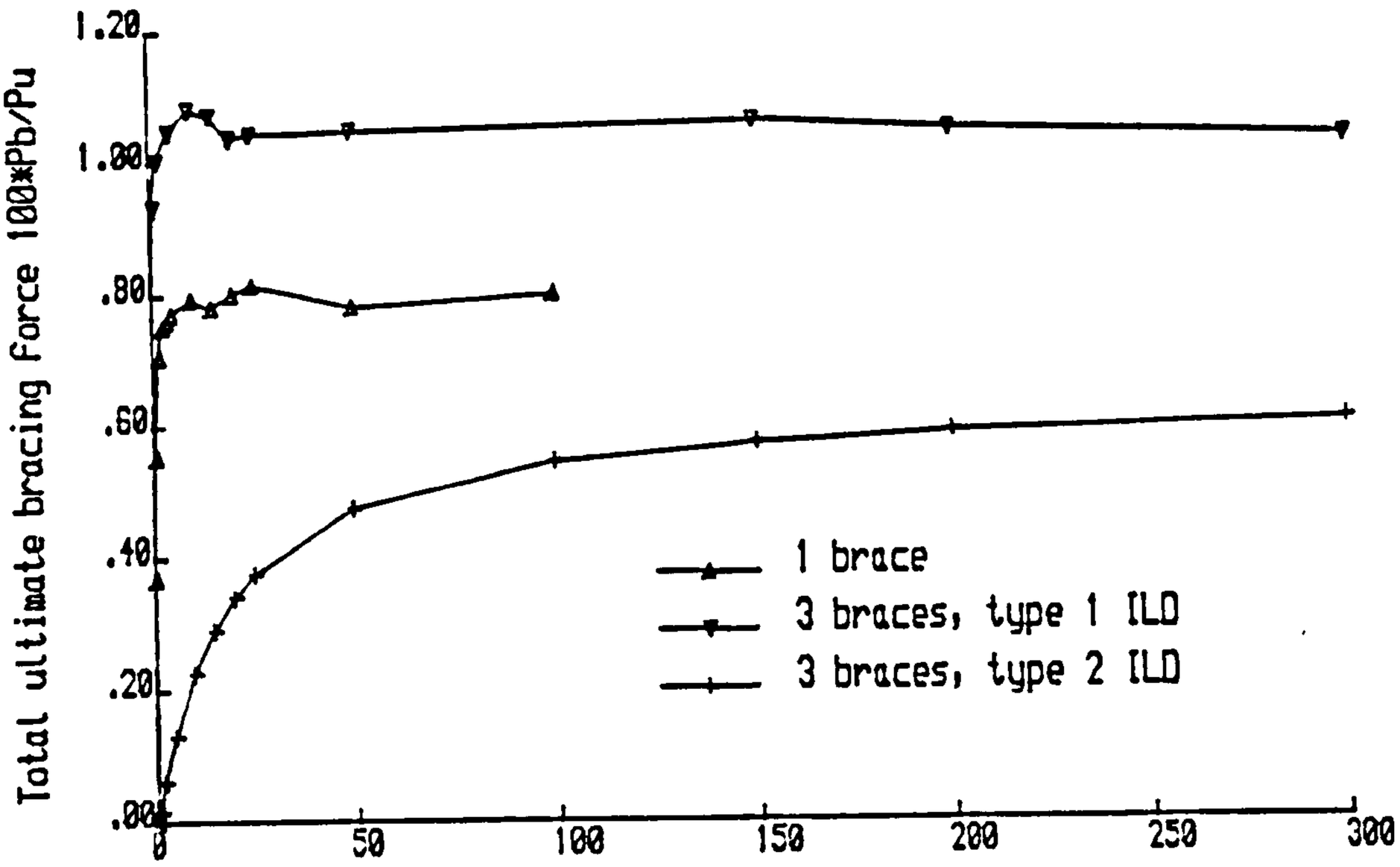

Fig. 8.9a Bracing Force-bracing stiffness curves
for Column Loading (CL) and Flange (F) bracing

Chapter 9

GENERAL CONCLUSIONS

9.1 Introduction

The theme of this research has been to study the effects of various restraints on the spatial behaviour and thus to predict the strengths of isolated beam-column members and subframes. The purpose has been fulfilled by modifying an existing program[1] for the ultimate strength analysis of beam-column members with simple end conditions (i.e. simply supported or fixed) and conducting a number of parametric studies using the new program. This chapter is intended to give a brief summary of some of the more interesting conclusions which have resulted from this study.

9.2 Modification of the Existing Program

A brief review of literature in Chapter 2 indicated that there was a need to conduct a systematical investigation into the effects of various restraints i.e. from beam column connections and secondary members, on the behaviour

of the main structure. The computer program[1] based on the analysis by Rajasekaran[2] was modified to incorporate the effects of these nonlinear end restraints and intermediate bracings. The problems of isolated beam-column members and subframes were addressed separately in Chapter 3 and Chapter 6. The close agreement with other analytical and experimental studies clearly showed the capacity of the modified program to deal with various problems.

9.3 Effect of End Restraints on Lateral-Torsional Buckling of Beam-Columns

The modified program was extensively utilised to generate a detailed parametric study into the effects of various practical end supporting conditions on the ultimate strengths of beams under flexural bending about the major axis. It was clearly shown that for an isolated member, the effect of the connection was reflected by reducing the deformation and balancing the flexural moment distribution along the member thus increasing the strength of the beam. The U.K. steelwork design code[3] recognises the strengthening effect of this 'favourable' pattern of moment distribution and proposes an n factor to reduce the beam effective length. Comparison between this method and the author's analytical results confirmed the validity of the design approach.

The sensitivity study of the effect of three main imperfections namely, initial lateral deflection, residual stress and discrepency in modelling the connection's $M-\phi$ curves showed that the initial deflection had a significant effect on the load-deflection behaviour and ultimate loads of beams, especially if substantial end restraint existed. The effect of residual stress depended on the degree of yield penetration in the beam. Apprently, if a plastic hinge

formed or the beam failed elastically, the beam's strength would not be affected at all. If the yield was modest, the reduction in the beam's strength due to residual stress would be maximum, although this value was rather small. This study also suggested that in predicting the beam's load-carrying capacity, the precision of the connection's force-deformation characteristics was not an important factor.

The foregoing investigations were concentrated on the effect of the connection's in-plane behaviour. In order to get a complete picture of the connection's influence, limited studies were conducted on the effect of the connection's various out-of-plane restraints i.e. minor axis restraint, torsional restraint and warping restraint. Making use of the prelimilary test results of Ref.[59] on flange cleat connections and web cleat connections, it was observed that the effect of minor axis restraint of these connections was negligible on the lateral-torsional buckling of the beam. Nevertheless, the lateral-torsional buckling of the beam was greatly influenced by end torsional restraints. Furthermore, even the practically weakest connection i.e web cleats might be accepted as providing full torsional restraint. For beams of open sections, the warping effect is great. However, due to the difficulty in identifying the warping force and warping displacement, their interrelationships are unknown for practical connections. The beam's strength against end warping restraint stiffness relationships were investigated and it was proposed that the end warping restraint was most active when its stiffness value fell in the region between $0.1\frac{EI_w}{L}$ and $100\frac{EI_w}{L}$. Obviously, some tests are necessary to determine the end warping characteristics of practical connections.

9.4 Effects of Bracing on I-Beams

Many studies have been devoted to this problem. However, most of them were confined to searching for the improved performance of the braced member by various bracings. The problem of determining the bracing reaction seemed to be overlooked. A selection of representive cases was studied. The force-deformation relationship of a brace was assumed to be linear although the method and the general conclusions were applicable to nonlinear cases. Both bracing strength requirements and the main member's performance were addressed, but the study was largely concentrated on the former.

It was found that provided the brace had adequate stiffness, its strength requirement was insensitive to the variation of the main member's slenderness. Studies on three beam slendernesses of 100, 300 and 600 indicated that a value of one percent of the maximum force in the main member's flange was required of a single bracing system to ensure its effectiveness in restraining the main member, which is in accord with the requirement specified in the design code for lateral and torsional bracings. A value of two percent was considered necessary for the total bracing reaction for the case of a multiple bracing system. In this case, the bracing force induced in each brace depended on such factors as its type, stiffness and position; the main member's initial deflection; the load level and load type acting on the main member.

9.5 Effect of Beam-Column Connections on 3-D Column Subassemblages

Having completed the study of various restraints on isolated beam-column members, it was felt necessary to progress the investigation into subframes since this would offer a complete illustration of the connection's effects as part of a frame. In this instance, the connection exhibited a two-fold role in affecting the ultimate load of a column subassemblage i.e. providing restraint (thereby enhancing strength) and transferring moment from beams to the column (thus reducing the load-carrying capacity). The overall influence of the connection would depend on the net effect of these two aspects. When the first effect was dominant, as in the case of slender columns, the use of stiffer connections was always accompanied by higher ultimate loads; however, when the latter controlled e.g. subassemblages with short columns or mainly under major axis loading, the weakening effect of the overstiff connection would be observed.

For the column subassemblage, the connection's torsional restraint was equivalent to providing the column with flexural restraints. Since the restraint was small compared with the flexural restraint from the connection, its effect might be ignored. The minor axis restraint provided the column with torsional restraint; therefore, no effect was noticed since for column type problems, the structure was not affected by torsional restraint alone.

The approach in the U.K. design code[3] provides a safe estimation of the load-carrying capacity of the column subassemblage. The predication of the ultimate load using Wood's 'variable stiffness' method[63] seemed to be closer to the author's analysis. This might be attributed to the overlooking

of the moment shedding phenomenan in the column observed in the analysis by the the U.K. design method.

9.6 Bracing Effects on 3-D Column Subassemblages

In order to complete the study of various restraints on ultimate strengths of 3-D beams and column subassemblages, the investigation in chapter 8 was performed. This study gave rise to the conclusion that the effect of joint flexibility was negligible if the column subssemblage was mainly under direct column loading and suggested that a value of one percent of the column buckling load be taken as the bracing strength requirement for one brace. It also confirmed the conclusions by Zuk[33] that the bracing strength requirement for one bracing system could be applied to each brace of the multiple bracing system and by Dooley[38], which implied that the effect of different pitches for offset braces was insignificant.

9.7 Recommendation for Future Work

This thesis presents an analytical study capable of tracing the spatial behaviour and thus predicting the ultimate strengths of both isolated members and column subassemblages allowing for the effects of various restraints. The following further work is thought to be of interest for the better understanding of spatial behaviour of restrained structures.

1. As mentioned in the introductory chapter of the thesis, a small deflection theory was assumed in the basic theory. The inclusion of direct

torsional effects was therefore hampered. The extension of the present study to allow for large torsional effects may be made by using the most sophisticated formulation presented by El-Khenfas[1];

2. The study in Chapter 7 indicated that an experimental investigation into the effect of semi-rigid connections on the behaviour of 3-D column subassemblages would be both necessary and beneficial; this work is currently in progress at Sheffield;

3. Due to the lack of data on connection's out-of-plane force-deformation characteristics, the work reported in this thesis is incomplete as far as this aspect is concerned. Detailed study may be carried out only if sufficient connection test data is available;

4. The present study was confined to beams and column subassemblages. The complementary version of this i.e columns and beam subassemblages would naturally be the choice of the next study;

5. The post-buckling behaviour of a member has a great effect on the performance of a complete frame. It would be useful to study the effect of restraints on the post-buckling behaviour of various members.

Bibliography

[1] El-Khenfas,M.A., "Analysis of Biaxial Bending and Torsion of Open Section Beam Columns", PhD Thesis, Department of Civil and Structural Engineering, University of Sheffield, UK, 1987

[2] Chen,W.F. and Atsuta,T., "Theory of Beam-Columns", Chapter 12, Vol. 2, McGraw-Hill International Book Company, 1980

[3] British Standards Institution, "BS 5950: Part 1, Structural Use of Steelwork in Building", London, BSI, 1985

[4] Nethercot,D.A.,"Steel Beam-to-Column Connections - A Review of Test Data", CIRIA Project Record 338, September, 1985, p.77

[5] Goverdhen,A.V., "A Collection of Experimental Moment-Rotation Curves and Evaluation of Predicting Equation for Semi-Rigid Connections", Doctoral Dissertation, Vanderbilt University, Nashville, Tennessee, 1984

[6] Kishi,N. and Chen,W.F., "Data Base on Steel Beam-to-Column Connections", CE-STR-86-26, School of Civil Engineering, Purdue University, 1986

[7] Jones,S.W., "Semi-Rigid Connections and Their Influence on Steel Column Behaviour", PhD Thesis, Department of Civil and Structural Engineering, University of Sheffield, UK, 1980

[8] Sugimoto,H. and Chen,W.F., "Small End Restraining Effects on the Strength of H-Columns", Journal of Structural Division, ASCE, Vol. 108, No. 3, 1982, pp. 661-687

[9] Nethercot,D.A. and Chen,W.F., "Effect of Connections on Columns" Steel Beam to Column Connections, Special issue, Journal of Constructional Steel Research, to be published in 1988

[10] Shen,Z.Y. and Lu.L.W., "Analysis of Initialy Crooked End Restrained Steel Columns", Journal of Constructional Steel Research, Vol. 3, No. 1, 1983, pp.10-18

[11] Razzaq,Z., "End Restraint Effect on Steel Column Strength", Journal of Structural Engineering, ASCE, Vol. 109, No. 2, Feburary, 1983, pp. 314-334

[12] Lui,E.M. and Chen,W.F., "Analysis and Behaviour of Flexibly Jointed Frames", Engineering Structures, Vol. 8, No. 2, April 1987, pp.107-118

[13] Gerstle,K.H., "Flexibly Connected Steel Frames", Steel Framed Structures: Stability and Strength, Edited by R. Narayanan, Elsevier Applied Science Publishers, 1985, pp. 205-239

[14] Anderson,D. and Lok,T.S., "Elastic Analysis of Semi-Rigid Steel Frames", Research Report CE/17, Department of Engineering, University of Warwick, January, 1985

[15] Davison,J.B., "Strength of Beam-Columns in Flexibly Connected Steel Frames", PhD Thesis, Department of Civil and Structural Engineering, University of Sheffield, UK, 1987

[16] Rifai,A.M., "Behaviour of Column Subassemblages with Semi-Rigid Connections", PhD Thesis, Department of Civil and Structural Engineering, University of Sheffield, UK, 1987

[17] Chen,W.F. and Atsuta,T.,"Theory of Beam-Columns", Vol. 2, McGraw-Hill International Book Company, 1980

[18] Hechtmann,R.A., Hattupp,J.S., Styer,E.E. and Tiedemann,J.C., "Lateral Buckling of Rolled Steel Beams", Transactions, ASCE, 122, November 1955, pp. 823-843

[19] Timoshenko,S.P. and Gere,J.M., "Theory of Elastic Stability", 2nd Edition, McGraw-Hill Book Company, 1961

[20] Trahair,N.S., "Stability of I-Beams with Elastic end Restraints", Journal of the Institution of Engineers, Australia, Vol. 37, No. 6, June 1965, pp. 157-168

[21] Schmidt.L.C., "Restraints Against Elastic Lateral Buckling", Journal of Engineering Mechanics Division, ASCE, Vol. 91, No. EM6, December 1965, pp.1-10

[22] Standards Association of Australia, "AS 1250-1981 SAA Steel Structures Code", SAA, Sydney, 1981

[23] Yoshida,H. and Imoto,Y., "Inelastic Lateral Buckling of Restrained Beams",Journal of Engineering Mechanics Division, ASCE, Vol. 99, No. EM2, April 1973, pp. 343-365

[24] Vinnakota, S. and Aoshima.Y., "Spatial Behaviour of Rotationally and Directionally Restrained Beam-Columns", IABSE Reprint from Vol. 34-II of the Publications, Zunich, 1974, pp. 169-194

[25] Gent,A.R. and Milner,H.R., "The Ultimate Load Capacity of Elastically Restrained H-Columns under Biaxial Bending", ICE Proceeding, Vol. 41, December 1968, pp.1685-1704

[26] Santathadporn,S. and Chen,W.F., "Analysis of Biaxially Loaded Steel H-Columns", Journal of Structural Division, ASCE, Vol. 99, No. ST3, March 1973, pp.

[27] Massonnet.CH., "Elements de Statique des constructions", Notes de Cours, Fascicule 2 Construction Metallique, Universik de Liege, 1972, p. 184

[28] Ojalvo,M. and Chambers,R.S., "Effect of Warping Restraints on I-Beam Buckling", Journal of Structural Division, ASCE, Vol. 103, No. ST12, December 1977, pp. 2351-2360

[29] Lindner,J. and Giezelt,R. "Influence of End-Plates on Ultimate Load of Laterally Unsupported Beams", Instability and Plastic Collapse of Steel Structures, Ed. by Morris,L.T., London, Granada Publishing, 1983, pp. 538-546

[30] Vacharajittiphan,P. and Trahair,N.S., "Warping and Distortion at I-Section Joints", Journal of Structural Division, ASCE, Vol. 100, No. ST3, March 1974, pp. 547-564

[31] Trahair,N.S. and Nethercot,D.A., "Bracing Requirements in the Thin-Walled Structures", Development in Thin-Walled Structure - 2, edited by Rhodes,J. and Walker,A.C., Elsevier Applied Science Publishers, 1984, pp.93-130

[32] Flint,A.R., "The Influence of Restraints on the Stability of Beams", the Structural Engineer, September 1951, pp.235-246

[33] Zuk,W., "Lateral Braicng Forces on Beams and Columns", Journal of Engineering Mechanics Division, ASCE, Vol. 82, No. EM3, July 1956, pp. 1032(1-11)

[34] Winter,G., "Lateral Bracing of Columns and Beams", Journal of Structural Division, ASCE, Vol. 84, No. ST2, March 1958, pp. 1561(1-22)

[35] Nethercot,D.A.,"Bracing of Slender Members", Civil Engineering and Public Works Review, November 1972, pp. 1158

[36] Hartmann,J., "Elastic Lateral Buckling of Continous Beams", Journal of Structural Division, ASCE, Vol. 93, No. ST4, pp. 11-26

[37] Massey,C., "Lateral Bracing Force of Steel I-Beams", Journal of Engineering Mechanics Division, ASCE, Vol. 88, No. EM6, pp.89-113

[38] Dooley,J.P., "on the Torsional Buckling of Columns of I-Section Restrained at Finite Intervals", Interanal Journal of Mechanics Science, Vol. 9, 1967, pp.1-9

[39] Dooley,J.P. and Locke,J., "Flexural-Torsional Buckling Tests on Beam-Columns with Sheeting Rail Type Restrints", International Journal of Mechanics Science, Vol. 16, 1974, pp.893-921

[40] Harung,H.S. and Miller,M.A., "Lateral Restrained Beam-Columns with uniform Biaxial Loading", International Journal of Mechanics Science, Vol. 15, 1973, pp. 765-773

[41] Tam,"Non-Uniform Torsional Behaviour of Structural Joints and Frames" Ph.D Thesis, Department of Civil and Structural Engineering, University of Manchester Institute of Science and Technology, May 1978

[42] Medland,I.C., "A Basis for the Design of Column Bracing", The Structural Engineer, Vol. 55, No. 7, July 1977, pp.301-307

[43] Nethercot,D.A. and Trahair,N.S., "Design of Diaphragm-Braced I-Beams", Journal of the Structural Division, ASCE, 101(ST10), October 1975, pp. 2045-61

[44] Wakayabashi,T. and Nakamura,M.,"Buckling of Lateraly Braced Beams", Engineering Structures, Vol. 5, No. 2, April 1983, pp. 108-118

[45] Wong-Chung,A.D. and Kitipornchai,S., "Partially Braced Inelastic Beam Buckling Experiments", Journal of Constructional Steel Research, Vol. 7, No. 3, 1987, pp. 189-211

[46] Milner,H.R. and Gent,A.R., "Ultimate Load Calculation for Restrained H-Columns under Biaxial Bending", Civil Engineering Transactions, Australia, April 1971, pp. 35-44

[47] Taylor,D.A., "An Experimental Study of Continuous Columns", Proceeding, ICE, 53(2), June 1973, pp.1-17

[48] Joint Committee's First Report, "Fully Rigid Multi-Storey Welded Steel Frames", the Institution of Structural Engineers and the Welding Institute, December 1964

[49] Joint Committee's Second Report, "Fully Rigid Multi-Storey Welded STeel Frames", the Institution of Structural Engineers and the Welding Institute, May 1971

[50] Wood, R.H., Needham,F.H. and Smith,R.F., "Test of a Multi-Storey Rigid Steel Frames", the Structural Engineers, Vol. 46, No. 4, April 1968, pp. 107-119

[51] Smith,R.F. and Roberts,E.H., "Test of a Fully Continuous Multi-Storey Frame of High Yield Steel", the Structural Engineers, Vol. 49, No. 10, October 1971, pp.451-466

[52] Lott,J.F. Unnikrishna,P. and Ellis,J.S., "Three-Dimensional Inelastic Subassemblage Design", Journal of Structural Division, ASCE, Vol. 97, No. ST5, May 1971, pp. 1445-1464

[53] Lightfoot,E. and LeMmessurier,A.P., "Instability of Space Frames Having Elastically Connected and Offset Members", 2nd International Conference on Space Structures, September 1975, pp. 143-149

[54] Ang,K.M.and Morris,G.A., "Behaviour of Three Dimensional Flexibly Connected Steel Frames", Research Report, Department of Civil Engineering, University of Manitoba, Canada, November 1983

[55] Renton,J.D., "On the Transmission of Non-Uniform Torsion Through Joints", Report 1086/74, Department of Engineering Science, Oxford University, 1974

[56] Sharman,P.W., "Analysis of Structures with Thin-Walled Open Sections", International Mechanics Science, Vol. 27, No. 10, 1985, pp. 665-377

[57] Vlasov,V.Z., "Thin-Walled Elastic Beams", 2nd edn, National Science Foundation, Washington,D.C., and Department of Commerce, U.S.A., by the Israel Program for Science Translation, Jerusalem, 1961, p.292

[58] Yoshida,H. and Haegawa,K., "Lateral Instability of I-Beams with Imperfections", ASCE Journal of Structural Division, Vol. 110, No. 8, August 1984, pp.1875-92

[59] Celikag,M. and Kirby,P.A., "Standardised Method for Measuing Three Dimensional Response of Semi-Rigid Joints", State of the Art Workshop on Connections - Strength and Design of Steel Structures, Cachan, France, May 1987, pp.203-210

[60] Bathe,K.J. and Wilson,E.L., "Numerical Methods in Finite Element Analysis", Prentice-Hall, INC, Englewood Cliffs, New Jersey, 1976

[61] Ackroyd,M.H. and Gerstle,K.H., "Strength of Flexibly Connected Steel Frames", Enginerring Structures, Vol. 5, January 1983, pp. 31-38

[62] Poggi, C. and Zandonini,R., "Behaviour and Strength of Steel Frames with Semi-Rigid Connections", in "Connection Flexibility and Steel Frames", Edited by Chen,W.F., ASCE, 1986, pp.57-76

[63] Wood,R.H., "A New Approach of Column Design, with Special Reference to Restrained Steel Stanchions", Building Research Station Report, HMSO, 1974

[64] Taylor,J.C., "Semi-Rigid Beam Connection's Effects on Column Design: B.20 Code Method", Joints in Structural Steelwork, Proceedings of the International Conference, Teeside Polytechnics, Middlesborough, Pentech Press, London, pp. 5.50-5.57

[65] Janss,J., Jaspart,J. and Maquoi, R., "Strength and Behaviour of Inplane Weak Axis Joints and of 3-D Joints" in Connection in Steel Structures, Behaviour, Strength and Design, edited by Bjorhovde,R., Vrizzetti,J. and Colson,A. Elsevier Applied Science Publisher, 1987 pp. 60-68

Appendix A1: Member Flexural and Geometrical Stiffness Matrices

1. Flexural Stiffness Matrix $[K_s]$

$$[K_s] =$$

$$\begin{bmatrix}
a & 0.0 & 0.0 & 0.0 & 0.0 & 0.0 & 0.0 & -a & 0.0 & 0.0 & 0.0 & 0.0 & 0.0 & 0.0 \\
 & b & c & 0.0 & 0.0 & 0.0 & 0.0 & 0.0 & -b & c & 0.0 & 0.0 & 0.0 & 0.0 \\
 & & d & 0.0 & 0.0 & 0.0 & 0.0 & 0.0 & -c & e & 0.0 & 0.0 & 0.0 & 0.0 \\
 & & & f & g & 0.0 & 0.0 & 0.0 & 0.0 & 0.0 & -f & g & 0.0 & 0.0 \\
 & & & & h & 0.0 & 0.0 & 0.0 & 0.0 & 0.0 & -g & i & 0.0 & 0.0 \\
 & & & & & j & k & 0.0 & 0.0 & 0.0 & 0.0 & 0.0 & -j & k \\
 & & & & & & l & 0.0 & 0.0 & 0.0 & 0.0 & 0.0 & -k & m \\
 & & & & & & & a & 0.0 & 0.0 & 0.0 & 0.0 & 0.0 & 0.0 \\
 & & & & & & & & b & -c & 0.0 & 0.0 & 0.0 & 0.0 \\
 & & & & & & & & & d & 0.0 & 0.0 & 0.0 & 0.0 \\
 & & & & & & & & & & f & -g & 0.0 & 0.0 \\
 & & & & & & & & & & & h & 0.0 & 0.0 \\
 & & & & & & & & & & & & j & -k \\
 & & & & & & & & & & & & & l
\end{bmatrix}$$

$$a = \frac{EA}{L}$$

$$b = \frac{12EI_\zeta}{L^3} \quad f = \frac{12EI_\eta}{L^3} \quad j = \frac{1.2GK_T}{L} + \frac{12EI_w}{L^3}$$

$$c = \frac{6EI_\zeta}{L^2} \quad g = \frac{6EI_\eta}{L^2} \quad k = 0.1GK_T + \frac{6EI_w}{L^2}$$

$$d = \frac{4EI_\zeta}{L} \quad h = \frac{4EI_\eta}{L} \quad l = \frac{4}{30}GK_TL + \frac{4EI_w}{L}$$

$$e = \frac{2EI_\zeta}{L} \quad i = \frac{2EI_\eta}{L} \quad m = -\frac{1}{30}GK_TL + \frac{2EI_w}{L}$$

2. Geometrical Stiffness Matrix

$$[K_G] =$$

$$\begin{bmatrix}
a & b & & & k & l & -a & b & & & m & n \\
 & c & & & o & p & -b & d & & & -o & r \\
 & & a & b & -k' & -l' & & & -a & b & -m' & -n' \\
 & & & c & -o' & -p' & & & -b & d & o' & -r' \\
 & & & & e & f & -k & -s & k' & s' & -e & g \\
 & & & & & h & -l & u & e' & -u' & -f & i \\
 & & & & & & a & -b & & & -m & -n \\
 & & & & & & & c & & & s & t \\
 & & & & & & & & a & -b & -m' & -n' \\
 & & & & & & & & & c & -s' & -t' \\
 & & & & & & & & & & e & -g \\
 & & & & & & & & & & & j
\end{bmatrix}$$

$$\begin{array}{llllllllll}
a & = & \frac{1.2F_\xi}{L} & h & = & 0.1M_{w1}L + \frac{1}{30}M_{w2}L & o & = & -0.1m_\eta - 0.2F_\zeta \\
b & = & \frac{1}{10}F_\xi & i & = & -\frac{1}{60}(M_{w1} + M_{w2})L & p & = & -\frac{4}{30}m_\eta L - \frac{1}{30}F_\zeta L \\
c & = & \frac{4}{30}F_\xi L & j & = & \frac{1}{30}M_{w1}L + 0.1M_{w2}L & r & = & \frac{1}{30}m_\eta L \\
d & = & -\frac{1}{30}F_\xi L & k & = & -\frac{1.2m_\eta}{L} - 0.1F_\zeta & s & = & 0.1m_\eta - 0.1F_\zeta L \\
e & = & \frac{1.2M_{w1}}{L} + 0.6\frac{M_{w2}-M_{w1}}{L} & l & = & -0.1m_\eta & u & = & \frac{1}{30}m_\eta L + \frac{1}{30}F_\zeta L^2 \\
f & = & 0.1M_{w1} & m & = & \frac{1.2m_\eta}{L} + 1.1F_\zeta & & & \\
g & = & 0.1M_{w1} & n & = & -0.1m_\eta - 0.1F_\zeta L & & &
\end{array}$$

$k', l', m', n', o', p', r', s', t', u'$ are obtained by replacing m_η *and* F_ζ by m_ζ *and* F_η

in the expressions k,l,m,n,o,p,r,s,t,u.

Appendix A2 Transformation Matrices

1. $[T_1]$ to transfer stiffness matrix from principal axes to segment coordinates

$$[T_1] =$$

$$\begin{bmatrix}
1.0 & 0.0 & -y_c & 0.0 & -z_c & 0.0 & 0.0 \\
0.0 & cos\alpha & 0.0 & sin\alpha & 0.0 & y_0 sin\alpha - z_0 cos\alpha & 0.0 \\
0.0 & 0.0 & cos\alpha & 0.0 & sin\alpha & 0.0 & y_0 sin\alpha - z_0 con\alpha \\
0.0 & -sin\alpha & 0.0 & con\alpha & 0.0 & z_0 sin\alpha + y_0 con\alpha & 0.0 \\
0.0 & 0.0 & -sin\alpha & 0.0 & con\alpha & 0.0 & z_0 sin\alpha + y_0 con\alpha \\
0.0 & 0.0 & 0.0 & 0.0 & 0.0 & 1.0 & 0.0 \\
0.0 & 0.0 & 0.0 & 0.0 & 0.0 & 0.0 & 1.0
\end{bmatrix}$$

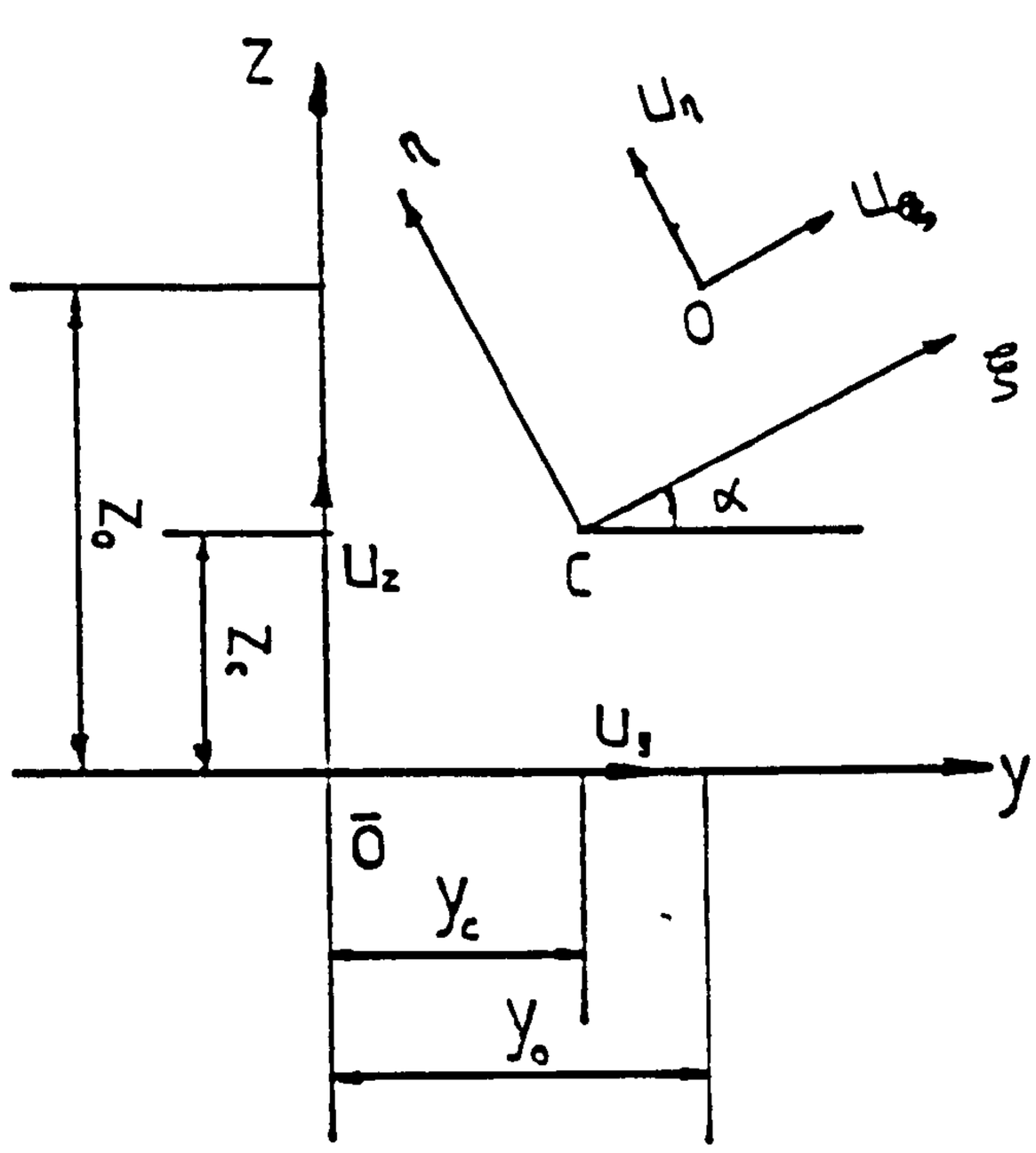

2. $[T_2]$ to transfer stiffness matrix from segment coordinates to member coordinates

$$[T_2] =$$

$$\begin{bmatrix}
1.0 & \frac{\Delta u_y}{L} & 0.0 & \frac{\Delta u_z}{L} & 0.0 & 0.0 & 0.0 \\
\frac{-\Delta u_y}{L} & 1.0 & 0.0 & sin\theta & 0.0 & 0.0 & 0.0 \\
0.0 & 0.0 & 1.0 & 0.0 & sin\theta & \frac{-\Delta u_z}{L} & 0.0 \\
\frac{-\Delta u_z}{L} & -sin\theta & 0.0 & 1.0 & 0.0 & 0.0 & 0.0 \\
0.0 & 0.0 & -sin\theta & 0.0 & 1.0 & \frac{\Delta u_y}{L} & 0.0 \\
0.0 & 0.0 & \frac{\Delta u_z}{L} & 0.0 & \frac{-\Delta u_y}{L} & 1.0 & 0.0 \\
0.0 & 0.0 & 0.0 & 0.0 & 0.0 & 0.0 & 1.0
\end{bmatrix}$$

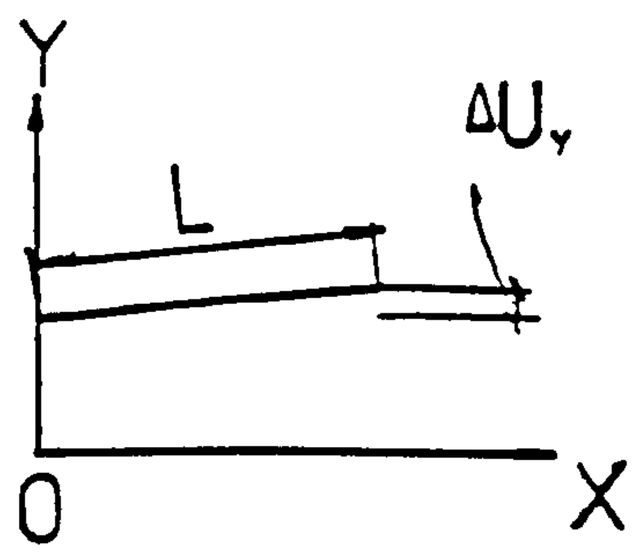

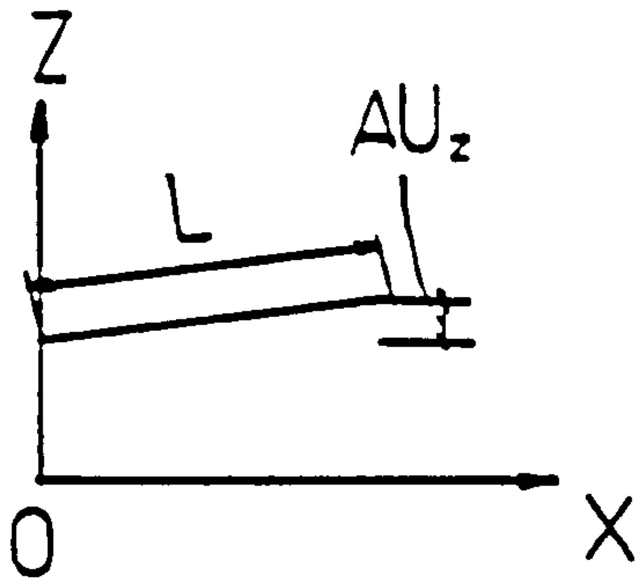

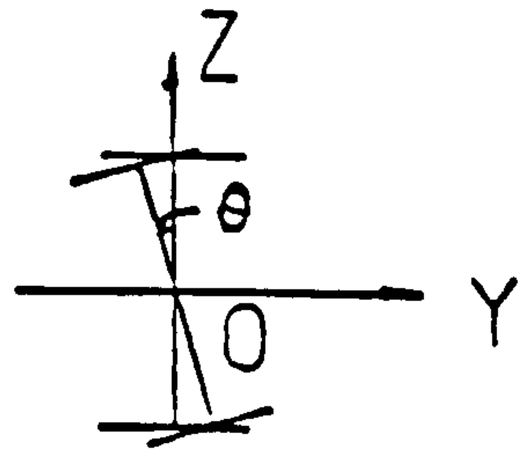

Appendix A3:Transformation and Stiffness Matrices for an Offset Brace

1. Transformation matrix $[T_b]$

$$[T_b] = \begin{bmatrix} 1.0 & 0.0 & -(d_{XY} - Y_c) & 0.0 & -(d_{XZ} - Z_c) & 0.0 & 0.0 \\ 0.0 & 1.0 & 0.0 & 0.0 & 0.0 & -(d_Z - Z_0) & 0.0 \\ 0.0 & 0.0 & 1.0 & 0.0 & 0.0 & 0.0 & 0.0 \\ 0.0 & 0.0 & 0.0 & 1.0 & 0.0 & (d_Y - Y_0) & 0.0 \\ 0.0 & 0.0 & 0.0 & 0.0 & 1.0 & 0.0 & 0.0 \\ 0.0 & 0.0 & 0.0 & 0.0 & 0.0 & 1.0 & 0.0 \\ 0.0 & 0.0 & 0.0 & 0.0 & 0.0 & 0.0 & 1.0 \end{bmatrix}$$

2. Stiffness matrix $[K_b]$

$$[K_b] =$$

$$\begin{bmatrix} S_{tx} & 0.0 & -S_{tx}(d_{XY} - Y_c) & 0.0 & -S_{tx}(d_{XZ} - Z_c) & 0.0 & 0.0 \\ & S_{ty} & 0.0 & 0.0 & 0.0 & -S_{ty}(d_Z - Z_0) & 0.0 \\ & & S_{rx}+ & 0.0 & S_{tx}(d_{XY} - Y_c) & 0.0 & 0.0 \\ & & S_{tx}(d_{XY} - Y_c)^2 & & \times(d_{XZ} - Z_c) & & \\ & & & S_{tz} & 0.0 & S_{tz}(d_Y - Y_0) & 0.0 \\ & & & & S_{ry}+ & 0.0 & 0.0 \\ & & & & S_{tx}(d_{XZ} - Z_c)^2 & & \\ & & & & & S_{ty}(d_Z - Z_0)^2+ & \\ & & & & & S_{tz}(d_Y - Y_0)^2 & 0.0 \\ & & & & & +S_{rx} & \\ & & & & & & S_w \end{bmatrix}$$

Appendix B1 Transformation Matrix $[T_3]$ for Different Cases of Beam-Column Framing

1. Case A

$$[T_3] = \begin{bmatrix} 0.0 & 1.0 & 0.0 & 0.0 & 0.0 & 0.0 & 0.0 \\ 0.0 & 0.0 & 0.0 & 1.0 & 0.0 & 0.0 & 0.0 \\ 0.0 & 0.0 & 0.0 & 0.0 & 0.0 & 1.0 & 0.0 \\ 1.0 & 0.0 & 0.0 & 0.0 & 0.0 & 0.0 & 0.0 \\ 0.0 & 0.0 & -1.0 & 0.0 & 0.0 & 0.0 & 0.0 \\ 0.0 & 0.0 & 0.0 & 0.0 & -1.0 & 0.0 & 0.0 \\ 0.0 & 0.0 & 0.0 & 0.0 & 0.0 & 0.0 & -1.0 \end{bmatrix}$$

2. Case B

$$[T_3] = \begin{bmatrix} 0.0 & 1.0 & 0.0 & 0.0 & 0.0 & 0.0 & 0.0 \\ 1.0 & 0.0 & 0.0 & 0.0 & 0.0 & 0.0 & 0.0 \\ 0.0 & 0.0 & -1.0 & 0.0 & 0.0 & 0.0 & 0.0 \\ 0.0 & 0.0 & 0.0 & -1.0 & 0.0 & 0.0 & 0.0 \\ 0.0 & 0.0 & 0.0 & 0.0 & -1.0 & 0.0 & 0.0 \\ 0.0 & 0.0 & 0.0 & 0.0 & 0.0 & -1.0 & 0.0 \\ 0.0 & 0.0 & 0.0 & 0.0 & 0.0 & 0.0 & 1.0 \end{bmatrix}$$

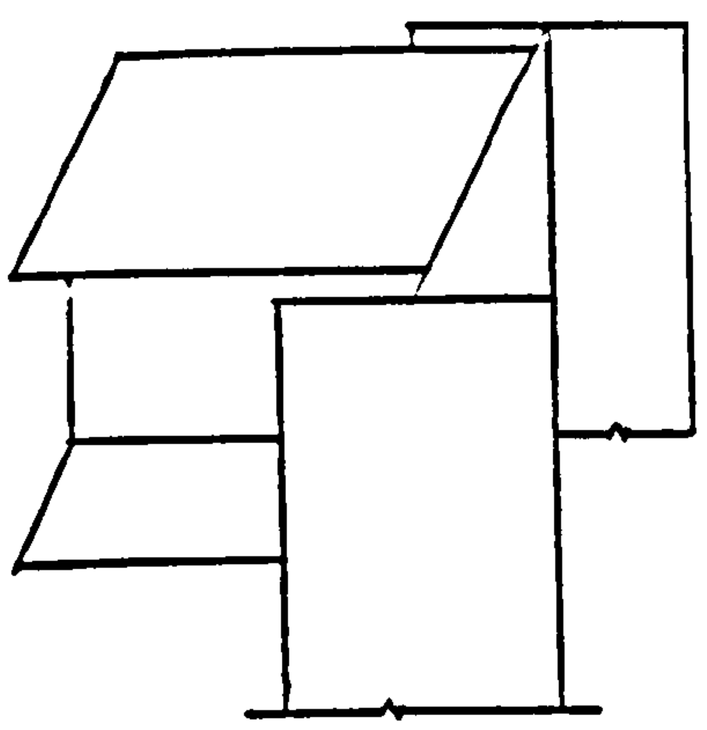

Case A

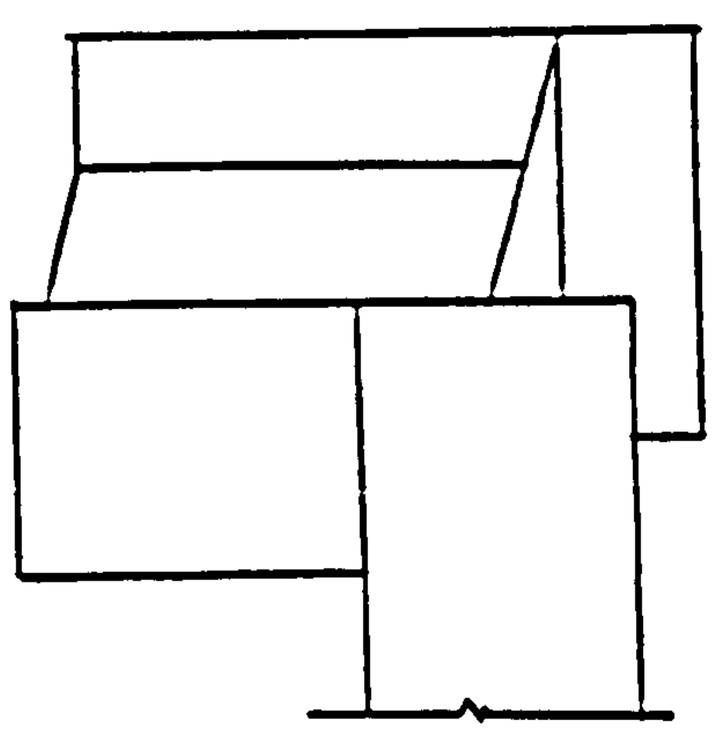

Case B

3. Case C

$$[T_3] = \begin{bmatrix} 0.0 & 0.0 & 0.0 & 1.0 & 0.0 & 0.0 & 0.0 \\ 0.0 & -1.0 & 0.0 & 0.0 & 0.0 & 0.0 & 0.0 \\ 0.0 & 0.0 & 0.0 & 0.0 & 0.0 & 1.0 & 0.0 \\ 1.0 & 0.0 & 0.0 & 0.0 & 0.0 & 0.0 & 0.0 \\ 0.0 & 0.0 & 0.0 & 0.0 & -1.0 & 0.0 & 0.0 \\ 0.0 & 0.0 & 1.0 & 0.0 & 0.0 & 0.0 & 0.0 \\ 0.0 & 0.0 & 0.0 & 0.0 & 0.0 & 0.0 & -1.0 \end{bmatrix}$$

4. Case D

$$[T3] = \begin{bmatrix} 0.0 & 0.0 & 0.0 & 1.0 & 0.0 & 0.0 & 0.0 \\ -1.0 & 0.0 & 0.0 & 0.0 & 0.0 & 0.0 & 0.0 \\ 0.0 & 0.0 & 0.0 & 0.0 & 1.0 & 0.0 & 0.0 \\ 0.0 & -1.0 & 0.0 & 0.0 & 0.0 & 0.0 & 0.0 \\ 0.0 & 0.0 & 0.0 & 0.0 & 0.0 & 1.0 & 0.0 \\ 0.0 & 0.0 & 1.0 & 0.0 & 0.0 & 0.0 & 0.0 \\ 0.0 & 0.0 & 0.0 & 0.0 & 0.0 & 0.0 & 1.0 \end{bmatrix}$$

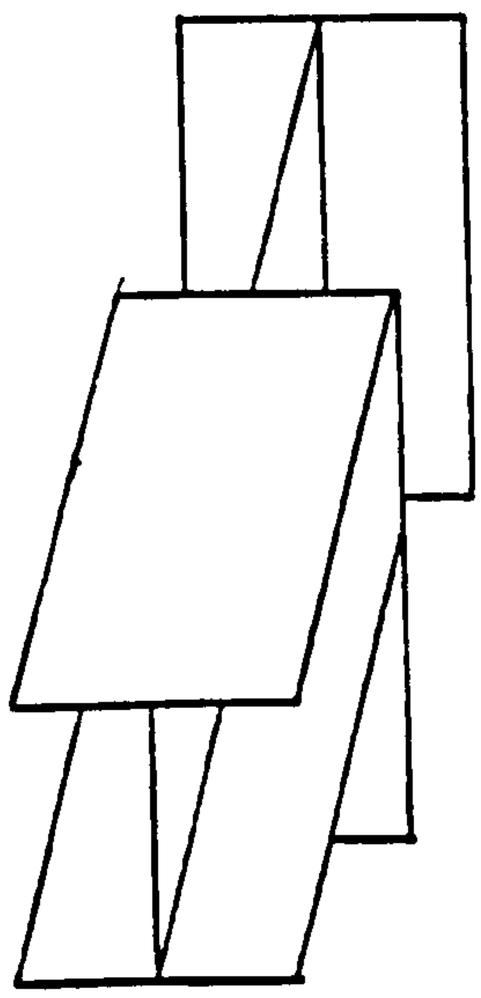

Case C

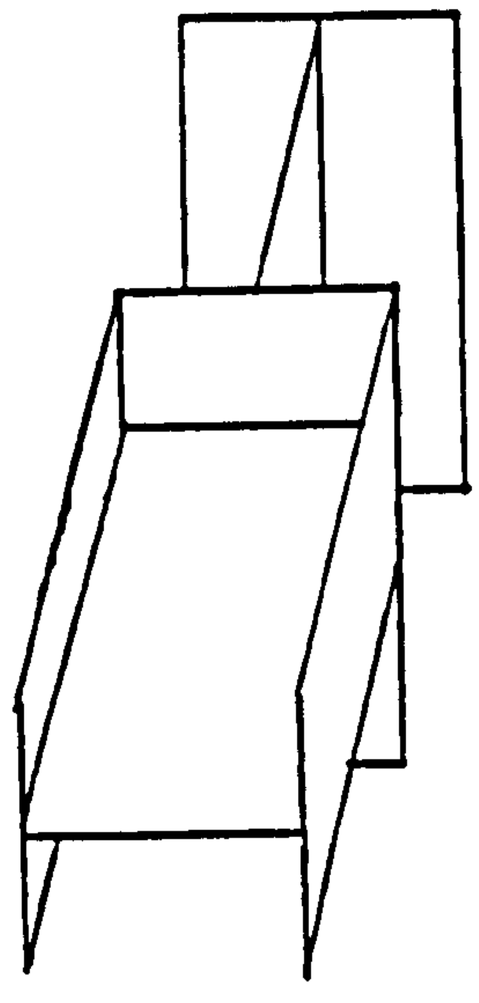

Case D

Appendix C1: Calculation of Moment Distribution in Column Subassemblages

Due to the negligible torsional effect on the behaviour of the column subassemblage, the three dimensional structure may be decoupled into a pair of planar subassemblages. Figure C1.1 illustrates one of these planar column subassemblages for the previously investigated structure.

Because of the nonlinear characteristics of the connection $M-\phi$ curves, the calculation of moment distribution has to be carried out incrementally. The incorporation of $M-\phi$ curves follows the procedure in the computer program.

The initial crookedness of the column is assumed to be triangular along the length of the column with the maximum value at the centre of the column. The deformation is thus assumed to be linear over each member.

In figure C1.1, P_{re} is the axial load in the column prior to the application of increment loads ΔP_1 and ΔP_2 , which are the loads applied on the beam and on the top of the column respectively. δ_0 and $\Delta\delta$ are the previous column deflection (including the initial value) and the deflection increment respectively. The second moment effect $(P-\Delta)$, which is profound under high levels of axial load, is taken into considertation in the calculation.

The force method is used and the connection moments are treated as redundancies. The moment distribution diagrams under these redundant forces, the applied loads and $P\Delta$ effect are given in figures C1.2a-C1.2d. The moment diagrams corresponding to unit values of each of these redundant moments and the unit force at the column mid-span are shown in Figs C1.3a-C1.3c.

Assuming elastic behaviour, applying each unit force in turn, and employing the virtual work principle, three equations will result. Reorganising these equations gives:

$$\left(\frac{1}{K_1}+\frac{1}{EK_{b1}}+\frac{1}{3EK_c}\right)\Delta M_1+\frac{1}{3EK_c}\Delta M_2-\frac{(\Delta P+P_{re})}{4EK_c}\Delta\delta = \frac{\Delta P\delta_0}{4EK_c}-\frac{\Delta P_1 a(1-\frac{a}{2L_{b1}})}{EK_{b1}} \qquad (.1)$$

$$\frac{1}{3EK_c}\Delta M_1+(\frac{1}{K_2}+\frac{1}{EK_{b2}}+\frac{1}{3EK_c})\Delta M_2-\frac{\Delta P+P_{re}}{4EK_c}\Delta\delta = \frac{\Delta P\delta_0}{4EK_c} \qquad (.2)$$

$$-\frac{L_c}{16EK_c}\Delta M_1-\frac{L_c}{16EK_c}\Delta M_2+\left(\frac{(\Delta P+P_{re})L_c}{12EK_c}-1\right)\Delta\delta = \frac{\Delta P_1\delta_0 L_c}{12EK_c} \qquad (.3)$$

where

$$K_{b(n)}=\frac{I_{b(n)}}{L_{b(n)}} \qquad n=1,2 \qquad (.4)$$

$$K_c=\frac{I_c}{L_c} \qquad (.5)$$

Once ΔM_1 , ΔM_2 and $\Delta\delta$ are calculated, the moment distribution diagram of the column subassemblage is readily obtained. The problem of other types of column subassemblages with different beam locations may be treated in a similar manner. Because of the small number of degrees of freedom, the use of a micro-computer is most suitable.

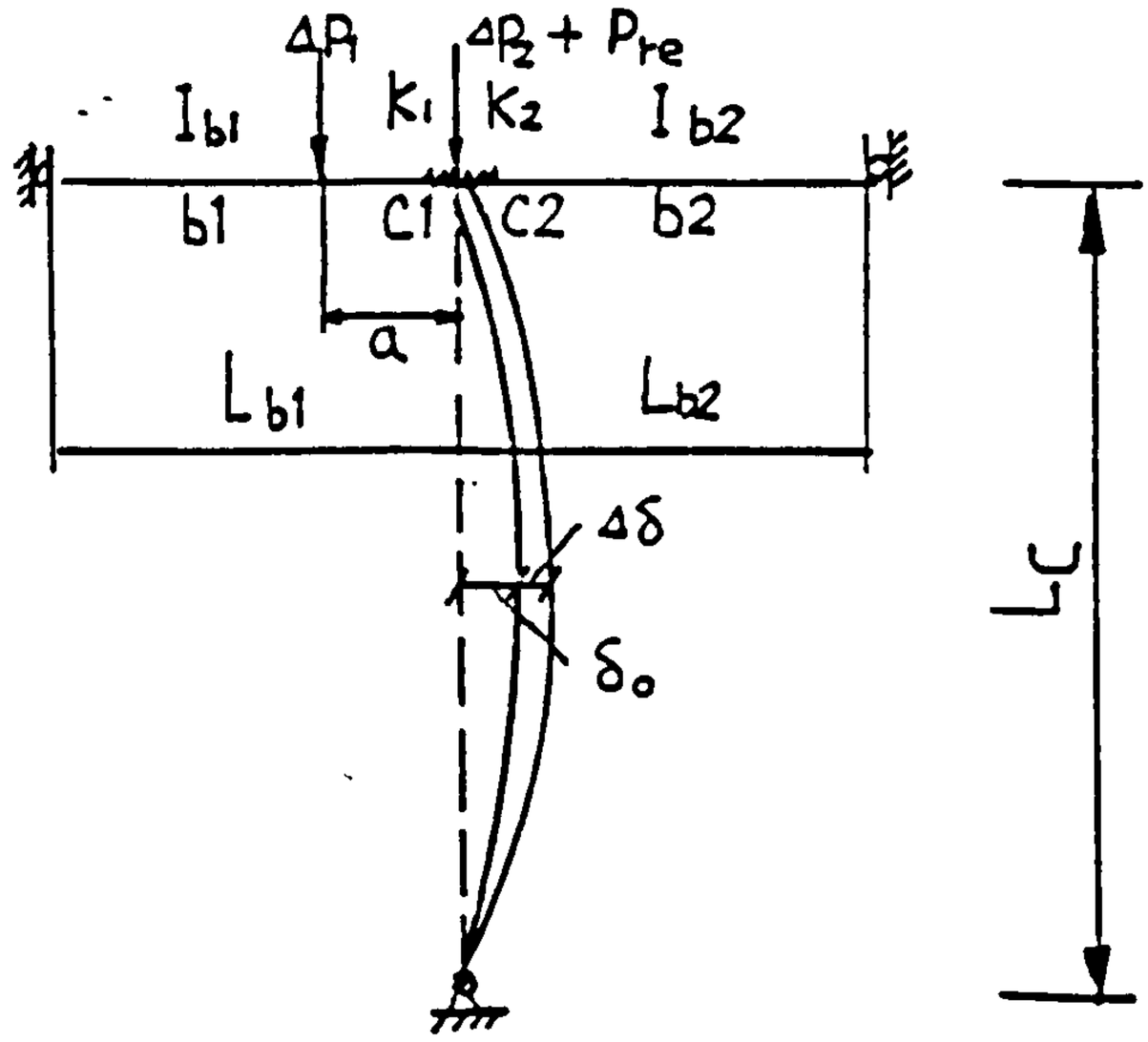

Fig. C1-1 General view of one planar subassemblage

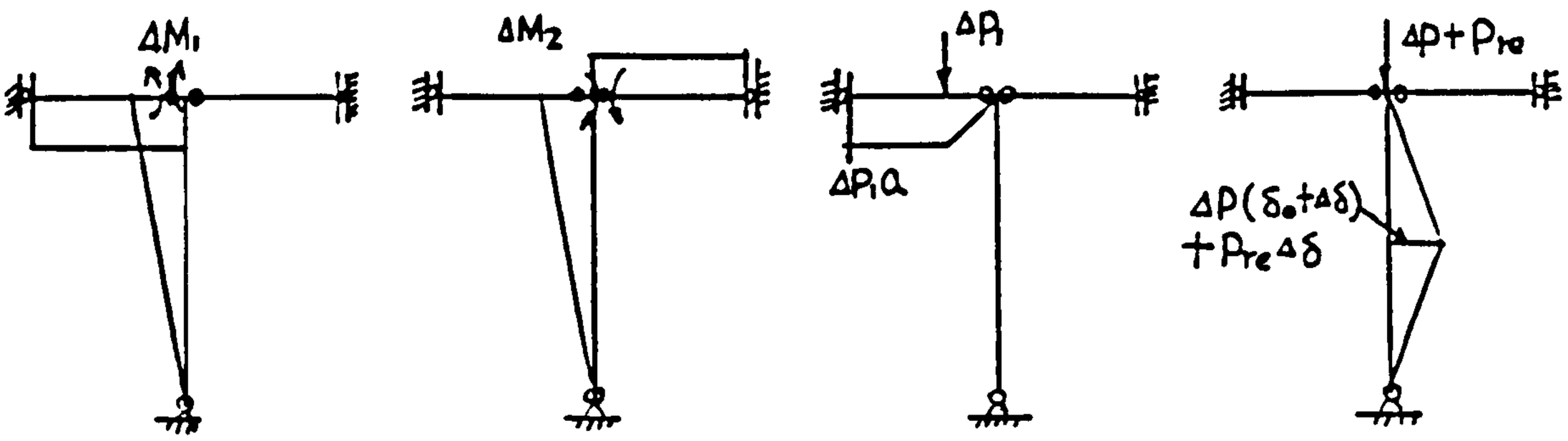

Fig. C1·2 Moment diagrams of the basic structure under different loads

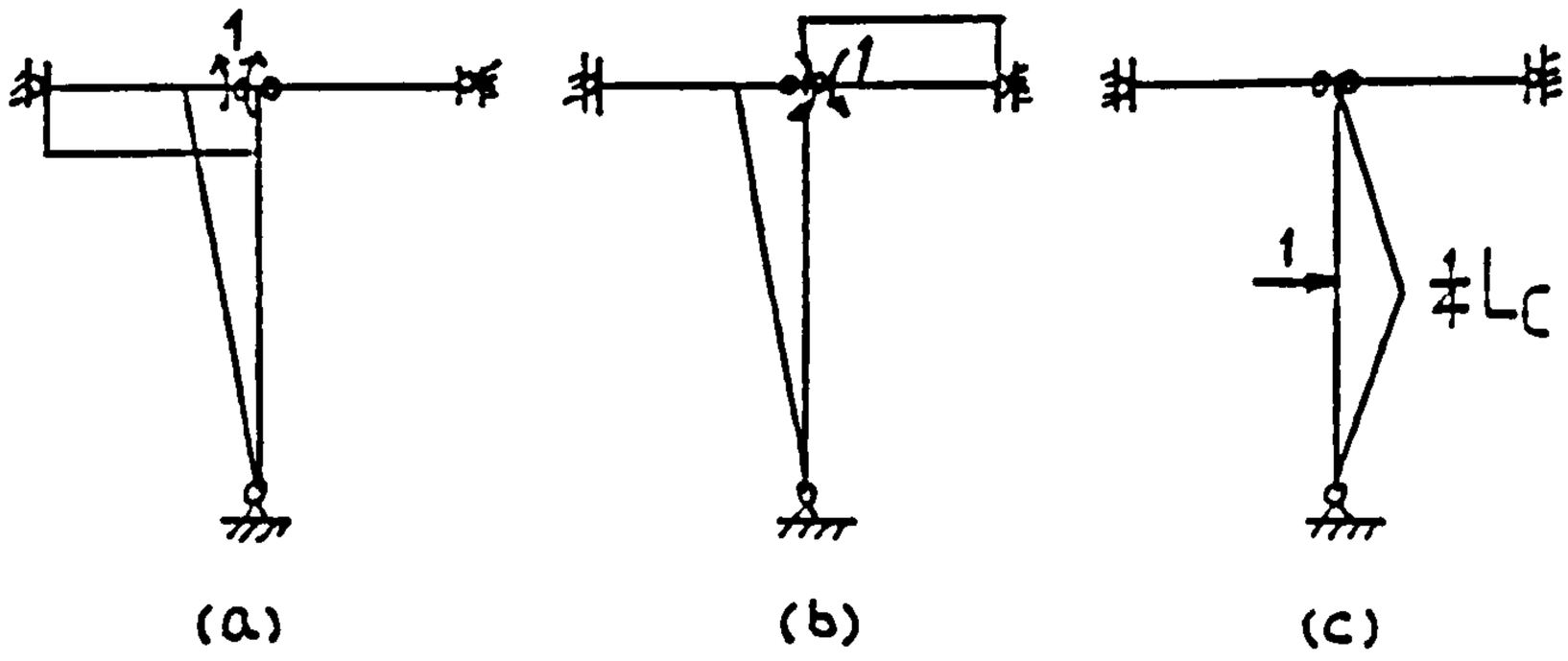

Fig. C1 3 Moment diagrams of the basic structure under different unit loads